DYNAMIC CHARACTERISTICS OF A 30 STOREY BUILDING DURING CONSTRUCTION DETECTED FROM AMBIENT VIBRATION MEASUREMENTS

by

NORMAN DAVID SCHUSTER

Honours B.A.Sc., The University of Waterloo, 1992

A THESIS SUBMITTED IN PARTIAL FULFILLMENT OF

THE REQUIREMENTS FOR THE DEGREE OF

MASTER OF APPLIED SCIENCE

in

THE FACULTY OF GRADUATE STUDIES
Department of Civil Engineering

We accept this thesis as conforming
to the required standard

THE UNIVERSITY OF BRITISH COLUMBIA

October 1994

Department of CIVIL ENGINEERING

The University of British Columbia
Vancouver, Canada

Date 10 OCT 1994

ABSTRACT

The dynamic response of building structures to earthquakes has become an issue in the province of British Columbia because of increased awareness of the seismic hazard in this region. While there is a great deal of knowledge about structural dynamics, the majority of this knowledge is based on uniform structures. Hence, there is concern about extrapolating these results to the behaviour of nonuniform building which emerge from current architectural trends. The focus of this study was to monitor and to quantify the dynamic characteristics of a 30 storey, reinforced concrete building during its construction. This building is representative of the type of construction in Vancouver, B.C. and is therefore a useful case study. In addition, the lateral force resisting system in this structure is uniform in plan and elevation while the distribution of storey mass is asymmetrical due to its geometry as well as a major setback at one corner.

Dynamic characteristics were determined by analyzing ambient vibrations of the structure. These vibrations were acquired and processed using a testing system developed at the University of British Columbia (Department of Civil Engineering). Several computer programs were developed during this project to complement the existing software.

The objectives of this study included determining mode shapes and periods, determining the effect of architectural components, assessing base motion, and assessing the manner of the core's deformation. In addition, a dynamic analysis was performed to assess the accuracy of modeling techniques. Finally, some aspects of current building codes were assessed.

Ambient vibration testing methods proved very practical and useful. Torsional motion and modal coupling were found to be very significant, while little motion was detected at the base of this building. Natural frequencies decreased and tended to converge as the building height increased. Architectural components did not significantly influence the dynamic characteristics. The dynamic behaviour of this building could be accurately represented using dynamic analysis. Finally, the building code provisions considered in this study appear to be appropriate.

TABLE OF CONTENTS

LIST OF TABLES

LIST OF FIGURES

ACKNOWLEDGMENTS

I would like to thank my advisor, Dr. Carlos Ventura. His experience with instrumented buildings and signal processing, along with his guidance and encouragement, contributed to the success of this project. His assistance in all of the City Tower vibration surveys was most helpful. Finally, his thoughts and suggestions during his review of early drafts of this thesis, are appreciated.

I am indebted to my colleague Dr. Andreas Felber. He developed the data acquisition system and analysis software which was used in this study. He also served as my trainer; offering insightful guidance about ambient vibration testing and spectral analysis. He was also instrumental during all of the ambient vibration surveys performed on City Tower, and his help is appreciated. Finally his company, EDI Ltd., made some additional software programs available for use in this study.

I would also like to thank those people involved with the City Crest Tower development. Mr. Don Ho of Trans City Properties Ltd. permitted the vibration measurements of his building. Mr. John Pao of Bogdonov Pao Associates Ltd. encouraged this study. He also provided contract drawings of the building and participated in the first test at City Tower. Mr. Jim Desroches, also of Bogdonov Pao Associates Ltd., was my liaison. Finally, the cooperation and assistance of Mr. Vince Kehoe, of Ledcor Industries, was very helpful to the preparation and execution of all the tests which were performed at City Tower.

The financial support of the Natural Science and Engineering Research Council (N.S.E.R.C.) of Canada is gratefully acknowledged. This includes a Postgraduate Scholarship as well as Research and Equipment Grants. The grants were used to augment the dynamic testing equipment at UBC as well as finance my attendance at EERI conferences (held in Los Angeles, California and Chicago, Illinois) to present research papers based on my research.

I would like to thank Mr. Howard Nichol, earthquake lab technician, for maintaining and explaining several components of the data acquisition system.

I would also like to thank all of the other people from UBC who provided invaluable assistance during the field tests. These people include Dr. Helmut Prion; graduate students Steve Yee, Rhonda Steinke, Tom Schmalz, Mike Baraka, Isabelle Villemure, and Markus Seethaler; and undergraduate student Aloysius Fekete.

Finally, I would like to thank Dr. P. Adebar and Dr. R. Foschi who, along with Dr. Ventura, reviewed the first draft of this thesis.

To my late grandfather, Peter . . .

I always cherished his pride in me in everything I did

CHAPTER 1
INTRODUCTION

This chapter presents an overview of this research project. A general description of the problem is discussed in the first section (§1.1). This is followed by a literature review (§1.2). The next section describes the scope and objectives of this study (§1.3). An outline of this thesis is presented at the end of this chapter (§1.4).

1.1 OVERVIEW OF PROJECT

Most civil engineering structures (buildings, bridges, etc.) are prototypes. Hence, an evaluation of a structure's behaviour prior to or even decades after its construction is based on mathematical analysis as well as engineering judgment and experience with similar types of structures. In recent years, the dynamic response of a structure during an earthquake has become a concern in the province of British Columbia (B.C.). In this case, a dynamic analysis of the structure is performed in order to predict its capacity to given seismic demands. This type of analysis is very sensitive to changes in a system's parameters; these being stiffness, damping, and mass. Moreover, the spatial distribution of these parameters, complicated by a structure's interaction with the soil upon which it rests, makes this task very difficult.

There has been a great deal of research in the area of structural dynamics and the behaviour of building systems. However, the majority of this research has focused on uniform buildings; i.e. buildings with rectangular shaped floor plans as well as regular and symmetrical layouts of the load bearing walls and columns. In contrast, current trends in architecture have produced very imaginative and oddly shaped buildings. Consequently, there is concern about extrapolating the behaviour of a *uniform* building to the behaviour of one of these *modern* buildings.

While fundamental engineering principles can be applied in the analysis of these *modern* buildings, there is a need to verify that predictions of building response determined through such applications are accurate. One method to verify the accuracy of these predictions is to measure

the vibrations of the structure, and by using signal processing methods, determine the dynamic characteristics of the structure. These characteristics can then be compared to those determined using analytical models.

A very popular method of determining dynamic characteristics is to analyze ambient vibrations of the building. These types of vibration result from wind, traffic on neighbouring streets, people moving about in the building, etc. For this study, an ambient vibration data acquisition and analysis system at the University of British Columbia was available to perform these measurements.

The focus of this study was on the dynamic behaviour of a high-rise building, called City Tower, which is located in Vancouver, B.C. This behaviour was quantified by recording and analyzing ambient vibrations of the structure. This was a very interesting case study for a number of reasons. First, the dynamic characteristics were determined at selected points in time during the building's construction. Thus, the evolution of this behaviour as the structural system is assembled up to the point in time when all of the architectural components are installed was monitored. Second, the asymmetrical distribution of storey mass in this structure created some interesting torsional effects in the vibration mode shapes. Moreover, the effect of two major setbacks along the height of this building was considered.

As mentioned, this ambient vibration survey was conducted as the building was being constructed. Specifically, measurements were taken at the building following the completion of 10, 15, 20, 25, and 32 levels during a 5 month period from January to June 1993. A final measurement was conducted in October 1993 when all of the major architectural components were in place.

1.2 CURRENT RESEARCH

The analysis of ambient vibration measurements of a wide variety of engineering structures has been documented over the last few decades. A few studies from 1982 to present are discussed below.

Four high-rise buildings located in New York City were recently tested by Gavin, Grossman, et al. (1992) using ambient and wind induced vibrations. This study focused on the response of tall flat-plate buildings representative of the construction in this region. Although the number of measurement points in these building was rather low, several vibration mode shapes and frequencies along with estimates of damping ratios were determined. The scope of this research was similar to the project discussed in this thesis. In particular, the type of construction of these buildings is similar to that of the building being studied in this research project. In addition, one of these buildings was tested prior to the installation of architectural components. The latter building was scheduled to be tested once it was finished.

Three different structures were successfully tested in Germany using ambient vibration measurements (Luz, 1992). These structures include a 12 storey office building (located at Stuttgart University) along with a church tower and a single span railway bridge. The fundamental vibration modes and several higher vibration modes were determined, along with their corresponding frequencies, for all of these structures. This effectively demonstrated the versatility of ambient vibration testing.

Ambient vibration measurements, along with strong motion vibration measurements from several earthquakes, were used to study several buildings on the west coast of the United States. One study involved a six storey building which contained strong motion instrumentation provided by the California Division of Mines and Geology (Pardoen, 1983). In another study, five multi-storey buildings in seismically active regions in San Francisco, California and Seattle, Washington, were tested by Neuss, Maison, and Bouwkamp (1983). In yet another study, five different buildings which experienced the ground motions of the Loma Prieta earthquake

(October 17, 1989) were studied by Marshall, Phan, and Çelebi (1994). In the latter study, comparisons were made between results obtained from ambient vibration measurements (using the existing strong motion instrumentation in the buildings) with the results obtained from analyzing the strong motion records.

An ambient vibration study was also conducted on several buildings in Vancouver by To and Cherry (1982). In this study, three *identical* buildings (Gage Residence) at the University of British Columbia were tested for comparison. In addition, the modal properties of three buildings located in downtown Vancouver, namely the Harbour Centre Building, and the IBM and Toronto Dominion Bank Towers, were also determined.

Considering the wide spread use of ambient vibration measurements to successfully determine dynamic characteristics of buildings, it was decided that this method of testing would be used to study City Tower.

1.3 SCOPE AND OBJECTIVES OF THIS STUDY

The objective of this investigation was to monitor and to quantify the dynamic characteristics of a multi-storey building whose structural system was representative of the type found in downtown Vancouver. The dynamic characteristics of interest were vibration mode shapes and corresponding periods in the three principal directions (torsional and two translational) of the building.

In addition to modal properties, several other aspects of the building's dynamic behaviour were studied. These include the effect of non-structural components, motion at the base of the building, and core deformations during the vibration mode shapes. The effect of non-structural components was determined based on differences in frequencies and vibration mode shapes as well as changes in damping ratios.

Following the experimental analysis, a dynamic modal analysis was performed on 5 models of the building corresponding to the construction stages where ambient vibration measurements

were taken. The objective of the dynamic analysis was to calibrate the models so that the resulting frequencies (periods) and mode shapes corresponded to those obtained experimentally. This would demonstrate the accuracy of state-of-the-art modeling techniques. Experimental and analytical periods determined from this study were also compared with periods obtained from the dynamic analysis used to design the building, as well as periods obtained using expressions in two building design codes. In addition, calculations of base shear and overturning moments were also made.

While several aspects of this building can be studied, only the topics mentioned above form the scope of this research. This limitation was due to time constraints. Moreover, other aspects of this building's behaviour can always be explored in the future.

1.4 OUTLINE OF THESIS

This thesis is comprised of six chapters and eight appendices. The second chapter presents background information on signal analysis. Chapter Three describes the high-rise building studied. The next two chapters discuss the ambient vibration tests and the results obtained from the analysis of the collected data. The last chapter presents the results from the dynamic analysis of the building. Finally, conclusions and recommendations for future research are presented.

Appendix A includes details of the ambient vibration tests and instrumentation. Appendices B through E contain descriptions and operating instructions of several software programs that were developed through the course of this research. Appendices F and G show plots of several signal processing functions determined from the experimental data. The plots in Appendix F were used to assess the performance of the instruments which recorded the building's vibrations. The plots in Appendix G were used to detect natural frequencies. Finally, Appendix, H contains selected results from the dynamic analysis of the building.

CHAPTER 2
BACKGROUND ON SIGNAL ANALYSIS

This chapter presents an overview of ambient vibration theory (§2.1) as well as a discussion of the signal processing functions which were used in this study (§2.2).

2.1 AMBIENT VIBRATION TESTING

2.1.1 AMBIENT VIBRATIONS

A popular method for determining modal frequencies and shapes of a structure is by analyzing its ambient vibrations. This method is favoured over forced-vibration testing for several reasons. First, it is very economical. Second, several of the vibrational modes are excited and can be detected from a single measurement using signal processing methods. Third, there is the possibility that forced-vibrations could damage the structure. The disadvantage of using ambient vibrations to determine modal characteristics is that improper data collection and analysis can lead to erroneous conclusions. Also, damping ratios cannot be determined reliably.

Ambient vibrations can be characterized as a random process combined with a deterministic signal. The former can be attributed to the response of the structure during its normal modes of vibration, while the latter can be attributed to the randomness of the environmental excitation as well as noise present in the signal (Diehl, 1991; Luz, 1992). The basis of using these vibrations to determine dynamic characteristics of a structural system is presented below.

2.1.2 PREREQUISITES FOR AMBIENT VIBRATION ANALYSIS

The method used to analyze ambient vibration time histories has several prerequisites. For this method of analysis, the structural *system* under consideration must have the following attributes:

(1) The *process* being measured is *stationary*
(2) The system behaves linearly
(3) Vibration modes of interest are significantly excited
(4) Vibration modes are well separated and lightly damped
(5) Structure is *classically damped*

Stationary simply means that the process being studied (in this case the ambient vibrations of the structure) is independent of time. Thus, measurements of the process can be made at any point in time, and the results obtained from analyzing these measurements will be the same. In addition to being stationary, the structure must behave as a linear system. In other words, the response of the system to a series of forces is equivalent to the superposition of the response of the system to each individual force.

The remaining three prerequisites ensure that meaningful information can be derived from the spectral analysis functions. First, in order to detect a modal frequency and its corresponding mode shape from the ambient vibrations, its contribution must be present in the measured time histories. Second, ambient vibration theory presumes that the response at a natural frequency is dominated by the corresponding mode shape. Furthermore, frequencies and mode shapes can only be isolated provided there is sufficient separation between them in the frequency domain. Lightly damped systems tend to have very narrow spikes in their spectra thus facilitating this requirement. Finally, *classically damped* implies that the resulting mode shape values are real, and therefore the signals from two degrees of freedom are either perfectly in-phase or perfectly out-of-phase at a natural frequency. This avoids the problem of interpreting complex valued mode shapes.

In general, the prerequisites described above were met while analyzing the ambient vibration measurements taken at City Tower.

2.1.3 FORMULATIONS

The basis of ambient vibration theory begins with the solution of the multi-degree of freedom equation of motion. The displacement response for an n degree of freedom system, in terms of its modal components, is given by Equation 2.1.

$$\{x(t)\} = \{\phi_1\}\alpha_1(t) + \{\phi_2\}\alpha_2(t) + \ldots + \{\phi_n\}\alpha_n(t) \quad (2.1)$$

This particular equation is based on the assumption that the displacement response of the

structure in the time domain, $x(t)$, can be expressed as a summation of corresponding products between the system's time invariant, vibration mode shape, ϕ, and a time varying amplitude function, $\alpha(t)$. This is a fundamental basis of several dynamic formulations which can be found in several text books (see for example Clough and Penzien, 1975, or Humar, 1990).

Transforming Equation 2.1 into the frequency domain gives:

$$\{X(\omega)\} = \{\phi_1\}H_1(\omega)P_1(\omega) + \ldots + \{\phi_n\}H_n(\omega)P_n(\omega) \quad \text{.....(2.2)}$$

Note that the modal amplitude is now expressed as the product of the frequency response function, $H(\omega)$, and the Fourier transform of the excitation, $P(\omega)$. The corresponding acceleration response is given by Equation 2.3.

$$\{\ddot{X}(\omega)\} = \omega^2\left[\{\phi_1\}H_1(\omega)P_1(\omega) + \ldots + \{\phi_n\}H_n(\omega)P_n(\omega)\right] \quad \text{.....(2.3)}$$

Now consider the acceleration response at the ith degree-of-freedom of the structure which is given by the following equation:

$$\ddot{X}_i(\omega) = \omega^2\left[\phi_{1i}H_1(\omega)P_1(\omega) + \ldots + \phi_{ni}H_n(\omega)P_n(\omega)\right] \quad \text{.....(2.4)}$$

Using the basis that modal frequencies are well separated and modal damping is small, then it follows that the response of the system at a natural frequency is dominated by the corresponding mode of vibration. Therefore, the acceleration response at the jth natural frequency, ω_j, can be can be approximated as:

$$\ddot{X}_i(\omega_j) \cong \omega_j^{\,2}\phi_{ji}H_j(\omega)P_j(\omega) \quad \text{.....(2.5)}$$

Finally, if two acceleration records are obtained simultaneously at locations a and b, then modal ratios can be estimated using:

$$\frac{\ddot{X}_a(\omega_j)}{\ddot{X}_b(\omega_j)} \cong \frac{\omega_j^{\,2}\phi_{ja}H_j(\omega_j)P_j(\omega_j)}{\omega_j^{\,2}\phi_{jb}H_j(\omega_j)P_j(\omega_j)} = \frac{\phi_{ja}}{\phi_{jb}} \quad \text{.....(2.6)}$$

In order to assemble vibration mode shapes, all that is necessary is to obtain a series of vibration

measurements at different locations of the structure, and calculate modal ratios with respect to a common measurement. This is analogous to the method used to calculate mode shapes in an Eigenvalue analysis (Clough and Penzien, 1975).

2.1.4 IMPLEMENTATION

In order to assemble the mode shape using the method described in the previous section, it is necessary to have two sets of sensors: *reference* sensors and *roving* sensors. The reference sensors are located at a point in the structure which contains information about the vibration mode shapes of interest; and they remain in this location during the entire test. The roving sensors are systematically placed at other locations in the structure where a component of the vibration mode shape is desired. After each measurement, the roving sensors are relocated to different locations. This continues until all of the measurements have been taken.

Since the modal ratios are calculated as the ratio between the reference sensor and the roving sensor, it is essential that the reference sensor is not located at a node in the vibration mode shapes of interest. This is unavoidable in some situations, and therefore it is necessary to use several reference sensors located at different locations and orientations in order to obtain information about different mode shapes. In this way some of the mode shapes can be detected with respect to (w.r.t.) one of the reference sensors, while the other mode shapes can be detected w.r.t. another reference sensor. For the City Tower tests, 4 reference sensors (2 pairs oriented in the north and east directions) were located on the top floor of the building while 4 roving sensors were systematically located on the floor below. These locations are discussed further in Chapters 4 and 5 as well as Appendix A.

2.2 SIGNAL PROCESSING FUNCTIONS USED IN THIS STUDY

All of the ambient vibration data collected in this study was analyzed using signal processing functions. This involved transforming the acceleration time histories into the frequency domain, and then generating certain functions to locate frequencies (periods) and mode shapes. Some of the more useful functions used to relate one signal to another signal include the cross-spectral density function, power-spectral density function, coherence function, and transfer function. These functions and their significance are discussed in the sections below.

It should be noted that the ambient vibration acceleration time histories collected during this study are actually expressed as voltage, not acceleration. However, no conversion is necessary since most of the signal processing functions involve a ratio thereby producing a dimensionless quantity, and also since the sensitivities of each of the sensors used for the vibration measurements are practically the same. For those functions which do not involve a dimensionless quantity, the magnitude is incorrect. However, only the overall shapes of these functions, not the magnitude, was of interest in this study.

2.2.1 SPECTRAL DENSITY FUNCTIONS

The functions described below are based on statistical principles of a random process. In addition, these functions assume single-input-single-output (SISO) behaviour of the system under consideration. Thus one signal is assumed to be the input (in this case the signal from the reference sensor) while the other signal is assumed to be the output (in this case the signal from the roving sensor).

This section only provides highlights of the spectral density functions that were used in this study. A more detailed discussion of random vibrations is made by Newland (1975). A more detailed discussion of signal processing and spectral analysis is made by Bendat and Piersol (1992).

2.2.1.1 Cross-Spectral Density Function

The *cross-spectral density function*, $G_{ij}(f)$, is a measure of the amount of energy in two signals. One definition of this function is given by Equation 2.7.

$$G_{ij}(f) = X_i^*(f)X_j(f) \quad \text{(2.7)}$$

Note that this function is the product of the complex conjugate of the Fourier transform of the ith signal, $X_i^*(f)$, and the Fourier transform of the jth signal, $X_j(f)$. While this function was not used directly in the analysis of the ambient vibration measurements, it is the basis of several other functions which were used. These functions are discussed below.

2.2.1.2 Power Spectral Density Function

The *power spectral density* (PSD) or *autospectral density* function, $G_{ii}(f)$, is a special case of the cross-spectral density function (Equation 2.7) where $i=j$ The PSD is given by Equation 2.8.

$$G_{ii}(f) = X_i^*(f)X_i(f) \quad \text{(2.8)}$$

The PSD is a measure of the frequency distribution of the mean square value of the data. This function was used to detect possible locations of natural frequencies of the system being measured. These locations correspond to peaks or spikes in the PSD function.

2.2.1.3 Coherence Function

The *coherence* function, $\gamma_{ij}^2(f)$, is a measure of correlation between two signals at a given frequency, Equation 2.9. It is also an indication of the amount of noise present in two signals. Coherence values (at a particular frequency) of unity or close to it indicate good correlation between the two signals, while values of zero or close to it indicate either poor correlation or that excessive noise is present in the signal.

$$\gamma_{ij}{}^2(f) = \frac{|G_{ij}(f)|^2}{G_{ii}(f)G_{jj}(f)} \quad \text{(2.9)}$$

Note that the coherence function combines the information obtained from both the cross-spectral density function and the power spectral density function. This function is used when determining the authenticity of mode shapes at a particular frequency.

2.2.1.4 Transfer Function

Analogous to the modal ratio function (Equation 2.6) is the *transfer function*, $T_{ij}(f)$. This function is given by the signal ratio of a roving sensor and a reference sensor, Equation 2.10.

$$T_{ij}(f) = \frac{\ddot{X}_j(f)}{\ddot{X}_i(f)} = \frac{\ddot{X}^*_i(f)\ddot{X}_j(f)}{\ddot{X}^*_i(f)\ddot{X}_i(f)} = \frac{G_{ij}(f)}{G_{ii}(f)} \quad \text{(2.10)}$$

Note that the transfer function can be expressed as the ratio between the cross-spectral density function and the power spectral density function of the reference sensor's signal. This function can also be expressed in terms of its modulus, $\Phi_{ij}(f)$, and its phase angle, $\Theta_{ij}(f)$, which is often referred to as a phase function. These expressions are given by Equation 2.11.

$$\Phi_{ij}(f) = \left|T_{ij}(f)\right| \quad \text{(2.11a)}$$

$$\Theta_{il}(f) = \arctan\left(\frac{imag[T_{il}(f)]}{real[T_{il}(f)]}\right) \quad \text{(2.11b)}$$

The modulus, Equation 2.11a, is used to determine where high and low relative response occurs between the two signals. The phase angle, Equation 2.11b, is used to determine whether the two signals are in-phase (0° apart) or out-of-phase (180° apart). These two components of the transfer function are the basis of the potential modal ratio functions (discussed in §2.2.1.6) which are used to assemble and determine the location and shape of vibration modes.

2.2.1.5 Averaged Normalized Power Spectral Density Function

The process of reviewing PSD functions in order to determine natural frequencies becomes very time consuming when several records are involved. In order to accelerate this review, a utility function was developed by Felber (1993) which would take a set of related PSD functions,

normalize them, and then average them. This weighs all of the PSD functions evenly so that the entire frequency distribution of the structure, in the frequency range of interest, can be seen in a single plot. This function, which is called an *averaged normalized power spectral density* (ANPSD) *function*, is given by:

$$ANPSD(f_k) = \frac{1}{l}\sum_{m=1}^{l}\left[\frac{G_{ii}(f_k)\big|_m}{\sum_{k=0}^{k=n} G_{ii}(f_k)\big|_m}\right] \quad \text{.....(2.12)}$$

where l is the number of PSD functions, and n is the number of points in the PSD array.

2.2.1.6 Potential Modal Ratio Function

Traditional methods of analyzing ambient vibration records involve checking PSD functions along with phase functions and coherence for individual pairs of signals. This is a very time consuming task, especially if there are several records involved. To greatly accelerate this procedure, a utility function was developed by Felber (1993) which would incorporate the magnitude and phase information obtained from the transfer function, with the correlation information obtained from the coherence function. This function, called the *potential modal ratio* (PMR) *function*, $M_{ij}(f)$, is given by Equation 2.13.

$$M_{ij}(f) = \left|T_{ij}(f)\right| \bullet PW_{ij}(f) \bullet CW_{ij}(f)$$

where

$$PW_{ij}(f) = \begin{cases} 1 & 0° \le \theta_{ij}(f) \le \theta_c \\ -1 & 180° - \theta_c \le \theta_{ij}(f) \le 180° \\ 0 & \textit{otherwise} \end{cases} \quad \text{.....(2.13)}$$

$$CW_{ij}(f) = \begin{cases} 1 & \gamma_c^2 \le \gamma_{ij}^2(f) \le 1 \\ 0 & \textit{otherwise} \end{cases}$$

This function is simply the modulus of the transfer function multiplied by a phase window and a coherence window. Phase and coherence is checked by specifying *cutoff* values. If the signal at a given frequency is within a certain phase, θ_c, and is above a specified value of coherence, γ_c^2, its value is passed through. Otherwise its value is automatically set to zero.

These functions are later used to assemble mode shapes. Thus a mode shape can be authenticated simply by inspecting it. The coherence and phase need not be checked separately since they have been incorporated into this mode shape.

2.2.2 MODAL ASSURANCE CRITERIUM (MAC)

Comparisons are often made between the shape of two vibration modes. One method to correlate these two shapes is a *modal assurance criterium* or MAC (Ewins, 1984), Equation 2.14.

$$MAC(a,x) = \frac{\left[\{\phi_a\}^T\{\phi_x\}\right]^2}{\left[\{\phi_a\}^T\{\phi_a\}\right]\left[\{\phi_x\}^T\{\phi_x\}\right]} \quad \text{.....(2.14)}$$

Note that this function is similar to the coherence function. As with the coherence function, values near unity indicate good correlation while values near zero indicate poor correlation. A matrix of MAC values can be assembled to compare two sets of mode shapes obtained experimentally and/or analytically.

2.2.3 SIGNAL PROCESSING SOFTWARE

All of the ambient vibration data which was collected in this study was processed using three software packaged called ULTRA, VISUAL, and P2. ULTRA was developed at the University of British Columbia specifically for processing ambient vibration records (Felber, 1993). This program calculates all of the functions described above and can be used to process several records quickly and efficiently. A companion program, called VISUAL, was developed simultaneously with ULTRA (Felber 1993). VISUAL is used to animate and visualize potential mode shapes based on PMR functions created by ULTRA. Finally, the program P2 (EDI Ltd., 1993) was used to generate ANPSD functions.

2.2.4 PROBLEMS ASSOCIATED WITH DIGITAL DATA

Some problems arise when continuous (analog) signals are represented by discrete points (digital data). Three common problems include data resolution, aliasing, and leakage.

2.2.4.1 Resolution

Resolution refers to the intervals between discrete points. In the case of a digitized time history, the resolution, Δt, is given by the inverse of the sampling rate. In the case of a time history which has been transformed into the frequency domain, the resolution, Δf, is given by the inverse of the time history's duration, T. The time resolution determines the threshold of frequencies which can be determined from the time history. The frequency resolution affects the precision of the frequency values.

To illustrate the effect of signal resolution, consider the plots shown in Figure 2.1. This figure shows three sine waves with frequencies of 6, 12, and 18 Hz which have been digitized using a sampling rate of 40 Hz. As shown, as the frequency of the sine wave increases, the quality of the digitized signal degrades since there are less discrete points representing the time signal.

In general, reliable values of frequency (and corresponding vibration mode shapes) can be detected up to one quarter of the sampling frequency. Frequencies above this value are more difficult to detect and the quality of the corresponding mode shapes degrades with increasing frequency. Examples of this can be seen in the mode shapes presented in Chapter 5.

2.2.4.2 Aliasing

As discussed in the previous section, as the frequency component of the waveform increases, the digital representation of the waveform degrades. This degradation continues to the point where the representation becomes misleading. This point corresponds to the highest frequency that can be resolved from a discrete time history; which is equal to one half of the sampling frequency. This frequency is often referred to as the Nyquist or cutoff frequency, and can be expressed as:

$$f_c = \frac{1}{2\Delta t} \qquad (2.15)$$

where Δt is the sampling interval, and f_c is the Nyquist frequency.

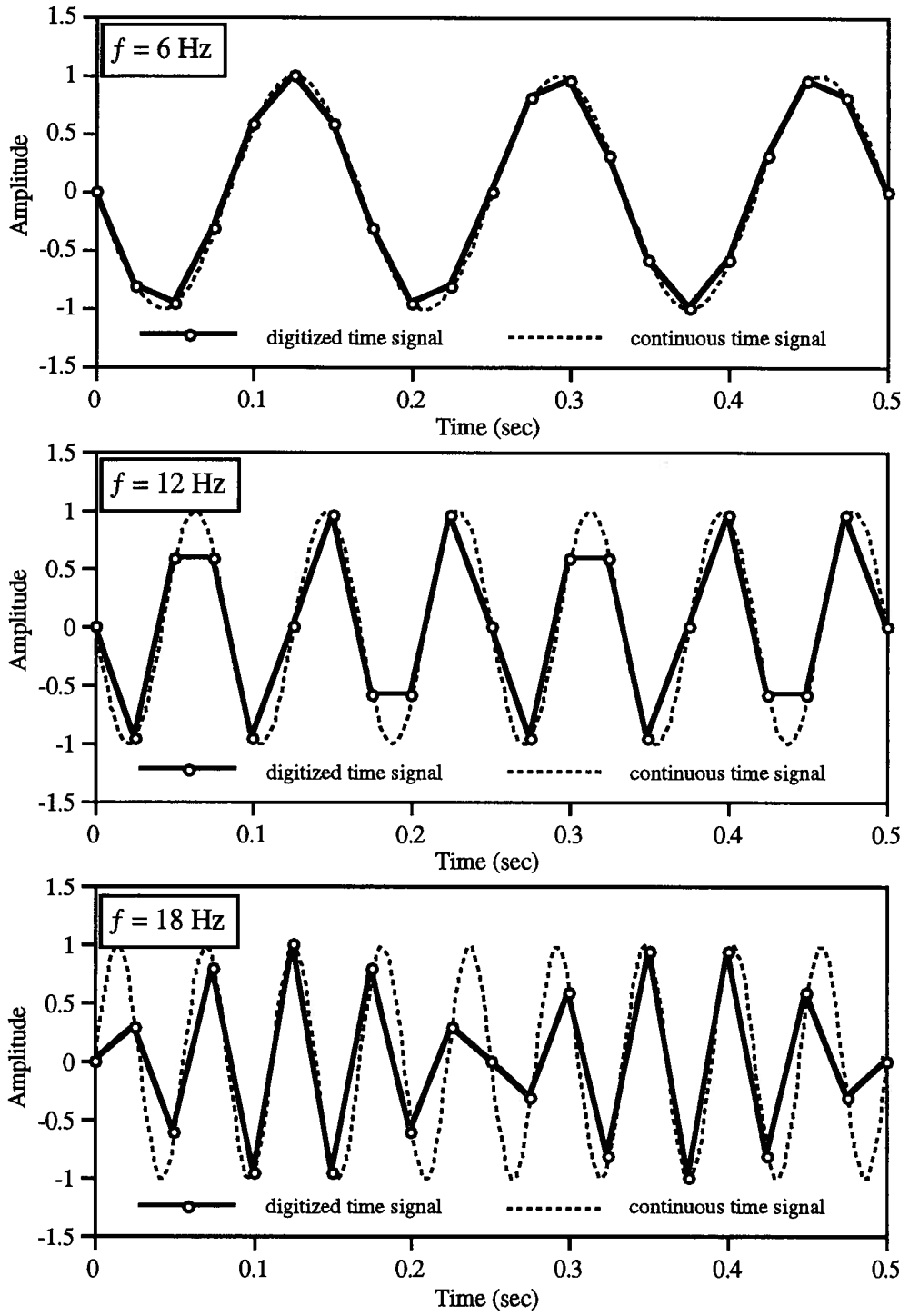

Figure 2.1. Digitized sine waves sampled at 40 Hz.

If the signal being measured contains a frequency component greater than the Nyquist frequency then, in the process of digitizing this signal, a false low-frequency waveform, called an *alias*, will be produced which differs from the true analog signal. The frequency of the alias can be

determined using Equation 2.16.

$$f_a = 2mf_c - f_t; \quad f_t > f_c, \quad m = 1,2,\ldots \textit{ such that } f_a < f_c \qquad (2.16)$$

where f_a is the alias frequency and f_t is the true frequency.

For example, if a sampling frequency of 40 Hz (f_c = 20 Hz) is used, and there is a frequency component of 22 Hz in the time signal, then the latter frequency will appear as an alias with a frequency of 18 Hz. Note that frequency components of 62 Hz and 102 Hz will also appear as an alias with a frequency of 18 Hz. An illustration of the aliasing effect is shown in Figure 2.2. This figure shows a sine wave with a frequency of 22 Hz along with its digitized representation (sampled at 40 Hz) and the resulting alias waveform.

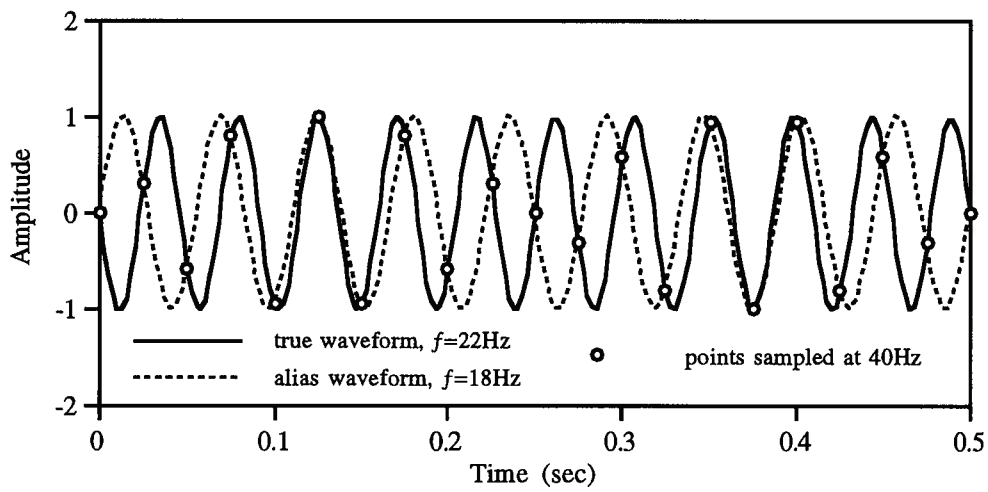

Figure 2.2. Sine wave with a frequency of 22 Hz and its digital representation (sampled at 40 Hz) and the resulting alias waveform.

To eliminate aliasing during the data acquisition process, low pass filters were used to screen out higher frequencies. In this study, data was acquired using a sampling rate of 40 Hz (f_c = 20 Hz) with a low pass filter of 12.5 Hz with the exception of some special measurements.

2.2.4.3 Leakage And Time Windows

The discrete Fourier transform (DFT), which is used to generate the signal processing functions described above, is only valid for periodic signals. In order to use the DFT, the time signals are

treated as periodic signals, with a period equal to its duration, T. However, the time signals are not periodic in general. Consequently, abrupt transitions (see Figure 2.3) between the end of the time signal and the beginning of the time signal can cause a leakage effect. This effect produces extraneous frequency components in the signal processing functions. These extraneous components may be incorrectly interpreted as belonging to the system being studied.

One method to suppress leakage is to multiply the discrete time signal by a time window which tapers the signal to allow a more gradual entrance and exit. This product is performed before the signal is transformed into the frequency domain.

Several time windows are available. However, one window which often produces very good results for analyzing ambient vibration data is the *Hanning window* (Dally, Riley, and McConnell, 1993). An expression for the Hanning window is given by Equation 2.17.

$$w_h(t) = \begin{cases} \frac{1}{2}\left(1 - \cos\frac{2\pi t}{T}\right) & 0 \le t \le T \\ 0 & otherwise \end{cases} \qquad (2.17)$$

An illustration of applying this window is shown in Figure 2.3. Figure 2.3b shows a discontinuous waveform which will cause leakage when it is transformed into the frequency domain. Figure 2.3c shows the same waveform after it has been multiplied by a Hanning window. Note that the Hanning window has transformed this waveform into a continuous signal. The Hanning window was used exclusively when processing the ambient vibration records.

2.3 CLOSING REMARKS

This chapter presented an overview of ambient vibration theory as well as signal processing functions which were used to analyze the ambient vibration records in this study. In addition, problems associated with digital data were addressed. Chapter 5 describes the method whereby dynamic characteristics of the building were determined using all of the functions just described. The next two chapters describe the building which was tested as well as the ambient vibration surveys.

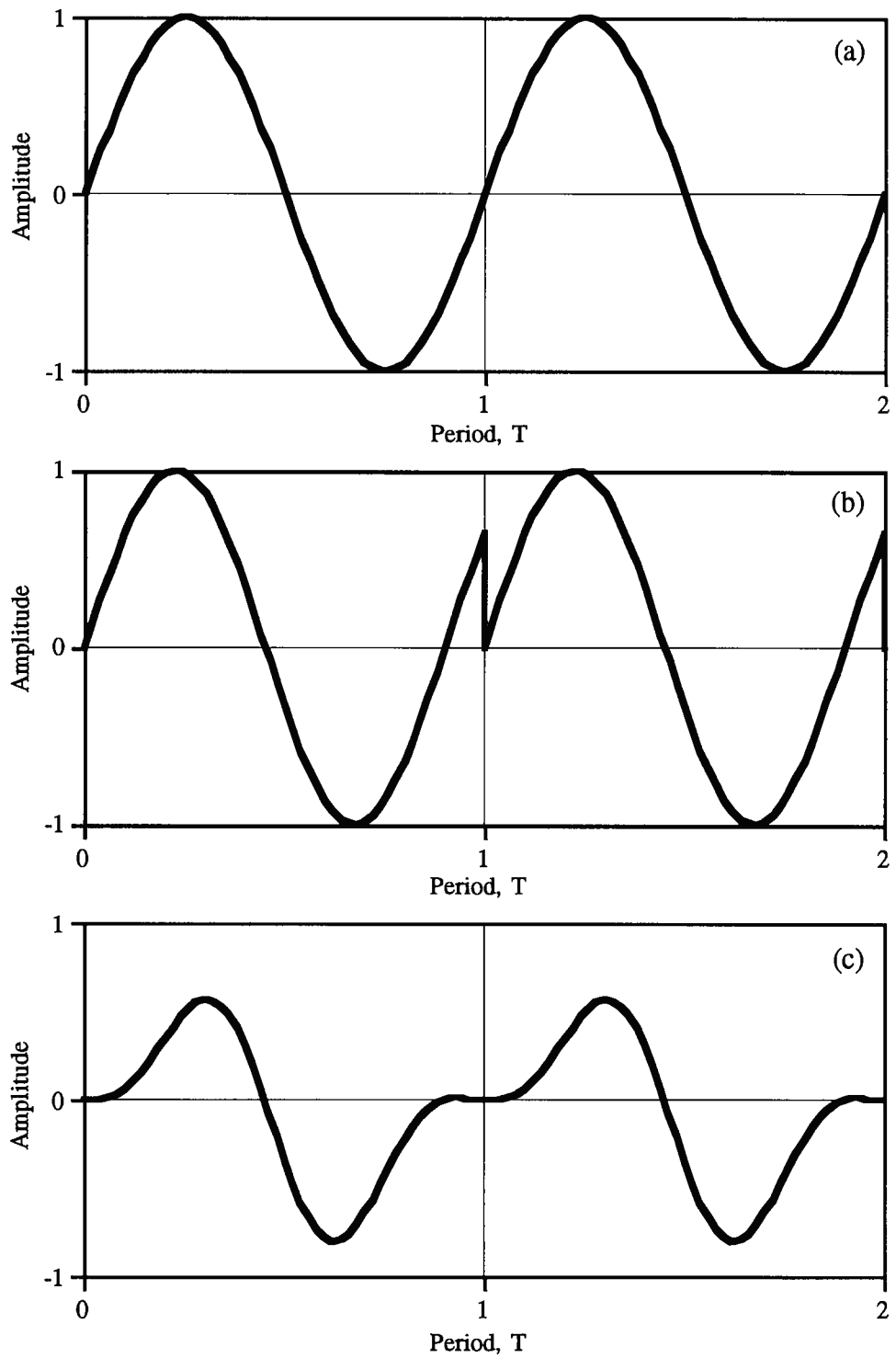

Figure 2.3. Plot of two sine waves. Plot (a) shows a sine wave which fits perfectly within the analysis window of period *T*. Plot (b) shows a sine wave which has a slope and magnitude discontinuity at its ends while plot (c) shows the same waveform after being multiplied by a Hanning window.

CHAPTER 3
DESCRIPTION OF BUILDING

This chapter describes the high-rise building which was studied. The first section (§3.1) contains a general description, while the second section (§3.2) contains a more detailed description of the structural system. The third section (§3.3) presents photographs of the building during the time that the ambient vibration measurements were made.

3.1 GENERAL DESCRIPTION OF CITY TOWER

3.1.1 OVERVIEW

The building under consideration is a thirty storey, high-rise residential tower located in downtown Vancouver (Figure 3.1). This building is representative of the type constructed in this region. On the east side of the tower is a two storey townhouse linked to the tower by two pedestrian bridges. On the north side of the tower is a terrace extending from the second floor. This terrace is monolithically linked to the tower via the floor slab. An underground parking garage, consisting of 6 staggered levels, is located beneath the tower and the townhouses. The building contains 136 residential units (including those in the townhouse), a weight room and party room opening onto the terrace, and also commercial space on the ground floor.

The building is 85 m (279 ft.) in height from ground level. The parking levels are located beneath ground level with a depth of 9.4 m (31 ft.). The first storey is 4 m (13 ft.) in height while the other storeys are 2.6 m (8.7 ft.) high. The residential floors on levels 3 through 10 are approximately 600 m^2 (6,000 ft^2) in area, reducing to about 500 m^2 (5,000 ft^2) on levels 11 through 25. The remaining upper level areas are reduced further. The parking levels are about 1100 m^2 (12,000 ft^2) each.

The building was designed by the architectural firm Baker McGarva Hart Inc. with structural consultants Bogdonov Pao Associates; both of Vancouver B.C. Construction of the tower began

in autumn 1992 and was completed in January 1994.

Figure 3.1. South-East Elevation of City Crest Tower.

3.1.2 STOREY REFERENCING CONVENTION

Some clarification is required regarding references (in this thesis) to the storeys and levels in this building. There are actually 31 storeys in this building including the mechanical penthouse. This corresponds to 32 levels from the ground floor to the roof. Ambient vibration tests at the building are referenced with respect to the number of levels which were completed at the building at the time the test was performed. For instance, *CT15* refers to the test which was

performed when 14 *storeys* or 15 *levels* of the building were completed.

3.2 STRUCTURAL SYSTEM

This building is a reinforced concrete structure consisting of irregular shaped flat plate slabs, a centrally located rectangular core, and several columns along the perimeter of each floor. The columns and core, in general, are continuous throughout the height of the tower. A typical floor plan of the building is shown in Figure 3.2.

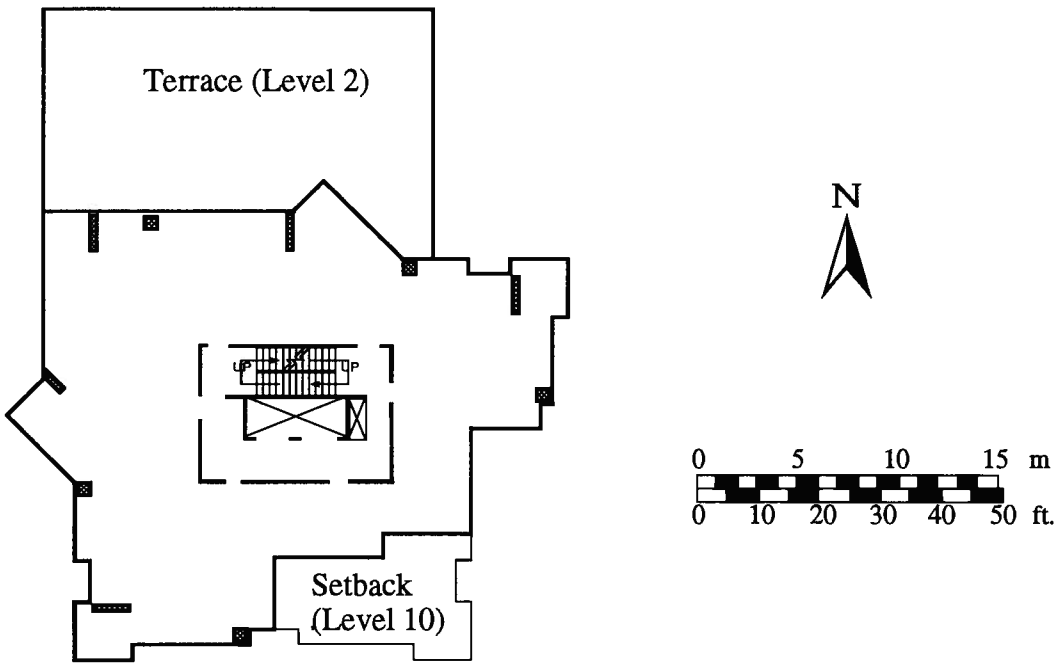

Figure 3.2. Typical floor plan of City Tower.

The core houses the corridor leading to the residential units, the elevator shaft and stair wells, as well as mechanical and electrical conduits. It is the primary lateral force resisting element of this structure. The core measures 10.3 m by 7.6 m (34 ft. by 25 ft.) in plan while the wall thickness varies from 450 mm (18") at the bottom gradually reducing to 350 mm (14") at the top floors. The core headers were designed as coupling beams with diagonal reinforcing for energy absorption (a typical detail is shown in Figure 3.3). The base of the core is designed to yield first forming a plastic hinge in this region.

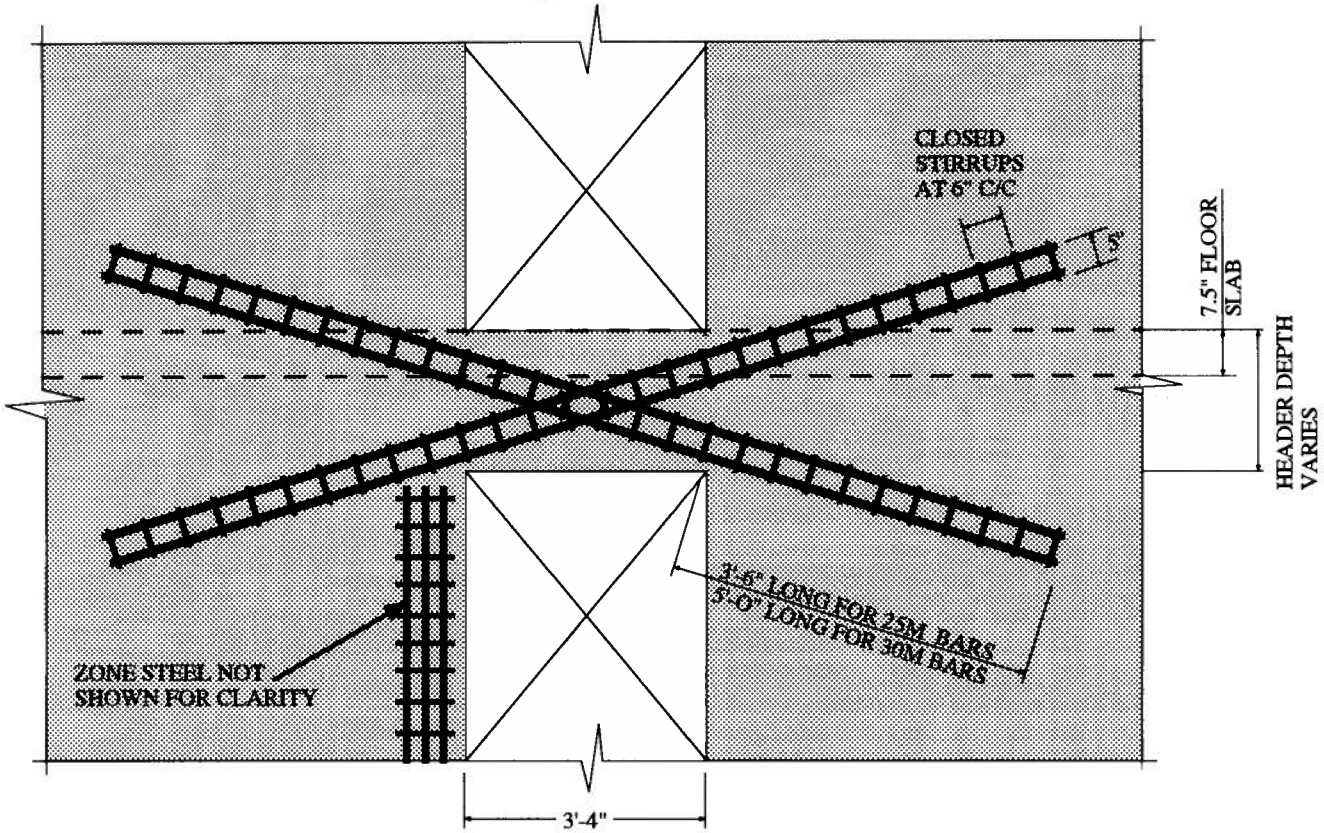

Figure 3.3. Typical detail of diagonal reinforcing in the core headers.

The floor slabs are 190 mm (7.5") thick, and about 28.3m by 24.7m (93 ft. by 81 ft.) in length. There is a major setback at the South-East (SE) corner of Level 10, as well as several minor setbacks at the top of the building above Level 25. These set backs can be seen in figure 3.1.

There are twelve columns along the perimeter of Levels 3 to 9. These consists of five 1.8 m by 0.3 m (6 ft. by 1 ft.) columns and seven 0.6m (2 ft.) square columns. The number of columns reduces to ten at Level 10 due to the setback. Above Level 10, the SE corner of the slab is supported by a wall projecting from the core. The primary function of the columns (and the wall at the SE corner) is to carry gravity loads. Specified concrete strengths for all of the building components are summarized in Table 3.1.

Table 3.1. Specified Concrete Strengths.
(Bogdonov Pao Associates Ltd., 1992, Drawing S-1)

Description		Strength
• footings and walls (excluding core)		25 MPa
• tower core	Levels P6 - 5	25 MPa
	Levels 6 - 32	30 MPa
• suspended slab & beams, retaining walls		30 MPa
• columns	Levels P6 - 4	25 MPa
	Levels 5 - 9	30 MPa
	Levels 10 - 19	35 MPa
	Levels 20 - 32	40 MPa
• surfaces subject to de-icing slats		35 MPa
• all other concrete		20 MPa
• reinforcing steel		grade 400

The foundation of this building is bearing on reasonably stiff glacial till (specified bearing capacity: 480 MPa). The footings consist of several pad footings for the core and columns, and a strip footing for the parking level retaining walls. The footing for the core is 3.1 m (7 ft.) thick with dimensions 16.2 m (53 ft.) by 12.8 m (42 ft.). The dimensions of the column footings vary between 2.4 m (8 ft.) square to 4.3 m square (14 ft.). The strip footing is 0.6m (2 ft.) in breadth. A schematic of the footings is shown in Figure 3.4.

The structure was designed in accordance with Vancouver Building By-Law 6134, CAN/CSA-S413-87 for parking structures, and the Canadian reinforced concrete design standard CSA CAN3-A23.3-M84. Specified gravity loads are summarized in Table 3.2. A dynamic analysis was also performed by the structural designers to estimate the fundamental periods of the structure as well as to understand the torsional behaviour resulting from the stepped floors.

Table 3.2. Specified Design Loads.
(Bogdonov Pao Associates Ltd., 1992, Drawing S-1)

Specified Design Loads		Live Load kPa (psf)	Dead Load kPa (psf)
roof	snow load based on ground snow load of	1.6 (34)	varies
	plus rain load of	0.3 (6.3)	-
A. parking slabs		2.4 (50)	-
B. firetruck access		12 (250)	varies
C. assembly areas and ground floor		4.8 (100)	varies
D. residential areas		1.9 (40)	1.0 (20)

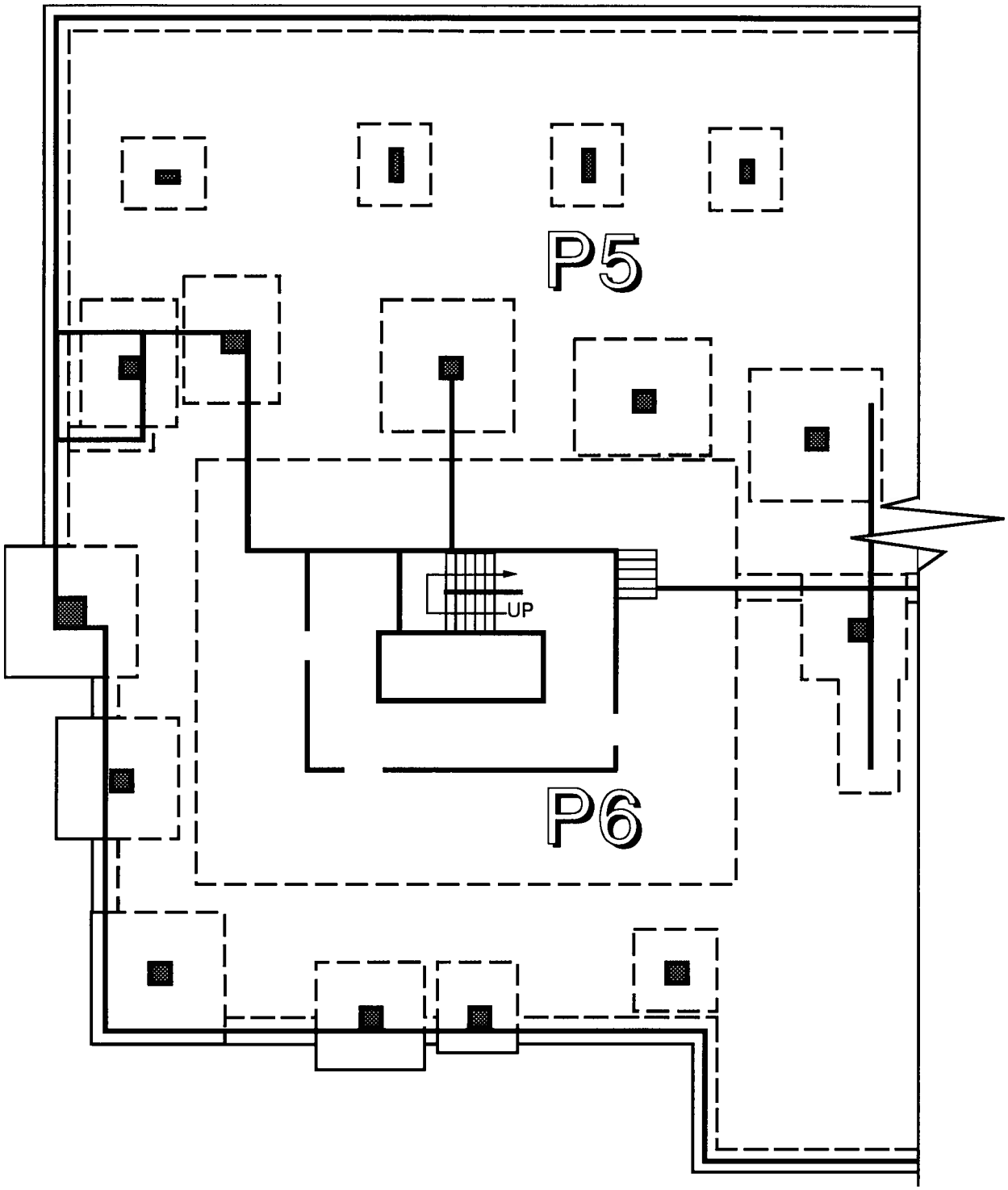

Figure 3.4. Schematic of footings supporting the building core, columns, and retaining walls. (Footings on the interior are shown with dotted lines).

3.3 THE TOWER DURING CONSTRUCTION

This section presents several photographs of the tower during construction. The first six figures (3.5 through 3.10) show an elevation view of the building at the six points in time when the ambient vibration measurements were taken[1]. Note that as the building's structure is assembled, architectural components are already being installed on the lower storeys. The remaining photographs show details of the building during construction. Figure 3.11 shows the shoring used to support the upper concrete floor slab as it was being poured and as it cured. This assemblage caused both floors to move as a rigid body in the experimental mode shapes. Figure 3.12 shows a portion of the platform projecting from the side of the building. This platform was used when lifting the cables used during the ambient vibration measurements. Also shown in this photograph is the lift located at the North-West (NW) corner of the building. In addition, the crane shaft, which typically pierced about 10 floors before reaching the top of the building, is shown on the right side of this photo. Figures 3.13 and 3.14 show a typical floor before and after the stud walls and additional components were installed.

3.4 CLOSING REMARKS

This chapter introduced the building which was the focus of this study. In the next chapter, the ambient vibration tests which were performed at this building are described.

---

[1]The photograph of the building when the structure was completed is an exception. The latter was taken about 6 weeks after the structure was finished, or about 4 weeks after the corresponding ambient vibration test.

Figure 3.5. City Tower following the completion of Level 10.

Figure 3.6. City Tower following the completion of Level 15.

Figure 3.7. City Tower following the completion of Level 20.

Figure 3.8. City Tower following the completion of Level 25.

Figure 3.9. City Tower following completion of the structure.

Figure 3.10. City Tower with all of the architectural components installed.

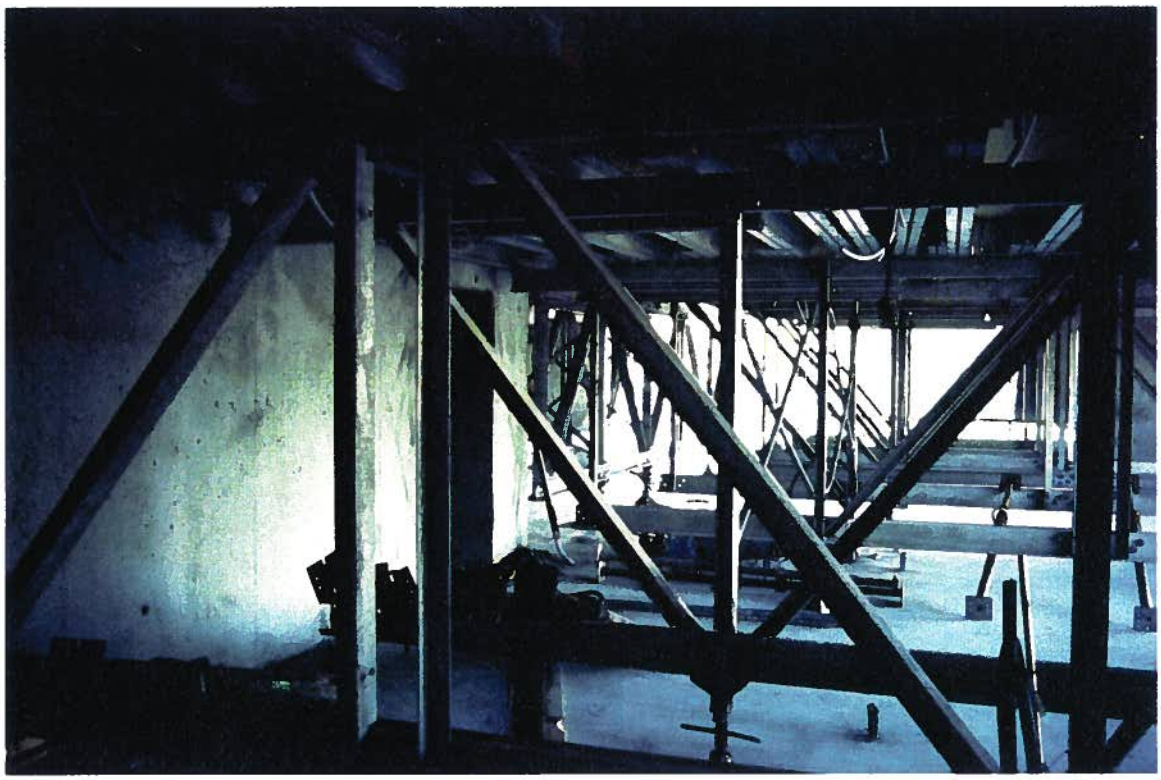

Figure 3.11. Detail of shoring which supports the level above it as the concrete is curing.

Figure 3.12. Platform used when pulling up cables to the top floor (left) and the crane tower which passes through the concrete floors (background right).

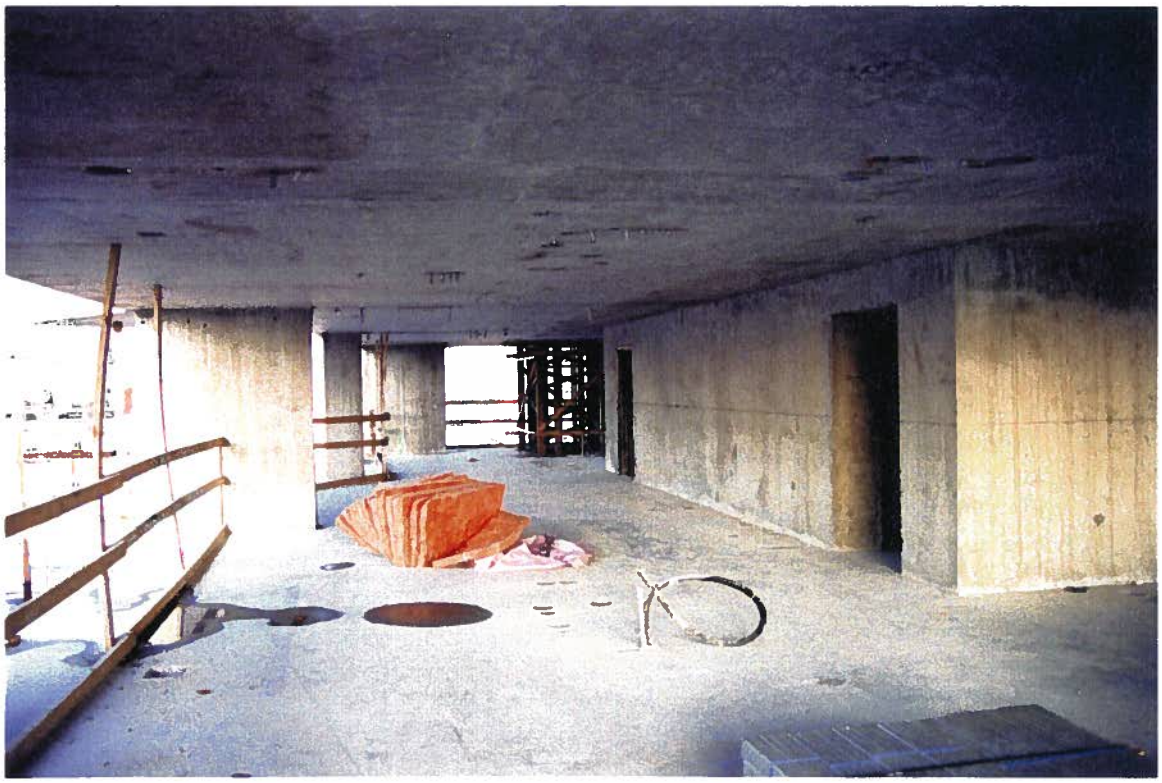

Figure 3.13. Typical floor before the installation of architectural components.

Figure 3.14. Typical floor with galvanized steel stud walls prior to the installation of drywall.

CHAPTER 4
AMBIENT VIBRATION TESTS

This chapter presents an overview of the ambient vibration tests. The first section (§4.1) deals with the data acquisition system which was used, and modifications which were made to it throughout this study. The next section (§4.2) lists the general testing objectives and the sensor locations. The following section (§4.3) contains a critique of each of the 6 tests which were performed at the building. The final section (§4.4) presents an error assessment of the collected data.

4.1 AMBIENT VIBRATION EQUIPMENT USED FOR THIS STUDY

4.1.1 THE HYBRID BRIDGE EVALUATION SYSTEM

During the course of his graduate studies towards a doctorate degree in Civil Engineering, Felber assembled and developed a data acquisition and analysis system that could be used for vibration measurements and system identification of bridge structures. This system was named the *Hybrid Bridge Evaluation System* (HBES). The aim of his research was to develop a system which could do this evaluation quickly and inexpensively.

The need for such a system arose from current economic trends. At present, existing bridges are being maintained and/or retrofitted for increased traffic demands as well as for strengthening them to withstand seismic loads. A retrofit process begins with an evaluation of the existing structure. Evaluations are usually based on an analytical model which is used to predict the behaviour and possible damage arising from a seismic event (or any other loading which needs to be considered). These models, in turn, are based on geometric properties obtained from old drawings as well as material properties obtained from core specimens at key locations in the structure. In addition, several assumptions need to be made about the soil on which the bridge supports rest as well as any interaction or composite action which occurs between separate spans or components of the bridge. Since this results in a certain amount of uncertainty, there is a need

to verify that these models are accurate. This would lead to increased confidence in the results derived from these analyses.

Modal properties of a bridge can be determined by measuring its vibrations when it is subjected to some form of excitement. One method of exciting the bridge is to use a forced input such as a sinusoidal force created by an eccentric mass shaker. This method has the advantage of exciting a single mode of the structure at a given frequency. In addition, good estimates of damping can be obtained from measuring the resulting vibrations. The disadvantages of this method is that it is expensive, and it is usually not convenient to shut down a bridge for an extended period to perform this type of test. An alternative to forced vibration measurements is to simply measure ambient vibrations. This has several advantages. First, these types of vibrations were provided by the traffic using the bridge as well as other sources. Second, the bridge did not need to be shut down to perform these tests. Finally, the measurements could be conducted at any time.

One problem with vibration measurements is the amount of time required to process the data. This activity could take anywhere from several weeks to several months to complete. Therefore, Felber also developed a software package, called ULTRA, which could be used for manual or automatic reduction of the ambient vibration records. In this way, data could be analyzed immediately in the field to check the quality of the data and also to obtain some preliminary results. In addition to this, measurements could be repeated or sensor arrangements modified if the measured data did not meet the test objectives. So instead of taking several months to process the data, the data was already processed and preliminary results obtained, the same day that the test was performed. Additional and more detailed analyses could be carried out later.

For a more detailed discussion of the development of this system, see Felber (1993).

4.1.2 ADAPTING THE HBES FOR BUILDING AMBIENT VIBRATION TESTS

The HBES had been used successfully to test the Colquitz River bridge near Victoria, B.C. as well as a wharf located in Squamish, B.C. Also, an ambient vibration survey of the

Queensborough bridge, located in New Westminster B.C., was already underway at the onset of the City Tower study.

Because of the success using this system, it was decided to use it to perform an ambient vibration survey of City Tower. Practically no modification to the HBES was necessary. However, as the tests progressed, several hardware and software components were added to the system to accommodate both the tests and subsequent analysis of the building's ambient vibrations.

With the addition of several new cables with lengths of 150 m (500') and 300 m (1000'), cable spools had to be constructed and wired so that they could be located away from the data acquisition equipment and connected to the system using a patch cable. It was also necessary to build stands to support these spools as the cable was being wound and unwound.

Several computer programs were also developed throughout this study. The first program was developed to plot the ambient vibration time histories so that they could be inspected prior to performing detailed analyses. This program, called HPPLOT, is discussed in §4.1.4 and in Appendix C. Revisions were also made to the data acquisition program, AVTEST, and an enhanced version of it, called AVDA, was developed. Details of these revisions appear in §4.1.3 and in Appendix B. Two other programs were developed for data analysis. One of these programs, named SLAVE, was used to enhance the three dimensional appearance of the mode shapes. The other program, called MAC, was used to perform a modal correlation analysis between analytical mode shapes and experimental mode shapes. The latter two programs are discussed in Chapter 5 and in Appendices D and E, respectively. All of these programs are intended to complement the existing software. To illustrate, a software hierarchy is shown in Figure 4.1. This figure shows which files serve as input files to the respective programs and which files serve as output files. The file types are designated by their extension while arrows denote input/output behaviour.

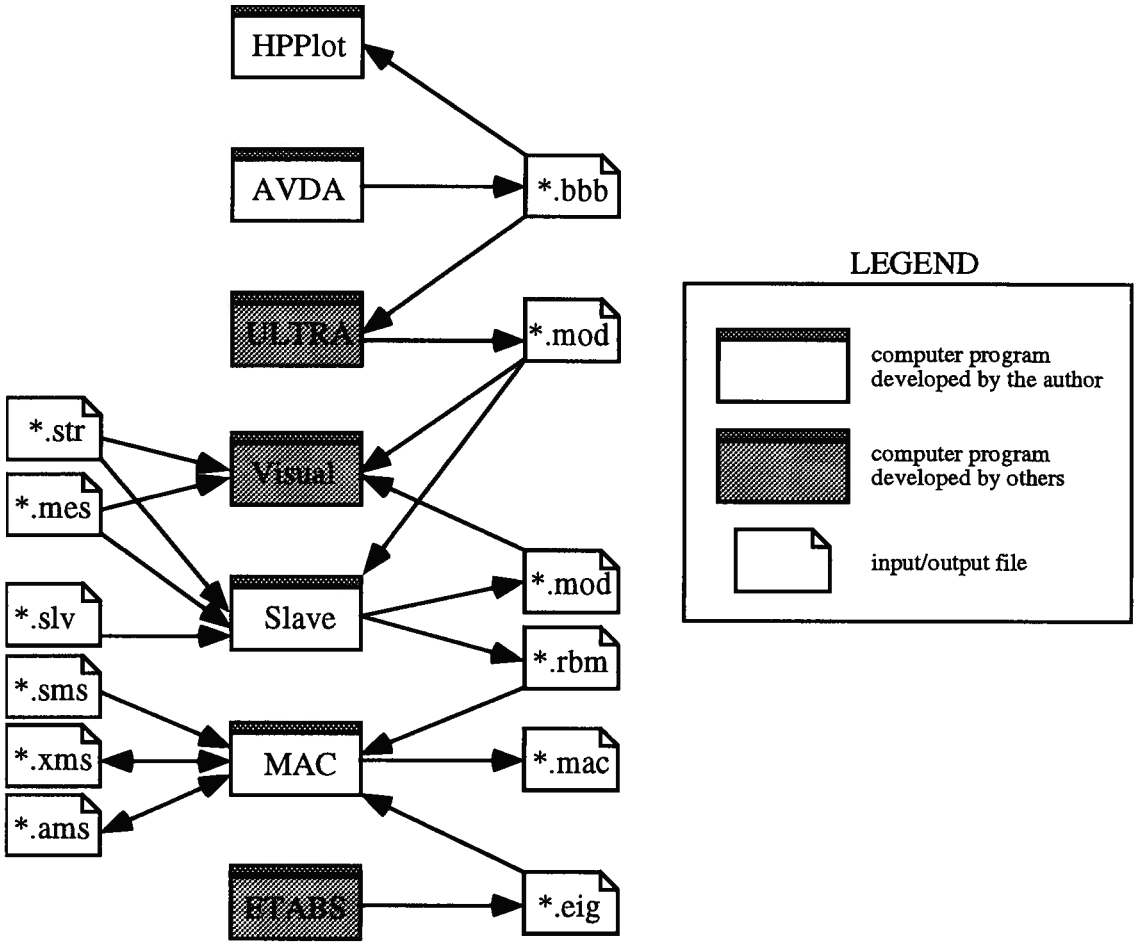

Figure 4.1. Software hierarchy for data acquisition and analysis.

4.1.3 MODIFICATIONS TO DATA ACQUISITION PROGRAM

Throughout this study, revisions were made to improve the data acquisition program named AVDA (formerly AVTEST). These modifications helped improve the quality of the recorded data and also increased the automation of the system. Details of these revisions, and operating instructions, can be found in Appendix B.

4.1.4 CHECKING TIME HISTORY RECORDS

Due to electrical anomalies, noise, and *forces unknown*, the ambient vibration time histories acquired with this system are occasionally susceptible to drift and contamination. In order to check for electronic drift, spikes, or shorts occurring in one or several channels, a program was developed which would plot the time histories of each channel, for each data segment, on the

same page. This allowed a comparison between all of the signals that had been recorded simultaneously. Two examples of signal drift and also signal contamination are shown in Figures 4.2 and 4.3, respectively. As can be seen in Figure 4.2, channels 5 and 7 show an excessive level of electronic drift while the other channels show normal vibrations of the structure. Also, channel 6 shows a slight offset from zero which could indicate that the sensor was not balanced correctly or that this instrument was tilted during the measurement. Figure 4.3 shows an example of signal contamination. Channels 3, 4, and 8 show an unidentified anomaly in the signals while the other channels show normal response. By inspecting the time histories in this manner, the user can decide which records need to be corrected, and which records are unreliable.

While this program was originally developed to check the quality data, it can also be used to inspect the vibration behaviour of the structure being tested. Figure 4.4 shows a set of records from one setup at City Tower. Channels 1 through 4 were located on the same floor; channels 1 and 2 are oriented in the North-South (NS) direction while channels 3 and 4 are oriented in the East-West (EW) direction. Since identical vibrations can be seen in these 4 channels, it follows that the building is vibrating in a torsional mode. In this case, these vibrations correspond to the fundamental torsional mode (f=1.504 Hz, T=0.665 s). Another example is shown in Figure 4.5 where translational motion was evident. In this figure, the sensor arrangement for the first four channels is identical to the arrangement described above. At 45-55 seconds into the measurement, the NS fundamental mode (f=1.543 Hz, T=0.648 s) was dominant in the records. This is indicated by the high amplitude, sinusoidal vibrations in channels 1 and 2 and low amplitude vibrations in channels 3 and 4. At 80-100 seconds into the measurement, the EW fundamental mode (f=1.875 Hz, T=0.533 s) becomes dominant. Vibration associated with this mode was detected in the same manner as the NS fundamental mode except that the high amplitude vibrations occur in channels 3 and 4 while low amplitude vibration occurs in channels 1 and 2. This type of behaviour confirms that fundamental modes usually dominate the response of a building structure. Operating instructions for this program can be found in Appendix C.

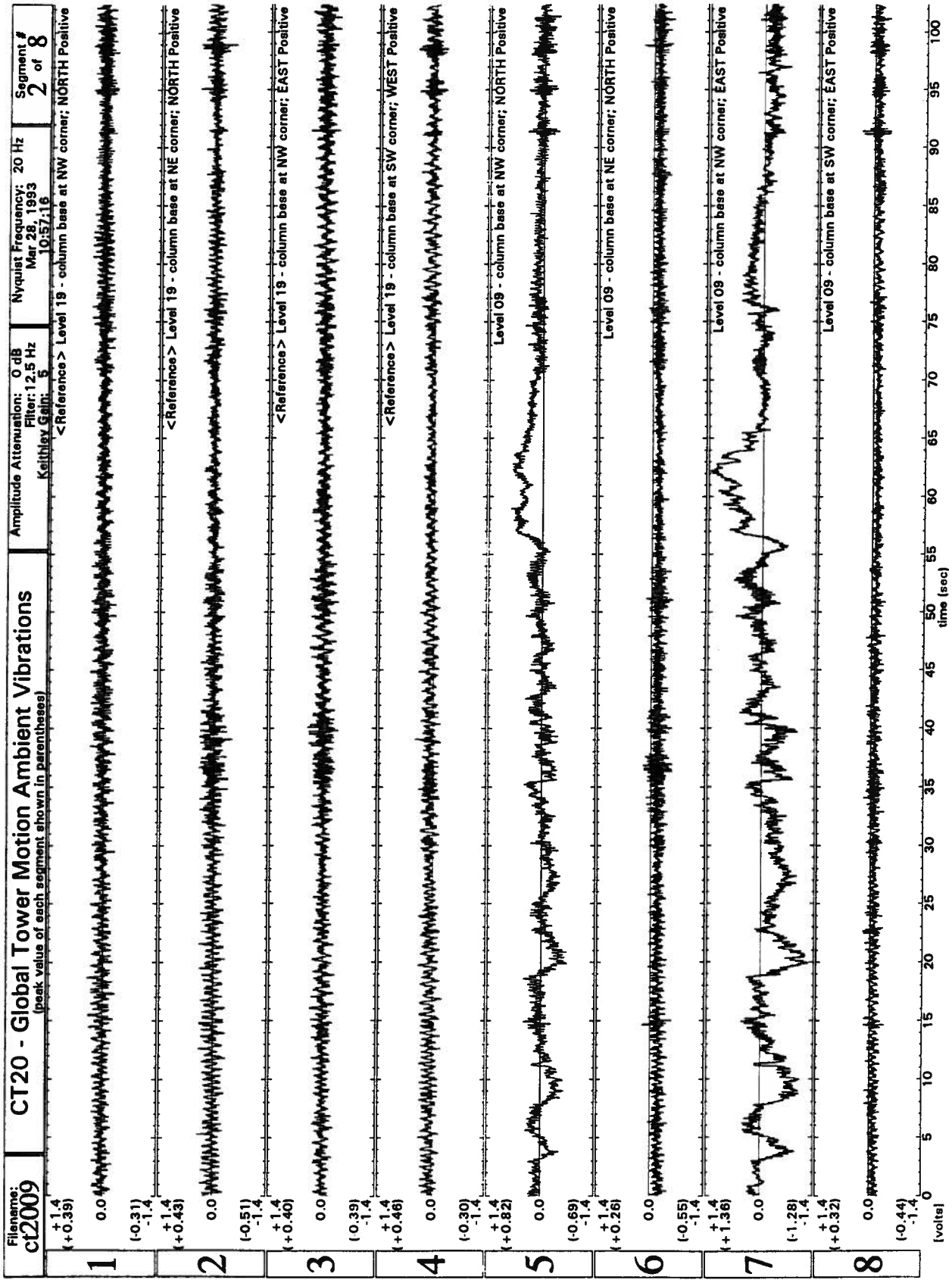

Figure 4.2. Ambient vibration time histories with signal drift in channels 5 and 7.

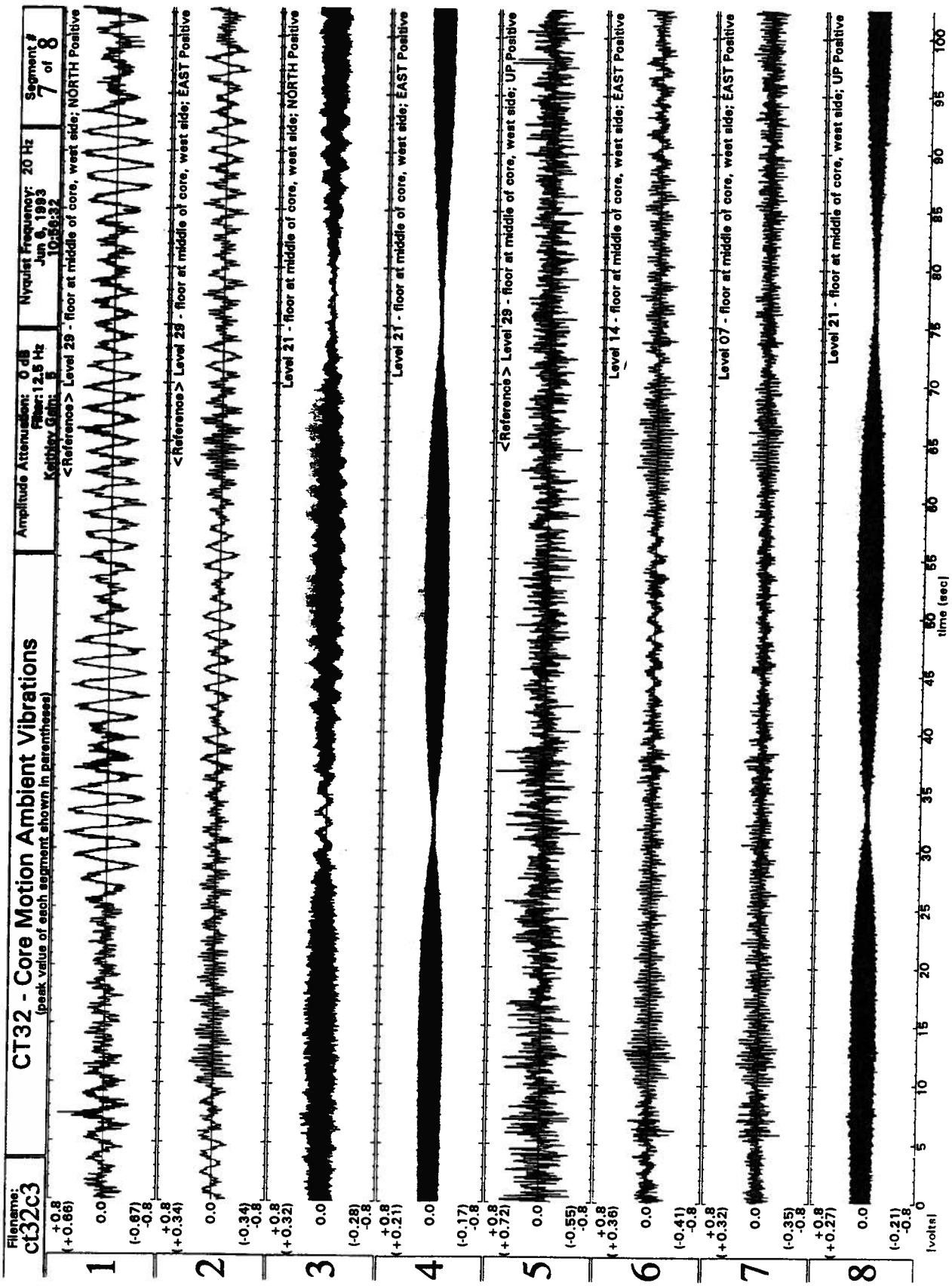

Figure 4.3. Ambient vibration time histories with signal contamination in channels 3, 4 and 8.

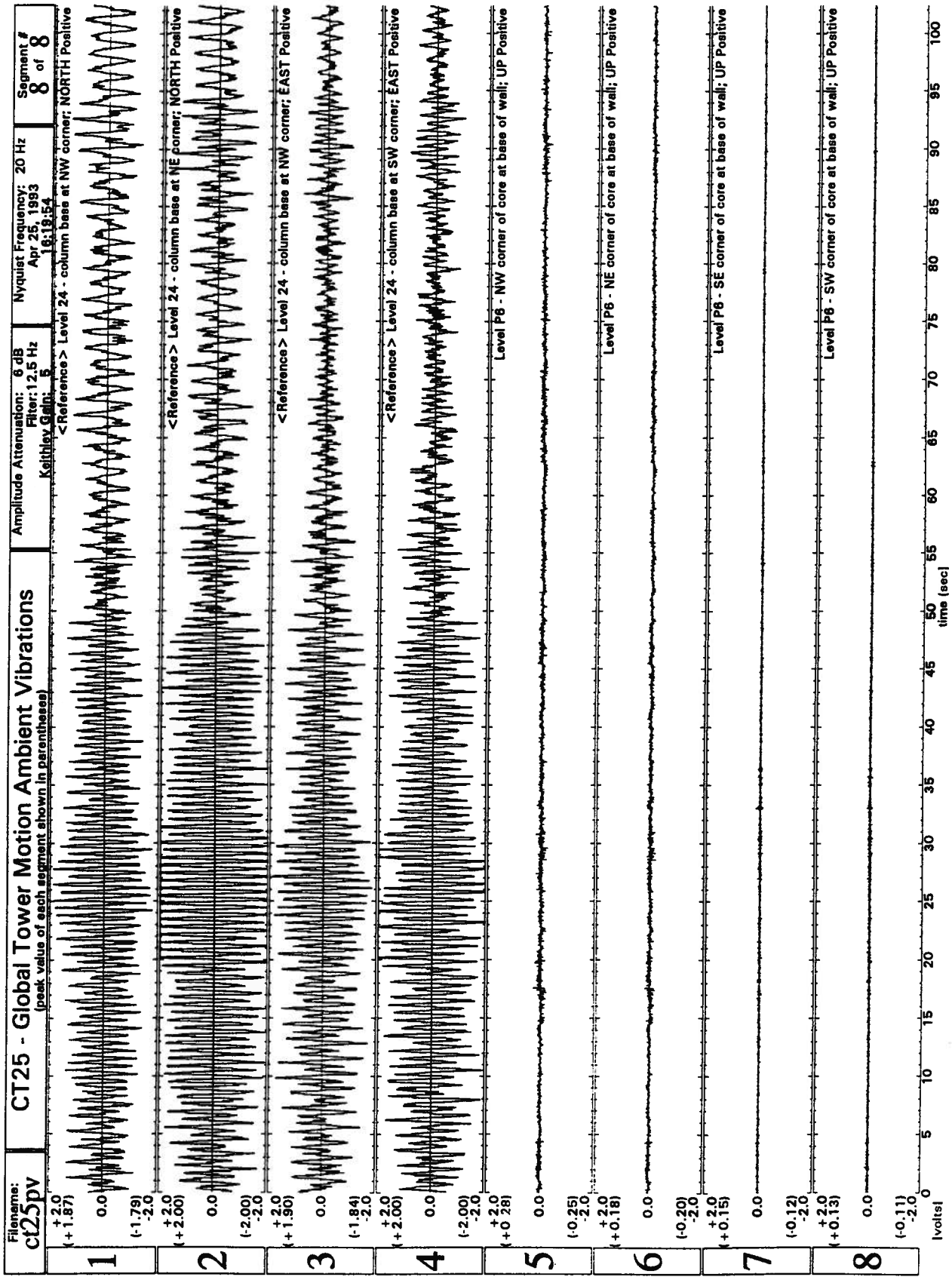

Figure 4.4. Ambient vibration time histories showing dominant torsional response.

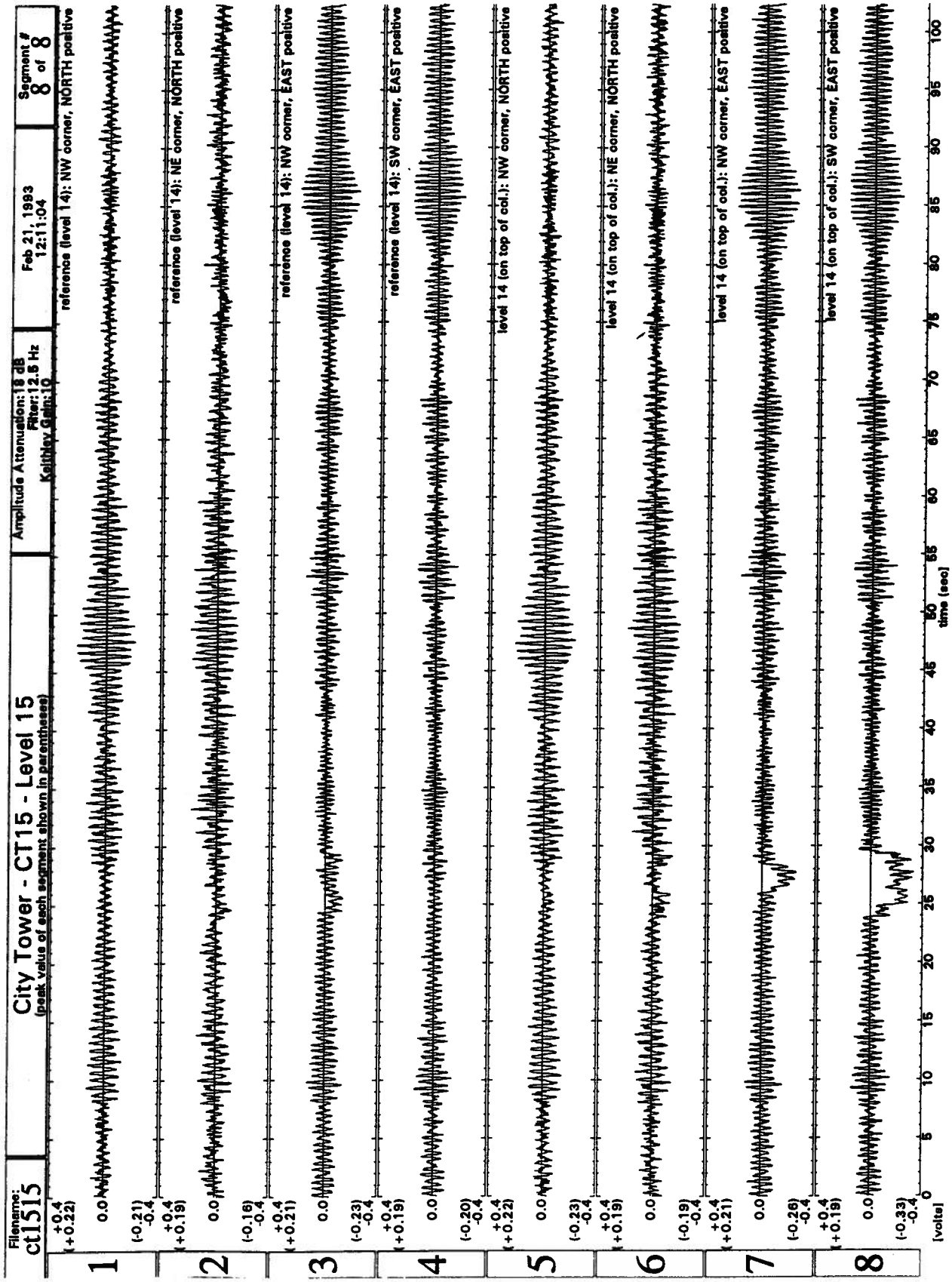

Figure 4.5. Ambient vibration time histories showing dominant translational response.

4.2 OVERALL OBJECTIVES AND TESTING PROCEDURES

4.2.1 GENERAL TEST OBJECTIVES

The primary objective of this study was to determine changes in dynamic characteristics of a high-rise building as construction progressed; based on ambient vibration measurements of the structure. The dynamic characteristics of interest were the vibration mode shapes along with the corresponding modal periods (frequencies). These modal properties are typically required in any type of dynamic analysis. Modal periods are an indication as to which modes will be excited by the dominant frequencies of the time-varying load under consideration, while the mode shapes indicate deformations of the structure which create stresses in its members.

There were some other objectives in addition to obtaining modal characteristics. The second objective was to assess foundation motion at ambient vibration levels. This was done by measuring the rocking motion of the base of the core[1] and also lateral motion at ground level and at the lowest parking levels (P5 and P6). The effect of architectural components on the building's vibration characteristics was also of interest. This was determined by making a comparison between the bare structure and the structure with all of the major architectural components installed. Comparisons were based on changes in periods, mode shapes and damping. Another objective was to measure vertical core motion in order to assess the nature of its deformation; i.e., shear or flexure.

4.2.2 DECIDING THE SENSOR LOCATIONS

With the exception of some special measurements (which will be discussed in §4.3), only lateral motion of each floor of the building was of interest. Moreover, only the *global* behaviour would be studied. Local vibrations of the columns or floors was not of interest.

---

[1]The core is resting on a 2.1 m (7 ft.) thick pad footing which is independent of the footings supporting the perimeter columns as well as the parking structure retaining walls

The location of the sensors were very important for a number of reasons. First, since this entire study was comparative in nature, it was decided that the sensors would be placed in the same location for each of the six tests. Also, because the sensors would be mounted using anchor bolts, it was desirable to choose a location where the bolts could remain in place until all of the tests were completed[2], and in a location which did not interfere too much with the construction process. Of course, the most important consideration was that the sensors should be placed in locations such that modal information could be extracted from the vibration records. Also, to maintain quality control, the same sensor layout for the *roving* sensors (i.e. sensors which were relocated from setup to setup) was used on each floor to minimize the chance of error when reconnecting the sensors to the cables after each move.

When deciding the sensor locations, two documents were consulted (A.S.C. S2, 1990; Rojahn and Matthiesen, 1977). Both of these documents provide guidelines for placing a limited number of sensors in a building structure. A review of California Strong Motion Instrumentation Program (CSMIP) documents which showed the sensor layout of several instrumented high-rise buildings in California, U.S.A. also proved helpful (CSMIP, 1989). With this information, the sensor layout shown in Figure 4.6 was chosen. In this figure, the arrows indicate the positive orientation of the accelerometer sensors. This sensor arrangement could be used quite effectively to isolate translational and torsional motion of each floor in both the North-South (NS) and East-West (EW) directions. Following the first test however, the location of the 4th sensor was changed to the NW corner in order to improve the appearance of the resulting mode shapes (see §4.3.3 for more information).

The location of the *reference* sensors (i.e. sensors which remain in the same location throughout the test) also had to be decided. As discussed in §2.1.4, the reference sensors must be situated wherever there are antinodes in the vibration modes of interest. The top floor of the building was

---

[2]several of these bolts had to be replaced from test to test since they were removed by workers whenever it interfered with their work.

chosen for this purpose where four sensors were positioned using the same layout as the roving sensors. This provided a redundant measurement in each of the two principal directions.

The sensor layouts will be discussed in more detail in §4.3. Specific details can also be found in Appendix A.

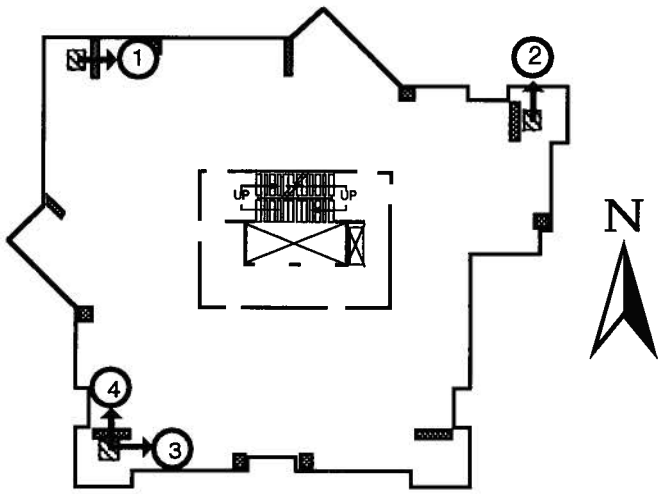

Figure 4.6 Typical sensor layout for the roving sensors used in the first building test.

4.2.3 TYPICAL TESTING PROCEDURE

Before the measurements could begin, the cable used to connect the sensors to the data acquisition equipment had to be laid out. Following this, the data acquisition station was set up while the *reference* sensors were installed and connected. While a preliminary measurement was taken to verify that the equipment was working correctly, the remaining four *roving* sensors were installed and connected. Following each measurement, the roving sensors were systematically located from floor to floor until the test was completed.

A schematic of the data acquisition system is shown in Figure 4.7. A photograph of the data acquisition equipment is shown in Figure 4.8. Acceleration measurements were obtained using 8 Kinemetrics force balanced accelerometers (model FBA-11). A typical sensor arrangement is shown in Figure 4.9. Several lengths of cable were available to connect the sensors to the signal conditioner. These cables included: 5-90m (300'), 2-150m (500'), and 4-300m (1000') as well as several shorter cables which served as *patch* cables for the longer cables. The signal

conditioner is a Kinemetrics model containing 8 cards (model AM-3I) which were used to filter and amplify the signals. Conditioned signals could be monitored on a 2 channel Zonic spectrum analyzer or digitized and stored on disk via a Keithley 575 analog-to-digital (A/D) converter. Two PC computers were also included in this setup. The data acquisition computer, a Compaq portable with an Intel 80286 processor, was dedicated to acquiring the ambient vibration records. In between measurements, the data files from the previous setup were transferred to the data analysis computer using a commercial software package called LapLink. This second computer was a PC with an Intel 80486DX processor. This arrangement allowed data to be collected on one computer while the second, and faster, computer could be used to process the data in-situ to check its quality as well as to perform some preliminary analyses. Once the data had been checked, the roving sensors could be relocated to the next floor and the next setup recorded.

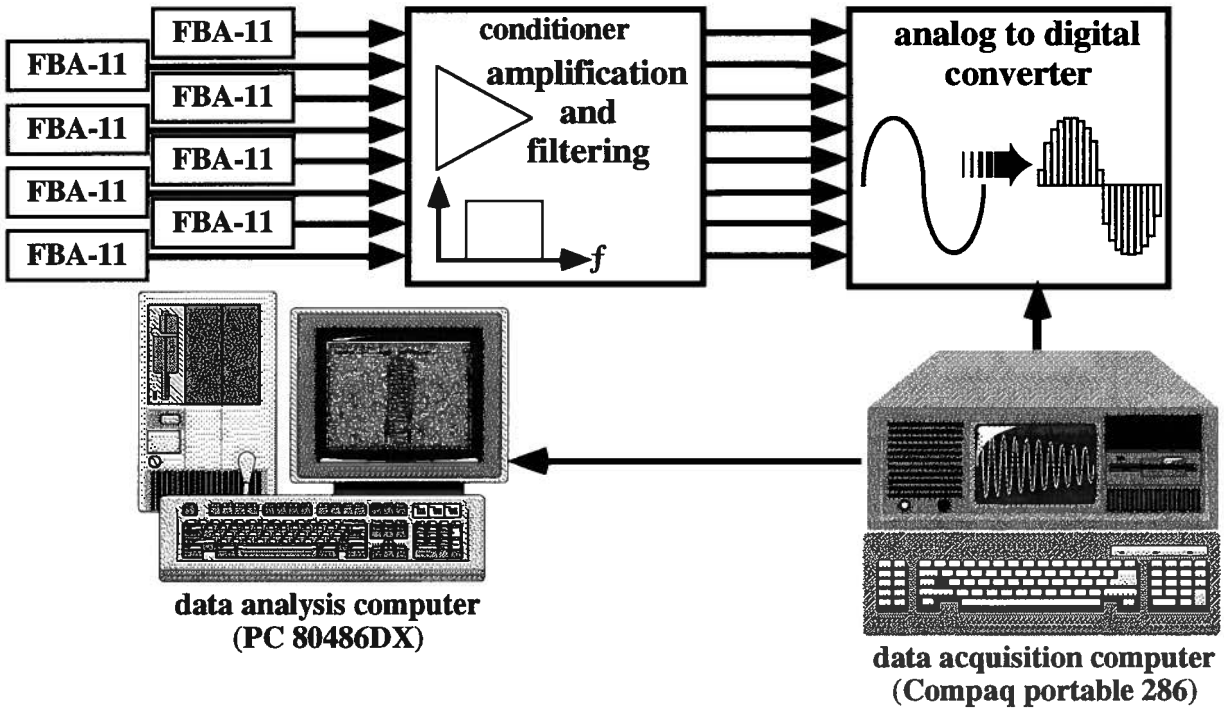

Figure 4.7. Schematic of the data acquisition equipment.

Figure 4.8. Data acquisition equipment (taken during the CT25 test).

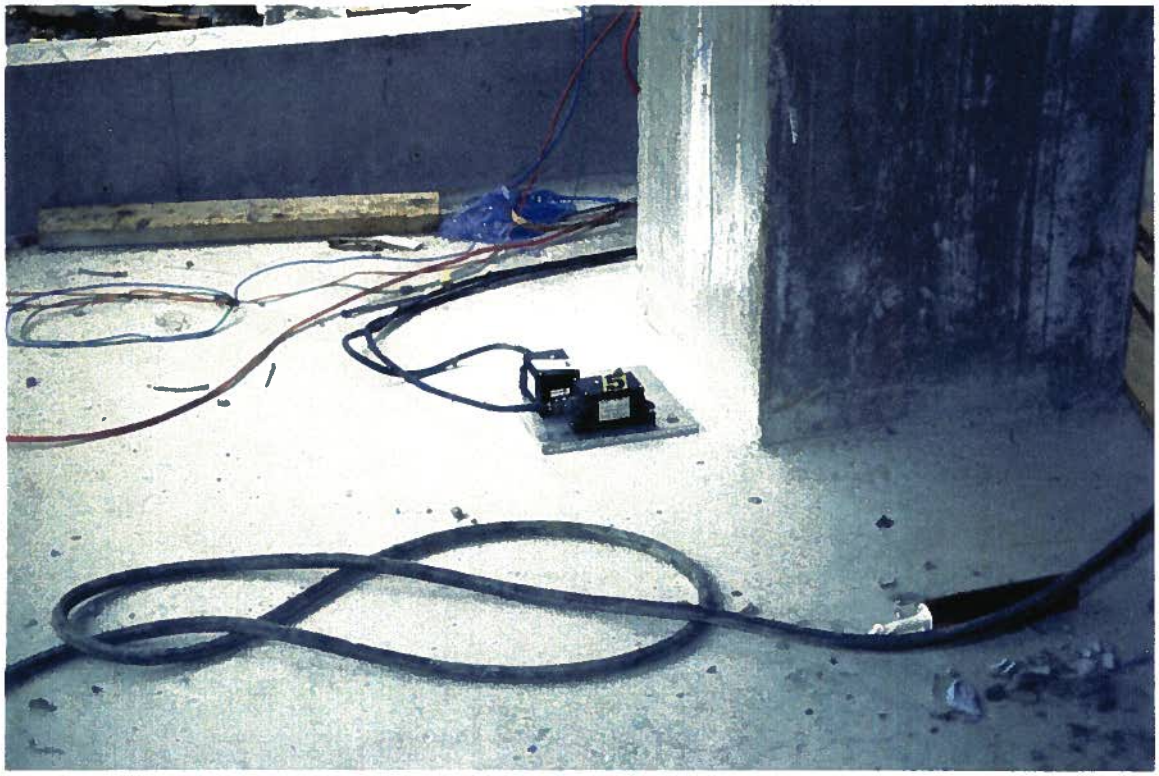

Figure 4.9. Two FBA-11 accelerometers in position during data acquisition.

4.3 SPECIFIC DETAILS OF THE CITY TOWER TESTS

4.3.1 OVERVIEW

Successful ambient vibration surveys require a great deal of planning. The schedule of the City Tower surveys was critical since tests were to be conducted following the completion of every 5 storeys. Therefore it was necessary to follow the contractor's progress very closely. At the onset of construction, each floor was completed in about 5 working days, but this rate was later accelerated to 4 working days. Once the required number of storeys were in place, measurements were taken during the following weekend.

The first step in the planning of every test was to visit the City Tower construction site. Two visits were made - one about 5 days before the test, and a second visit one day before the test. The purpose of the first visit was to inspect the building and the surrounding site in order to determine where to place the data acquisition equipment (hereafter referred to as the *station*), where and how the cables would be laid out, and identify any restrictions which would hamper the test. The purpose of the second visit was to obtain keys from the contractor in order to gain access to the site, and to install anchor bolts wherever the sensors would be located. The latter task helped speed up the test and also helped the crew when positioning the sensors.

A crew was necessary for these surveys to help with all of the physical work involved. The size of these crews varied from test to test and it was found that a 5 member crew worked best for the building surveys. The crew was typically made up of professors, graduate and undergraduate students, and engineers.

One of the most time consuming task of these surveys is unwinding and laying out the cables. Therefore, it is very important to plan this task so that it may be done as efficiently as possible. The location of the station is another consideration. Since walkie-talkies were used for communication, it was necessary to have a clear communication path between the station and the crew on the upper floors who were in charge of relocating the sensors from setup to setup.

The sensors were usually mounted on aluminum plates which were fastened to the concrete floor (or wall in some situations) using the anchor bolts. A different strategy for fastening these plates was necessary for the last test (CTTC) since ceramic tiles and carpet had been installed over the concrete floors. For the tiled surfaces, the plates were fastened using double sided carpet tape. This worked very well though it was sometimes difficult to remove the plate afterwards. Special plates were assembled for situation where the sensors needed to be positioned on a carpeted surface. Three 5mm (3/16") bolts were attached to these plates in order to act as *feet*. In this way, the weight of the plate was concentrated at the tips of these bolts which were in contact, as close as possible, to the building structure[3].

Measurements typically began at the top of the building. Roving sensors were systematically placed on the levels to be measured as the crew worked its way down the building. This order was reversed for the last test, CTTC, since cables had to be lowered from the top of the building rather than pulling them up from the ground.

The testing procedure changed and was improved from test to test. Highlights and methodology from the individual tests are discussed in the sections which follow.

4.3.2 CT10 - 10 LEVELS COMPLETED

4.3.2.1 Measurement Objectives

The objectives of this test were to obtain:

- lateral mode shapes and periods
- torsional mode shapes and periods
- assess effect of discontinuities
- assess rocking of foundation

---

[3]This method of fastening the sensors was tested prior to the test using a collocation measurement in order to ensure that reliable measurements could be made.

4.3.2.2 Setup

The first test of this study took place on Saturday, January 16, 1993. At this point in time, the 10th floor had just been cast a few days before. This floor was being supported by the floor below it (Level 9) with shoring and jack-posts while the concrete was curing.

The *station* was located on Level 9 for a number of reasons. First, since only 8 cables were available at this point in time (2-15m, 2-30m and 4-90m), the station had to be situated very close to the reference sensors so that they could be connected to the signal conditioner using the short cables. Also, since this floor was heated (for curing the concrete in the winter), it provided a comfortable location for conducting the measurements and data analyses.

The reference sensors were mounted on the side of the columns about 500mm (20") from the soffit of Level 10. The roving sensors were systematically placed on all floors; beginning with Level 9. The 90m cables used to connect to the roving sensors was passed through a hole in the concrete floor to Level 8 where they were unwound. From here, these cables were dropped between the stairways since it was open all the way to Level 1.

Specific sensor locations and signal conditioning information can be found in Appendix A.

4.3.2.3 Test Evaluation

Being the first test, it was perhaps the most difficult for a number of reasons. First, construction workers who were on site that day interfered with the test. Curious workers stopped by the station several times to see what was going on. Some other workers were curious enough to dismantle one of the accelerometers. Fortunately, the sensor was not damaged. In addition to this, a concrete *grinder* was being operated that day which may have banded the frequency range of the excitation. This is undesirable for an ambient study.

Another problem was the location of the station. Although the lift was available in the morning to transport all of our equipment to the 9th floor, it was not available at the end of the test.

Therefore *all of the equipment* had to be carried down 9 flights of stairs. Also, since there were two flights of stairs, the generator used to power the data acquisition equipment was accidentally left behind on one of the landings. It had to be retrieved the following morning.

As far as the test was concerned, it was found that Level 9 and 10 moved together as a consequence of the shoring which was supporting Level 10. Hence it was not necessary to instrument the top floor. Instead, positioning the reference sensors at the base of the columns on Level 9 would have sufficed.

In future tests, it was decided that the station would be situated at or near ground level. Also, the location of the reference sensors would be mounted on the floor one level below the level which had just been cast. Finally, the test would take place on a Sunday when there were no workers at the site.

4.3.3 CT15 - 15 LEVELS COMPLETED

4.3.3.1 Measurement Objectives

The objectives of this test were:

- obtain at least three vibration modes and frequencies in the three principal directions.
- position the sensors to provide improved mode shapes, and better measurement of base "rocking".

4.3.3.2 Setup

The second test of this study took place on Sunday, February 21, 1993. At this point in time, the 15th floor had just been cast 2 days before. This floor was being supported by the floor below it (Level 14) with shoring and jack-posts while the concrete was curing.

This test was performed in sequence with two tests at the Queensborough bridge. Hence, the station was located at ground level in a cube van which housed the station during the bridge tests. The addition of 2-150m (500') cables and 4-300m (1000') cables to the equipment made it feasible to install the reference sensors at the 14th level.

The sensor layout was similar to the previous test with the following changes. First, the FBA located at the south-west (SW) corner, which was oriented in the NS direction, was relocated to the north-west (NW) corner. This was done to improve the definition of the vibration mode shapes. Second, in order to enhance the base-motion analysis, two of the reference sensors were relocated to the building core for two of the setups. In addition, sensor #6 was moved to inside the core on Level P6 and oriented vertically to improve the observed motion of the core rocking. Finally, due to time constraints, only every other floor was measured during this test.

As with the previous test, cables were passed through the opening between the stairways. Some of the other cable, as an experiment, was pulled up to the 14th floor from the outside of the building. The test proceeded as before. Measurements were made starting at the underground parking level, and then progressively on every second floor beginning with Level 15.

Specific sensor locations and signal conditioning information can be found in Appendix A.

4.3.3.3 Test Evaluation

The biggest criticism of this test was that the cables got severely tangled as they were brought down from the 14th floor. In addition to this, the 150 m cables had to be completely unwound and laid out in the alley neighbouring the building site. In contrast, the cable which had been pulled up to the upper floors from the *outside* of the building was collected very easily and efficiently.

As far as the test was concerned, Level 14 proved to be a good location for the reference sensors. In addition, Level 14 and Level 15 moved together. It was found that the sensors which were relocated to the building core for two of the setups did not enhance the base motion analysis. Therefore, this procedure was not used again. The quality of the signals appeared to be better than those of the previous test. It is believed that this can be attributed to a better location of the reference sensors, and the absence of construction activity during the measurements.

This test introduced several refinements which would be used in the tests which followed. First,

the reference sensors would be positioned on the level just below the floor which had just been poured as they were in this test. Further, it was clear that the two floors at the top of the building moved together, and therefore the motion of the highest floor was not measured in subsequent tests. Second, Sunday proved to be a good day to conduct these tests since all construction at the site had ceased. Third, the cables would be pulled up from the outside of the building (as opposed to the inside) in future tests. In addition, *male* plugs would be added to the 150m cables so that they did not need to be unwound completely in order to use them[4].

4.3.4 CT20 - 20 LEVELS COMPLETED

4.3.4.1 Measurement Objectives

The objectives of this test were:

- obtain at least three vibration modes and frequencies in the three principal directions.
- perform man-excited vibration measurements
- high-frequency vertical measurement (for soil-structure interaction analysis)

4.3.4.2 Setup

The third test of this study took place on Sunday, March 28, 1993. At this point in time, the 20th floor and the core walls above this level were in place. Level 20 was still being supported from the 19th level with shoring.

In this test, the reference sensors were located on Level 19. Roving sensors were positioned on every other floor beginning with Level 17. The station was located in one of the finished rooms at ground level. Two platforms which projected out from the side of the building, one on the north side of the building and one on the south side, facilitated pulling the cable up from the ground. The cable spools were positioned at ground level. Thus, as the cable was lowered from floor to floor throughout the day, the slack could be wound up. By the time the cable reached the ground, it was all wound up and could be placed back onto the truck since it was no longer

---

[4]This type of connection had already been implemented in two of the four 300 m cables at that time.

needed.

Man excited tests of the building were also performed. The building was excited by two crew members, located on the top floor, who were rocking back and forth with the same period as the building's NS fundamental period (1.07 s). A sample of the building's response is shown in Figure 4.10. In this figure, channels 1 and 2 show the response of the structure due to the man excitement while channels 3 and 4 show normal ambient vibrations. As can be seen, the crew members were able to amplify the motion of the structure 5 times above ambient levels. Also note the *beating* effect caused by a slight difference between the building's period and the period of the excitation.

The sensor layout was similar to the previous test with the following changes. First, reference sensor #4 was accidentally oriented in the opposite direction. In addition to this, the reference sensors remained in the same location for the entire test (unlike CT15 where two of them were relocated to inside the core).

Specific sensor locations and signal conditioning information can be found in Appendix A.

4.3.4.3 Test Evaluation

This test went very well. The only problems encountered had to do with drift and shorts in some of the signals. It was later found that this may have been caused by one of the crew members disturbing the connection between a patch cable and one of the 300 m cable spools.

In future tests, it was decided to follow the same procedure as this test since it worked very well. Also, any contact with the cable during the measurements was avoided in order to prevent shorts in the signals.

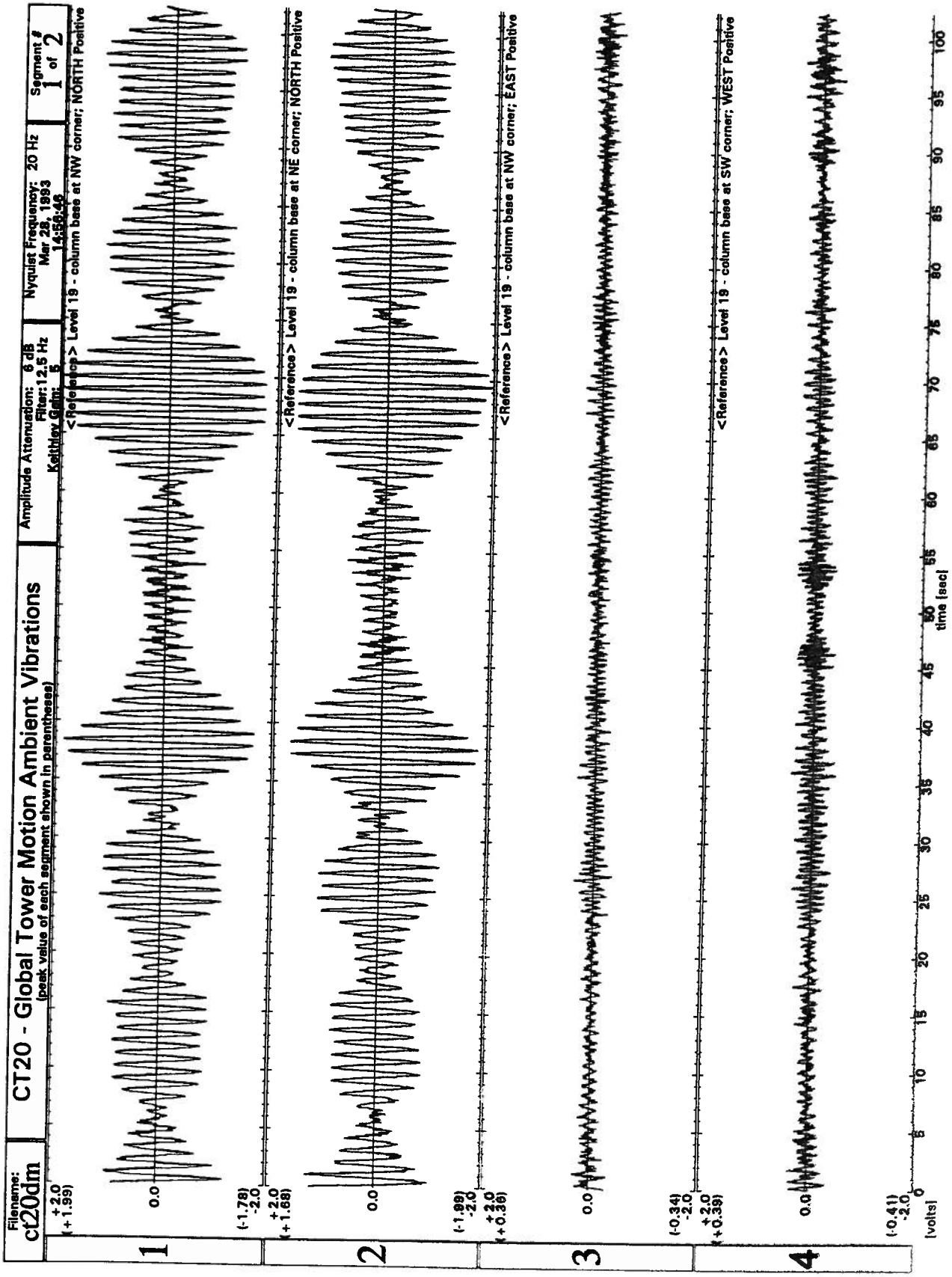

Figure 4.10. Building response during man excited test in the NS direction.

4.3.5 CT25 - 25 LEVELS COMPLETED

4.3.5.1 Measurement Objectives

The objectives of this test were:

- obtain at least four vibration modes and frequencies in the three principal directions.
- high-frequency vertical measurement (for soil-structure interaction analysis)

4.3.5.2 Setup

The fourth test of this study took place on Sunday, April 25, 1993. At this point in time, the 25th floor and the core walls above this level were in place. Level 25 was still being supported from the 24th level with shoring.

The sensor layout was similar to the previous test except that sensor #4 was oriented in the east direction as it should have been in the previous test. The station was located on the second floor.

Specific sensor locations and signal conditioning information can be found in Appendix A.

4.3.5.3 Test Evaluation

This was perhaps the best test. Everything went smoothly. The only problems encountered had to do with shorts in some of the signals. In addition to this, most of the signals recorded from sensor #4 appeared to be contaminated. However, since this was a redundant reference sensor, it was not a concern.

It was decided that the procedure followed in this test was excellent and should be used in the following test.

4.3.6 CT32 - 32 LEVELS COMPLETED

4.3.6.1 Measurement Objectives

The objectives of this test were:

- obtain at least four vibration modes and frequencies in the three principal directions.
- sensor collocation measurement
- measure core deformation
- diaphragm motion of a typical floor

4.3.6.2 Setup

The fifth test of this study took place during the weekend of June 5-6, 1993. At this point in time, the entire structure had been completed. Level 32 had been cast about 2 weeks before.

The sensor layout and procedure was the same as the previous test with some additional setups. The motion of the crane was measured since at the time it was believed that it was interacting with the building. A special measurement was also conducted on Level 27 in order to estimate damping. Some additional sensor setups were planned. However, as will be discussed shortly, the data collected from these setups was unreliable.

Specific sensor locations and signal conditioning information can be found in Appendix A.

4.3.6.3 Test Evaluation

This test did not run as smoothly as the previous test but was nevertheless done well. The quality of the data collected on the first day of the test was good with the exception of some drift and contamination in some of the channels. The quality of the data collected on the second day, though, was poor. The majority of the signals were contaminated by an unknown source (see Figure 4.3). This contamination may have been caused by a high voltage power cable which ran up to the crane from the second floor where the station was located. Consequently, all of the measurements made on this day were considered unreliable.

4.3.7 CTTC - TOWER COMPLETED

4.3.7.1 Measurement Objectives

The measurements collected during the final test were made primarily to assess the contribution of non-structural elements to the dynamic behaviour of the building. Specific objectives were as follows:

- Determine frequencies of the finished building and acquire sufficient data to assemble partial vibration mode shapes to properly categorize these frequencies.
- Estimate damping for the first two vibration modes in each principle direction.
- Take vertical measurements around the perimeter of the building core in order to determine how the core is deforming (shear and/or flexure)[5]. As a bonus, axial modes of vibration may also be determined using these measurements.
- Take two measurements of a representative setup, one at 40 Hz, and the other at 80 Hz to determine if any aliases are being created in the 0-20 Hz range.
- Take a collocation measurement to assess the signal variance between *reference* and *roving* sensors.

The analytical result for the last two objectives are discussed in §4.4.

4.3.7.2 Sensor Locations and Setup

The final test of this study took place on Wednesday, October 27, 1993. At this point in time, all of the major architectural components had been installed. Suites up to the 25th floor had been finished while the floors above it were currently being finished.

Several factors influenced the location of the sensors. First, based on the analysis of the past 5 tests, it was concluded that only 2 orthogonal reference sensors (located at the top of the building) were required to generate the mode shapes instead of 4. Second, due to increased confidence in the program named SLAVE (see Chapter 5) , it was decided that only 3 lateral

---

[5]This measurement was attempted during the second day of the previous test (CT32), but as discussed, the majority of the data collected on that day was contaminated by an unknown source rendering it unreliable. Therefore, this is a second attempt to gather this information.

measurements were required on each floor; one in the north direction (NS) and two in the east direction (EW). The remaining 3 sensors were available to simultaneously take vertical measurement of the core. This arrangement of sensors (2 lateral reference, 3 lateral/floor, 3 vertical at core) was preferred since the same setup would be used on each floor thereby minimizing the chance of error. Also, to accommodate workers on Level 29, the reference sensors were placed on Level 30; not Level 29 as originally planned.

Based on the results from the last test, excellent spectra which contained *spikes* from each vibration mode of interest could be obtained on Level 17 and Level 19. It was also desirable to obtain mode shapes to verify that these spikes were genuine. There were also implementation constraints since the majority of the building was closed off and since the elevator was only operating during week days. Given these requirements, it was decided to set up the data acquisition equipment on Level 29. Cables could then be lowered from Level 28 to the sensors located on the floors below. It was decided to only instrument half of the building; beginning with Level 17 (to generate spectra for comparisons) and then every third floor above this level (to generate mode shapes). This was done to reduce the time required to conduct the test, and because only the top portion of the mode shape was necessary for the purpose of identification (based on results from CT32).

For the measurements used to estimate damping, the same sensor arrangement as CT32 was used, except that reference sensors 1, 3, and 4 had to be located on Level 30 to accommodate the workers on Level 29.

The collocation measurement simply involved placing all the sensors on a single plate (in the same direction and orientation) and then taking a measurement as usual. It was expected that each sensor should record the same signal.

Specific sensor locations and signal conditioning information can be found in Appendix A.

4.3.7.3 Test Evaluation

While this test only had about half of the setups as the previous tests, a great deal of information was obtained. The procedure and sensor layout was optimal and proved to be very effective in generating the required dynamic characteristics of the building. Indeed, this setup is recommended in future studies of buildings with a similar configuration.

4.4 ERROR ANALYSIS

A scientific study is incomplete without some mention of error. One source of error results in the digitization process whereby aliasing is introduced. To check for this, two measurements were taken using the same sensor setup at different sampling rates. Another source of error is caused by different sensitivities in the sensors. To quantify this, a collocation measurements was taken whereby all the sensors were aligned in the same direction and orientation. Finally, bias and random errors are also introduced in the signal processing functions. These three sources of errors are discussed in the following sections. The measurements associated with aliasing and sensor sensitivities were made during the last ambient vibration test, CTTC.

4.4.1 ALIAS CHECK

Based on the results from the CT32 test, Level 17 proved to be a good location to conduct this measurement since contributions from all the modes of interest appear in spectra generated at this level. Two measurements were made using the *standard* setup (see Figure A.7s) - one using a sampling rate of 40 Hz and the second using a sampling rate of 80 Hz[6]. For comparison, the portion of the spectra ranging from 0 - 20 Hz were plotted together. The portion of the spectra ranging from 20 - 40 Hz for the data sampled at 80 Hz was plotted in reverse order (i.e. from 40 - 20 Hz from left to right). Plotting the data in this manner allowed coincidental spikes to be easily found. According to these plots, there did not appear to be any folded frequencies for the lateral signals (see Figures F.1 through F.5). The vertical signals, however, show a significant

[6]Note that these sampling rates correspond to Nyquist frequencies of 20 Hz and 40 Hz respectively.

spike around 21.5 Hz with a corresponding alias at 18.5 Hz (see Figures F.6 through F.8). There are also two other significant spikes around 37 Hz - one of which coincides with the spike associated with the second torsional mode. However, it is unlikely that the spike around 3 Hz is an alias since it has already been shown to correspond to the second torsional mode, and since the spikes at 37 Hz is much higher than the low-pass filter used (25 Hz[7]). In any event, these aliases do not affect the frequencies determined throughout the analysis, and therefore these frequencies were considered to be genuine.

4.4.2 COLLOCATION MEASUREMENT

Since the basis of the vibration mode shapes (determined in this analysis) is a *transfer function* between a given signal and a reference signal, it is important that all of the sensors respond in a similar manner. In order to check this a *collocation* measurement was conducted. Thus the sensors should be measuring the same motion. Coherence functions (CF), Phase functions (PF), and Frequency Response functions (FRF) were generated for the roving sensors (Number 3, 4, 5, 6, 7, and 8) relative to the reference sensors (Number 1 and 2) (figures appear in Appendix F).

The Coherence functions (Figures F.9 and F.10) showed an overall value of unity except for a drop off below 0.5 Hz. The only other exceptions were sensors 5 and 6 which showed an anomaly between 2 to 3 Hz. However, these anomalies correspond to a *valley* in the PSD functions and is therefore of no concern. Also, since the lowest mode is at 0.55 Hz, the drop off is also of no consequence.

The Phase functions (Figures F.13 and F.14) showed an overall variance of roughly ±3°. In a similar manner to the CF, there is a *jump* just below 0.5 Hz as well as an anomaly with sensors 5 and 6 in the same frequency region as before (2 to 3 Hz). Sensor #4 shows a significant drift up to ±10°. In any event, a phase cut-off of 20° was used when generating the PMR functions, and therefore these phase variances are within tolerance.

---

[7]In retrospect, a low-pass filter of 12.5 Hz should have been used as was used for the measurement sampled at 40 Hz.

Finally, the frequency response functions (Figures F.11 and F.12) show a drop off below 0.5 Hz, an overall value of unity in the range 0.5 to 9 Hz, and a gradual drop off up to 20 Hz. Since the trend in these functions is similar, generating ratios (as is done with a transfer function) between them should not produce any major errors. Furthermore, the frequency range of interest is between 0.5 to 10.5 Hz which is in the unity range - therefore, the effects of the gradual drop is of no concern anyway.

4.4.3 RANDOM AND BIAS ERRORS

Both the Power Spectral Density (PSD) function and the Coherence function (CF) have bias and random errors which are a consequence of averaging the spectra in the frequency domain. Bias error refers to the variance in frequency while random error refers to the variance in the value of the function at a given frequency.

As mentioned in Chapter 2, the correct magnitude of the PSD was not of interest in this study. Therefore, neither was the random error. However, the bias error is of concern since PSD plots were used to locate natural frequencies. Bias errors in the PSD functions ranged from -2% to -33%. This means that a frequency determined from this plot could be lower than the actual frequency by as much as 33%. This error was evident since in some cases the mode shape was found at a frequency which was greater than the corresponding peak in the PSD.

The bias error for the coherence function is undefined. The corresponding random error is a function of frequency, and due to resolution problems, it can become very high (Bendat and Piersol, 1992). This was the case in this study. Coherence between the reference sensors and some of the roving sensors, at some levels in the building, was found to be surprisingly low. Since there was sufficient foreknowledge of the mode shapes being detected, coherence was generally ignored when reviewing the mode shapes. This was done by using a coherence cutoff of zero in the potential modal ratio functions.

CHAPTER 5
AMBIENT VIBRATION ANALYSIS RESULTS

This chapter presents the analytical results of the ambient vibration records. The first section (§5.1) presents the method whereby modal frequencies and the corresponding mode shapes were determined. This is followed by a discussion of the mode shapes (§5.2) and a discussion of frequency ratios and frequency trends (§5.3). The last sections deal with the effect of architectural components (§5.4).

5.1 METHOD FOR DETECTING MODE SHAPES AND FREQUENCIES

The following subsections discuss the procedure followed when determining the dynamic characteristics of City Tower. The signal processing functions mentioned herein are discussed in more depth in Chapter 2.

5.1.1 DETERMINING NATURAL FREQUENCIES

Prior to any detailed analysis, all of the records were plotted using HPPLOT to visually inspect and assess the quality of the signals. Signals containing excessive signal drift were conditioned to improve their quality before they were used in the analysis. In some cases, some signals were contaminated and were not considered reliable. Such records were discarded from further analysis.

Natural frequencies were determined by generating averaged *power spectral densities* (PSD) of each signal. Peaks in this function may correspond to natural frequencies or may indicate that a natural frequency is within the vicinity. Therefore, the corresponding frequency of each of these peaks were noted and later verified when the associated mode shapes were reviewed.

Since there was a pair of sensors oriented in both the NS and EW directions of each floor, translational and torsional motion could be enhanced by combining these signals. In order to accelerate this process, a program called P2 (EDI Ltd., 1993) was used to generate *averaged*

normalized power spectral density (ANPSD) functions. Thus, an overview of the frequency content of the structural system could be viewed in a single plot. ANPSD functions from the fifth test (CT32) are shown in Figure 5.1.

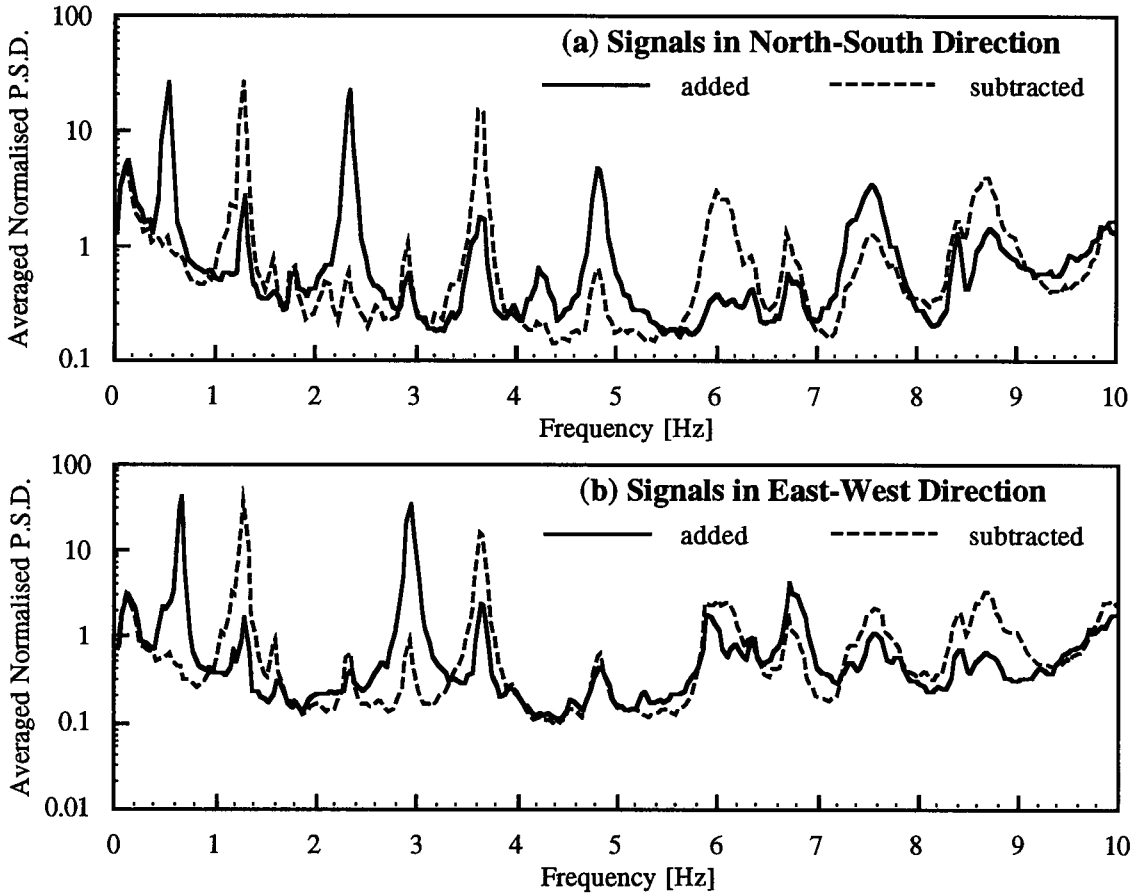

Figure 5.1. Averaged normalized power spectral densities for parallel signals in the NS and EW directions (response of the building when its structure was completed).

The two ANPSD functions shown in Figure 5.1 were created using pairs of sensors in the NS and EW directions respectively. These pairs of signals were combined before the transformation. As can be seen, by adding two parallel signals (as shown by the solid line), peaks associated with translational motion are enhanced while peaks associated with rotational motion are diminished. The reverse is true when the same two signals are subtracted (as shown by the dashed line). These plots also give indications of modal coupling (i.e., vibration modes which have both translational and rotational motion). The second torsional mode (f = 3.65 Hz) is a good example of this behaviour. This modal coupling can be attributed to the asymmetrical distribution of the

storey mass of the tower. ANPSD plots from all of the tests can be found in Appendix G.

5.1.2 DETERMINING MODE SHAPES

Once possible values of the natural frequencies have been determined, the next step was to generate and inspect the corresponding mode shapes. The procedure was as follows. First, potential modal ratio (PMR) values were generated for all of the signals with respect to the four reference sensors[1] using the program ULTRA. Second, these values were assembled into deflection shapes which were animated and viewed from a variety of angles using a companion computer program called VISUAL. By viewing the deflection shape at or near a frequency determined from an ANPSD, the frequency was either verified as a frequency of the structure or discarded. In the former case, the deflection shape was verified as being a vibration mode shape while the frequency was verified as being a natural frequency. Both of these modal properties were then categorized depending on the dominant component of the mode shape (translational, torsional, etc.).

There was a lot of judgment involved when verifying modal properties in this manner. Deflection shapes which were smooth were accepted while those which were erratic were rejected. Some foreknowledge of the building's mode shapes also proved helpful. In particular, the fundamental mode shapes, along with its harmonics in sequential order, were expected. For instance, if (for a given direction) a fundamental and a third mode was located, then it followed that there must be a second mode located between these two modes. Moreover, the mode shapes were typical of those described in structural dynamic text books (Clough and Penzien, 1975; Humar, 1990).

One observation that was made when reviewing higher mode shapes (those higher than the second mode shape) was that sometimes the well defined mode shape had a frequency which was

---

[1]Only two reference sensors were used in the final test, CTTC

slightly higher than the corresponding peak obtained from the ANPSD plots. This can be attributed to bias errors in the PSD functions.

5.1.3 TYPICAL MODE SHAPES

5.1.3.1 Mode Shape Appearance

In order to simplify the appearance of the mode shapes, each floor in the building is represented by either a quadrilateral or a triangle as shown in Figure 5.2. The vertices of the triangles represent the sensor locations. This simplification should be kept in mind when looking at the mode shapes.

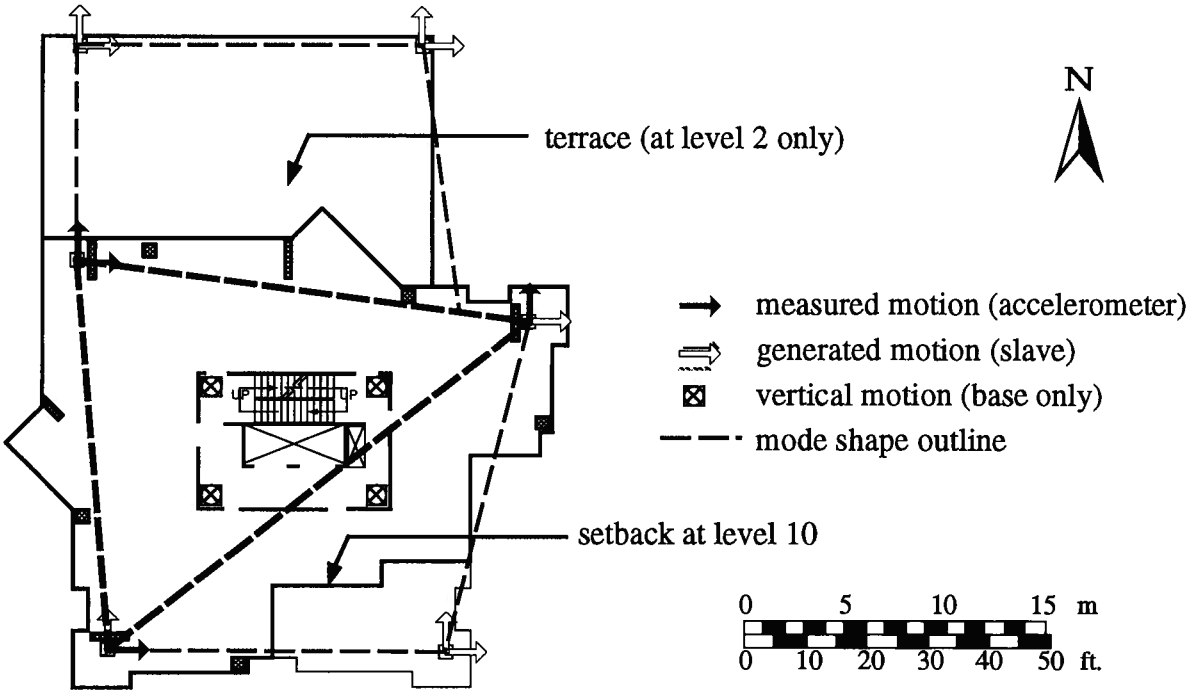

Figure 5.2. Typical floor plan showing sensor locations, slave motion locations, and lines used to represent the floors in the mode shapes presented below.

5.1.3.2 Importance Of Reference Sensors

The choice of reference sensor proved to be very important when creating the mode shapes since each reference sensor contained different components of these modes. For instance, a reference sensor oriented in the NS direction produced very smooth NS translational modes and torsional modes, but produced very erratic EW translational modes. It is likely that this reference sensor

contained very low or zero amplitude motion in the EW direction at the frequencies corresponding to the EW translational modes. Therefore, when the transfer functions were calculated, the resulting values were very large thereby producing the erratic displacement of the mode shape. Thus, some mode shapes could only be obtained using one of the reference sensors while the other mode shapes had to be obtained by using one of the other reference sensors - even if the reference sensors were parallel.

An excellent example of the importance of reference sensor locations arose while studying an incident of modal interference (this phenomenon is discussed in more depth in §5.2.4.2). In this case, two completely different mode shapes, with identical frequencies, were produced by using two different, but *parallel*, reference sensors. These two mode shapes are shown in Figure 5.3.

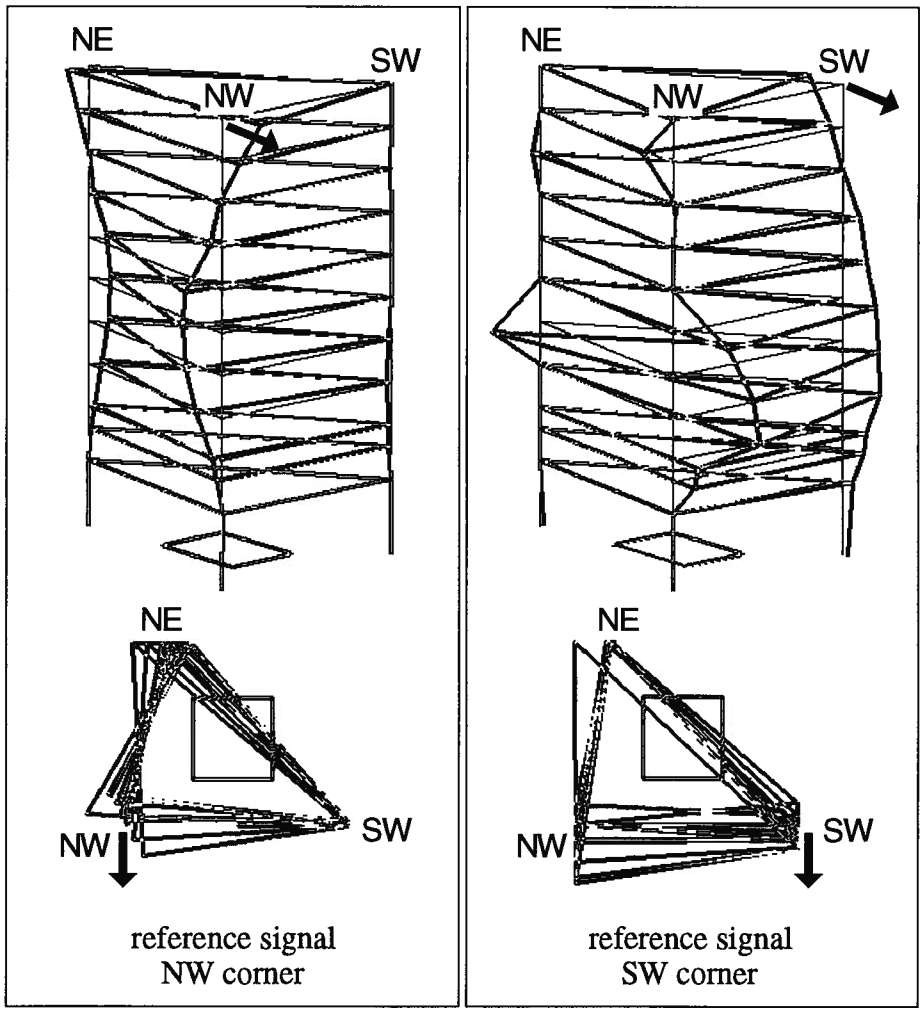

Figure 5.3. Orthographic and top views of two mode shapes which have identical frequencies but were reduced with respect to different reference sensors

The mode shape on the left was reduced w.r.t. the reference sensor located at the NW corner of the building while the mode shape on the right was reduced w.r.t. the reference sensor located at the SW corner of the building. The mode shape on the left shows a superposition of a translational and a torsional mode shape with closely spaced frequencies. In contrast, the mode shape on the right only shows the translational mode. It is likely that the reference sensor located at the NW corner contained information about both the translational and torsional modes while the reference sensor located at the SE corner only contained information about the same translational mode. Thus, the translational mode could be isolated by using one reference sensor but could not be isolated by using the other one. In this case, both of these reference sensors helped identify this interesting phenomenon.

Overall, the two reference sensors (oriented in the NS and EW directions) located at the NW corner of the building were used to find the majority of the mode shapes discussed in this thesis. In some cases though, it was necessary to use the other reference sensors to find the remaining mode shapes. This demonstrates the value of having redundant reference sensors.

5.1.3.3 Importance Of Signal Resolution

A significant factor affecting the quality of the mode shapes was the Nyquist frequency and resolution of the PMR functions. The Nyquist frequency defines the threshold of the frequency range. It was found that good quality mode shapes could be resolved in the range of zero to one half of the Nyquist frequency; which is consistent with previous studies (Ewins, 1984). Mode shapes with frequencies outside of this range tended to be very crude. Consequently, mode shapes in this range are more difficult to locate and categorize with any certainty. The appearance of the mode shapes can also be improved by using a lower resolution when averaging the signals. A lower resolution means that more averages are used when generating the PMR functions. This tends to smooth the function but at the cost of increasing the frequency resolution. For this study, mode shapes with frequencies below 10 Hz were reported with confidence while those above this frequency were often considered questionable. Generally, a

medium resolution (16 averages, $\Delta f = 0.156$ Hz) was used when generating ANPSD functions while a low resolution (32 averages, $\Delta f = 0.312$ Hz) was used when generating the PMR functions.

5.1.4 DEVELOPMENT OF SLAVE

One limitation of VISUAL is that it can only animate displacements which have been measured at a particular point of motion (POM). For City Tower, this represents 4 POMs per floor. Consequently, there was an inherent distortion in the mode shapes since motion at other points on the floor were not being animated. This distortion is illustrated in Figure 5.4. This figure shows translational motion of each floor as depicted by the mode shapes. If translational motion occurs in the NS direction (Figure 5.4c), points *A* and *B* move (since they were instrumented) while point *C* remains fixed thus distorting the shape of the triangle. A similar distortion occurs for translational motion in the EW direction (Figure 5.4b). Here, points *A* and *C* move while point *B* remains fixed. It was not too difficult categorizing the lower mode shapes with this type of distortion. However, the higher modes became impossible to categorize due to modal coupling. Since all of the higher modes had rotational components, torsional modes could not be distinguished from translational modes.

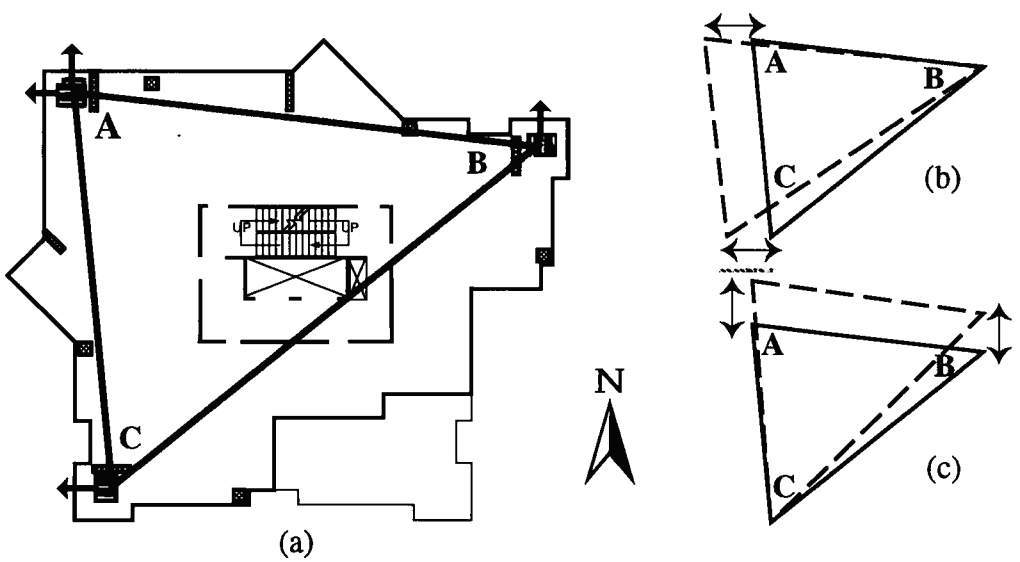

(a) typical floor plan of building showing sensor layout and orientation (denoted by arrows). (b) distortion created by motion associated with (b) east-west translation and (c) north-south translation.

Figure 5.4. Distortion created when animating experimental mode shapes

To deal with this problem, it was decided to calculate the motion at other points on the floor by treating each floor as a rigid body and then interpolating from the PMR values derived from the ambient vibration records. Fortunately, the mathematical formulation for this process had been developed previously (Çelebi, et al., 1987). These formulations were later implemented in a computer program called SLAVE. Specific formulations as well as instructions for using this program can be found in Appendix D.

Excellent results were obtained using the program SLAVE. As an example, consider the mode shapes shown in Figure 5.5. This figure shows orthographic and top views of the first three NS translational mode shapes (from CT25). The mode shapes at the top show vibrational motion with just the measured POMs (master nodes) while the mode shapes at the bottom show the vibrational motion with both the *master* and the *slave* nodes included in the plot.

As can be seen, the first and second modes in the top of Figure 5.5 can be categorized easily despite the distortion. However, it is unclear how the third mode shape should be categorized. Even the top view of the third mode did not provide sufficient information. Now, once the slave nodes have been generated and appended to the mode shape, a much clearer picture is formed. The distortion has been eliminated from all of the modes. Furthermore, the third mode shape can now be categorized with confidence. In this case, the third mode is in fact a translational mode with a rotational component (modal coupling). The program SLAVE was essential for enhancing and properly categorizing all of the mode shapes described in the following section.

5.1.5 DEVELOPMENT OF MAC

A portion of this study was concerned with correlating mode shapes based on a MAC analysis (see Chapter 2). To facilitate this analysis, a program was developed to compute the correlation coefficient between two sets of mode shapes which were obtained either experimentally or analytically. Details of this program as well as operating instructions can be found in Appendix E.

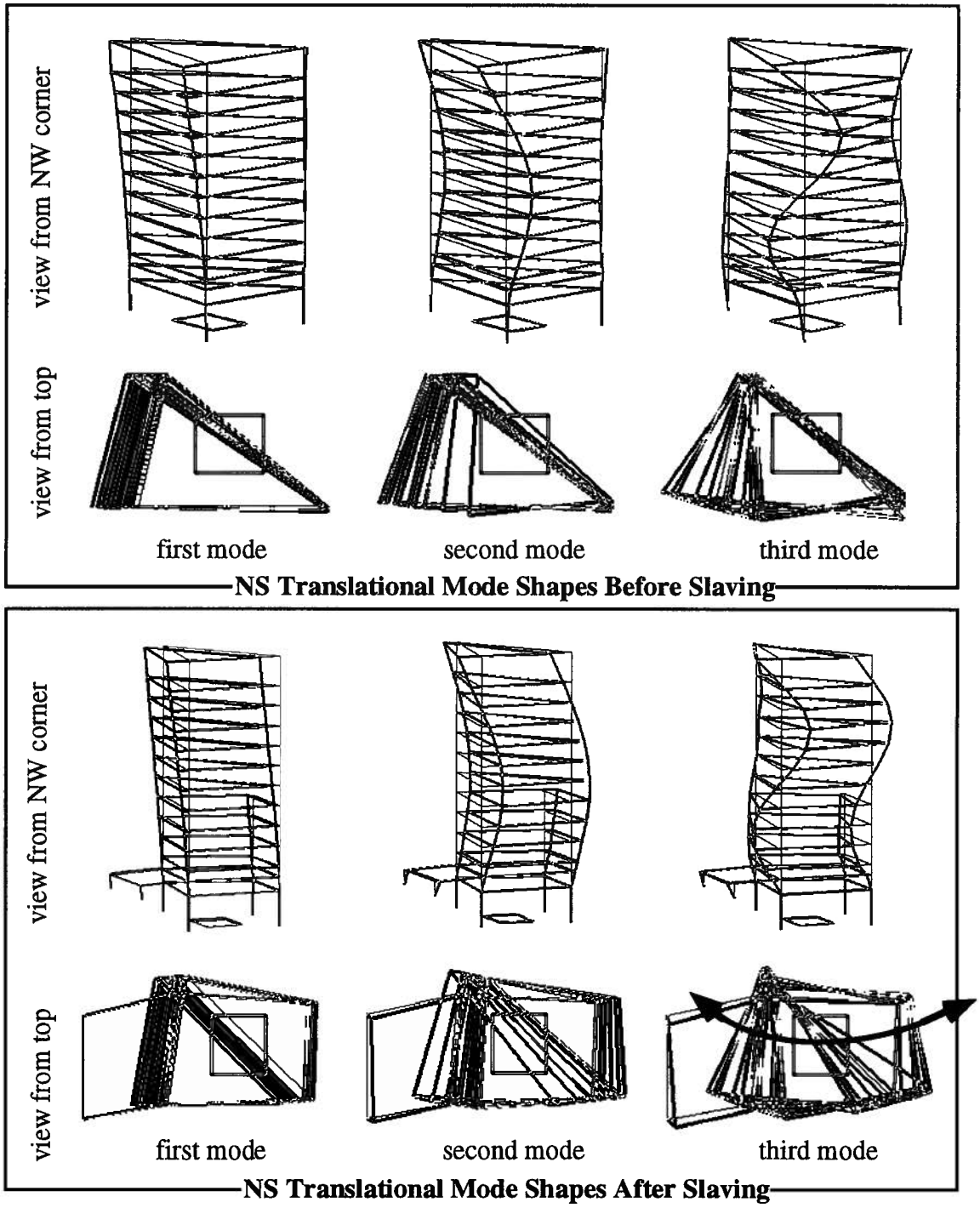

Figure 5.5. NS translational mode shapes - with and without slave nodes.

5.2 MODE SHAPES FROM INDIVIDUAL TESTS

This section presents all of the experimental mode shapes which were obtained from this study. The evolution of the building's dynamic behaviour is also discussed based on these vibration modes.

5.2.1 MODE SHAPE NAMING CONVENTIONS

The following conventions are used when referring to specific mode shapes:

Table 5.1. Vibration mode shape designations.

designation	description
NS•1, NS•2, ...	translational mode with dominant components in the north-south (NS) direction and corresponding order - i.e. fundamental, second, third, etc.
EW•1, EW•2, ...	translational mode with dominant components in the east-west (EW) direction and corresponding order - i.e. fundamental, second, third, etc.
T•1, T•2, ...	torsional mode and corresponding order
A•1, A•2, ...	axial mode and corresponding order

5.2.2 TEN LEVELS OF THE TOWER COMPLETED (CT10)

At this stage in the building's construction, 10 levels of the building were completed corresponding to a height of 25.1 m (82.3 ft.). Five vibration mode shapes were obtained from the ambient vibration records. These mode shapes, along with their corresponding frequencies (periods) are shown in Figure 5.6. In this figure, Levels 1 through 10, and the lowest parking level P6 of the building, are depicted in these mode shapes. Unlike the fundamental modes, the quality of the second modes was not very good. Moreover, the second EW translational mode could not be found with certainty due to a lack of definition.

The fundamental frequencies were very high. However, the building was also much stiffer than a typical building of this height since its core was designed for a 30 storey building, not a 9 storey building.

The mode shapes tend to be very directional with no evidence of modal coupling. The nodal

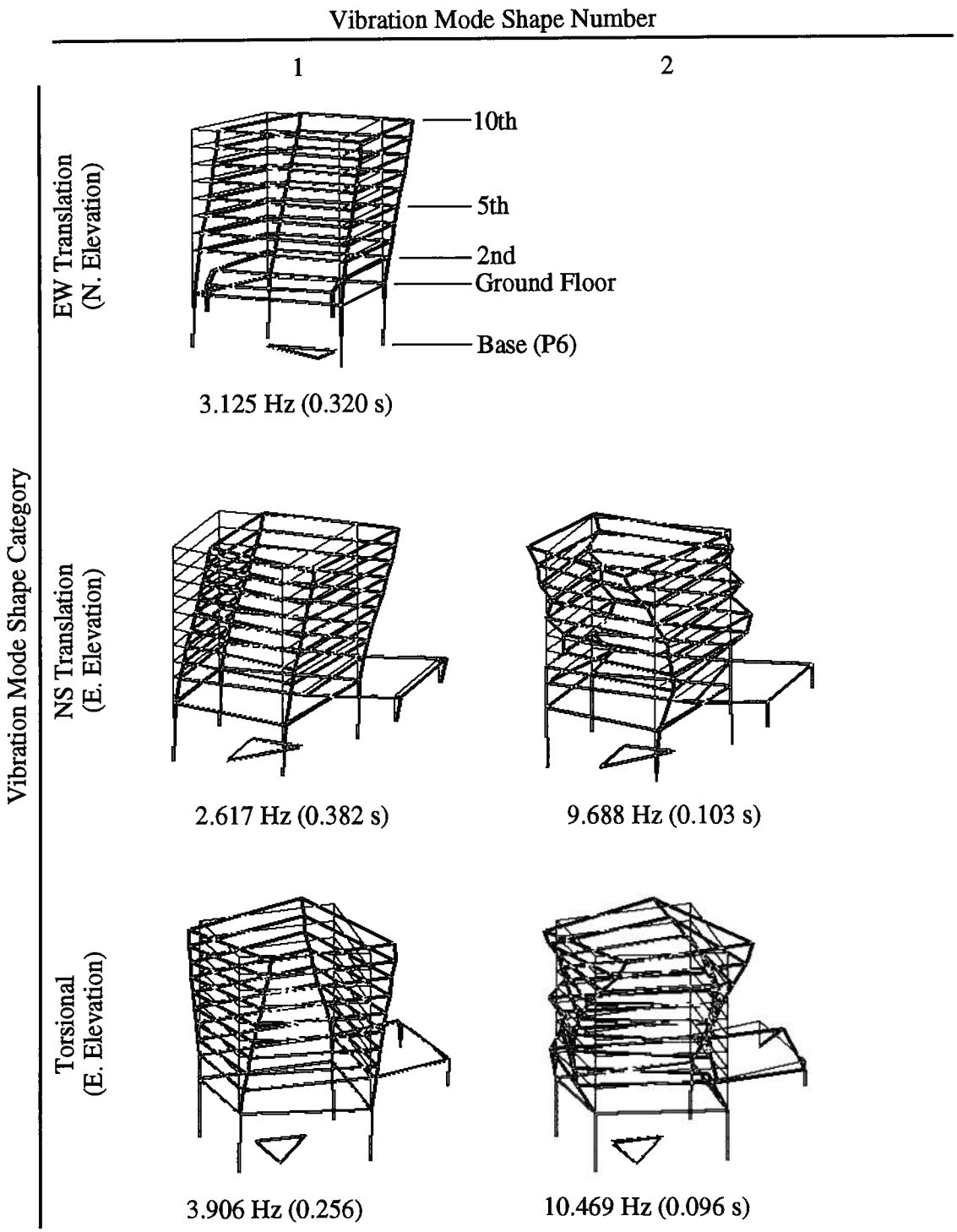

Figure 5.6. Vibration Modes shapes in each principal direction of the building, and corresponding frequencies (periods) following the completion of 10 levels.

point for the second modes were located between the 7th and 8th floor (approximately 74% of the building's height). There did not appear to be any significant rocking motion of the core. Also, the absence of lateral motion at the ground floor indicates no significant embedment effect; i.e. there is no significant difference between the motion at the ground floor and the motion at the base of the building. This can be attributed to the stiffening effect of the surrounding soil as well as the parking structure which the tower connects to at this level. The setback at level 2 as well as the tall first storey do not appear to affect the vibration modes at all.

5.2.3 FIFTEEN LEVELS OF THE TOWER COMPLETED (CT15)

At this stage in the building's construction, 15 levels of the building were completed corresponding to a height of 38.3 m (125.7 ft.). Nine vibration mode shapes were obtained from the ambient vibration records. These mode shapes, along with their corresponding frequencies (periods) are shown in Figure 5.7. In this figure, only every other floor is depicted with the exception of levels 2 and 14 as well as level P6. The definition of these modes shapes are better than those from the previous test. This was attributed to the relocation of the reference sensors, and that no construction was taking place at the building during the ambient vibration measurements.

There was a drop in all of the building's frequencies, compared with the previous test, due to the addition of five storeys. Specifically, there was a 40% drop in the translational modal frequencies and a 30% drop in the torsional modal frequencies.

Overall, the mode shapes tend to be directional though modal coupling is noticeable in the modes NS•2, NS•3, and EW•3. This coupling can be attributed to the setback located at the SE corner of level 10 which introduces a significant redistribution of the floor mass. The nodal point for the second modes is located at the 11th floor (approximately 72% of the building's height) while the nodal points for the third modes are located at the 7th and 13th floors (approximately 45% and 86% of the building's height, respectively). Rocking motion of the core is evident in mode EW•2 but is not evident in the other modes. Also, the embedment effect discussed in the

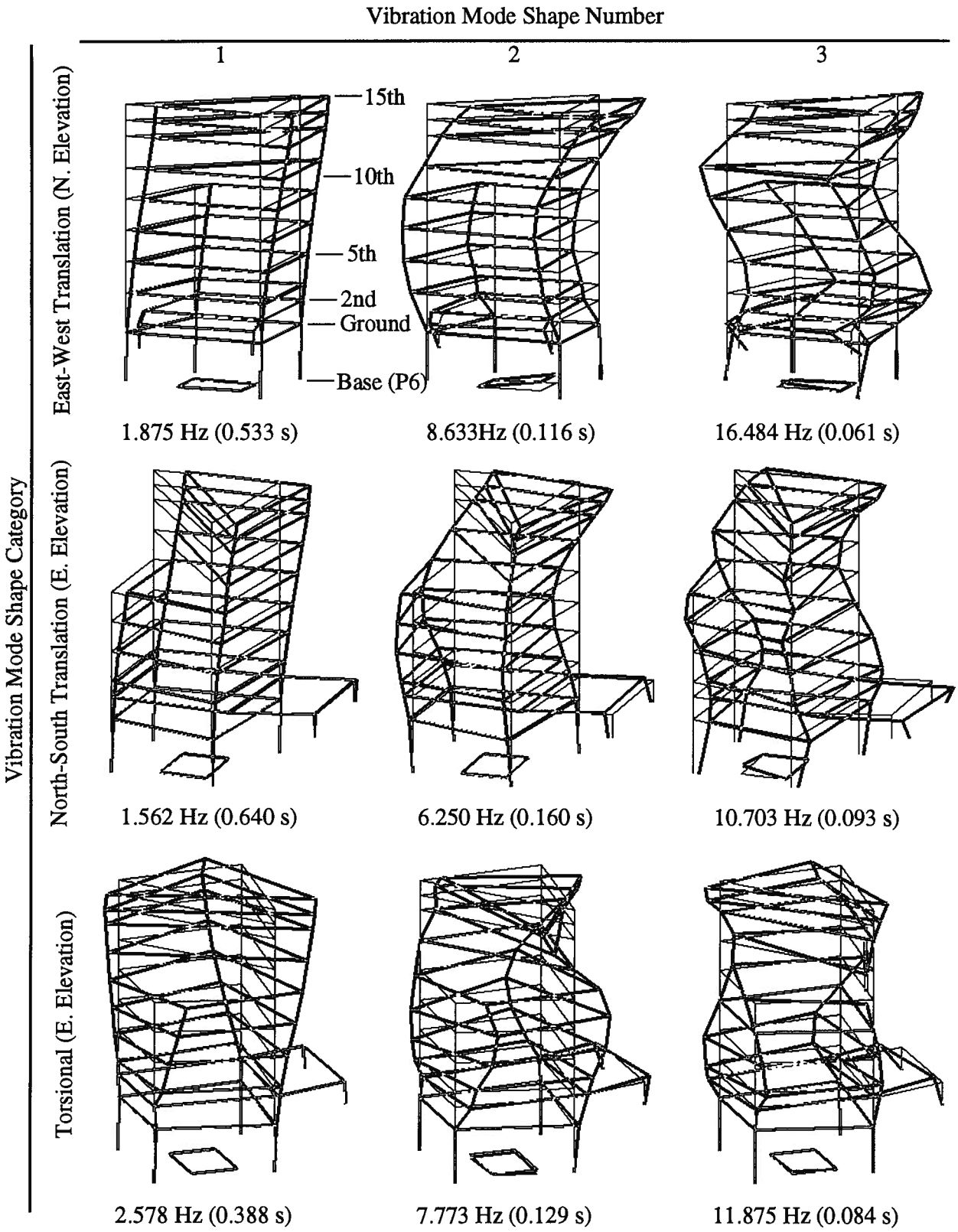

Figure 5.7. First three vibration mode shapes in each principal direction of the building, and corresponding frequencies (periods) following the completion of 15 levels.

previous section is not present in these modes. The setbacks at Level 2, along with the tall first storey, do not appear to affect the vibration modes at all.

5.2.4 TWENTY LEVELS OF THE TOWER COMPLETED (CT20)

5.2.4.1 Mode Shapes

At this stage in the building's construction, 20 levels of the building and the core above Level 20 were completed. This corresponded to a height of 54.2 m (177.7 ft.). Ten vibration mode shapes were obtained from the ambient vibration records that were collected during this test. These mode shapes, along with their corresponding frequencies (periods) are shown in Figure 5.8. In this figure, only every other floor is depicted with the exception of level 2 and level P6. The definition of these mode shapes is excellent, though a loss of definition can be seen in some of the higher modes (such as EW•3, EW•4 and T•3).

There was a drop in all of the building's frequencies, compared with the previous test, due to the addition of another five storeys. Specifically, there was a 40%, 30% and 25% drop in the EW translational, NS translational, and torsional modal frequencies, respectively.

As can be seen, the modal coupling in all of the higher translational modes is becoming more pronounced. This demonstrates that the setback at the corner of level 10 has an important effect on the vibration characteristics of this structure. The nodal point for the second modes are located at the 15th floor (approximately 71% of the building's height) while the nodal points for the third modes are located around the 10th and 17th floors (approximately 46% and 80% of the building's height respectively). Although the definition of the mode EW•4 is quite crude, the nodal points for this mode appear to be located at the 6th, 11th, and 17th floors (approximately 27%, 51%, and 80% of the building's height respectively). There did not appear to be any evidence of rocking motion of the core in any of these mode shapes. At this point, it seemed clear that the setback at Level 2, along with the tall first storey, are not significant factors in the building's vibrational behaviour. In contrast, the setback at Level 10 was a very important

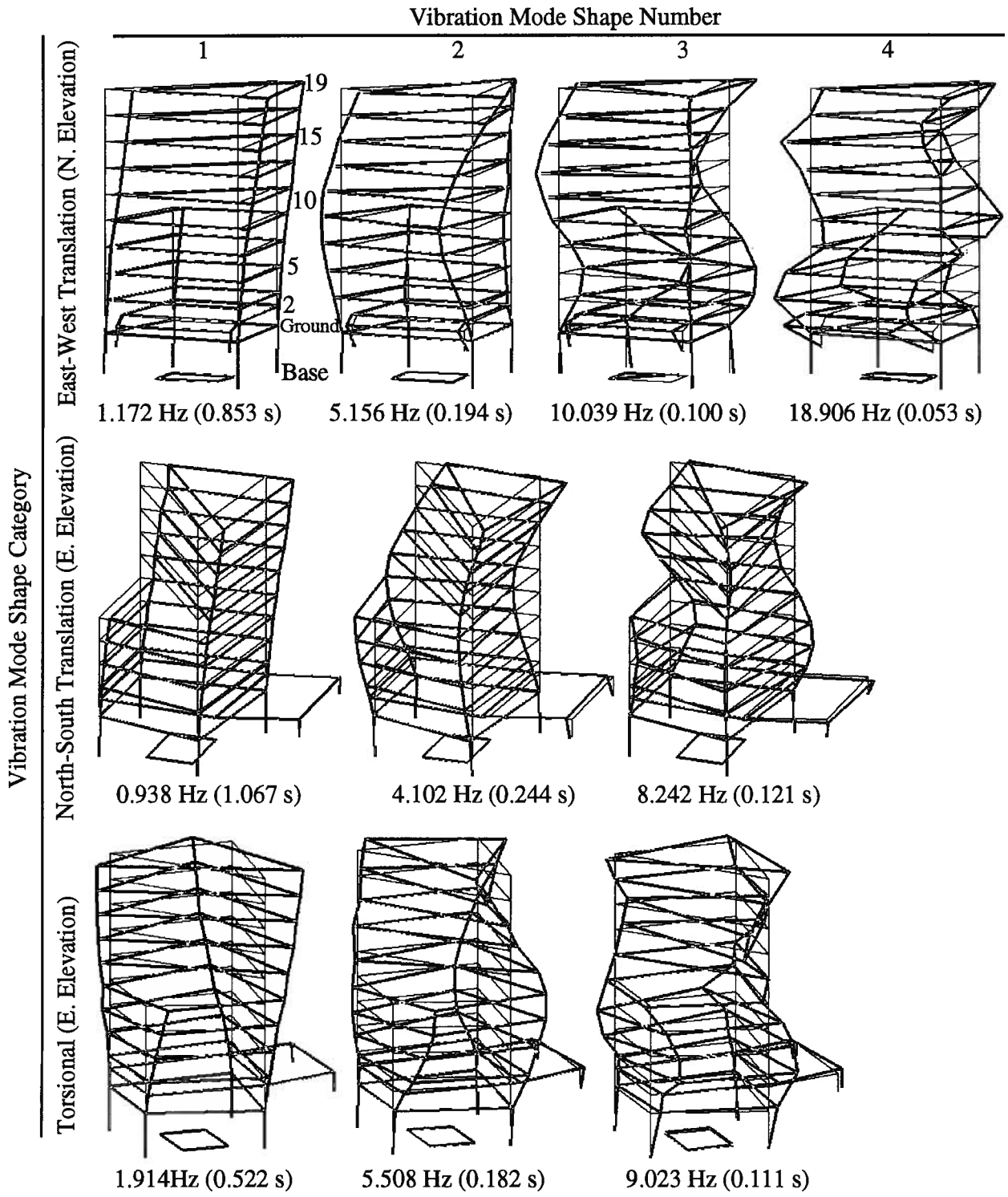

Figure 5.8. Lower vibration mode shapes in each principal direction of the building, and corresponding frequencies (periods) following the completion of 20 levels.

attribute since it had introduced significant torsional motion to almost all of the vibration modes.

5.2.4.2 Modal Interference Between Modes EW•2 And T•2

One of the most interesting observations made in this study was an incident of modal interference (Thomson, 1993). This involves the superposition of motion between modes which have closely spaced frequencies (periods).

This type of behaviour was found during the analysis of the data collected during the CT20 test. In this case, the motion of the second EW translational mode (f=5.16 Hz, T=0.194 s) and the second torsional mode (f=5.51 Hz, T=0.181 s) were combined, resulting in the mode shape shown in Figure 5.9. At first glance, the EW translational mode appeared to be the second torsional mode; rotating about an axis located at the SW corner of the building. However, this did not make sense since the second torsional mode had already been located, and since there was no structural element located at the SW corner which would cause this type of rotation. Upon closer inspection, it was surmised that if translational and rotational motion from the second EW translational mode and the second torsional mode, respectively, were combined as shown in Figure 5.9c, lateral motion (EW direction) would be increased at the NW corner and eliminated at the SW corner. This indeed was the case. The combination of motion just described can be seen clearly by looking at the top view of the mode shape (Figure 5.9b). Similar behaviour was observed for the corresponding torsional mode (Figure 5.9d). In this case the EW motion at the NW corner has been eliminated while the EW motion at the SW corner has been increased.

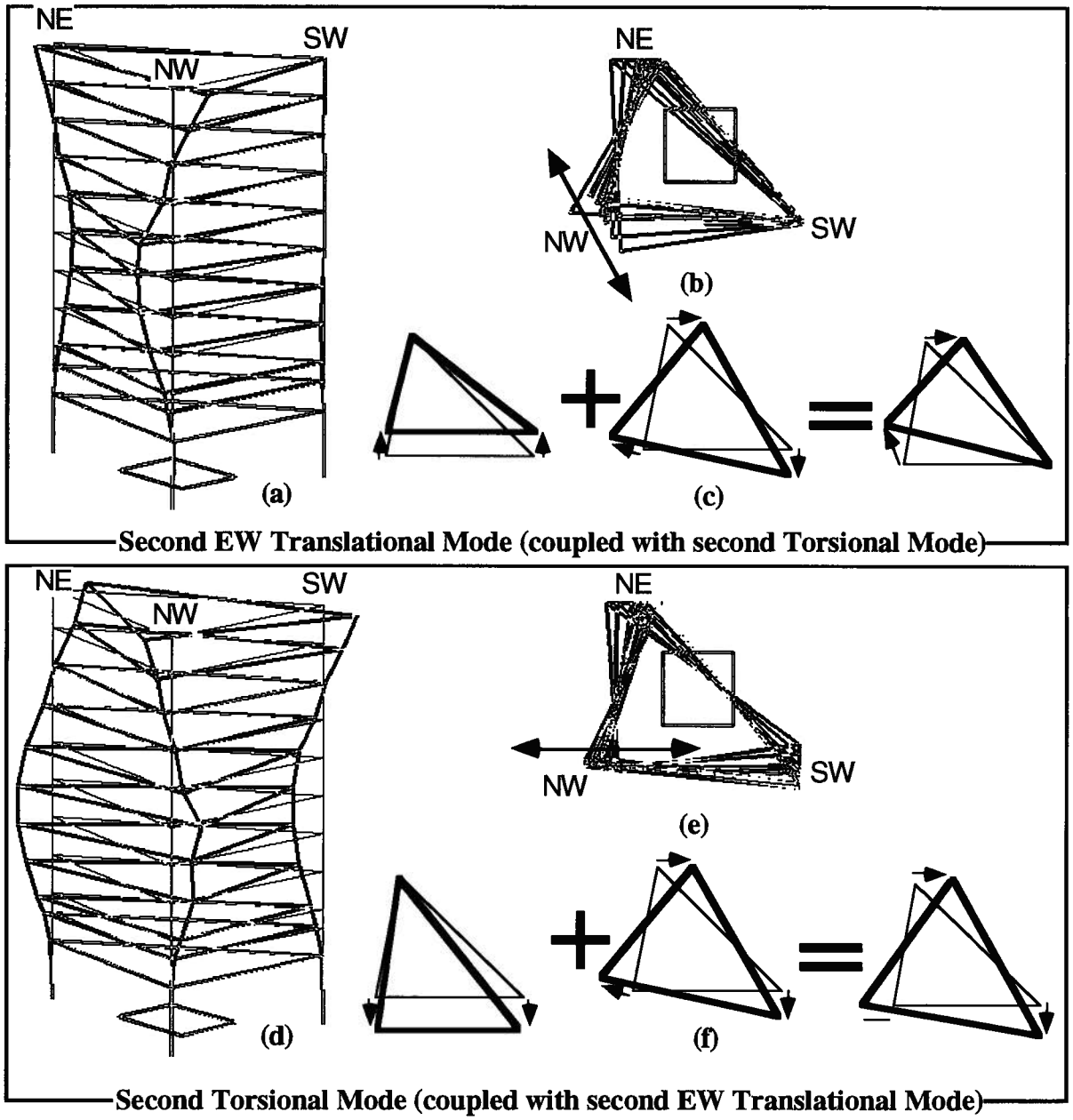

Second EW translational mode shape: (a) viewed from the north-west corner, (b) viewed from the top of the building, (c) probable superposition with second torsional mode (top view)
Second torsional mode shape: (d) viewed from the north-west corner, (e) viewed from the top of the building, (f) probable superposition with second torsional mode (top view)

Figure 5.9. Modal interference between second EW translational mode and second torsional mode.

5.2.5 TWENTY-FIVE LEVELS OF THE TOWER COMPLETED (CT25)

At this stage in the building's construction, 25 levels of the building and the core above Level 25 were completed. This corresponded to a height of 67.4 m (221.0 ft.). Ten vibration mode shapes were obtained from the ambient vibration records that were collected during this test. These mode shapes, along with their corresponding frequencies (periods) are shown in Figure 5.10. In this figure, only every other floor is depicted with the exception of level 2 and level P6. Also, level 23 was not instrumented due to time constraints, and since measurements on this floor were not essential for determining the modal characteristics for this particular test.

There was a drop in all of the building's frequencies, compared with the previous test, due to the addition of another five storeys. Specifically, there was a 25% drop in the translational modal frequencies and a 20% drop in the torsional modal frequencies.

At this stage in the building's construction, the rotational component of the translational modes had increased in magnitude relative to the previous test. However, other aspects of the building's dynamic behaviour did not change from the previous test. There was still evidence of no significant embedment effect, and the structural configuration at the ground floor of the building (tall first storey, and setback at level 2) do not affect the dynamic behaviour. Also, there was no evidence of rocking at the base of the core. The nodal point for each of the second *translational* modes is located around the 19th floor (approximately 73% of the building's height) while the nodal point for the second *torsional* mode is located at the 17th floor (approximately 65% of the building's height). Note that there is a noticeable shift in the nodal point of the torsional mode at this stage. As for the other modes, the nodal points for the third modes are located around the 11th and 21st floors (approximately 41% and 80% of the building's height, respectively). The nodal points for the mode NS•4 are located at the 8th, 16th, and 23rd floors (approximately 29%, 61%, and 88% of the building's height, respectively).

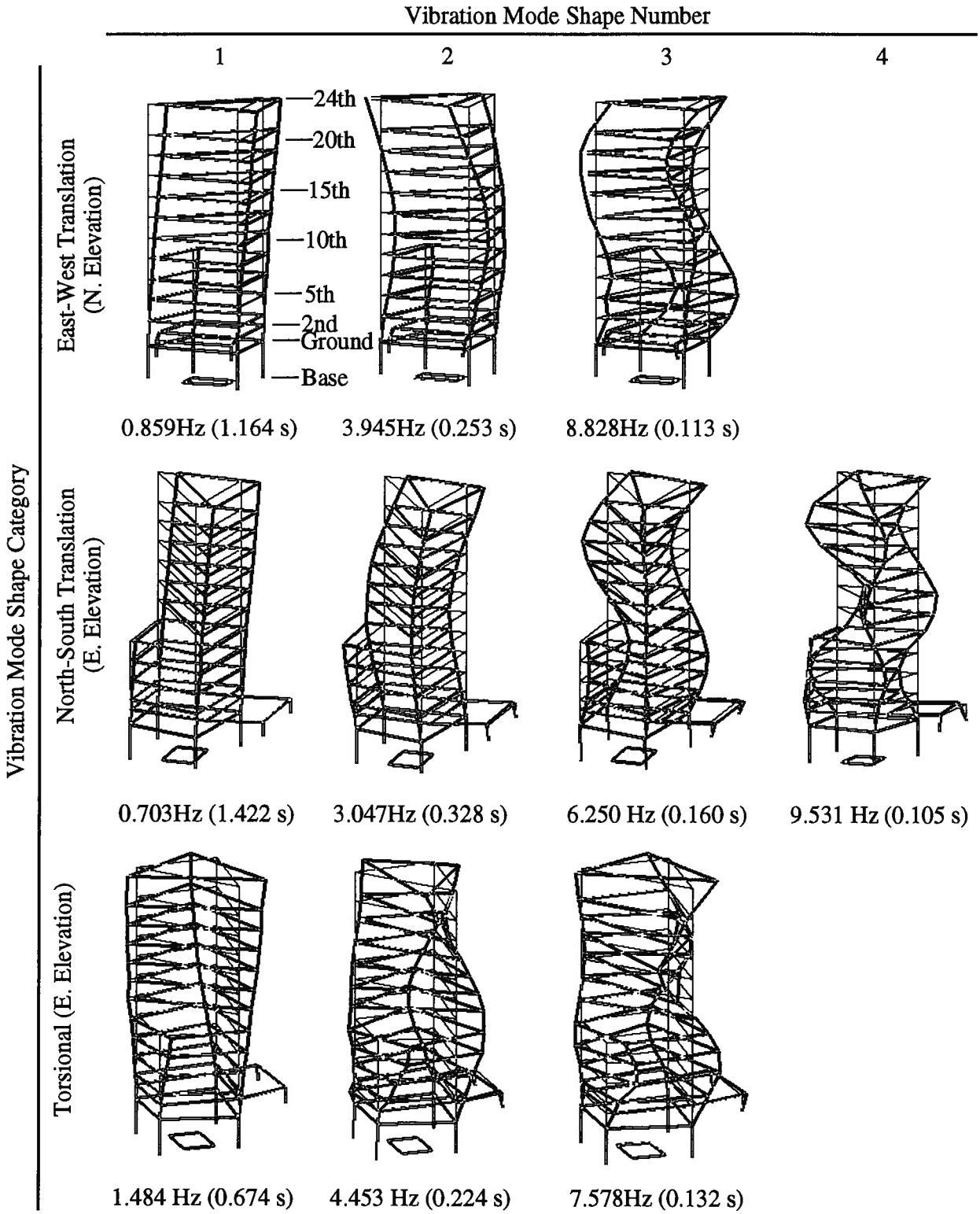

Figure 5.10. Lower vibration mode shapes in each principal direction of the building, and corresponding frequencies (periods) following the completion of 25 levels.

5.2.6 ALL THIRTY-TWO LEVELS OF THE TOWER COMPLETED (CT32)

At this stage in the building's construction, the entire structure (32 levels) was completed. This corresponded to a height of 83.2 m (273.0 ft.). Twelve vibration mode shapes were obtained from the ambient vibration records that were collected during this test. These mode shapes, along with their corresponding frequencies (periods) are shown in Figure 5.11. In this Figure, only every other floor is depicted with the exception of level 2 as well as level P6. Also, level 31 was not instrumented since these measurement were not required, and level 3 was not instrumented since that level was inaccessible during the test.

All of the mode shapes are very well defined with the exception of the mode EW•4. Here the mode shape is quite crude. There also appears to be considerable lateral movement at the ground floor in this mode. However, this can be attributed to either the crudeness of the mode shape or that the amplitude of this vibration mode is minute. In other words, the amplitude of this mode is the same as the amplitude of the ground motion in all of the other mode shapes.

There was a consistent drop in all of the building's frequencies, compared with the previous test, due to the addition of another seven storeys. Specifically, there was a 25% drop in the translational modal frequencies and a 20% drop in the torsional modal frequencies.

There had been little change in the building's dynamic behaviour compared to the previous test. The nodal point for the second modes is located around the 23rd floor (approximately 71% of the building's height) and the 19th floor (approximately 59% of the building's height) for the translational and torsional modes, respectively. The nodal points for the third modes are located around the 16th and 26th floors (approximately 49% and 81% of the building's height, respectively). Finally, the nodal points for the fourth modes are located at the 10th, 19th, and 27th floors (approximately 30%, 59%, and 84% of the building's height, respectively).

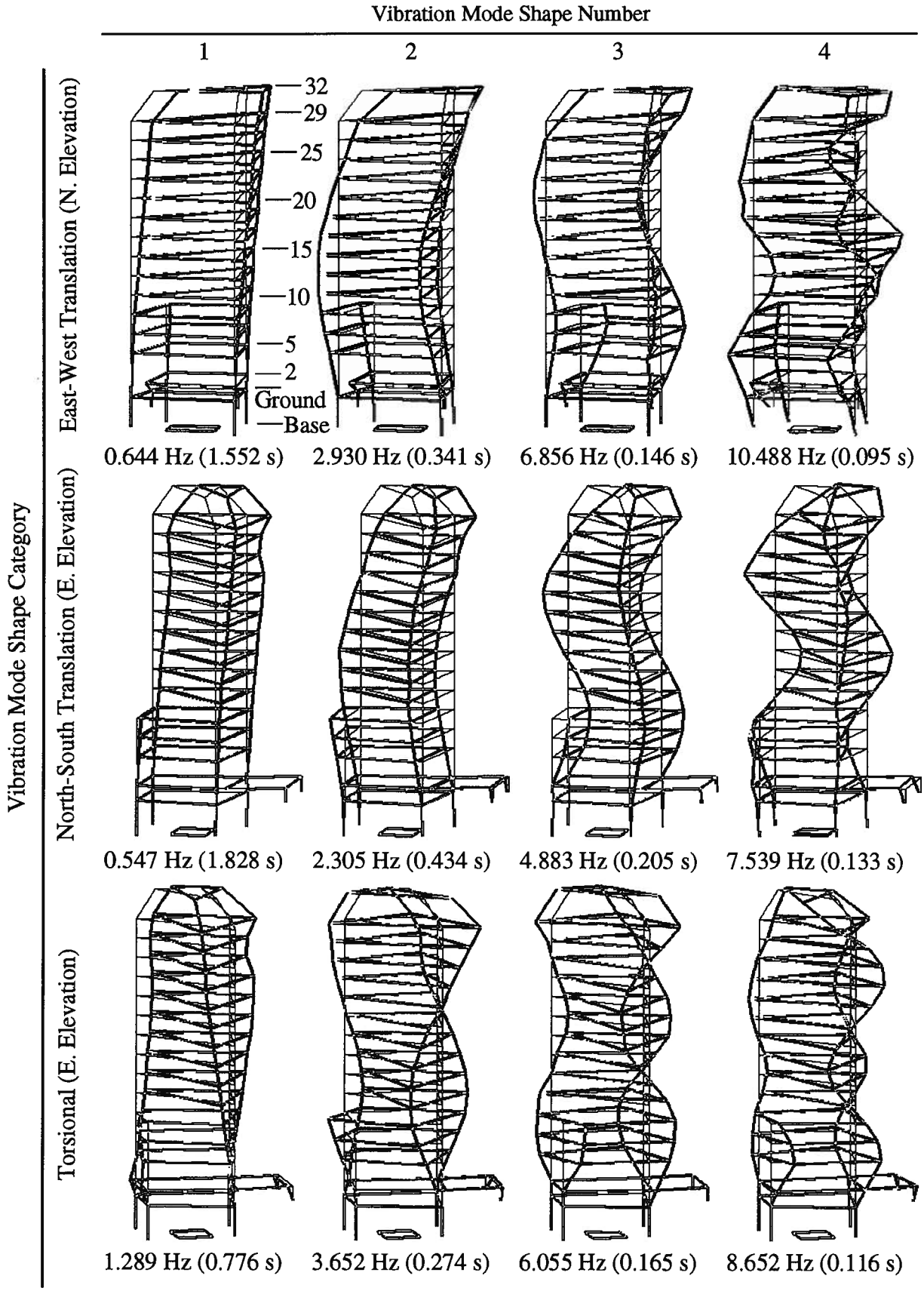

Figure 5.11. First four vibration mode shapes in each principal direction of the building, and corresponding frequencies (periods) for the bare structure (32 levels).

5.2.7 EVOLUTION OF THE MODE SHAPE

It is worthwhile examining all of the mode shapes as they evolved throughout the construction process. The first point worth mentioning is that modal coupling became significant after the setback was introduced at level 10. Moreover, the resulting torsional effects became more pronounced as the building became higher. The second point worth mentioning is that the overall proportion of these mode shapes tended to be the same. For comparison, the nodal points (expressed as a proportion of the building height) were tabulated, and can be found in Table 5.2. Although there are some variations, in general the nodal points occurred at the same point in the structure. There is also the shift in the nodal point for the second torsional mode encountered during the CT25 and CT32 tests. As another comparison, all of the second modes were tabulated and are shown in Figure 5.12. As can be seen, the mode shapes maintain the same proportion during its evolution.

Table 5.2. Nodal points expressed as a percent of the building's height

Test	2nd mode	3rd mode	4th mode
CT10	74		
CT15	72	45, 86	
CT20	71	46, 80	27, 51, 80
CT25	73 (65)*	41, 80	29, 61, 88
CT32	71 (59)*	49, 81	30, 59, 84

* torsional mode

5.2.8 BASE MOTION

Based solely on the mode shapes, there did not appear to be any significant movement at the base of this structure. The only rocking motion (of the core) appeared in a single mode shape (CT15, mode EW•2). Also, there was no significant lateral motion associated with the parking levels (i.e. those levels below ground level). This behaviour can probably be attributed to the sudden increase in stiffness as the tower frames into the parking structure and the neighbouring townhouses.

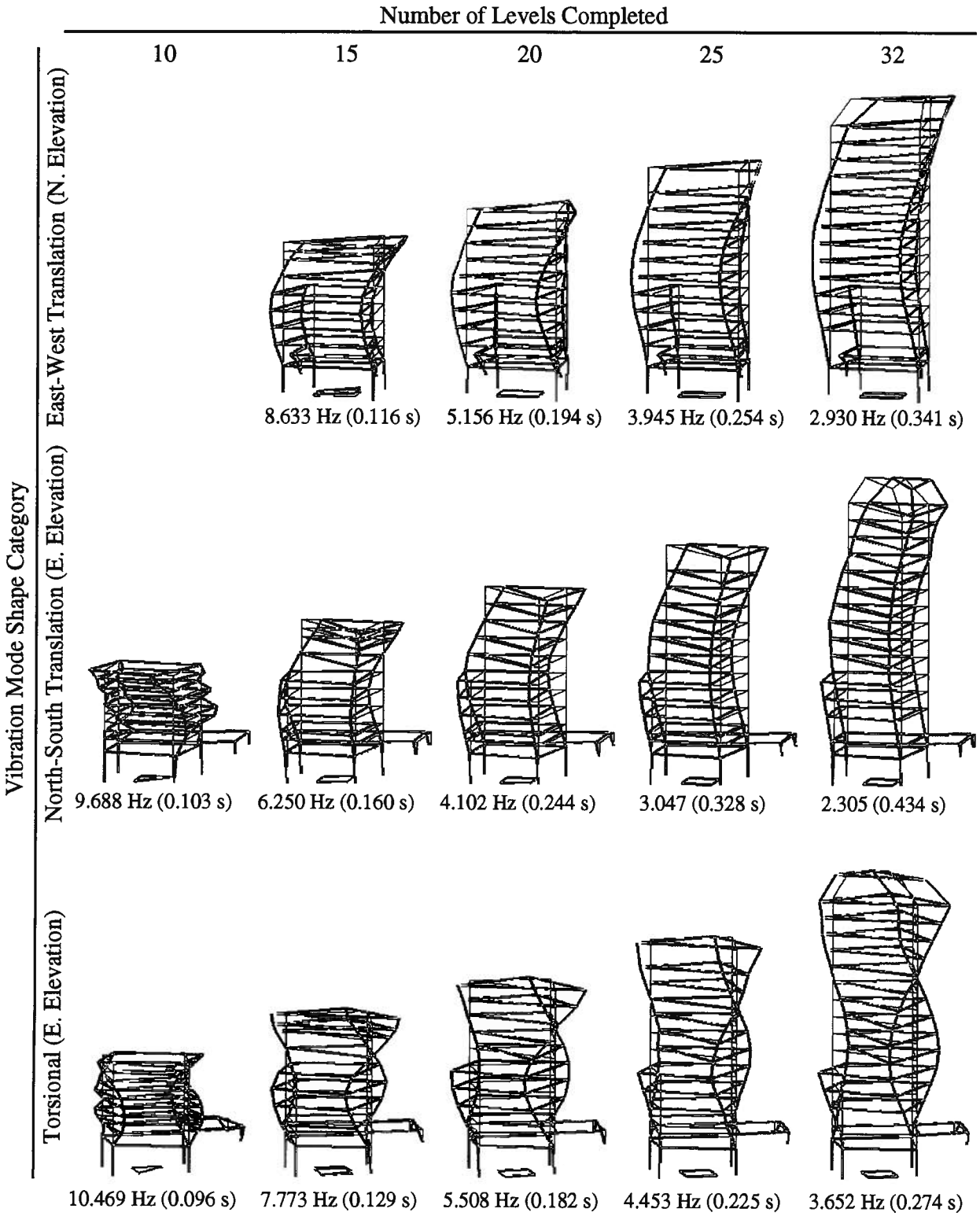

Figure 5.12. Evolution of the second vibration modes and corresponding frequencies (periods).

5.2.9 TOWER COMPLETED (CTTC)

Two aspects of the vibration mode shapes were investigated during this test. First, lateral motion of each instrumented floor was determined for comparison with the previous test (CT32). Second, vertical (and interpolated lateral motion) of the core was determined in order to investigate the manner in which the core deforms. Since a different sensor layout was used in this test, the *lines* used to represent each floor and the core in the resulting mode shapes are slightly different from the other tests. For reference, sensor locations and mode shape outlines for these mode shapes are shown in Figure 5.13.

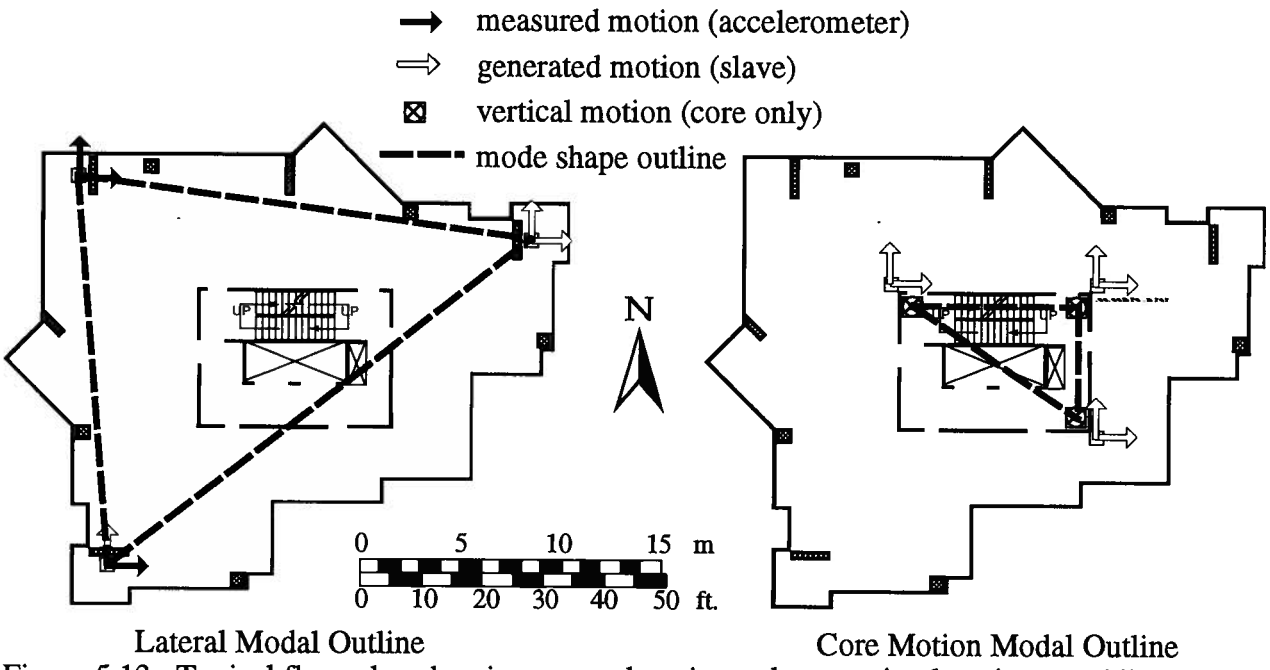

Figure 5.13. Typical floor plan showing sensor locations, slave motion locations, and lines used to represent the floors in the mode shapes presented below.

5.2.9.1 Lateral Modes

At this stage in the building's construction, the majority of the building was finished. All of the major architectural components such as glazing and partition walls were in place. Since the primary objective of this test was to compare frequency shifts due to the addition of the architectural components, only 5 storeys were instrumented in order to assemble partial mode shapes. These partial mode shapes were sufficient to verify the modal frequencies. Twelve

lateral vibration mode shapes were obtained from the ambient vibration records that were collected during this test. These mode shapes, along with their corresponding frequencies (periods) are shown in Figure 5.14. In this figure, only 5 levels are depicted, namely levels 17, 20, 23, 26, and 29.

The analysis showed that there was little or no change in the modal frequencies when compared with those from the last test (CT32). In addition, the shape of the vibration modes did not change; at least not the portion which was measured in this test. This is based on a MAC analysis between the mode shapes obtained from CT32 and the mode shapes obtained from this test.

5.2.9.2 Core Deformation And Vertical Modes

The core modal displacements are shown in Figure 5.15. According to these mode shapes, the core deforms primarily in flexure during the translational modes but there is no significant vertical core displacement associated with torsional modes. An interesting aspect of the first and second translational mode shapes is that the upper half of the building remains straight while flexure occurs in the lower half. The latter is based on comparisons between analytical and experimental mode shapes. This type of modal behaviour makes sense since less energy is required to deform the core in this way and since less energy is associated with the lower modes of vibration.

Although determination of modes dominant in the vertical direction of this structure was beyond the scope of this study, an attempt was made to locate some of these modes based on the vertical measurements of the core. Only a single axial mode could be found. This mode is included in Figure 5.15. As shown, all three corners of the core move in parallel and in phase. This type of motion suggests that this is the fundamental axial mode shape of the structure. However, since only a portion of the structure was measured, it is possible that this could be the second axial mode of the structure.

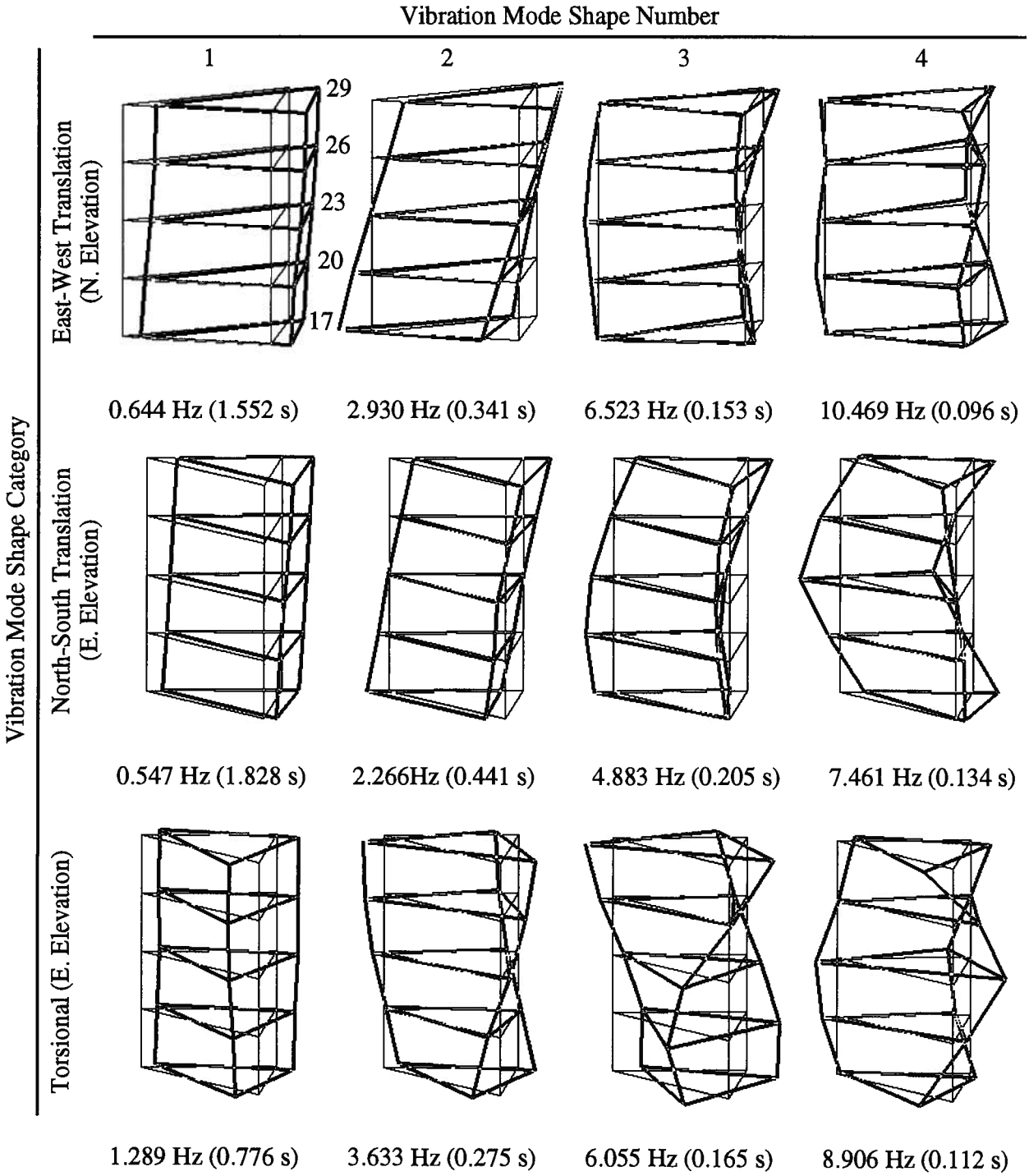

Figure 5.14. First four vibration mode shapes in each principal direction of the building, and corresponding frequencies (periods) of the finished building (CTTC). (Only the top half of the building is shown in these mode shapes).

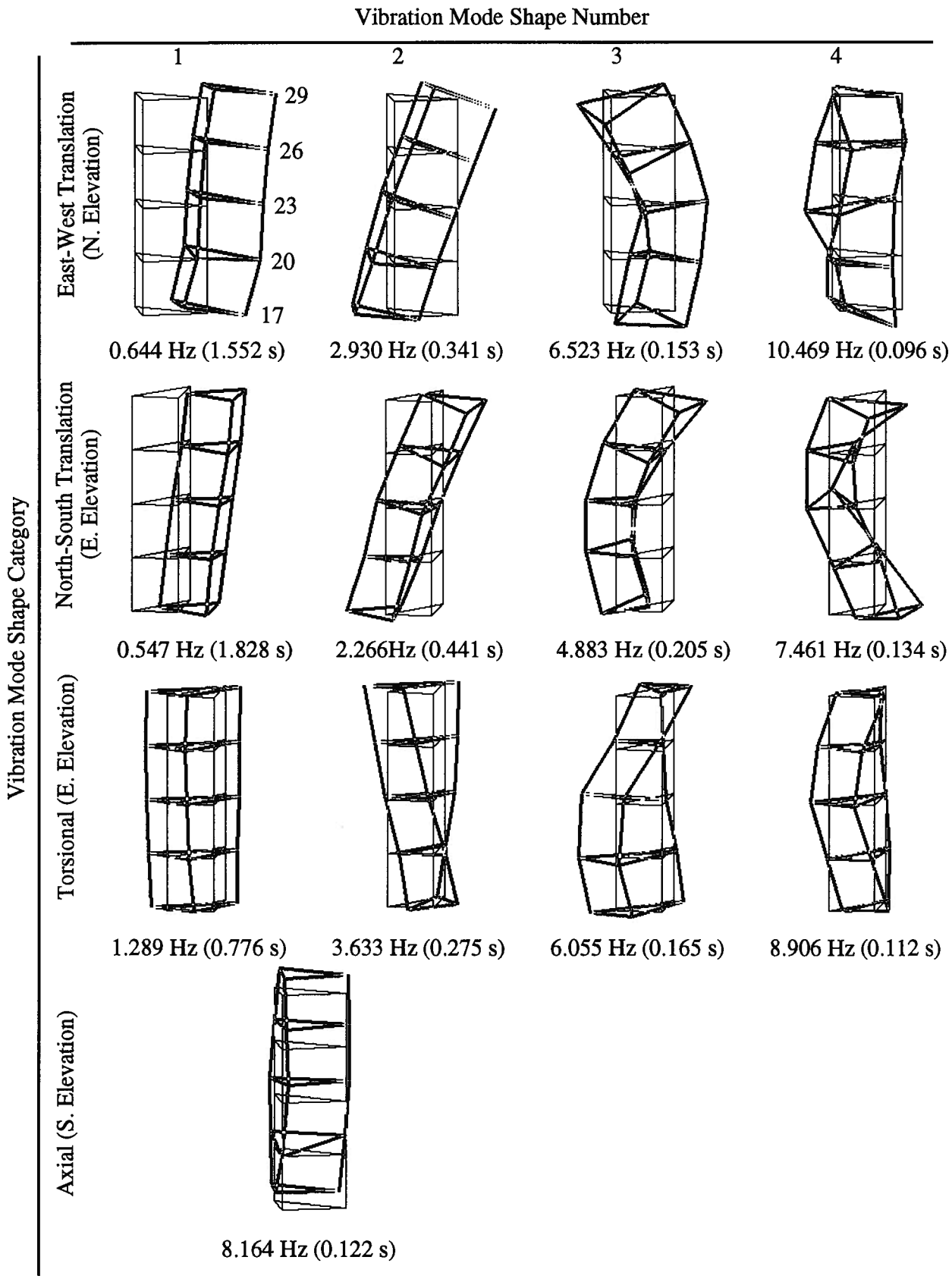

Figure 5.15. First four vibration mode shapes of the building core, in each principal direction of the building; and corresponding frequencies (periods) of the finished building (CTTC). (Only the top half of the building is shown in these mode shapes.

5.3 MODAL FREQUENCIES

This section presents all of the experimentally obtained frequencies and how they changed as the building was being constructed.

5.3.1 MODAL FREQUENCIES AND FREQUENCY RATIOS

Tabulated frequencies and frequency ratios appear in Tables 5.3 and 5.4 respectively. As to be expected, the modal frequencies decreased as the building increased in both height and mass. Modal frequency ratios between the higher modes and the corresponding fundamental mode were found to be consistent from test to test. Also, the overall sequence of these ratios tended to be 4-9-14, 4.5-10.5-16, and 3-5-7 for the NS translational, EW translational, and torsional directions respectively. Note that all of the numbers are equally spaced for each sequence (namely 5, 6, and 2 for the aforementioned directions). The higher spacing for the EW translational modes, compared with the spacing for the NS translational modes, can be attributed to the higher lateral stiffness in the EW direction.

Table 5.3. Frequencies (Hz) for City Tower from 5 stages in its construction.

corresponding mode shape	CT10	CT15	CT20	CT25	CT32
NS•1	2.62	1.56	0.94	0.70	0.55
NS•2	9.69	6.25	4.10	3.05	2.30
NS•3		10.70	8.24	6.25	4.88
NS•4					7.54
EW•1	3.13	1.88	1.17	0.86	0.64
EW•2		8.63	5.16	3.95	2.93
EW•3			10.04	8.83	6.86
EW•4			18.91		10.49
T•1	3.91	2.58	1.91	1.48	1.29
T•2	10.47	7.77	5.51	4.45	3.65
T•3		11.88	9.02	7.58	6.05
T•4					8.65

Table 5.4. Frequencies ratios for City Tower from 5 stages in its construction.

modal frequency ratio	CT10	CT15	CT20	CT25	CT32
NS•2/NS•1	3.7	4.0	4.4	4.3	4.2
NS•3/NS•1		6.8	8.8	8.9	8.9
NS•4/NS•1					13.8
EW•2/EW•1		4.6	4.4	4.6	4.5
EW•3/EW•1			8.6	10.3	10.6
EW•4/EW•1			16.1		16.3
T•2/T•1	2.7	3.0	2.9	3.0	2.8
T•3/T•1		4.6	4.7	5.1	4.7
T•4/T•1					6.7

5.3.2 FREQUENCY TRENDS

Trends for the modal frequencies were estimated by plotting the frequencies in Table 5.3 against the storey height of the building. This plot is shown in Figure 5.16. As can be seen, the change in frequency for both translational and torsional modes follow a similar trend. Furthermore, translational modal frequencies appear to be more sensitive to building height than torsional modal frequencies. Worth noting is the cross-over between the second EW translational frequencies and the second torsional frequencies. The intersection around 19 storeys coincides with the modal interference described previously in §5.2.4.2.

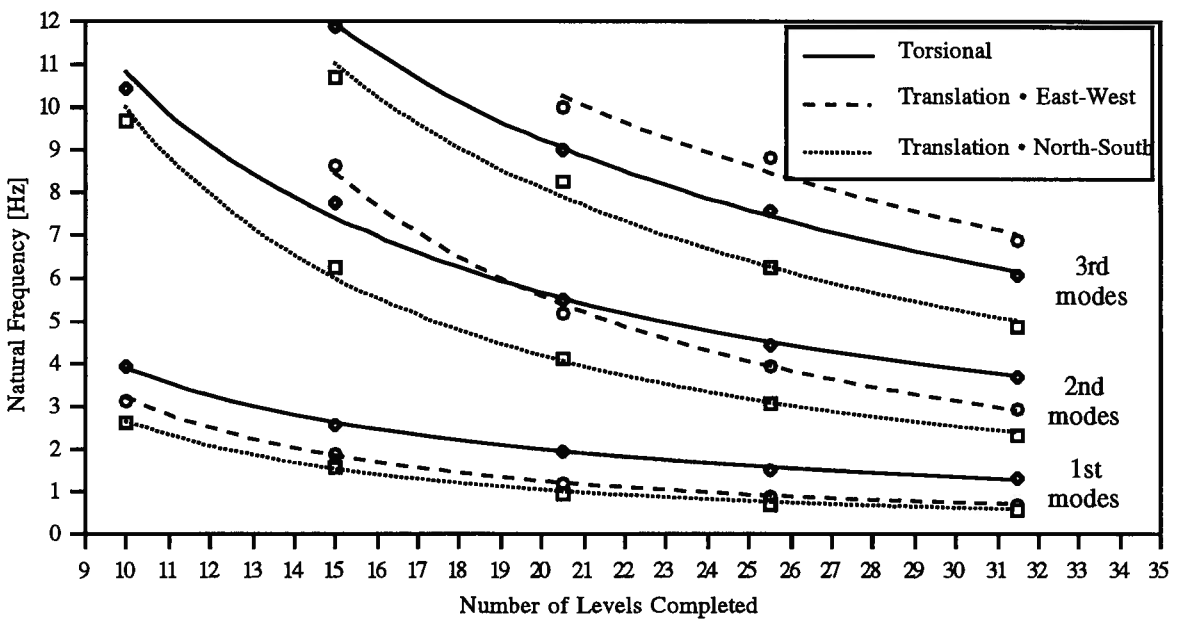

Figure 5.16. Frequency trends for the tower during its construction phase.

5.4 EFFECT OF ARCHITECTURAL COMPONENTS

One of the objectives of this study was to compare the dynamic characteristics of a bare structure with those of a structure with architectural components (such as drywall, cladding, and glazing) attached. This comparison was based on the mode shapes and frequencies (periods) as well as on estimates of damping obtained from the last two tests (CT32 and CTTC).

5.4.1 EFFECT ON FREQUENCY

The modal frequencies from the tests CT32 and CTTC are compared in Table 5.5. As can be seen, there has been little or no change in the modal frequencies. The only significant shifts occurred in the higher modes of vibration. These modes involve more complex deformations than the lower modes, therefore it makes sense that the architectural components would affect them during low amplitude vibration.

Table 5.5. Modal frequencies from CT32 and CTTC

mode shape designation	CT32 (Hz)	CTTC (Hz)	change (%)
NS•1	0.547	0.547	-
EW•1	0.644	0.664	3.1
T•1	1.289	1.289	-
NS•2	2.305	2.266	-1.7
EW•2	2.930	2.930	-
T•2	3.652	3.633	-0.5
NS•3	4.883	4.883	-
T•3	6.055	6.055	-
EW•3	6.856	6.523	-4.9
NS•4	7.539	7.461	-1.0
T•4	8.652	8.906	2.9
EW•4	10.488	10.469	-0.2

5.4.2 EFFECT ON MODE SHAPES

As mentioned earlier, the mode shapes themselves did not change with the addition of architectural components. A MAC analysis showed excellent correlation between the corresponding mode shapes obtained from the CT32 test (the bare structure) and from the CTTC

test (the finished structure). Note that this comparison is somewhat incomplete since only the upper portion of the building's mode shape was available for this comparison.

5.4.3 EFFECT ON DAMPING

Damping estimates derived from ambient vibration measurements are generally unreliable because of large errors due to time windows as well as digitization and noise present in the time signal (Brownjohn, 1988). Other studies have shown that damping levels are force dependent and are typically inconsistent during low amplitude vibrations (Okauchi, Miyata, et al., 1992). Moreover, damping levels under ambient conditions tend to be lower than damping levels under strong motion (Marshall, Phan, and Çelebi, 1994). Therefore, the actual *values* of damping determined from ambient vibrations appear to have little meaning. Furthermore, they certainly should not be used to predict structural behaviour under extreme loads such as earthquakes and hurricanes.

Despite all of the negative conclusions documented about damping estimates from ambient vibrations, an attempt to estimate damping for the lower 6 modes was made anyway. This was done for completeness, and also with the hope that a qualitative comparison could be made between the structure with and without architectural components installed. Measurements taken for the purpose of estimating damping were made on level 27 using a lower sampling rate (20 Hz) than was used for the other measurements (40 Hz). A level closer to the base of the building would have been preferred. However, this was not feasible since architectural components had already been installed on the lower floors at the time of the CT32 test.

5.4.3.1 Sensitivity Analysis

The method used to estimate the damping level was the bandwidth method (Clough and Penzien, 1975) using an averaged PSD function for each of the four measurements made on Level 27. However, several considerations had to be made. The first consideration was whether or not to apply a time window to the signal before transforming it to the frequency domain (as was usually

done). For instance, a *Hanning* window, compared with a *rectangular* window, tends to inflate the width of the spikes in the frequency domain thereby causing an increase in the calculated value of damping. The second consideration involved choosing the frequency resolution or number of averages to be used when calculating the PSD functions. The smoothing which results from several averages may also widen the width of the spike as well as reduce the height of the spike. Both of these factors would increase the calculated value of the damping using the band-width method.

In order to quantify the sensitivity of calculated damping values, several combinations of windows (rectangular and Hanning) and resolutions (high, medium, low, and very low)[2] were used. In addition to this, estimates were made using individual segments from one record (cttcd105). The results of this exercise are summarized in Figures 5.17 through 5.20. The first three figures (5.17, 5.18, and 5.19) show comparisons of damping estimates for the first and second vibration modes. The last of these figures (5.20) show damping estimates for a single record only.

Figures 5.17, 5.18, and 5.19 consistently show that damping estimates increase as the resolution decreases, and that there is a considerable variation in the damping values (damping estimates ranged from 1% to 5% for NS•1, 0.5% to 3% for EW•1, and 0.2% to 1.7% for T•1). Damping estimates also increased when a Hanning window was used.

Damping estimates were also made based on eight individual data segments from a single channel. The arithmetic mean of these values was also calculated. These values were compared to the values determined from averaging in the frequency domain. A summary is shown in Figure 5.20. As can be seen, damping values are consistent from data segment to data segment except for the mode NS•1 which shows some variation. The arithmetic mean appears to produce

---

[2]These are the designations used in the program "ULTRA" which was used for this analysis. High, medium, low, and very low correspond to 8, 16, 32, and 64 averages respectively.

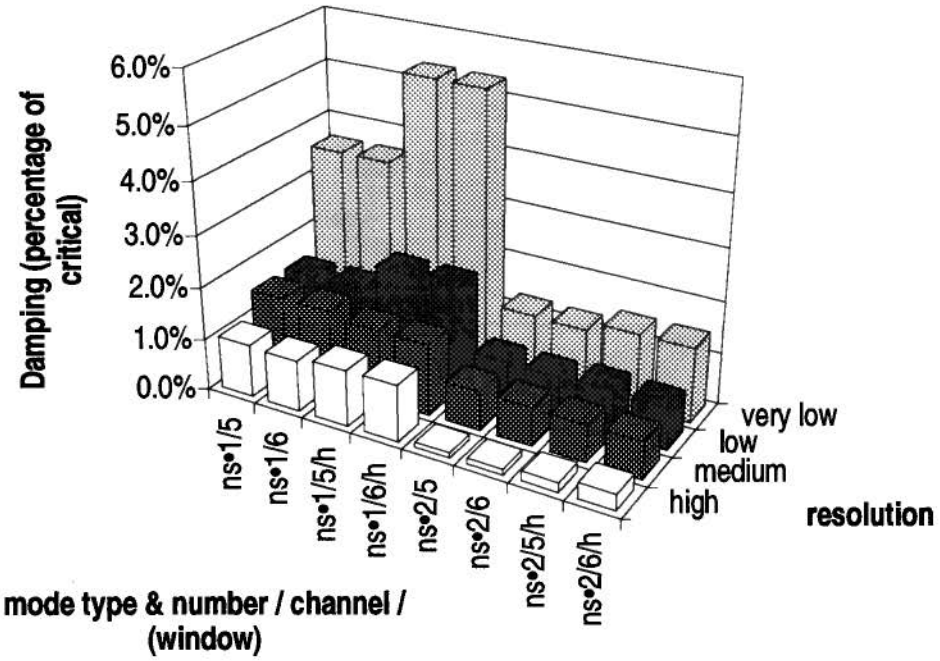

Figure 5.17. Damping estimates for 2 signals in the NS direction using different resolutions and windows.

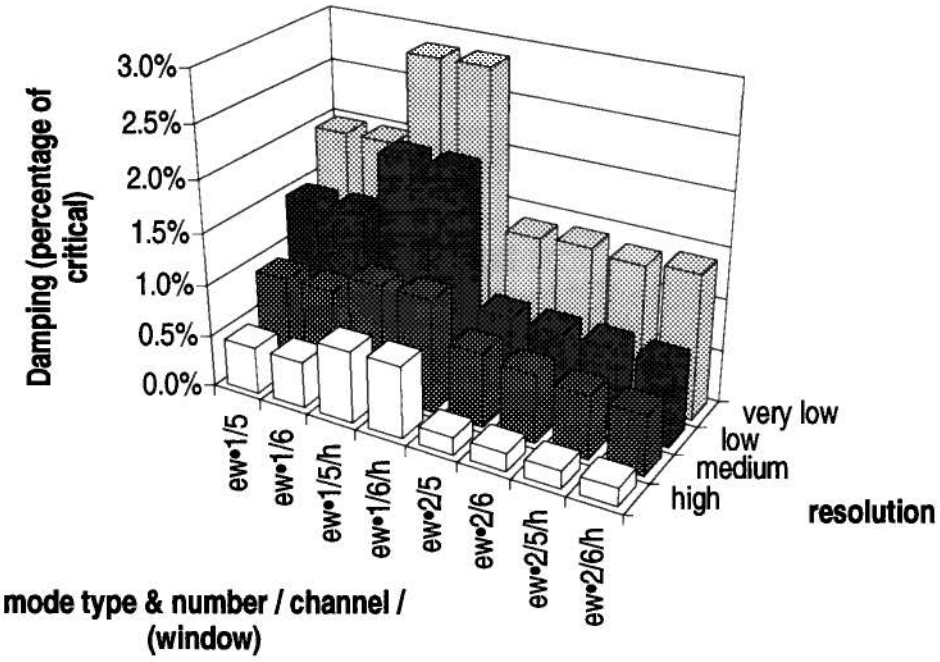

Figure 5.18. Damping estimates for 2 signals in the EW direction using different resolutions and windows.

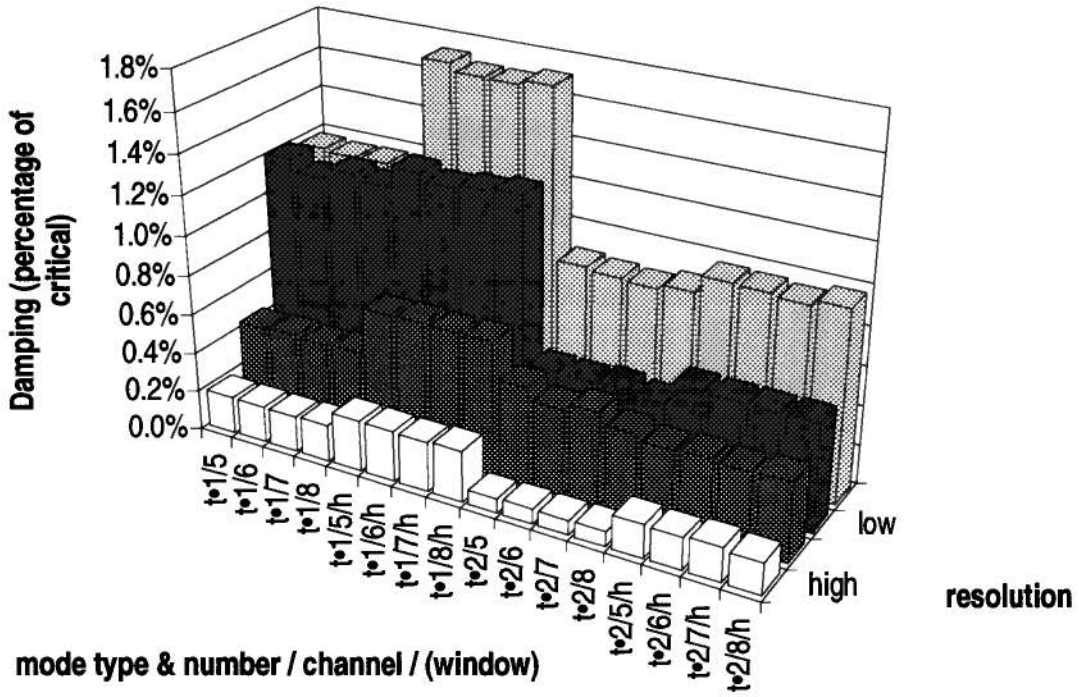

Figure 5.19. Damping estimates for 4 signals in the NS and EW directions (torsion) using different resolutions and windows.

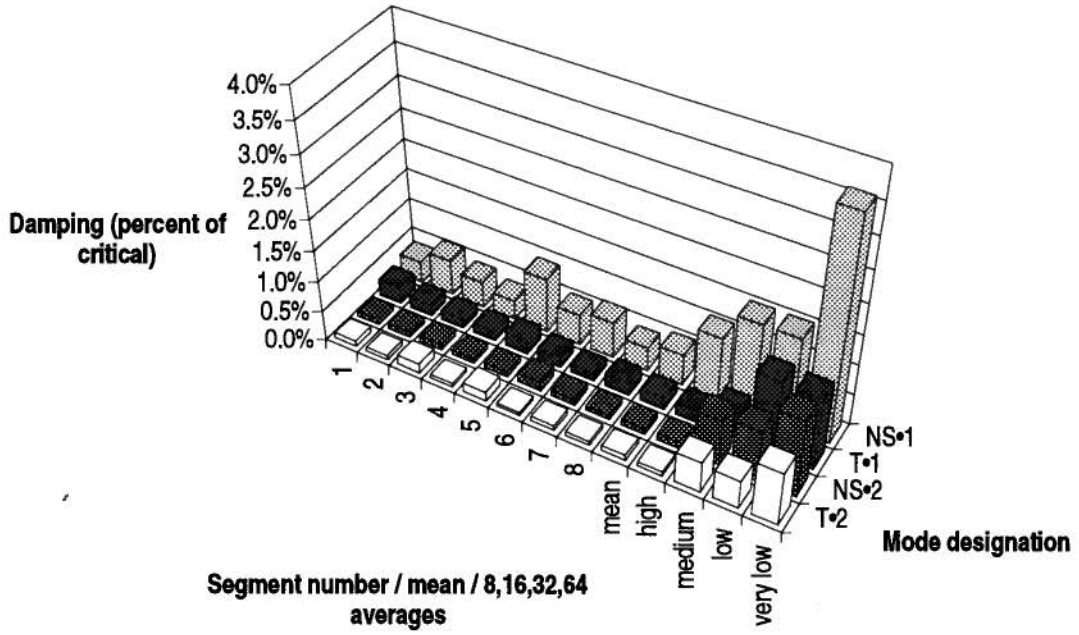

Figure 5.20. Damping estimates for one signal in the NS direction using individual segments, mean, and different resolutions (no window).

a good estimate. Estimates based on a high resolution produced results which were similar to the mean except for the mode NS•1. There was considerable variation in damping estimates based on lower resolutions (values ranged from 0.3% to 3.6% for NS•1 and 0.1% to 1.3% for NS•2).

Based on these results, it is clear that damping values are very difficult to quantify accurately. However, one conclusion that can be drawn from these figures (especially Figure 5.19 which shows damping estimates for the torsional modes) is that for a given window and resolution, the results are quite uniform. Therefore, it seemed reasonable that relative comparisons could be made between damping levels.

5.4.3.2 Comparison Of Bare Structure And Finished Building

Using the basis that relative comparisons of damping values could be made (as discussed in the previous section), it was decided to compare damping estimates from the CTTC test and the previous test, CT32, using a rectangular window, and a high resolution. The results appear in Figure 5.21.

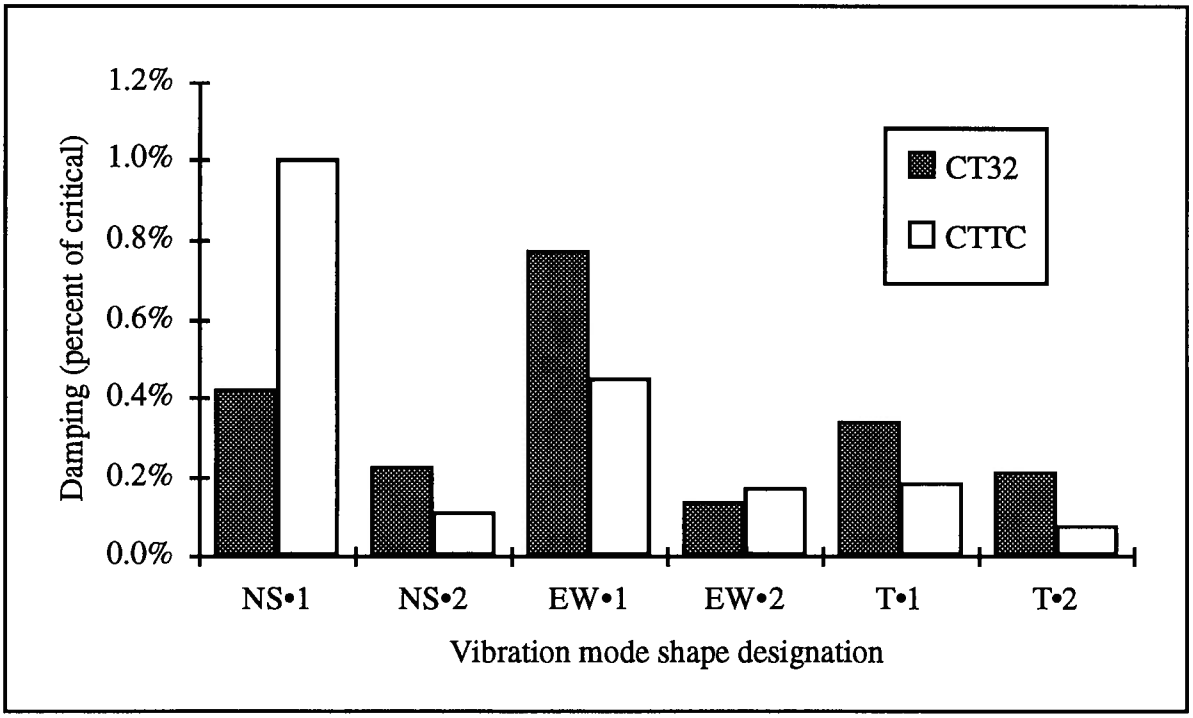

Figure 5.21. Modal damping comparison between the bare structure and structure with architectural components in place.

According to this figure, the addition of architectural components to the structure results in a modest increase in damping of the fundamental NS translational mode (from 0.4% to 1%) as well as the second EW translational mode (from 0.14% to 0.17%). The remaining modes showed a decrease in damping (from 0.8% to 0.5% for the mode EW•1 as well as a 0.15% drop in the other). These shifts in damping are quite small. Moreover, in light of all of the errors associated with damping estimates from ambient vibration records, one can conclude that there has been no significant change in the damping levels with the addition of the architectural components. However, this conclusion is based on ambient levels of vibration, and should not be extrapolated to high amplitude vibrations induced in the structure by a seismic event. In the latter case, it is believed that architectural components will contribute to dissipating energy (i.e. damping) if the structure undergoes large displacements.

CHAPTER 6
DYNAMIC ANALYSIS OF THE BUILDING

This chapter presents a discussion of dynamic analyses of the building (§6.1). In addition, design considerations based on the results of this study are also discussed (§6.2).

6.1 COMPUTER ANALYSIS

To complete this study, a dynamic analysis of the building was performed. This was done to determine if the building's dynamic characteristics could be accurately represented by an analytical model.

6.1.1 CHOICE OF DYNAMIC ANALYSIS PACKAGES

The program ETABS (CSI Ltd. 1992) was chosen for this analysis for two reasons. First, it is specialized for the analysis of building systems. Second, this software package is commonly used for design by engineering consultants, and thus serves as a useful benchmark.

6.1.2 CALIBRATION OF THE BASE MODEL

A very precise model of the building, with 32 levels and the parking levels in place, was created using information from the contract drawings of this building (Bogdonov Pao Associates Ltd., Baker McGarva Hart Inc.). The objective of developing this model was to calibrate it such that its frequencies (periods) and mode shapes, obtained through dynamic analysis, corresponded to the experimental results. Several revisions and adjustments were made to the model in order to satisfy this objective.

The *calibrated* (base) model of City Tower corresponding to the CT32 test is shown in Figure 6.1. A detailed description of this model is given below.

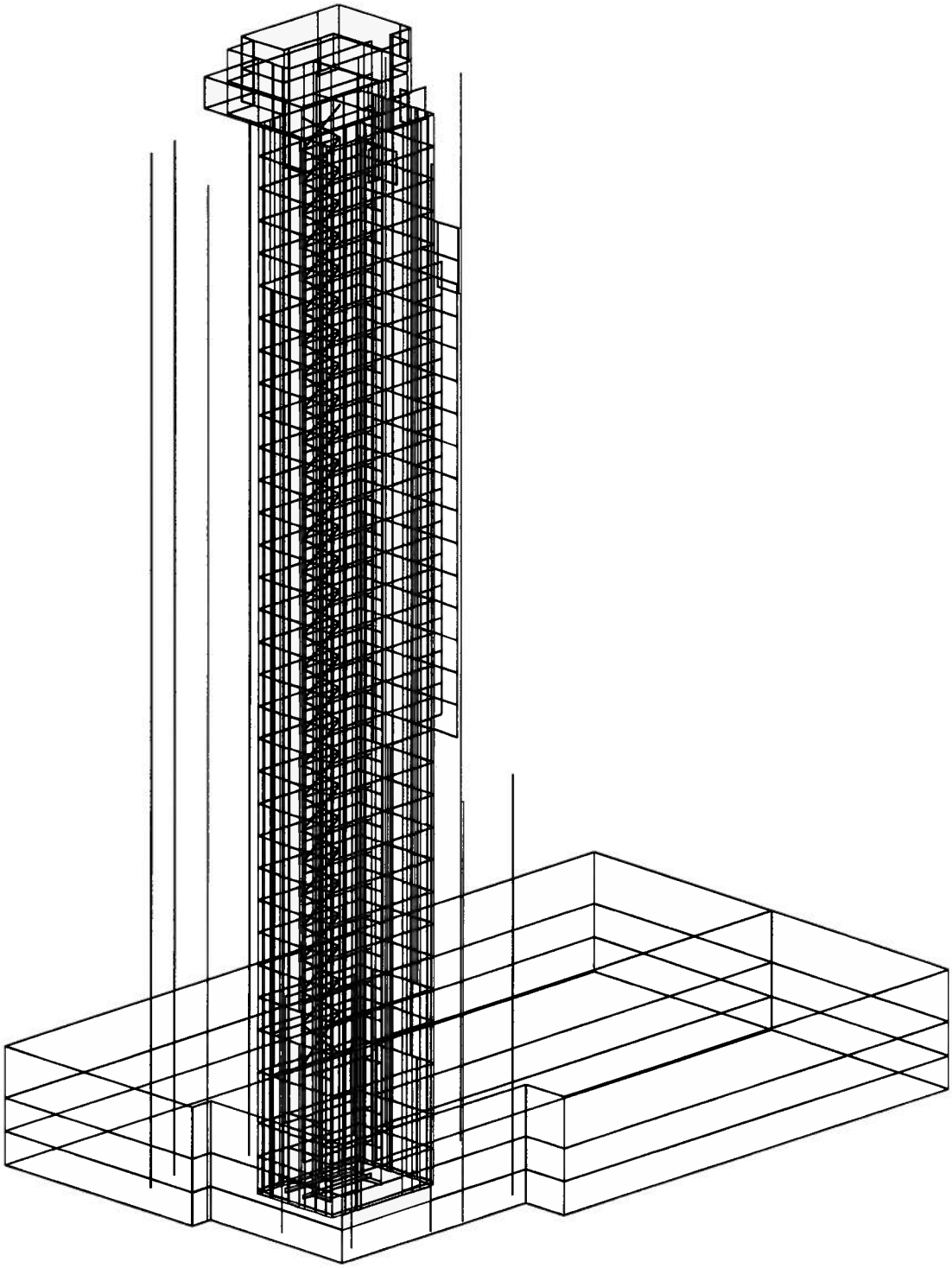

Figure 6.1. ETABS model of the building with all 32 levels.

The core was modeled as an assemblage of shear panels; taking into account all door and wall openings. The stiffness of these panels was represented by using the same wall thicknesses specified on the drawings (ranging from 450mm (18") at the base to 350 mm (14") at the top) along with the secant stiffness (based on specified values of f'_c - see Table 3.1) to represent the concrete. Shear panels were also used to model the parking level retaining walls.

Columns were modeled as *stick* elements accounting for all geometric and material properties. Stairways were modeled as X-bracing. Vertical soil stiffness was modeled by providing an additional storey at the base of the building. Columns and shear walls were extended to this storey and their properties appropriately modified to model the soil. Lateral and torsional springs, representing the soil, were added to the parking levels acting through the centre of mass of the core.

The floor slabs were not modeled directly since an intrinsic assumption in ETABS is that these slabs behave as rigid diaphragms. However, the distribution of floor mass was meticulously accounted for. A density of 24 kN/m^3 was used to model the weight/mass of all of the reinforced concrete in this building.

About 20 revisions, which included modifications and adjustments to the model, were made before the model was *calibrated* satisfactorily. The revisions which significantly affected the modal properties are as follows. First, the addition of the header beams properly modeled the torsional stiffness of the core. Second, the addition of both the retaining walls and lateral soil springs to the parking storeys also helped improve the match of both the frequencies and the shape of the vibration modes. Finally, the upper storeys (above Level 25) were found to be too heavy. Reducing the reinforced concrete density from 24 kN/m^3 to 20 kN/m^3 at these levels improved the values of the analytical fundamental frequencies (which were too low prior to this change). This change reflects the lower steel percentage in the core[1] above Level 25. The

---

[1]Note that the density of steel (7850 kg/m^3) is over 3 times the density of concrete (2430 kg/m^3). Therefore a reduction in the steel percentage also reduces the overall density of the reinforced concrete.

revisions to this model which did not significantly affect the modal properties include the stairway (acting as cross-bracing) and a torsional spring, representing soil stiffness, applied at the parking levels.

Once the base model (all 32 levels) was calibrated, 4 other models of the building were created corresponding to the state of the building at the time of the other ambient vibration tests (CT10, CT15, CT20, and CT25). These models were created simply by taking the base model and removing the upper storeys such that the number of storeys in the model was the same as the number of storeys in the building at the time of the aforementioned tests. It was found (through dynamic analysis) that these other models accurately represented the dynamic behaviour of the building, at the corresponding stage in its construction, without further modifications.

The results of the original calibration and subsequent modeling of the building at other stages in its construction are discussed in the following sections.

6.1.3 COMPARISON OF ANALYTICAL AND EXPERIMENTAL FREQUENCIES

Comparisons between corresponding analytical and experimental frequencies (for all 5 models) were based on percentage differences, and also by plotting these frequencies against each other. In terms of differences between analytical and experimental frequencies, it was found that most of the corresponding frequencies were within 5% of each other. The remaining frequencies differed by as much as 24%. Tabulated frequency comparisons can be found in Appendix H.

Plots of experimental versus analytical frequencies were also made for comparison; these appear in Figure 6.2. In these plots, the closer each *point* comes to the diagonal, the better the correspondence of the analytical frequency to the experimental frequency. Since most of these points came very close to this line, it was concluded that there was very good correspondence.

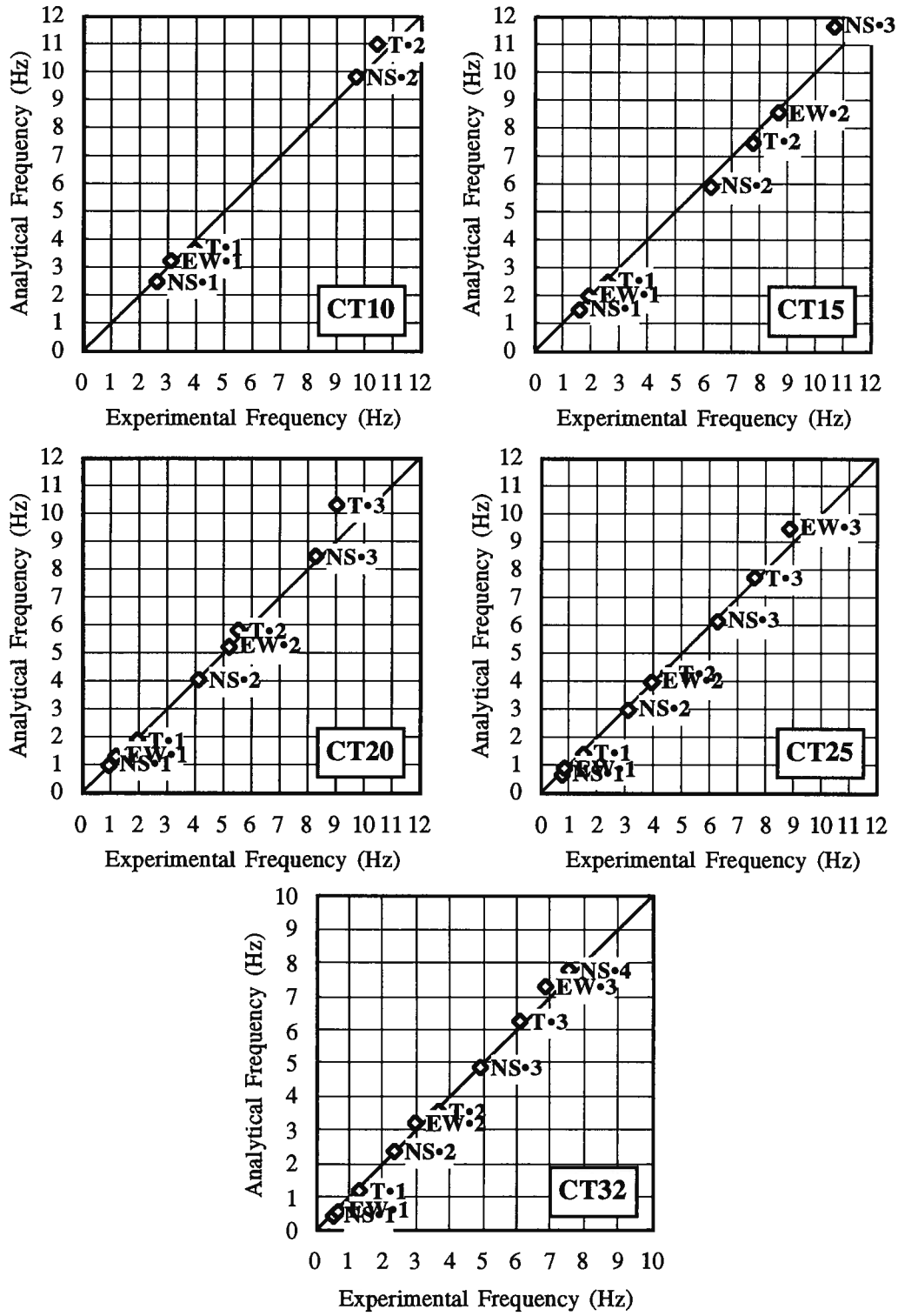

Figure 6.2. Experimental versus analytical frequencies.

6.1.4 COMPARISON OF ANALYTICAL AND EXPERIMENTAL MODE SHAPES

While frequencies are an important measure of dynamic response, vibration mode shapes are perhaps more important since they determine the deformation of the structure. These deformations induce strains and stresses in the structural members. Therefore, it is important that these vibration mode shapes are properly represented by an analytical model.

Experimental mode shapes were generated relative to the center of rotation of each instrumented floor using the programs SLAVE and MAC. This was done so that direct comparisons could be made with the mode shapes produced by ETABS[2]. Comparisons were made based on a MAC analysis and also by overlaying the mode shapes on a plot.

6.1.4.1 Comparison Based On A MAC Analysis

MAC values were generated between analytical and experimental mode shapes. These values are shown in Table 6.1. Overall, the *dominant* components of the corresponding first and second mode shapes were well correlated (MAC values of 99% and 100%) while the corresponding third and fourth mode shapes showed moderate correlation (MAC values of 81% to 91%). These values are shown in **bold** in Table 6.1.

Care had to be taken when interpreting MAC values. In particular, it was found that sometimes experimental and analytical fundamental modes (NS translation, EW translation, and torsional) were all well correlated to each other. For example, the analytical mode EW•1 shows good correlation with the experimental modes NS•1, EW•1, and T•1 (from Table 6.1a, MAC values are 98%, 100%, and 95%, respectively). Though this result was puzzling at first, it was later realized that this made sense since the *shape* of each of these vibration modes was similar. Therefore, it followed that the correlation between the dominant component of these mode shapes should be quite good. An example of similarities in mode shape components is shown in

---

[2]The mode shapes produced by ETABS consists of two translational and a single rotational component of each floor at the centre of mass of that floor.

Figure 6.3. In this figure, the dominant component of the analytical fundamental modes are plotted. As can be seen, the shape of the translational modes are virtually identical while the shape of the torsional mode (rotations) is similar to the others.

Table 6.1. MAC values (percentage) between experimental and analytical mode shapes.

(a) EW component (experimental modes along the top; analytical modes along the left side)

A\X	NS•1	NS•2	NS•3	NS•4	EW•1	EW•2	EW•3	EW•4	T•1	T•2	T•3	T•4
NS•1	84	1	35	11	89	20	7	4	76	37	0	0
EW•1	98	5	13	8	**100**	2	3	5	95	12	0	0
T•1	91	17	10	19	92	1	13	2	89	8	6	3
NS•2	4	12	53	4	2	89	10	1	9	69	1	0
EW•2	1	12	69	1	1	**100**	3	0	0	92	1	0
T•2	2	13	80	4	4	97	6	2	0	95	0	2
NS•3	1	14	34	19	1	58	18	1	0	62	42	5
T•3	0	2	4	66	0	5	82	0	0	2	81	25
EW•3	0	1	15	74	1	13	**89**	1	0	8	79	11
NS•4	0	1	12	69	1	14	81	0	0	8	72	22
T•4	1	0	10	2	1	0	6	67	0	1	4	56
EW•4	1	1	24	18	3	1	15	**90**	0	2	8	56

(b) NS component (experimental modes along the top; analytical modes along the left side)

A\X	NS•1	NS•2	NS•3	NS•4	EW•1	EW•2	EW•3	EW•4	T•1	T•2	T•3	T•4
NS•1	**99**	2	0	5	89	5	3	5	88	10	5	3
EW•1	72	18	0	1	69	6	9	9	42	3	0	0
T•1	20	55	0	5	13	16	6	2	49	54	2	11
NS•2	1	**100**	0	0	0	56	7	1	14	69	7	0
EW•2	1	73	19	1	0	41	1	1	9	38	3	0
T•2	0	77	22	5	0	41	8	9	11	79	39	3
NS•3	1	9	**91**	0	0	5	36	17	6	27	81	0
T•3	1	12	85	5	0	9	20	16	6	30	86	8
EW•3	4	1	18	85	3	9	17	10	1	6	34	81
NS•4	4	1	10	**92**	3	7	29	9	0	4	22	82
T•4	5	2	17	74	5	10	12	7	1	6	36	85
EW•4	3	2	0	1	6	10	4	8	2	0	3	14

(c) rotational component (experimental modes along the top; analytical modes along the left side)

A\X	NS•1	NS•2	NS•3	NS•4	EW•1	EW•2	EW•3	EW•4	T•1	T•2	T•3	T•4
NS•1	70	17	1	1	92	0	0	6	99	1	0	1
EW•1	64	28	3	1	89	2	0	5	97	6	0	1
T•1	70	19	2	1	93	0	1	7	**100**	2	0	1
NS•2	7	94	24	3	15	75	8	3	19	88	3	0
EW•2	1	81	30	2	0	95	12	0	0	97	6	0
T•2	0	82	14	1	1	84	2	0	1	**99**	0	0
NS•3	1	31	98	13	1	40	71	6	3	19	86	2
T•3	0	12	89	6	0	25	76	1	1	6	**94**	0
EW•3	6	1	0	72	7	3	8	32	2	0	1	90
NS•4	3	17	68	78	2	13	31	31	2	10	57	55
T•4	2	1	14	84	4	0	0	13	2	0	12	**81**
EW•4	10	9	12	33	3	2	14	87	3	3	9	30

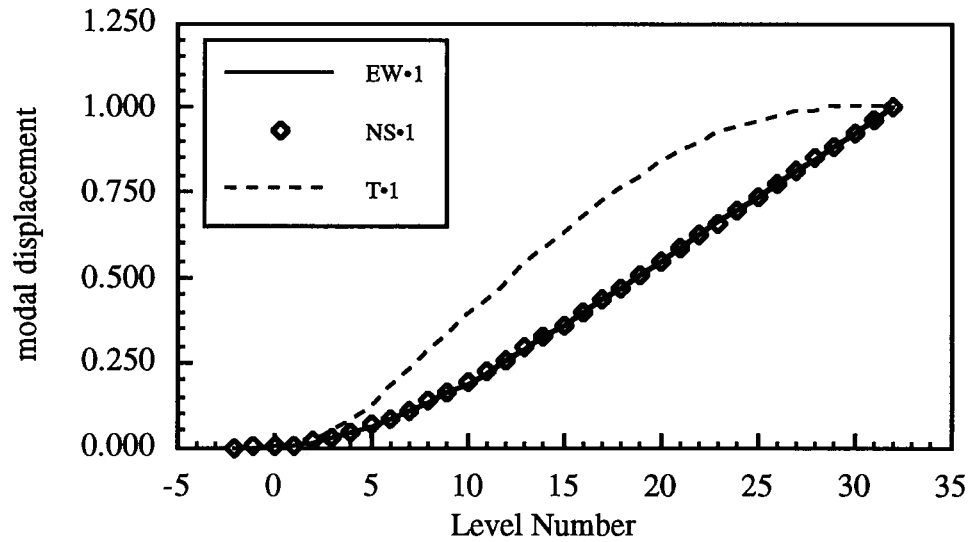

Figure 6.3. Dominant components of the fundamental mode shapes for the base model (CT32).

6.1.4.2 Comparison Based On Overlaying Mode Shape Components

Experimental and analytical mode shapes were normalized such that the displacement at the top storey was equal to unity. Each component of the normalized mode shapes were then plotted for comparison. This proved to be a good method. A typical set of these plots is shown in Figure 6.4. This figure shows the components for both the analytical mode shape (shown by the solid line) and the experimental mode shape (shown by the diamonds) for the second torsional mode of the base model (CT32). In this example, there is a very good match for all three components. Overall, the dominant component of the corresponding vibration mode shapes matched very well. In some cases, one or two of the other components also matched really well. In the other cases, the match was not that good. All of the comparative plots for the base model, CT32, can be found in Appendix H.

Based on the results of the MAC analysis and the comparison described above, it was concluded that the calibrated analytical models have represented the dynamic characteristics of the actual building very well.

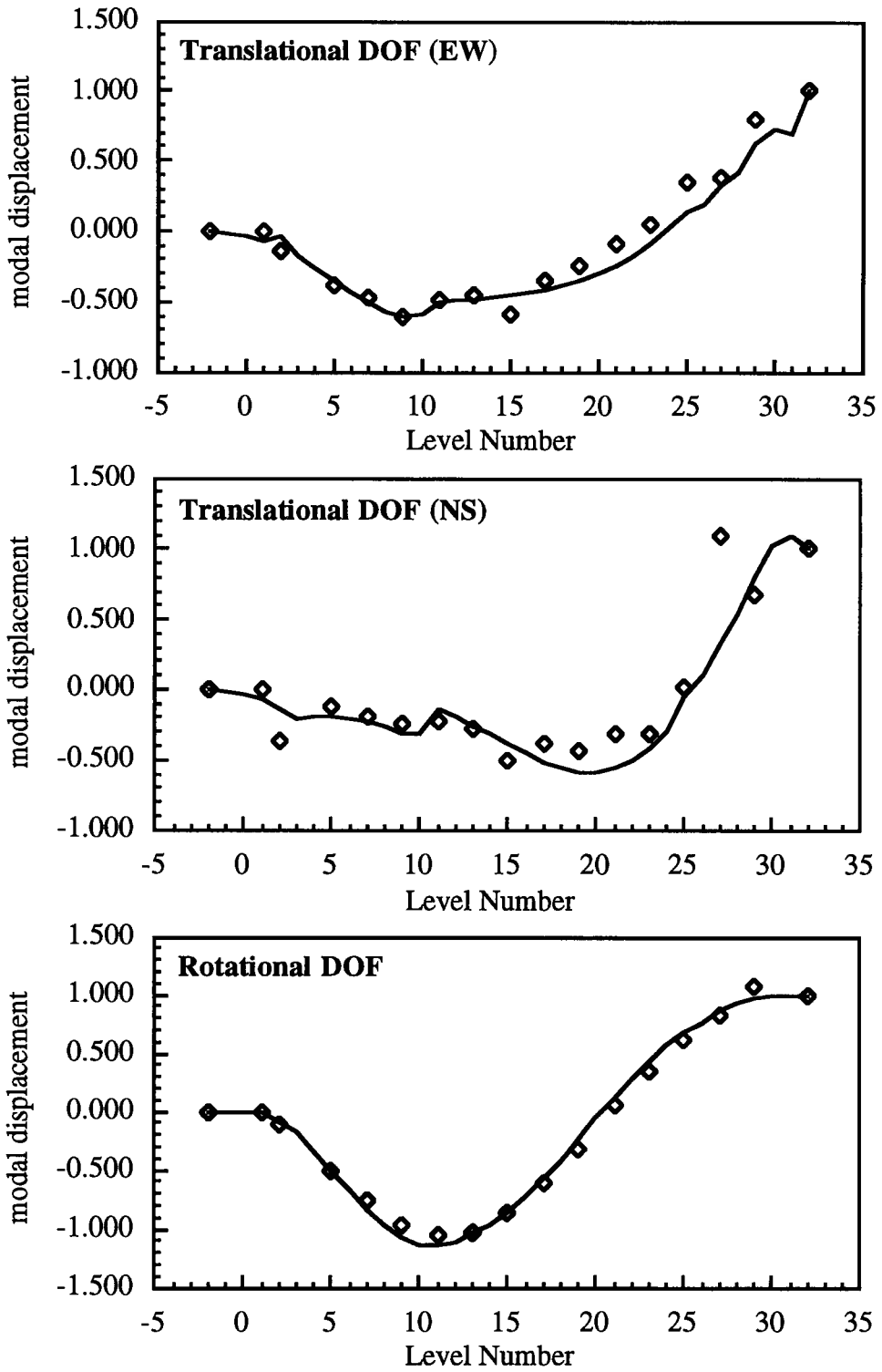

Figure 6.4. Comparison of experimental (◊) and analytical (——) mode shape components for the second torsional mode.

6.2 DESIGN CONSIDERATIONS

Results obtained in this study were also used to assess some aspects of building codes. In this section, periods estimated using code formulae are presented. In addition, seismic demand on the building at each stage in its construction, based on code response spectra, are also discussed.

6.2.1 DESIGN FREQUENCIES

Civil engineering structures are usually prototypes, and therefore prediction of its behaviour both statically and dynamically must be estimated based on fundamental engineering principles along with experience. In the case of City Tower, a dynamic analysis was performed by the structural consultants (Bogdonov Pao Ltd.) in order to understand the torsional behaviour of this building. This analysis was performed using the software package ETABS. However, unlike the model which was developed in this study, the *design* model was more simplified since the purpose was to determine an envelope of seismic loads.

Periods obtained during the design process along with the periods obtained experimentally are shown in Table 6.2. Also shown are periods, T, calculated using expressions in both the National Building Code of Canada (NBCC) (NRC, 1990) and the Uniform Building Code (UBC, 1991). The expression from the NBCC is given by Equation 6.1:

$$T = \frac{0.09h_n}{\sqrt{D_s}} \qquad (6.1)$$

where h_n is the height of the building (in metres) measured from its base, and D_s is the dimension of the wall (in metres) which constitutes the main lateral load-resisting system in the direction parallel to the applied forces. The expression from the UBC is given by Equation 6.2:

$$T = C_t h_n^{\frac{3}{4}}$$

where

$$C_t = \frac{0.1}{\sqrt{A_c}} \qquad (6.2)$$

$$A_c = \sum A_e \left[0.2 + \left(\frac{D_e}{h_n} \right)^2 \right]; \quad \frac{D_e}{h_n} \leq 0.9$$

where h_n is the height of the building (in feet), A_e is the minimum cross-sectional shear area at the first storey (in ft^2), and D_e is the wall length which is oriented parallel to the applied forces (in feet).

Table 6.2. Comparison of measured and design periods for the building.

Mode	NS Translation		EW Translation		Torsion	
	Measured	Design	Measured	Design	Measured	Design
1	- 1.828 s -	2.310 s 2.719 s* 1.891 s**	- 1.552 s -	1.767 s 2.335 s* 1.616 s**	- 0.776 s -	1.000 s - -
2	0.434	0.505	0.341	0.402	0.274	0.334
3	0.205	0.242	0.146	0.202	0.165	-

*NBCC; **UBC

In general, the design periods tended to be longer than those which were measured. However, this is to be expected since the design periods represent the structural response during an earthquake, while the measured periods represent the structural response during ambient conditions. Also worth noting is that the period calculated using the formula in the UBC came very close to the measured periods.

6.2.2 RESPONSE SPECTRA AND SEISMIC DEMANDS

Another consideration in the design process of the structure is its response if an earthquake should occur during its construction. This is a consideration which is often overlooked since the time period over which the construction occurs is quite short relative to the life of the structure. Usually only the loads which act on the structure as a result of the construction process (such as the shoring shown in Figure 3.14) are accounted for.

To illustrate seismic demands of City Tower as it was being constructed, fundamental (translational) periods for both the NS and EW directions of the building were plotted with their corresponding location on design "spectra" from both the NBCC and UBC. These spectra were normalized for Vancouver[3]. In addition, the fundamental periods estimated from the dynamic

[3] for NBCC "spectra": v=0.2, Z_a=Z_v, F=1; for UBC "spectra": seismic zone = 2b, S=1

analysis and the code equations were also included in this plot which is shown in Figure 6.5. According to this plot, it appears that the seismic demand on City Tower, in terms of spectral acceleration, was very high at the onset of construction but gradually decreased as the building was erected. In addition to this, the seismic demand corresponding to the periods obtained experimentally, analytically, or by using the code equations are similar.

Quantifying seismic demand in terms of spectral acceleration, though, is very misleading. In particular, while there is a high spectral acceleration early on in construction, only a portion of the total building mass is present. Therefore, the actual *force* acting on the structure is about the same. In order to demonstrate this, base shear and overturning moments were calculated in accordance with clause 4.1.9.1 of the NBCC. This was done using the fundamental translational periods obtained from the five ambient vibration tests at City Tower. The results appear in Figure 6.6. In this figure, the base shear is shown by the bars while the overturning moments are shown by the lines. As can be seen, the seismic demand in terms of base shear is constant throughout the construction phase. The overturning moment, however, increases as the building increases in both height and weight. Overall, it would appear the seismic demand on the structure during its construction phase is either lower or equal to the demand corresponding to the finished structure.

One final note should be made about the proximity of the frequencies as the building was constructed. As can be seen in either Table 5.3 or Figure 5.16, as the height of the building increases, frequencies corresponding to the higher modes come very close to the fundamental frequencies. Therefore, it is likely that these modes will get excited thereby contributing to the dynamic response of the structure during an earthquake. This confirms a provision in the NBCC whereby a portion of the lateral loads is concentrated at the top of the structure (NBCC clause 4.1.9.1(13)) to account for the contribution of higher modes.

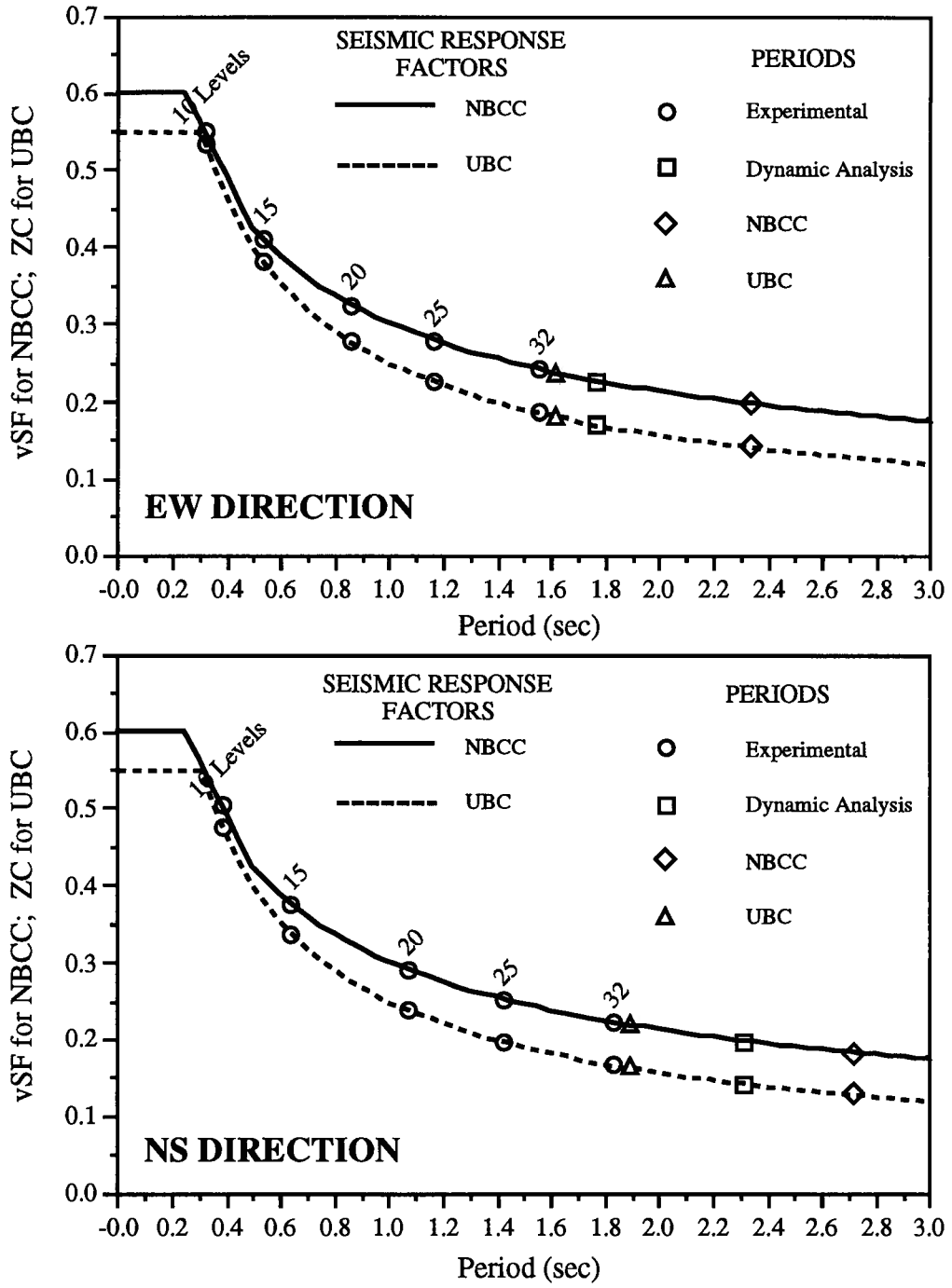

Figure 6.5. Spectral Acceleration curves from the NBCC and UBC building codes. Also shown are periods for the EW and NS directions obtained from ○ measurements, code equations (◇ NBCC and △ UBC) and □ dynamic analysis.

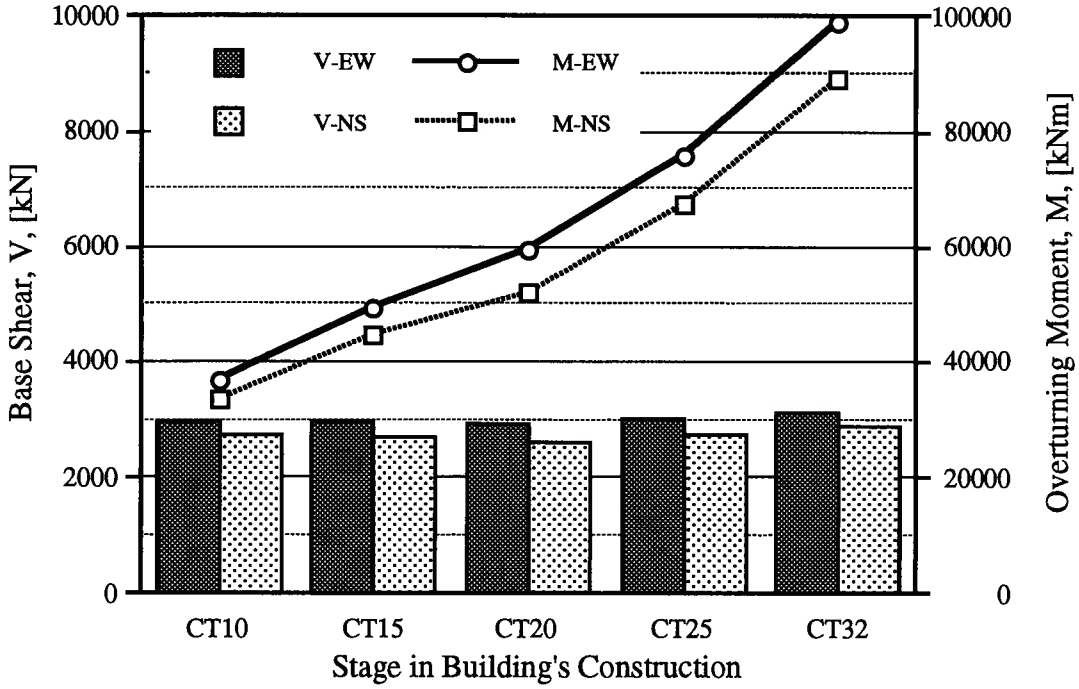

Figure 6.6. Base shears and overturning moments for the building, during its construction phase, determined using procedure outlined in the NBCC (R=3.5).

CONCLUSIONS

A number of conclusions can be drawn from the results of this investigation. These have been grouped into four sections; namely Ambient Vibration Testing, General Dynamic Behaviour, Special Dynamic Behaviour, and Analytical Analysis.

AMBIENT VIBRATION TESTING

- Determining dynamic characteristics of a building using ambient vibrations and signal processing functions is a very practical and useful method.
- Reliable estimates of damping are very difficult, if not impossible, to obtain from ambient vibration records.

GENERAL DYNAMIC BEHAVIOUR

- Asymmetry in building mass distribution can lead to significant rotational motion and modal coupling. Therefore, the dynamic consequences of setbacks should be carefully considered in the design of a building.
- The shape of the vibration modes remain invariant with the increase in building height.
- Modal frequencies decrease with increase in building height and mass (obviously). In addition, the spacing of the frequencies corresponding to the higher modes and the fundamental modes decreases as the building height increases. Also, translational modal frequencies are more sensitive to changes in height compared with torsional modal frequencies.

SPECIAL DYNAMIC BEHAVIOUR

The following conclusions are limited to the type of building considered herein. Moreover, the behaviour described below is for low amplitude vibrations. This behaviour may change during high amplitude vibrations.

- Architectural components do not appear to affect the frequency of vibration or the *shape* of the vibration modes. In addition, there is no significant changes in damping levels during ambient levels of vibration.
- The building core, which is often referred to as a *shear wall*, deforms in flexure during translational modes of vibration. There in no vertical motion of the core associated with the torsional modes of vibration.
- There is no significant base motion associated with this building. This can be attributed to the underlying soil which is very stiff as well as the stiffening effect created by the underground

parking structure.

ANALYTICAL ANALYSIS

- The dynamic behaviour of this building, in terms of frequencies and mode shapes, can be accurately represented using dynamic analysis.
- The expressions for estimating fundamental translational periods in building codes such as the NBCC and UBC appear to be reasonable for low levels of vibration.
- The calculated base shear and overturning moments for this building, during its construction phase, do not exceed those expected during its service life. Therefore, assessing these demands on a building of this type, during its (short) construction phase, does not seem warranted as part of the design process.

RECOMMENDATIONS FOR FUTURE RESEARCH

While this project explored many aspects of the dynamic response of this building, there are several additional aspects worth studying. First, an analysis of the soil-structure interaction of this building could be performed using appropriate signal processing methods. Second, further refinements could be made to the ETABS analytical model to improve the correlation between the analytical and experimental mode shapes and corresponding periods. Finally, a more detailed dynamic analysis could be performed using the ETABS models. In particular, stress distributions throughout the structure, resulting from a *design* earthquake, could be studied. Further, this analysis could be repeated using simplified models of the building to determine what level of detail is warranted in this type of analysis.

In future ambient vibration studies of buildings with configurations similar to City Tower, the sensor layout used for the last test, CTTC, is recommended. A great deal of information was obtained using this setup, and in conjunction with the software program SLAVE, well refined mode shapes were obtained. In addition, the length of the measurements (data segments) should be increased to improve the resolution and reduce the bias and random errors associated with the signal processing functions.

It would be interesting to conduct another ambient vibration survey of City Tower several years from now to determine if there have been any significant changes in its dynamic behaviour. However, this may be difficult to implement since public reaction to a "dynamic test" may be unfavourable.

Finally, VISUAL could be modified to incorporate the *slave node generator* routine used in the program SLAVE. This would make the analysis of building mode shapes more efficient in terms of time and computer disk space.

NOMENCLATURE

CW(f)	coherence window
f	frequency (Hz)
f_c	Nyquist frequency (Hz)
Δf	frequency resolution/increment (Hz)
G(f)	power spectral (autospectral) density function
H(ω)	transfer function
L_s	segment length (points)
M(f)	potential modal ratio function
P(ω), {P(ω)}	loading function in the frequency domain - single component and vector
PW(f)	phase window
t	time (sec)
Δt	time increment (seconds)
T	period (seconds)
T(f)	transfer function
x(t), {x(t)}	displacement response in the time domain - single component and vector
X(ω), {X(ω)}	displacement response in the frequency domain - single component and vector
X*(ω), {X*(ω)}	complex conjugate of the displacement response - single component and vector
$\ddot{X}(\omega), \{\ddot{X}(\omega)\}$	acceleration response in the frequency domain - single component and vector
y(t)	modal amplitude in the time domain
ϕ, {ϕ}	time invariant mode shape - single component and vector
$\Phi(f)$	modulus of the transfer function, T(f)
$\gamma 2(f)$	coherence function
$\Theta(f)$	phase function
ω	radial frequency (equal to $2\pi f$) (radians/s)

ABBREVIATIONS

ANPSD	Averaged Normalized Power Spectral Density
ASD	Autospectral Density
AV	Ambient Vibration
CF	Coherence Function
CSMIP	California Strong Motion Instrumentation Program
CT10	City Tower ambient vibration test - 10 levels completed
CT15	City Tower ambient vibration test - 15 levels completed
CT20	City Tower ambient vibration test - 20 levels completed
CT25	City Tower ambient vibration test - 25 levels completed
CT32	City Tower ambient vibration test - 32 levels completed
CTTC	City Tower ambient vibration test - Tower Completed
EW	East-West (direction)
FBA	Force-Balance-Accelerometer
FRF	Frequency Response Function
HBES	Hybrid Bridge Evaluation System
NBCC	National Building Code of Canada
NS	North-South (direction)
PF	Phase Function
PMR	Potential Modal Ratio
PSD	Power Spectral Density
SISO	Single Input Single Output
TF	Transfer Function
UBC	Uniform Building Code (or University of British Columbia)
w.r.t	With Respect To

REFERENCES

Accredited Standards Committee S2, Mechanical Shock And Vibration. (1990) American *National Standard - Vibration Of Buildings - Guidelines For The Measurement Of Vibrations And Evaluation Of Their Effects On Buildings* (ANSI S2.47-1990), New York, U.S.A.

Baker McGarva Hart Inc. (1992) *City Tower, 1155 Homer Street, Vancouver, B.C. Architectural Contract Drawings* (A1.01-A10.02). Vancouver, B.C., Canada.

Bendat, J.S., Piersol, A.G. (1993) **Engineering Applications of Correlation and Spectral Analysis, Second Edition**. John Wiley and Sons, Inc., New York, U.S.A.

Binstock, A., Babcock, D.P., and Luse, M. (1991) **HP LaserJet Programming**. Addison Wesley, Don Mills, Ontario, Canada.

Bogdonov Pao Associates Ltd. (1992) *City Tower, 1155 Homer Street, Vancouver, B.C. Structural Contract Drawings* (S1-S21). Vancouver, B.C., Canada.

Borland International Incorporated. (1991-92) **Borland C++** Version 3.1. Scotts Valley, California, U.S.A.

Brownjohn, J.M.W. (1988) **Assessment Of Structural Integrity By Dynamic Measurements**. Ph.D. Thesis, University of Bristol, United Kingdom.

Çelebi, M., Safak, A. et al. (1987) *Integrated Instrumentation Plan For Assessing The Seismic Response Of Structures - A Review Of The Current USGS Program.* USGS Circular 947. California, U.S.A.

Clough, R.W. and Penzien, J. (1975) **Dynamics of Structures**. McGraw Hill, New York, U.S.A.

CSI, Ltd. (1992) **ETABS Three Dimensional Analysis of Building Systems - Users Manual**. Computers and Structures, Inc., Berkeley, California, U.S.A.

Dally, J.W., Riley, W.F., and McConnell, K.G. (1993) **Instrumentation For Engineering Measurements, 2nd Edition**. John Wiley and Sons, Inc., New York, U.S.A.

Diehl, J. (1991) *Ambient Vibration Survey: Application, Theory And Analytical Techniques*. Application Note #3. Kinemetrics Systems, Pasadena California, U.S.A.

EDI Ltd. (1994) **U2, V2, and P2, Manual Version 2.0**. Experimental Dynamic Investigations Ltd., Vancouver, B.C., Canada.

Ewins, D.J. (1984) **Modal Testing: Theory and Practice**. John Wiley and Sons Inc., New York, U.S.A.

Felber, A.J. (1993) **Development Of A Hybrid Bridge Evaluation System**. Ph.D. thesis, University of British Columbia, Canada.

Hewlett-Packard Company. (1990) **HP PCL 5 Printer Language Technical Reference Manual**. (HP Part #33459-90903).

Humar, J.L. (1990) **Dynamics of Structures**. Prentice Hall, New Jersey, U.S.A.

KDAC 500. (1989) *Keithley KDAC500 Data Acquisition and Control Software* (Document #501-915-01 Rev. C; Software: KDAC500/B Version 1.4, P/N: 500-886; IBIN-A Interface card: Document # 501-910-01 Rev. C). Keithley Instruments Inc., Cleveland, Ohio, U.S.A.

Keithley 575. (1989) *Model 575 Measurement and Control System* (Document # 575-901-01 Rev. C). Keithley Instruments Inc., Cleveland, Ohio, U.S.A.

Kernighan, B.W. and Ritchie, D.M. (1988) **The C Programming Language, 2nd Edition**. Prentice Hall, New Jersey, U.S.A.

Luz, E. (1992) *Experimental Modal Analysis Using Ambient Vibration.* **International Journal Of Analytical And Experimental Modal Analysis** (v7 n1 pp.29-39).

Marshall, R.D., Phan, L.T., and Çelebi, M. (1994) *Full-Scale Measurement Of Building Response To Ambient Vibration And The Loma Preita Earthquake.* **Fifth U.S. National Conference on Earthquake Engineering Proceedings** (Volume II, pp. 661-670).

Microsoft Corporation. (1991) **Microsoft MS-DOS User's Guide and Reference - Operating System 5.0.**

Newland, D.E. (1975) **An Introduction to Random Vibrations and Spectral Analysis**. Longman Group Ltd., New York, U.S.A.

NRC (1990) **National Building Code Of Canada**. Associate Committee Of The National Building Code, National Research Council Of Canada, Ottawa.

Okauchi, I., Miyata, T., Tatsumi, M. and Kiyota, R. (1992). *Dynamic Field Tests and Studies on Vibration Characteristics of Long Span Suspension Bridges.* **ISCE Journal of Structural Engineering and Earthquake Engineering, 9** (pp.89-100).

Pardoen, G.C. (1983) *Ambient Vibration Test Results Of The Imperial County Services Building.* **Bulletin Of The Seismological Society Of America** (Volume 73, No. 6, pp. 1895-1902).

Rojahn, C. and Matthiesen, M. (1977) *Earthquake Response And Instrumentation Of Buildings* . **Journal Of The Technical Councils of ASCE**.

Shakal, A., Huang, M., Reichle, M., Ventura, C., Cao, T., Sherburne, R., Savage, M., Darragh, R., and Petersen, C. (1989) *Csmip Strong-Motion Records From The Santa Cruz Mountains (Loma Prieta), California Earthquake Of 17 October 1989*. Report # OSMS 89-06. California Department of Conservation, Division of Mines and Geology, Office of Strong Motion studies.

Stroustrup, B. (1993) **The C++ Programming Language, 2nd Edition**. Addison Wesley, New York, U.S.A.

To, Ngok-Ming (1982) **The Determination Of Structural Dynamic Properties Of Three Buildings In Vancouver, B.C., From Ambient Vibration Surveys**. M.A.Sc. thesis, University of British Columbia, Canada.

UBC (1991) **Uniform Building Code**. International Conference of Building Officials, Whittier, California, U.S.A.

A

APPENDIX A
DETAILS OF AMBIENT VIBRATION SURVEYS

This appendix shows the exact location of each sensor for each of the six City Tower ambient vibration surveys. In addition, filenames, attenuation and filter settings on the signal conditioner, and the nodes corresponding to the VISUAL input files are presented.

A.1 BUILDING INSTRUMENTATION

Figures A.1 to A.6 show the south elevation of the building at the particular stage in construction when the ambient vibration measurements were taken. Instrumentation on all of the floors where ambient vibration measurements were taken, is shown in these figures. In addition to this, floor elevations (relative to the ground floor) of each level are also shown.

A.2 EXACT SENSOR LOCATIONS AND CONDITIONING DETAILS

A.2.1 AMBIENT VIBRATION MEASUREMENTS

Specific details about the measurements are summarized in tables A.1 through A.6. These tables list each floor which was measured, along with the filename containing the ambient vibration data (in *.bbb format) and conditioning details (attenuation and filters). Each channel number has been cross-referenced with the node number used in the structure file used to assemble and animate the mode shapes in the program VISUAL.

A.2.2 SENSOR LOCATIONS

Each of the sensor setups is cross-referenced with figure A.7. The latter figure shows the exact locations and orientations of all of the setups described in the aforementioned tables.

The following legend applies to figures A.1 through A.6.

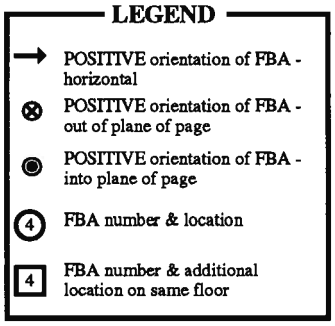

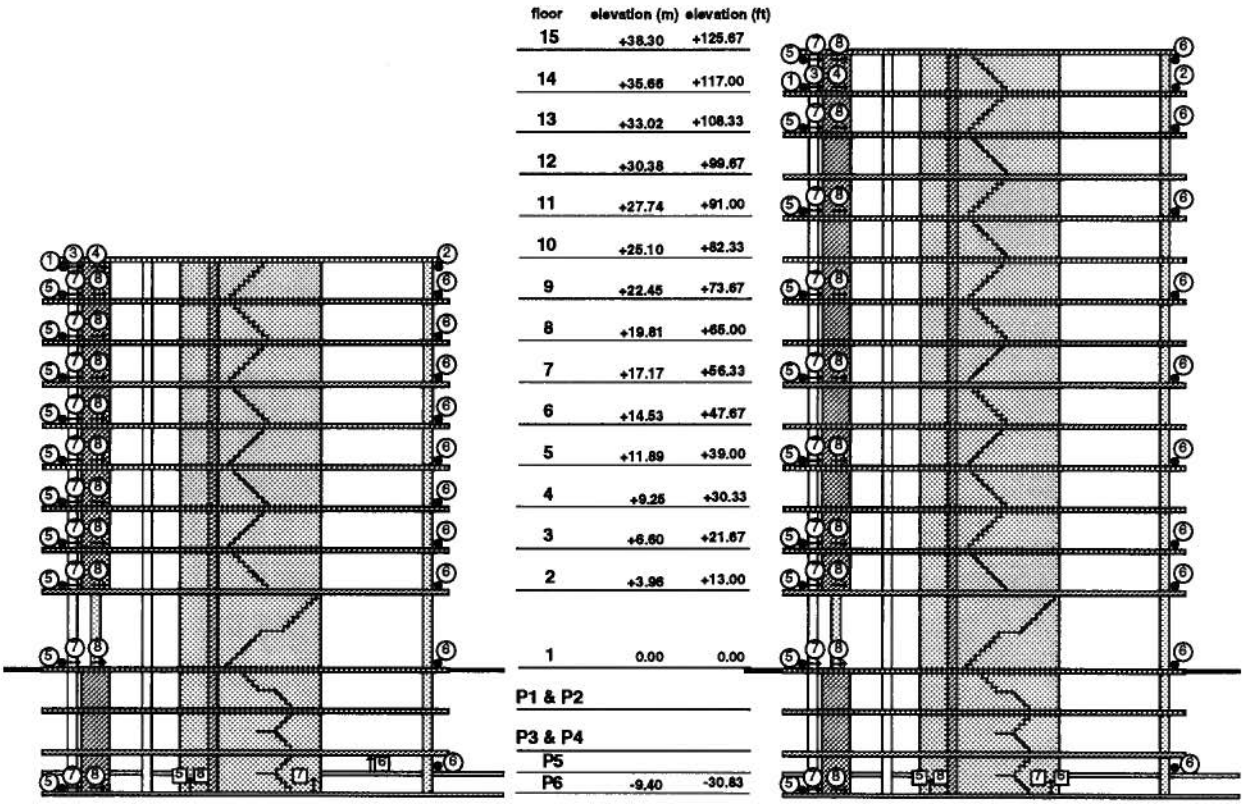

Figure A.1. Instrumentation of the building for the first ambient vibration survey; 10 levels completed (CT10).

Figure A.2. Instrumentation of the building for the second ambient vibration survey; 15 levels completed (CT15).

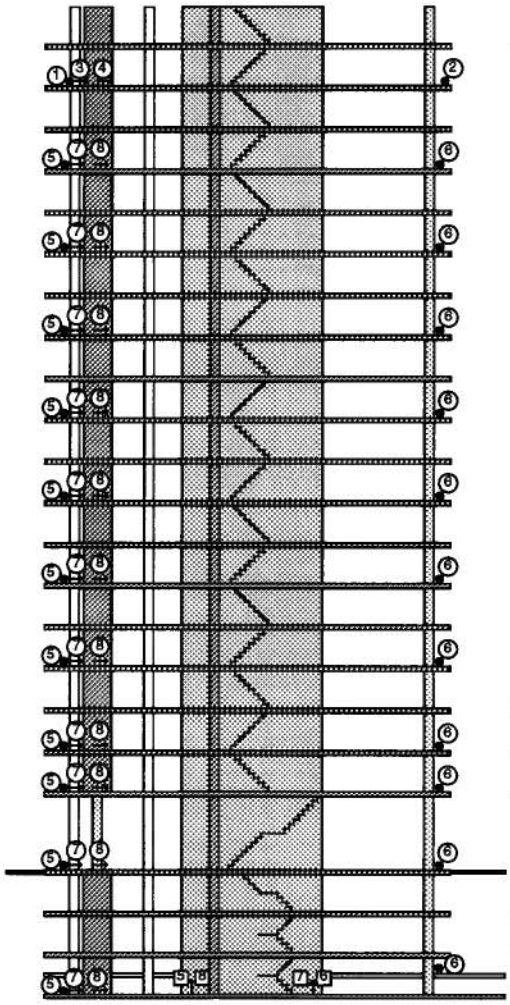

floor	elevation (m)	elevation (ft)
26	+67.36	+221.00
25	+64.72	+212.33
24	+62.08	+203.67
23	+59.44	+195.00
22	+56.79	+186.33
21	+54.15	+177.67
20	+51.51	+169.00
19	+48.87	+160.33
18	+46.23	+151.67
17	+43.59	+143.00
16	+40.94	+134.33
15	+38.30	+125.67
14	+35.66	+117.00
13	+33.02	+108.33
12	+30.38	+99.67
11	+27.74	+91.00
10	+25.10	+82.33
9	+22.45	+73.67
8	+19.81	+65.00
7	+17.17	+56.33
6	+14.53	+47.67
5	+11.89	+39.00
4	+9.25	+30.33
3	+6.60	+21.67
2	+3.96	+13.00
1	0.00	0.00
P1 & P2		
P3 & P4		
P5		
P6	-9.40	-30.83

Figure A.3. Instrumentation of the building for the third ambient vibration survey; 20 levels completed (CT20).

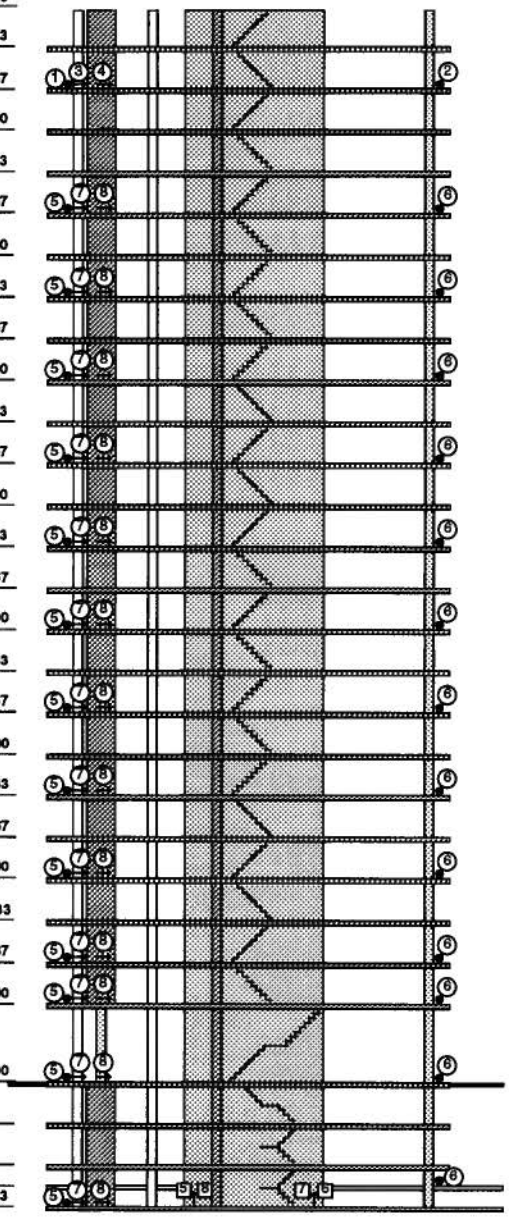

Figure A.4. Instrumentation of the building for the fourth ambient vibration survey; 25 levels completed (CT25).

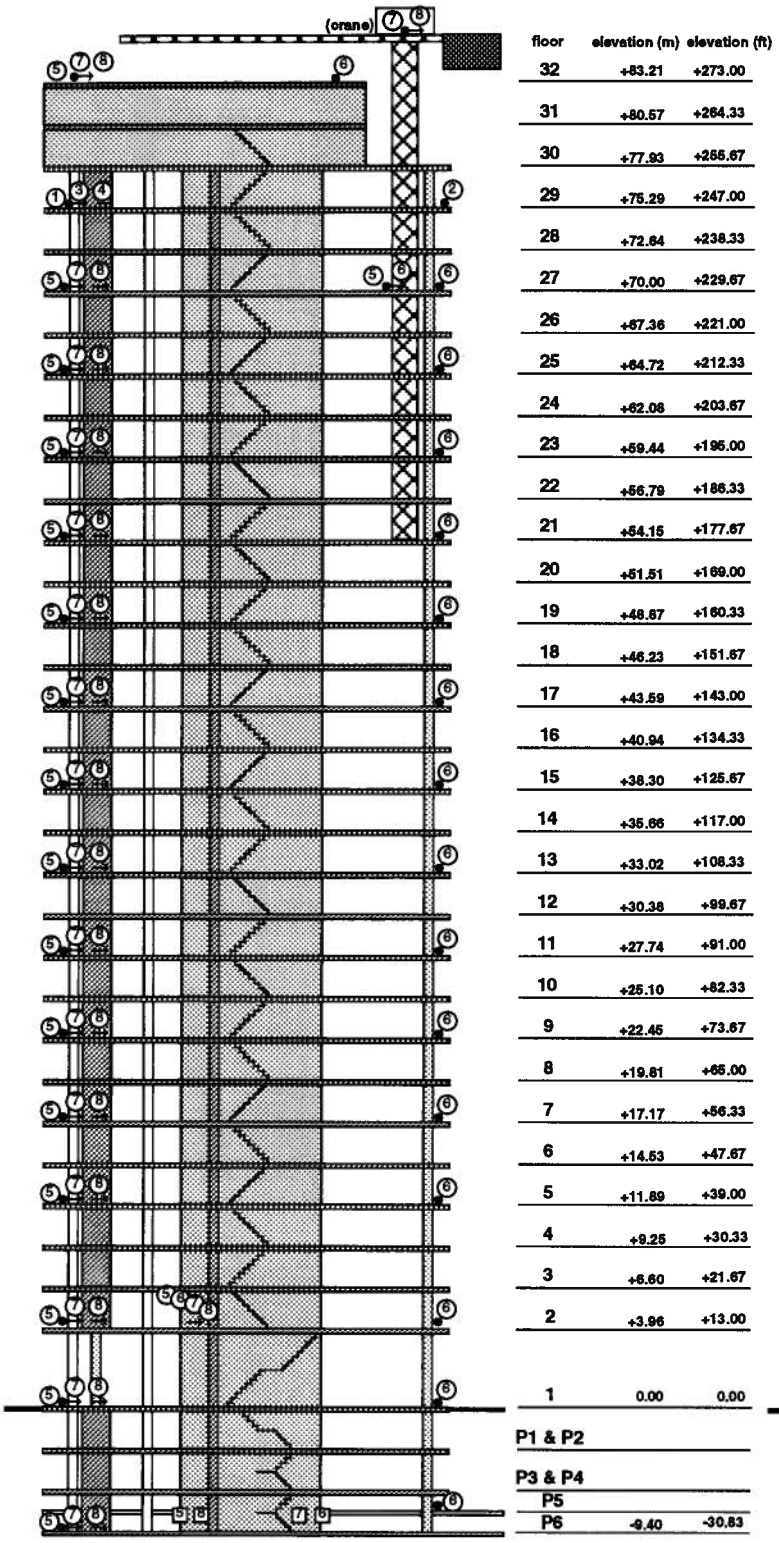

floor	elevation (m)	elevation (ft)
32	+83.21	+273.00
31	+80.57	+264.33
30	+77.93	+255.67
29	+75.29	+247.00
28	+72.64	+238.33
27	+70.00	+229.67
26	+67.36	+221.00
25	+64.72	+212.33
24	+62.08	+203.67
23	+59.44	+195.00
22	+56.79	+186.33
21	+54.15	+177.67
20	+51.51	+169.00
19	+48.87	+160.33
18	+46.23	+151.67
17	+43.59	+143.00
16	+40.94	+134.33
15	+38.30	+125.67
14	+35.66	+117.00
13	+33.02	+108.33
12	+30.38	+99.67
11	+27.74	+91.00
10	+25.10	+82.33
9	+22.45	+73.67
8	+19.81	+65.00
7	+17.17	+56.33
6	+14.53	+47.67
5	+11.89	+39.00
4	+9.25	+30.33
3	+6.60	+21.67
2	+3.96	+13.00
1	0.00	0.00
P1 & P2		
P3 & P4		
P5		
P6	-9.40	-30.83

Figure A.5. Instrumentation of the building for the fifth ambient vibration survey; all 32 levels completed (CT32).

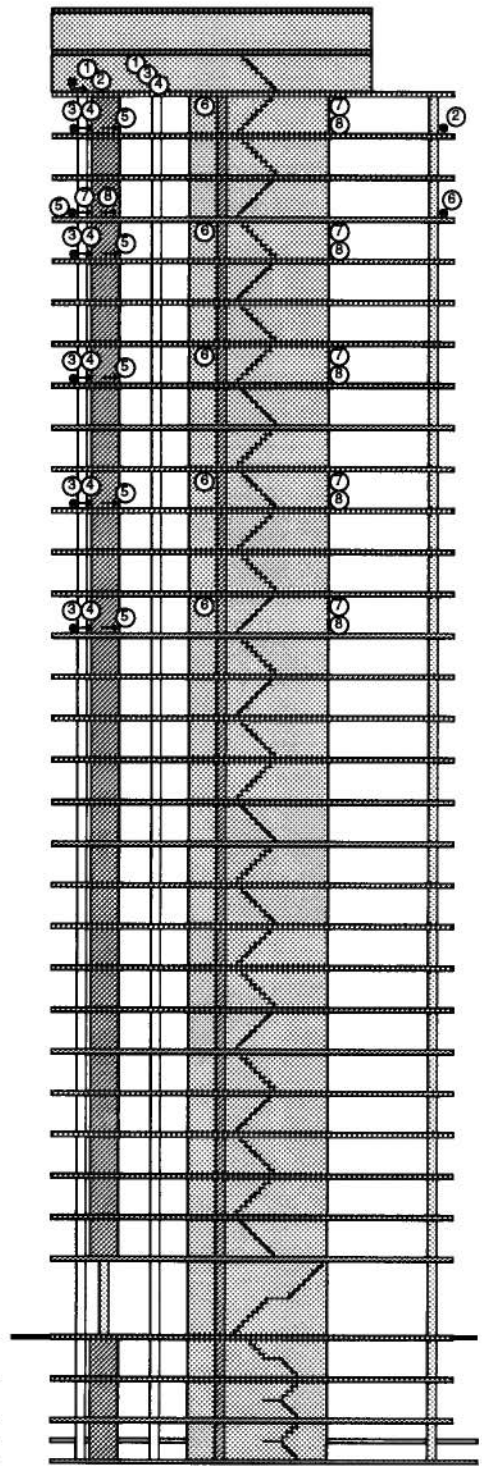

Figure A.6. Instrumentation of the building for the final ambient vibration survey; tower completed (CTTC).

Table A1. CT10 FBA setups and locations, conditioning and sampling details, VISUAL Nodal coordinates

setup #	setup figure number	floor(s)	filename prefix	att. [dB]	hi/lo pass filters [Hz]	Nyquist *f*	comments	VISUAL Nodal Coordinates							
								1	2	3	4	5	6	7	8
1	d/d	9	ct1009	12	0/12.5	20	saturation in segment #4	34E	35N	36N	36E	31E	32N	33E	33N
2	d	8	ct1008	12	0/12.5	20						28E	29N	30E	30N
3	d	7	ct1007	18	0/12.5	20						25E	26N	27E	27N
4	d	6	ct1006	18	0/12.5	20	worker dismantled FBA #5					22E	23N	24E	24N
5	d	5	ct1005	18	0/12.5	20						19E	20N	21E	21N
6	d	4	ct1004	18	0/12.5	20	short in channel #6					16E	17N	18E	18N
7	d	3	ct1003	18	0/12.5	20						13E	14N	15E	15N
8	c	2	ct1002	18	0/12.5	20	drift in channel #2					10E	11N	12E	12N
9	b	1	ct1001	18	0/12.5	20						07E	08N	09E	09N
10	a	P5/P6	ct10ph	18	0/12.5	20	drift in channels #6,7,8					04E	05N	06E	06N
11	a	P5/P6	ct10pv	12	0/12.5	20						00V	01N	02V	03V

reference: top of columns on level 9

Table A2. CT15 FBA setups and locations, conditioning and sampling details, VISUAL Nodal coordinates

setup #	setup figure number	floor(s)	filename prefix	att. [dB]	hi/lo pass filters [Hz]	Nyquist *f*	comments	VISUAL Nodal Coordinates							
								1	2	3	4	5	6	7	8
1	k/e	P6	ct15pv	0	0/12.5	20	short in all channels, segment #8	31N	32N	31E	33E	00V	01V	02V	03V
2	e	P5/P6	ct15ph	0	0/12.5	20						04N	05N	04E	06E
3	k/k	15	ct1515	6,seg.#1 18,seg.#2-8	0/12.5	20	some shorts; especially channels #2,6					34N	35N	34E	36E
4	l	13	ct1513	12	0/12.5	20	drift in channels #2,3,6,7,8					28N	29N	28E	30E
5	l	11	ct1511	18	0/12.5	20	"jumps" in channels #2,3,4,6,7,8					25N	26N	25E	27E
6	j	9	ct1509	12	0/12.5	20	short in all channels; anomalies in channels #6,8					22N	23N	22E	24E
7	j	7	ct1507	18	0/12.5	20	short in all channels; anomolies in channels #4,6,7,8					19N	20N	19E	21E
8	j	5	ct1505	12	0/12.5	20	anomolies in channels #6,7,8					16N	17N	16E	18E
9	j	3	ct1503	12	0/12.5	20	anomolies in channels #2,3,4,6,7,8					13N	14N	13E	15E
10	h	2	ct1502	12	0/12.5	20	"jumps" in all channels					10N	11N	10E	12E
11	f	1	ct1501	12	0/12.5	20	drift in channel #2					07S	08N	07E	09E

reference level 14

Table A3. CT20 FBA setups and locations, conditioning and sampling details, VISUAL Nodal coordinates

setup #	setup figure number	floor(s)	filename prefix	att. [dB]	hi/lo pass filters [Hz]	Nyquist *f*	comments	VISUAL Nodal Coordinates							
								1	2	3	4	5	6	7	8
1	m/l	17	ct2017	0	0/12.5	20	drift in channels #6,7,8; short and offset in channel #6	37N	38N	37E	39W	34N	35N	34E	36E
2	l	15	ct2015	0	0/12.5	20		reference level 19				31N	32N	31E	33E
3	l	13	ct2013	0	0/12.5	20	shorts in channels #5,6,7,8					28N	29N	28E	30E
4	l	11	ct2011	0	0/12.5	20	shorts in channels #5,6,7 - segment #1					25N	26N	25E	27E
5	j	9	ct2009	0	0/12.5	20	major drift in channels #4,6 - segment #1,2					22N	23N	22E	24E
6	j	7	ct2007	0	0/12.5	20	major drift in channels #4,6 - segment #1,2					19N	20N	19E	21E
7	j	5	ct2005	0	0.1/12.5	20						16N	17N	16E	18E
	j	19	ct20dn	0	0.1/12.5	20	man excited in NS direction, 1 segment, clipping								
8	j	3	ct2003	0	0.1/12.5	20						13N	14N	13E	15E
9	h	2	ct2002	0	0.1/12.5	20						10N	11N	10E	12E
10	f	1	ct2001	0	0.1/12.5	20						07N	08N	07E	09E
11	e	P5/P6	ct20ph	0	0.1/12.5	20						04N	05N	04E	06E
	m	19	ct20dm	6	0.1/12.5	20	man excited in NS direction, 2 segments, clipping								
	m		ct20d3	18	0.1/12.5	20	man excited in NS direction, 4 segments								
12	e	P6	ct20pv	18	0.1/12.5	20						00V	01V	02V	03V
	e		ct20pr	12	0.1/out	100									

Table A4. CT25 FBA setups and locations, conditioning and sampling details, VISUAL Nodal coordinates

setup #	setup figure number	floor(s)	filename prefix	att. [dB]	hi/lo pass filters [Hz]	Nyquist *f*	comments	VISUAL Nodal Coordinates							
								1	2	3	4	5	6	7	8
1	m/l	21	ct2521	6	0.1/12.5	20	short in channel #6	43N	44N	43E	45E	40N	41N	40E	42E
2	l	19	ct2519	0	0.1/12.5	20	drift in channel #4					37N	38N	37E	39E
3	l	17	ct2517	6	0.1/12.5	20	channel #4 suspect	reference level 24				34N	35N	34E	36E
4	l	15	ct2515	6	0.1/12.5	20	channel #4 suspect					31N	32N	31E	33E
5	l	13	ct2513	0	0.1/12.5	20	channel #4 suspect					28N	29N	28E	30E
6	l	11	ct2511	0	0.1/12.5	20	channel #4,8 suspect; saturation in segment #5					25N	26N	25E	27E
7	j	9	ct2509	0	0.1/12.5	20	channel #4 suspect					22N	23N	22E	24E
8	j	7	ct2507	6	0.1/12.5	20	channel #4 suspect					19N	20N	19E	21E
9	j	5	ct2505	0	0.1/12.5	20	channel #4 suspect					16N	17N	16E	18E
	j		ct255r	18	0.1/out	100	channel #4 suspect								
10	j	3	ct2503	0	0.1/12.5	20	channel #4 suspect					13N	14N	13E	15E
11	h	2	ct2502	0	0.1/12.5	20	channel #4 suspect; shorts in channel #6; windy					10N	11N	10E	12E
12	g	1	ct2501	6	0.1/12.5	20	channel #4 suspect, only 6 segments collected;					07N	08N	07E	09E
13	e	P5/P6	ct25ph	12	0.1/12.5	20	channel #4 suspect; windy					04N	05N	04E	06E
14	e	P6	ct25pv	6	0.1/12.5	20	data clipped					00V	01V	02V	03V
	e		ct25pr	12	0.1/12.5	100									
	e		ct25pf	6	0.1/out	100	channels 4,5,6 corrupt								

Table A5. CT32 FBA setups and locations, conditioning and sampling details, VISUAL Nodal coordinates

setup #	setup figure number	floor(s)	filename prefix	att. [dB]	hi/lo pass filters [Hz]	Nyquist *f*	comments	VISUAL Nodal Coordinates							
								1	2	3	4	5	6	7	8
1	o/q	crane, 27	ct32ch	12	0.1/12.5	20		52N	53N	52E	54E		TOP		TOP
2	p	32	ct3232	0	0.1/12.5	20						55N	56N	55E	57E
3	l	27	ct3227	0	0.1/12.5	20						49N	50N	49E	51E
	l		ct32d1	0	**0.1/5**	**10**									
4	l	25	ct3225	0	0.1/12.5	20	short in channel #5					46N	47N	46E	48E
5	l	23	ct3223	6	0.1/12.5	20	channel #5 suspect, att. possibly set to "0"					43N	44N	43E	45E
6	l	21	ct3221	0	0.1/12.5	20	drift in channel #6					40N	41N	40E	42E
7	l	19	ct3219	0	0.1/12.5	20						37N	38N	37E	39E
8	l	17	ct3217	0	0.1/12.5	20	drift in channel #5 - segment #1					34N	35N	34E	36E
9	l	15	ct3215	0	0.1/12.5	20						31N	32N	31E	33E
10	l	13	ct3213	0	0.1/12.5	20	short and drift in channel #6					28N	29N	28E	30E
11	l	11	ct3211	0	0.1/12.5	20						25N	26N	25E	27E
12	j	9	ct3209	0	0.1/12.5	20	drift in channel #8					22N	23N	22E	24E
13	j	7	ct3207	0	0.1/12.5	20	short in channel #6					19N	20N	19E	21E
14	j	5	ct3205	0	0.1/12.5	20						16N	17N	16E	18E
15	h	2	ct3202	6	0.1/12.5	20	channel #5 suspect, att. possibly set to "0"					10N	11N	10E	12E
16	i		ct32th	0	0.1/12.5	20									
17	g	1	ct3201	0	0.1/12.5	20						07N	08N	07E	09E
18	e	P5/P6	P5/P6	0	0.1/12.5	20						04N	05N	04E	06E
19	e	P6	ct20ph	0	0.1/12.5	20						00V	01V	02V	03V

reference level 29

Table A6. CTTC FBA setups and locations, conditioning and sampling details, VISUAL Nodal coordinates

setup #	setup figure number	floor(s)	filename prefix	att. [dB]	hi/lo pass filters [Hz]	Nyquist *f*	comments	VISUAL Nodal Coordinates							
								1	2	3	4	5	6	7	8
1	t	29	cttcco	12	0.1/12.5	20									
2	r,v	27/29	cttcd1	0	**0.1/5**	**10**									
3	u/s	17	cttc17	6	0.1/12.5	20		32N	33E	01N	01E	03E	04V	05V	06V
	s		cttc40	12	**0.1/25**	**40**	workers hammering causing transient spikes in data								
4	s	20	cttc20	6	0.1/12.5	20	channel #7 dead			07N	07E	09E	10V	11V	12V
5	s	23	cttc23	6	0.1/12.5	20				13N	13E	15E	16V	17V	18V
6	s	26	cttc26	6	0.1/12.5	20				19N	19E	21E	22V	23V	24V
7	t	29	cttc29	6	0.1/12.5	20				31N	31E	27E	28V	29V	30V

reference level 30

Figure A.7. Locations of FBA sensors during the ambient vibration measurements at City Tower.

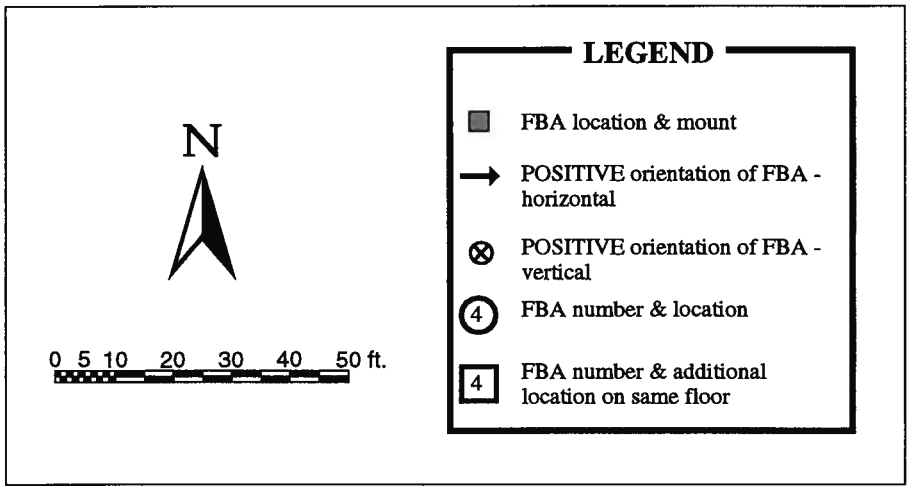

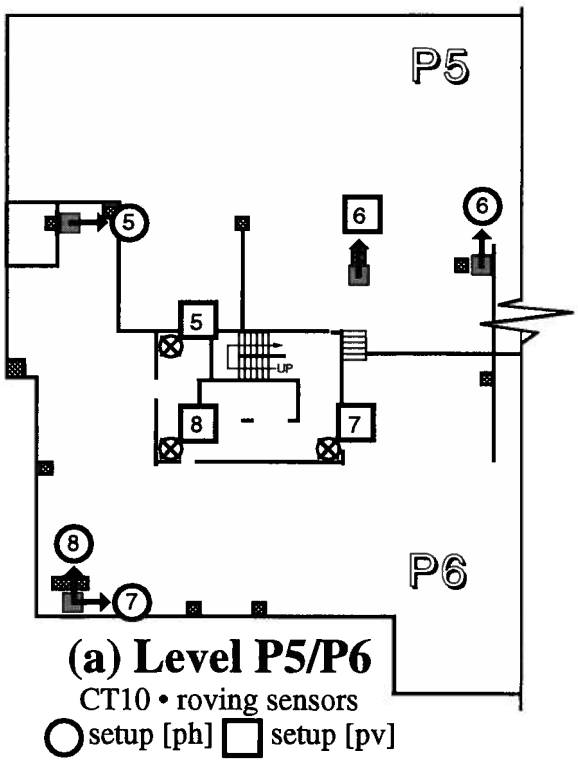

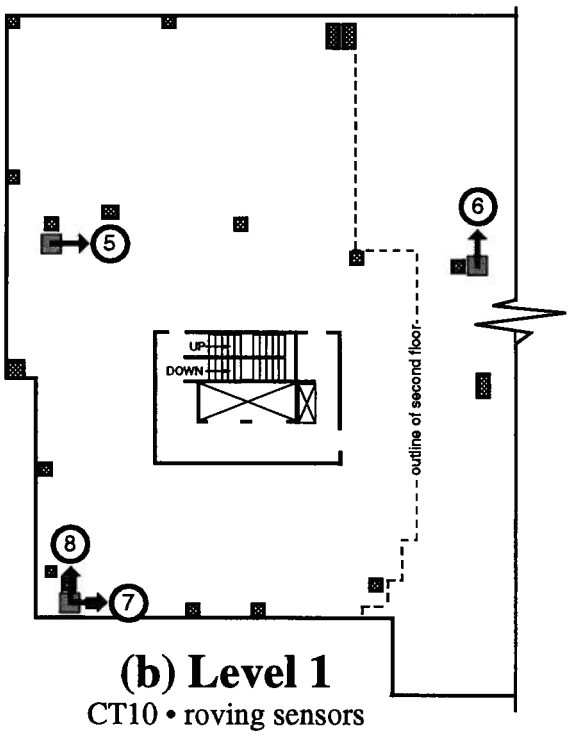

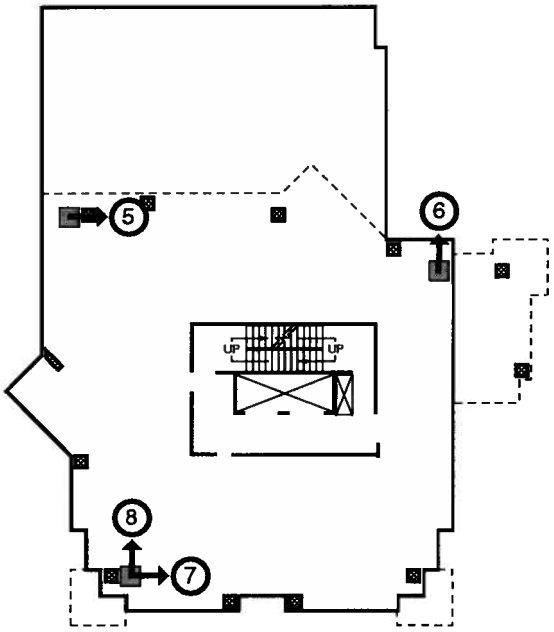

(c) Level 2
CT10 • roving sensors

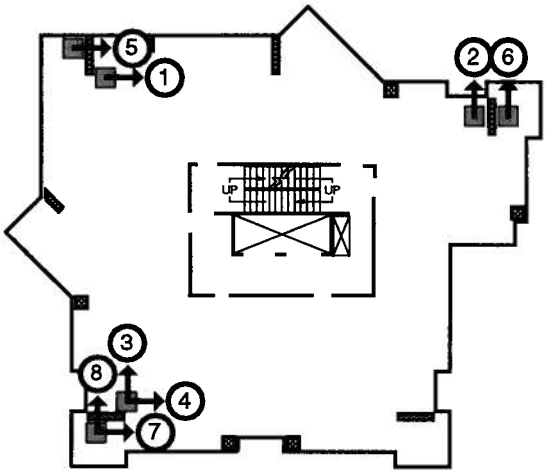

(d) Levels 3-9
CT10 • reference sensors (Level 9 only)
CT10 • roving sensors

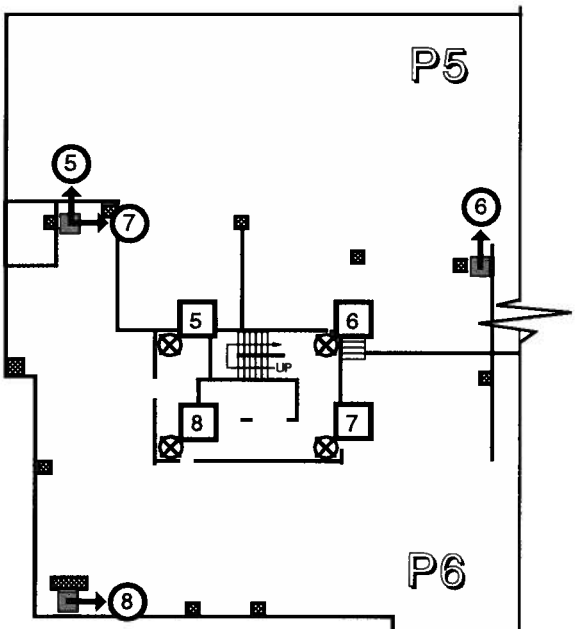

(e) Level P5/P6
CT15 • roving sensors
CT20 • roving sensors
CT25 • roving sensors
CT32 • roving sensors
○ setup [ph] □ setup [pv]

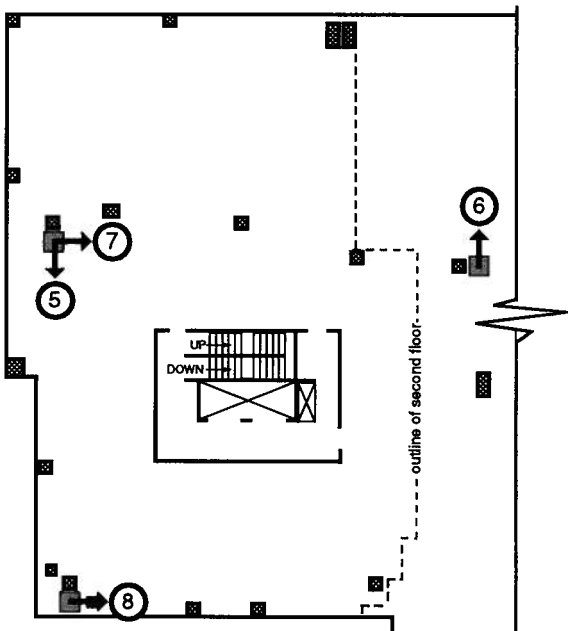

(f) Level 1
CT15 • roving sensors
CT20 • roving sensors

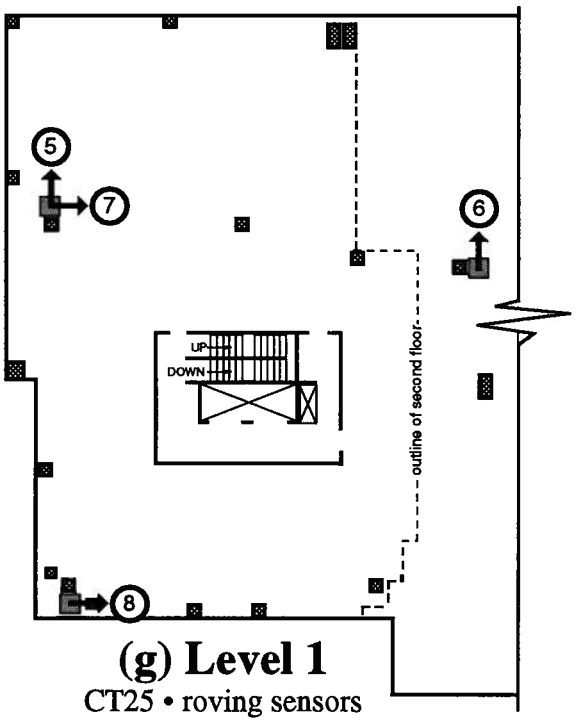

(g) Level 1
CT25 • roving sensors
CT32 • roving sensors

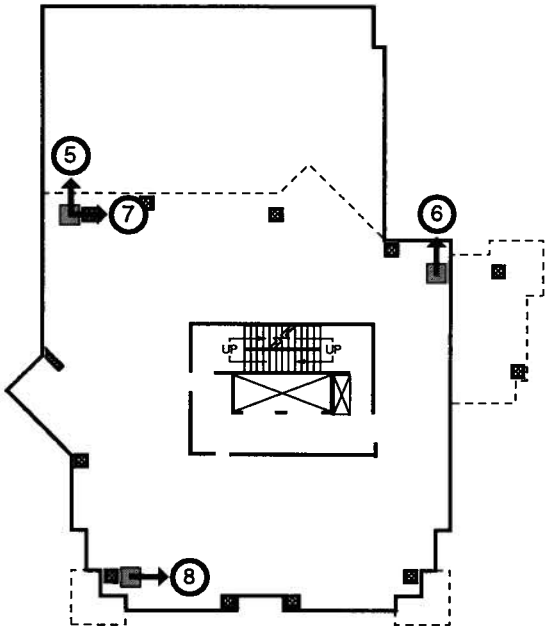

(h) Level 2
CT15 • roving sensors
CT20 • roving sensors
CT25 • roving sensors
CT32 • roving sensors

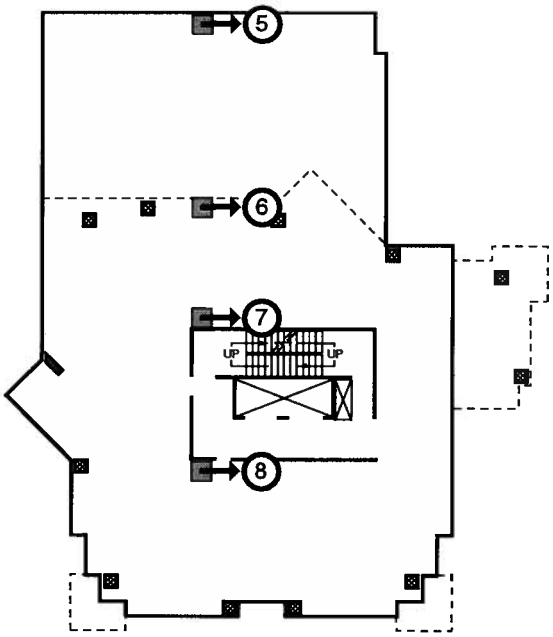

(i) Level 2
CT32 • roving sensors (setup TH)

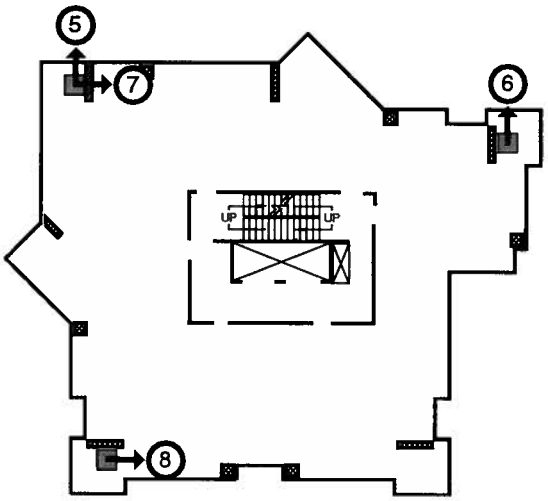

(j) Levels 3-9
CT15 • roving sensors
CT20 • roving sensors
CT25 • roving sensors
CT32 • roving sensors

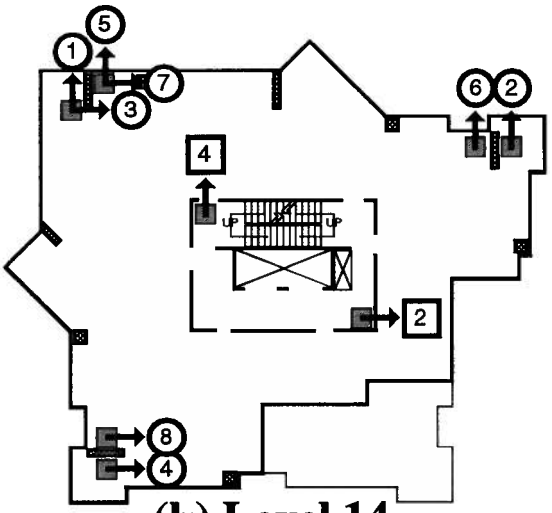

(k) Level 14

CT15 • reference sensors (setup PV,PH)
CT15 • reference sensors
CT15 • roving sensors (placed on top of columns)

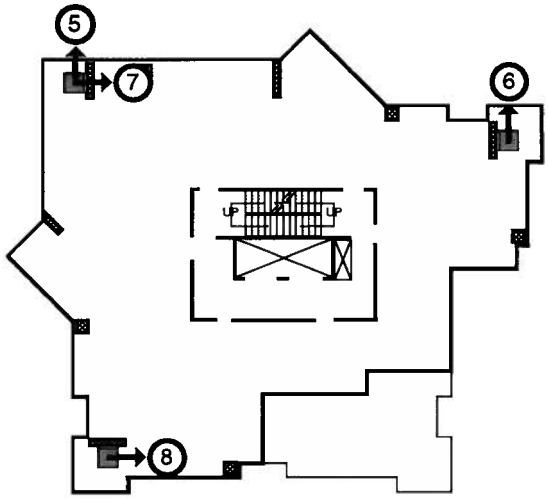

(l) Levels 11-25

CT15 • roving sensors
CT20 • roving sensors
CT25 • roving sensors
CT32 • roving sensors

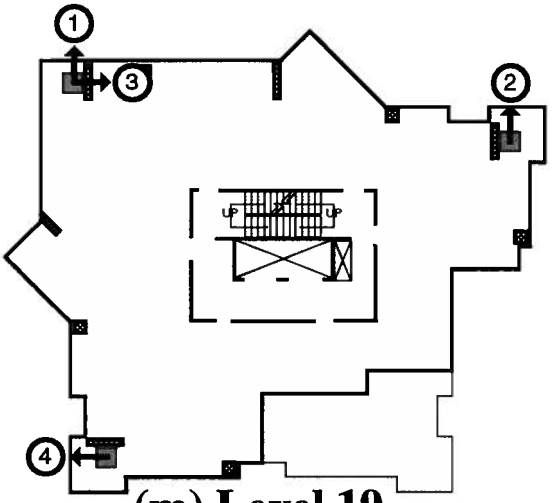

(m) Level 19

CT20 • reference sensors

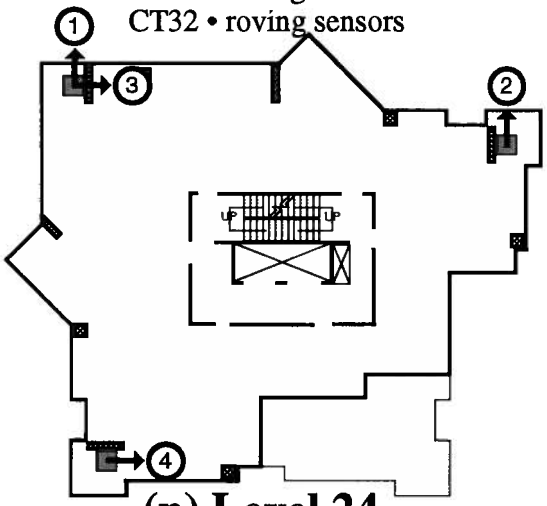

(n) Level 24

CT25 • reference sensors

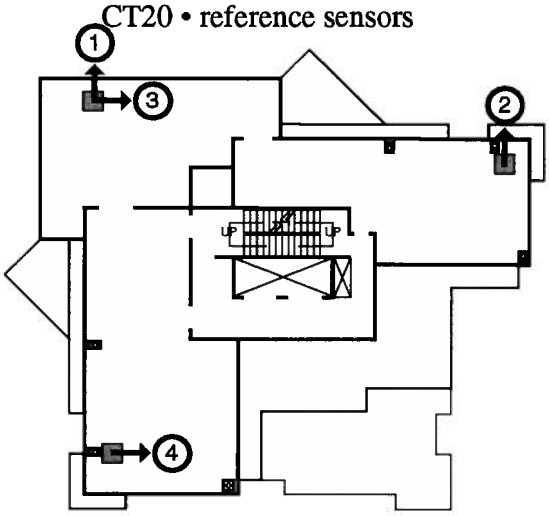

(o) Level 29

CT32 • reference sensors

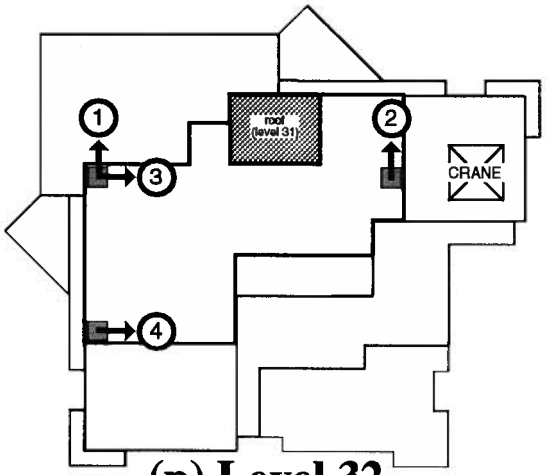

(p) Level 32

CT32 • roving sensors

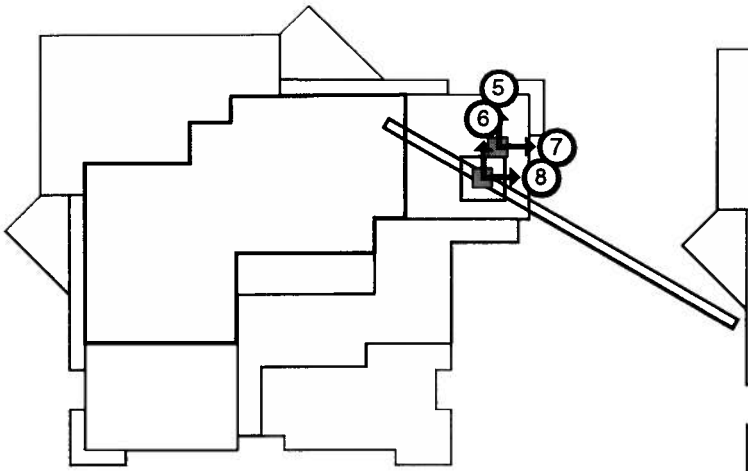

(q) Levels 27/30
CT32 • crane measurements

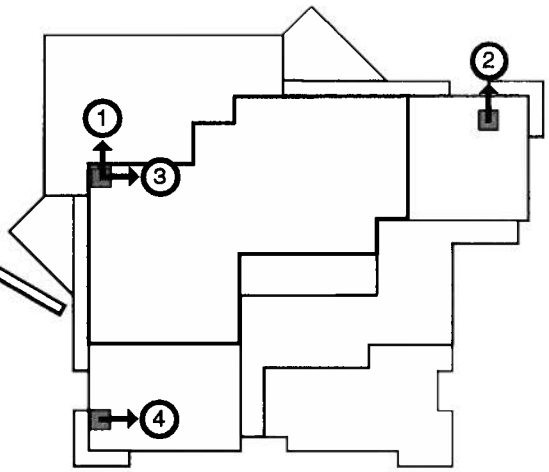

(r) Levels 29/30
CTTC • setup D1

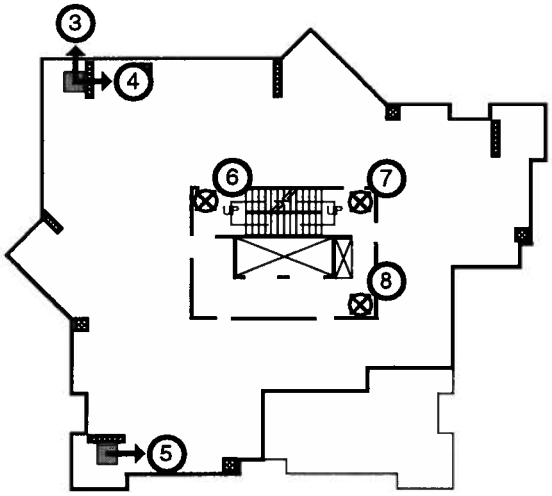

(s) Levels 17-26
CTTC • roving sensors

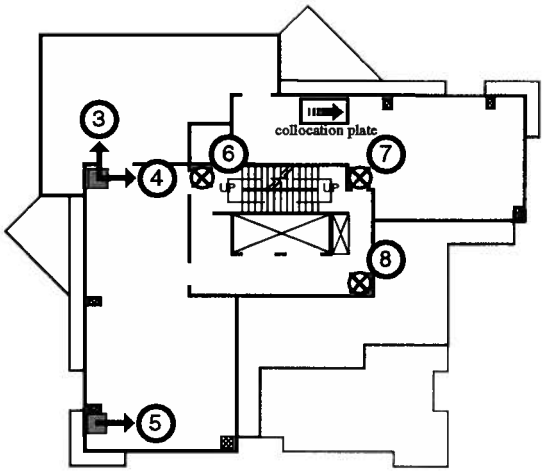

(t) Level 29
CTTC • roving sensors
CTTC • collocation setup

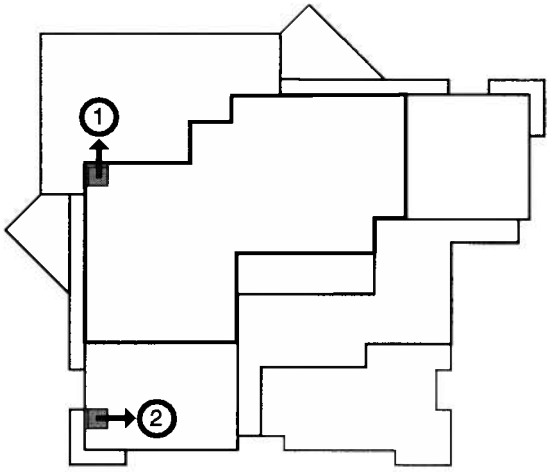

(u) Level 30
CTTC • reference sensors

B

APPENDIX B
AMBIENT VIBRATION DATA ACQUISITION SOFTWARE (AVDA) - OPERATING INSTRUCTIONS

B.1 OVERVIEW

B.1.1 DESCRIPTION

The software program AVTEST is one of the original components of the HBES software. Its function is to instruct the Keithley analog-to-digital (A/D) converter to sample data at a specified rate while plotting the channels *real time* on the screen. It also extracts this data and stores it on the hard drive of the field computer. During the course of this research, this program has undergone several revisions to enhance its capabilities and to improve quality control when acquiring data.

B.1.2 REVISIONS TO AVTEST

Modifications to the AVTEST source code were performed using a Borland C/C++ compiler (Borland International Inc., 1992) along with the library provided by the Keithley 500/B software (KDAC, 1989). All routines are written in C (Kernighan & Ritchie, 1988). Newer versions of the program were named AVDA - an acronym for Ambient Vibration Data Acquisition.

Table B.1 lists all versions of AVDA which were released during 1992-1994. Following this table is a description of all enhancements which were made to this program.

Table B.1. AVDA versions and compile dates.

Program Name	Program Version	Compile Date/Time
AVTest	0.1	07-09-92 11:02a
AVDA	0.2	06-03-93 12:21p
AVDA	0.2.1	10-25-93 12:44p
AVDA	0.3	11-26-93 10:21a
AVDA	0.3.1	02-07-94 11:47a
AVDA	0.3.2	03-23-94 4:01p
AVDA	0.3.3	04-09-94 12:35p
AVDA	0.4ß	04-29-94 12:17p
AVDA	0.4.1	05-31-94 11:31a
AVDA	1.0	15-10-94 12:34p

AVTEST and subsequent versions of AVDA were used extensively in several ambient and impact vibration studies. Through this use, several limitations of the program were identified and subsequent improvements were made to the program modules.

B.1.2.1 Data Saturation Check

One modification involved adding a routine that would check each individual segment for saturation (i.e. clipping) prior to storing it on disk (ver. 0.2). If any saturation was detected, all of the data collected in that particular segment would be discarded automatically and the acquisition repeated. In some cases though, the data segments saturated at the beginning of the acquisition and the user had to wait for the program to collect the entire segment - and then discard it. This represented a waste of valuable time. To improve this, an option was added which would allow the user to discard the segment manually (ver. 0.4ß). This modification provided automated and improved quality control over the collected data.

B.1.2.2 Check For Existing Filenames And Remaining Disk Space

In another revision of the program, a routine was added which would check whether or not the name of a data file was already in use, and if so, to warn the operator (ver. 0.2.1). In addition to this, the available hard disk space was checked to ensure that all of the data could be stored on the disk during the program's execution (ver. 0.3). These modifications were added since these mistakes occurred frequently; leading to loss of time and data.

B.1.2.3 Addition Of Sounds Corresponding To Certain Operations

Another modification involved providing feedback as the program performed its various operations (ver. 0.2). This was done by associating unique *sounds* to these operations. These include such actions as calibration, accepting and rejecting a segment (manually or automatically), an input error if a filename was already in use or if there was insufficient disk space or memory, and finally notification that all of the data had been collected. Thus the operator could concentrate on other activities unless he/she hears a sound requiring his/her

attention.

B.1.2.4 Increased Channel Capacity And Increased Size Of Data Arrays

The introduction of impact testing into the dynamic testing program at UBC prompted the need to rewire the A/D converter so that 16 channels of data could be acquired instead of only 8 channels. Consequently, AVDA also had to be modified to account for this change[1] (ver. 0.3). Also, since higher sampling rates would be used, memory had to be increased. This was done by using *far data* routines in AVDA for dynamically allocated memory as well as modifying a parameter in the BATch file *k.bat*. The latter parameter is described in more detail in §B.3.3.

Along with increasing the number of data acquisition channels, the size of the data segments was increased. Hence, beginning with version 0.3[2], the length of each data segment has been embedded in the output file header. This was a missing piece of information in the file headers and was necessary since segment lengths could now be larger than the default value of 4096. These files are still compatible with the program ULTRA. The details of the output file header appear in §B.3.4.

B.1.2.5 Flexible Sensor Calibration

Yet another modification involved providing alternative sensor calibration options. Instead of calibrating before and after collecting the data, or not at all, the operator has the option of calibrating *before* and/or *after* (ver. 0.4ß) and/or can simply *monitor* the signals without storing the data on disk (ver. 0.4.1).

The final version of this program, which was released along with this thesis, was version 1.0. A

---

[1]This in an important change and the operator should note that versions of AVTEST and AVDA prior to this version (0.3) WILL NOT WORK CORRECTLY since they assume that the Keithley A/D converter is wired for 8 channels, NOT 16 (as was the case at the time of this writing).

[2]In version 0.3, the segment length defaulted to the maximum allowable segment length. As of version 0.3.1, the segment length is the smaller of this number and the number of points to be acquired.

copy of the program source code and executable files are available from the computer graphics lab of the Civil Engineering Department.

B.2 INSTALLATION AND SYSTEM REQUIREMENTS

This program should run on any PC computer with a 80286 processor or higher, a CGA monitor, and at least 20 Mb of hard disk space (for storing the data files). In addition to this, an IBIN-A interface card which communicates with the Keithley 575 A/D converter must be installed in the computer and properly configured (see the documentation provided with the card for further information).

This program works correctly with MS-DOS 5.0 and will probably work with other versions as well. The system configuration should be kept simple, and it is very important that the Windows™ extension SMARTDRV.EXE is not installed since it interferes with the sampling interrupts.

This program works well in conjunction with the DOS utility DOSKEY (see a DOS 5.0 manual for details). This utility retrieves previous *command lines* thus eliminating the need to retype all of the input parameters at the DOS prompt. Usually, most of these parameters remain the same throughout the test. Also, the parameters which change more frequently, such as the filename, appear at the end of the parameter list so that they can be readily modified.

The files AVDA.EXE, AVDA.TBL and K.BAT must be copied into the directory containing the Keithley drivers. For more information of the installation of the latter drivers, refer to the Keithley 500/B documentation.

B.3 PROGRAM EXECUTION

B.3.1 RUNNING THE PROGRAM

Prior to executing AVDA, the memory resident program K500.EXE must be executed. The latter program sets up its own kernel in memory and then executes other programs including

AVDA (see the Keithley 500/B documentation for further information). This task is facilitated by using a BATch file called *k.bat*. This BATch file takes several arguments. The first argument is the name of the data acquisition program (in this case AVDA). The remaining arguments are passed on to AVDA. In other words, to run the program, type the following at the DOS prompt:

```
k avda <arg1> <arg2> ...
```

The arguments (arg1, arg2, etc.) are described in the following section (§B.3.2). If no arguments are specified, the program version and a descriptive list of the arguments is displayed on the screen as shown in Figure B.1. If all of the arguments are valid, then they will be echoed to the screen prior to acquiring the data. This allows the user to verify the parameters before proceeding. Warning messages, if any, will also be displayed.

```
        UBC Civil Ambient Vibration Data Acquisition Program - Version 1.0
                    16 Channel Interactive - October 1994
                 written by N. Schuster, A. Felber, and S. Yee

AVDA  Freq  NumPts  NumChan  GGain  Calib  Sat  filename

    Freq : Nyquist Frequency [Hz] (0.1-1000)
  NumPts : Total number of Points in k (1,2,4,8,16,32,64,128)
 NumChan : Number of Channels to be Sampled (1-16)
   GGain : Global gain (1,2,5,10)
   Calib : calibration: <b> before, <a> after, <m> monitor, <n> none
     Sat : allowable consecutive saturation points per segment (0-1024)
           --> specify -1 to disable saturation check routine
filename : filename prefix for storage
```

Figure B.1. Instructions displayed when AVDA is executed with no command line arguments.

For example, if the following line is entered at the DOS prompt:

```
k avda 20 32 8 5 ba 2 beer01
```

then the screen shown in Figure B.2 will appear when AVDA is executed.

At this point, the user can proceed or terminate the program if any of the parameters are incorrect. If the user chooses to proceed, then the program will do the following:

(a) if a BEFORE calibration was specified:
- acquire and store data for the sensor calibrations before the test
- scan all channels afterwards so that the user can set the attenuation levels

(b) if a MONITOR calibration was specified
- acquire and display data from each sensor (no data is stored on disk)
- scan all channels afterwards so that the user can set the attenuation levels

(c) acquire the data
- collect as many segments as necessary
- check each segment for saturation (if requested)
- store the data on disk

(d) if an AFTER calibration was specified:
- acquire and store data for calibrations after the test

While acquiring the data (step "c" above), the user can press <ESC>[3] followed by <R> to manually reject the segment. Alternatively, after pressing <ESC>, the user can press <X> to terminate the program prematurely[4].

```
        UBC Civil Ambient Vibration Data Acquisition Program - Version 1.0
                    16 Channel Interactive - October 1994
                 written by N. Schuster, A. Felber, and S. Yee

                      Nyquist Frequency : 20.00 Hz
                  Total Number of Points : 32768
                      Number of Channels : 8
                             Global Gain : 5
                             Calibration : BEFORE AFTER
Allowable Consecutive Saturation Points : 2

                         Filename Prefix : beer01

            Disk Space Required (bytes) :   1228800
           Available Disk Space (bytes) :  12345678
  Available KEITHLEY memory per channel :     12762
      Available CORE memory per channel :     45964

                          Segment Length : 8192
                      Number of Segments : 4
                 Duration of Measurement : 0:13:39

Press any key to proceed or 'X' to terminate
```

Figure B.2. Echo of the command line arguments.

---

[3]Pressing the ESC key is necessary in order to interrupt the real-time graphing routine (GRAPHRT). Note that this doesn't interrupt the sampling routine (BGREAD) which will continue in the background until it is finished or until the user presses the <R> or the <X> key.

[4]Before exiting, AVDA will warn the user if the length of the data array which is already stored on disk is not a power of 2. It will also try to update the "Number of Points" field in the output file header to reflect the actual number of data points saved on disk.

B.3.2 COMMAND LINE ARGUMENTS

The following list is a detailed description of each parameter which must be specified on the command line.

B.3.2.1 Nyquist Frequency (Freq)

The Nyquist frequency, f_c, represents the maximum frequency that can be resolved from the data. This determines the sampling rate that the program will use when acquiring the data; its value is equal to twice the Nyquist frequency. Legal values of the Nyquist frequency must be in the range of 0.1 to 1000 Hz, though an upper limit of 100 Hz is recommended for slower machines such as the portable Compaq II.

B.3.2.2 Number Of Points To Acquire (NumPts)

This is the total number of points (in kilobytes) that the program will collect for each channel. This number is specified using one of the index numbers shown in the following table.

Index	Number of points per channel
1	1024
2	2048
4	4096
8	8192
16	16384
32	32768
64	65536
128	131072

Due to DOS memory limitations, the data arrays for all of the channels being sampled must be collected in one or more data segments of equal length. The length of these segments depends on how much memory has been allocated by the K500.EXE module as well as the number of channels being sampled. AVDA determines the maximum feasible segment length prior to acquiring the data, and displays this value in the screen echo (see Figure B.2). Typical segment

lengths, L_s, include 4096, 8192, and 16384[5] points.

Note that the segment length and the Nyquist frequency affect the frequency resolution of the data. The frequency resolution, Δf, can be determined as follows:

$$\Delta f = \frac{2f_c}{L_s}$$

For example, the frequency resolution for a 4096 point segment with a corresponding Nyquist frequency of 20 Hz is equal to 2*20/4096 ≈ 0.00976 Hz.

B.3.2.3 Number Of Channels (NumChan)

This is the number of channels to be sampled by the A/D converter. This number must be in the range of 1-16. At the time of this writing, channels 1 through 8 are used for digitizing the signals from the Kinemetrics signal conditioner while the remaining channels receive input from the 8 BNC connectors on the Keithley A/D converter.

B.3.2.4 Global Gain (GGain)

The Keithley 575 A/D converter transforms the analog signals into 16 bit integer values. This corresponds to a resolution of 2^{16} or 65536 *steps*, which are used to represent the *shape* of the time signal. In order to optimize the signal resolution, a global gain is applied to the incoming signal. Note that the global gain defines the threshold of the time signal; which is numerically equal to ±10/(GlobalGain).

Legal values of global gains are shown in the following table:

sensor output voltage (V)	global gain
±1	10
±2	5
±5	2
±10	1

[5]AVDA limits the segment lengths to 16384. This is due to the fact that the Keithley routines do not allow arrays larger than 32767 points.

To illustrate this process, consider the plots shown in Figure B.3. This figure shows a sine wave with an amplitude of 2 volts which has been digitized using the four possible global gains. As can be seen, the signal resolution improves with increasing global gains. However, the global gain must be chosen to avoid clipping the signals. In this case, a global gain of 10 clips the sine wave while a global gain of 5 is the optimal gain that should be used to represent the signal. For the FBA-11 accelerometers, a global gain of 5 is typical.

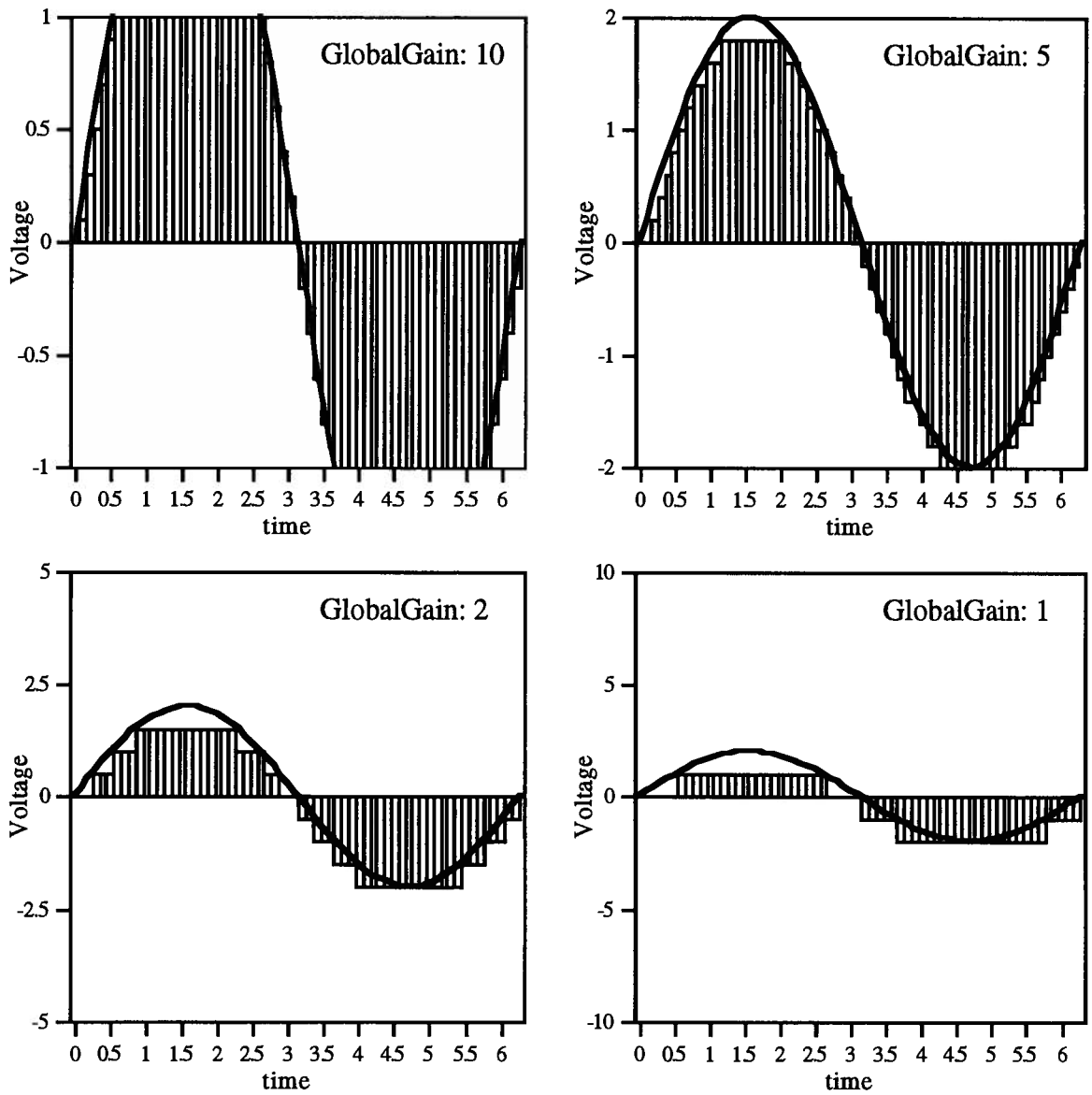

Figure B.3. A digitized sine wave and corresponding global gains.

B.3.2.5 Calibration Options (Calib)

This option is used to ensure that all of the Kinemetrics FBA-11 sensors are properly connected to the signal conditioner and are functioning correctly. Calibrations can be performed before sampling, after sampling, or not at all. These calibration records are also stored to disk using the file naming convention discussed in §B.3.2.7. The correct procedure for sensor calibration is discussed in §B.4. An alternative to calibration is to use the MONITOR option. This is similar to the calibration option except that the data is not stored on disk.

The calibration options are activated by specifying one or more of the parameters summarized in the table below. If more than one parameter is used, then they should be specified as a single string. For example if the user wants to calibrate before and after sampling the data, he/she should specify "ba" or "ab" for the calibration option.

option	parameter	program action
BEFORE	b	sample and save calibration data before data sampling
AFTER	a	sample and save calibration data after data sampling
MONITOR	m	sample and display each channel before data sampling
NONE	n	data sampling only

B.3.2.6 Allowable Number Of Consecutive Saturation Points (Sat)

After each data segment is acquired, and prior to storing the data onto disk, the program checks each data array to ensure that no clipping has occurred. Clipping occurs if the signal amplitude was higher than the threshold set by the global gain (see §B.3.2.4 for details). If clipping has occurred in any of the channels, then all of the data segments are discarded and the measurement repeated. Because of time constraints, several rejections might be undesirable. Therefore, if the user is willing to tolerate some saturation points, he/she may specify the number of consecutive points that will be ignored by this routine.

Legal values of *Sat* must be in the range of 0-1024. Values of 0 or 1 provide good quality control of data though values of up to 5 have been used in some bridge tests. This routine can also be disabled by specifying a negative one (-1) for the *Sat* parameter. The latter option can

help accelerate the data acquisition process.

B.3.2.7 Filename Prefix (Filename)

This program uses the DOS filename convention which consists of 8 characters with a 3 character extension. Due to this limitation, the first 6 characters (the filename prefix) of these filenames are specified by the user while the remaining two characters are used by AVDA to specify the type of file being created as well as the channel number. The extension appended to the filename is ".bbb". This filename convention is illustrated below:

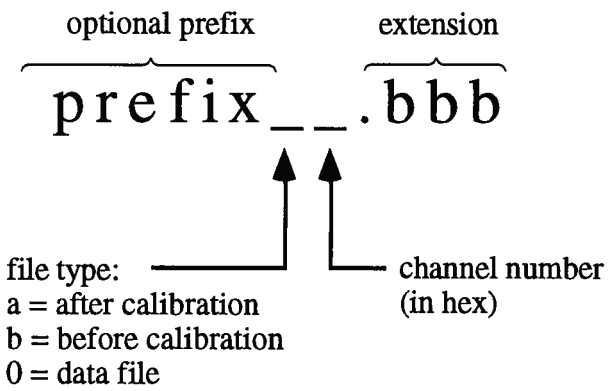

Note that since only one character is available to specify the channel number, hex (base 16) notation is used. A conversion table from decimal to hex is shown below.

channel #	1	2	3	4	5	6	7	8	9	10	11	12	13	14	15	16
label	1	2	3	4	5	6	7	8	9	A	B	C	D	E	F	0

B.3.3 MEMORY CONSIDERATIONS

As discussed in §B.3.1, AVDA is executed from another program, K500.EXE, which sets up its own kernel in RAM for video and for data arrays. The memory available for data arrays created by the Keithley 500 routines depends on a parameter specified in a BATch file named *k.bat*. The contents of this file are shown below for reference:

```
echo off
if exist %1 goto run_it
if exist %1.com %0 %1.com %2 %3 %4 %5 %6 %7 %8 %9
if exist %1.exe %0 %1.exe %2 %3 %4 %5 %6 %7 %8 %9
:run_it
K500 -m 12800 -c AVDA -q %1 %2 %3 %4 %5 %6 %7 %8 %9
```

Lines 2-4 appends the appropriate extension to the data acquisition program so that the K500 program can execute it correctly. The last line executes the K500 program. The *-m 12800* parameters shown on the last line instructs the Keithley software to allocate 12800 16-byte memory segments for use as data arrays. This number limits the length of the data arrays which can be collected before it is stored on disk and the memory purged. The user can optimize the amount of space used for data arrays by adjusting this number. However, the size of this array also reduces the amount of memory available for use by AVDA. To facilitate optimizing this number, AVDA displays the size of these data arrays (in terms of the number of data points which can be stored in memory for a given number of channels). These values can be seen in the echo screen shown in Figure B.2. Adjustments should only be made to the number following "-m". The other parameters should NOT be modified.

B.3.4 OUTPUT FILE FORMAT

All of the output files are stored in binary format. The data (in units of volts) is preceded by a header which identifies the file and includes all pertinent information. Specific details of this file are given below. A routine for reading these data files appears in §B.5.

file content (in sequence)	variable type	length (bytes)
identification string	char	42
reserved	long	4
segment length (points)	long	4
sampling interval (sec)	float	4
number of sampled points, N	long	4
channel number (on Keithley)	int	2
global gain	int	2
filename	char	80
site (currently not used)	char	80
setup (currently not used)	char	80
year	int	2
day	char	1
month	char	1
hour	unsigned char	1
minute	unsigned char	1
second	unsigned char	1
data points	float	4 * N

B.4 TYPICAL TESTING PROCEDURE

A typical setup procedure is as follows:

1. Verify connections between Keithley, signal conditioner, and data acquisition computer

2. Turn power switches to ON for all of the aforementioned equipment

3. Install the sensors at selected locations

4. Balance the sensors (if necessary)

5. Connect cables between sensors and signal conditioner

6. Set the signal conditioner to TEST

7.Run AVDA (from the KEITHLEY directory) and verify the input parameters

8. If calibrating:

   (a) set attenuation to 66dB and filters to OUT for all channels
   (b) press any key to begin sampling
   (c) after a short BEEP, the operator should turn the key on the signal conditioner from TEST to CALIBRATE.
   (d) after approximately 1 second, the key should be turned from CALIBRATE to NATURAL FREQUENCY and should remain in this position until calibration is complete.
   (e) once all of the data is acquired[6], inspect the individual calibration records for each channel, as they are displayed one by one, to ensure that the sensors are working correctly.
   (f) turn the key on the signal conditioner back to TEST
   (g) once all of the records have been displayed, the user has the option of repeating the calibration, or proceeding. If any of the sensors are not functioning, the problem can be remedied before proceeding.

9. Set attenuation and filters for recording

10. Proceed with the data acquisition

11. If calibrating after the data acquisition, repeat the procedure described in step #8.

12. Transfer data files to data analysis computer

13. Inspect recorded time histories using ULTRA (for quality control)

14. Relocate roving sensors to the next setup.

15. Repeat steps 3-14 until the test is finished.

If the user wishes to use the MONITOR option in lieu of calibration, the signal conditioner

---

[6]calibrations are sampled at 600 Hz and 2048 points are collected; this has a duration of 3.4 sec

should be plugged in and the key on the conditioner should be set to OPERATE ***before*** any of the sensors are moved. This ensures that the filter cards are not overloaded by the movement of the sensors as they are being relocated.

For further information about calibrating and balancing the FBA-11 accelerometers, see the operating instructions (Kinemetrics FBA-11).

B.5 ROUTINE TO READ "BBB" FILES

The following is a generic routine (written in C) for reading the binary files created by AVDA. The source code can be modified by the user to suit the application.

```
#include<stdio.h>
#include<stdlib.h>
#include<string.h>
#include<dos.h>

void ReadBBBFile( char *name );

/*****************************************************************************/
void ReadBBBFile( char *name )
{
     FILE                *fp;                /* file pointer to *.bbb file      */
     long                reserved;           /* reserved for future use         */
     long                segLen;             /* segment length                  */
     long                N;                  /* total number of points          */
     int                 n;                  /* Keithley channel number         */
     int                 mag;                /* global amplitude gain           */
     char                filename[80];       /* filename - embedded in data     */
     char                site[80];           /* site                            */
     char                setup[80];          /* setup                           */
     char                id[50];             /* identification string           */
     float               del;                /* time increment                  */
     struct date         d;                  /* date structure                  */
     struct time         t;                  /* time structure                  */

     long                i;                  /* counter                         */
     int                 j;                  /* segment number (counter)        */
     float               *data;              /* data array                      */
     int                 ns;                 /* number of segments              */
     fpos_t              filePos;            /* file position                   */

     const char BBBIdentifier[] = "Karg Weissbier ist das beste in der Welt";

/* open file */

     if( (fp = fopen( name, "r") == NULL )
     {
          printf("Error opening input file -- Terminating Program\n" );
          exit(EXIT_SUCCESS);
     }
```

```
/* header */

     printf( "Reading header information...\n" );
     fread( id, sizeof(char), 42, fp );
     if( strcmp( id, BBBIdentifier ) != 0 )
     {
          printf("Invalid file format! -- Terminating Program\n" );
          exit(EXIT_SUCCESS);
     }

     fread( &reserved, sizeof(long), 1, fp );
     fread( &segLen, sizeof(long), 1, fp );
     fread( &del, sizeof(float), 1, fp );
     fread( &N, sizeof(long), 1, fp );
     fread( &n, sizeof(int), 1, fp );
     fread( &mag, sizeof(int), 1, fp );
     fread( filename, sizeof(char), 80, fp );
     fread( site, sizeof(char), 80, fp );
     fread( setup, sizeof(char), 80, fp );
     fread( &(d.da_year), sizeof(int), 1, fp );
     fread( &(d.da_day), sizeof(char), 1, fp );
     fread( &(d.da_mon), sizeof(char), 1, fp );
     fread( &(t.ti_hour), sizeof(unsigned char), 1, fp );
     fread( &(t.ti_min), sizeof(unsigned char), 1, fp );
     fread( &(t.ti_sec), sizeof(unsigned char), 1, fp );

/* sort out segment length */

     if( reserved != 0L )
          segLen = 4096L;     /* default value (pre 0.3 version of AVDA) */
     segLen = ( segLen > N ) ? N : segLen;
     ns = N/segLen;

/* data */

     data = (float *)calloc( N, sizeof(float) );
     {
          printf("Memory allocation error! -- Terminating Program\n" );
          exit(EXIT_SUCCESS);
     }

     for( j = 0; j < ns; j++ )
     {
          printf("segment #%d\n", j+1);
          fread( &(data[j*segLen]), sizeof(float), segLen, fp );
     }

/*
 * -------> insert user code here <-------
 */
}
```

C

APPENDIX C
AMBIENT VIBRATION TIME HISTORY PLOTTER SOFTWARE FOR HP LASERJET III PRINTERS (HPPLOT) - OPERATING INSTRUCTIONS

C.1 DESCRIPTION

The program HPPlot is used to plot the ambient vibration and calibration records produced by the program AVDA (see Appendix B). Its function is to plot all of the channels on the same page for comparison. Thus the user is able to visually determine if any anomalies or signal contamination has occurred in one or more of the channels before any data analysis is done. A sample output created by this program is shown in Figure C.1.

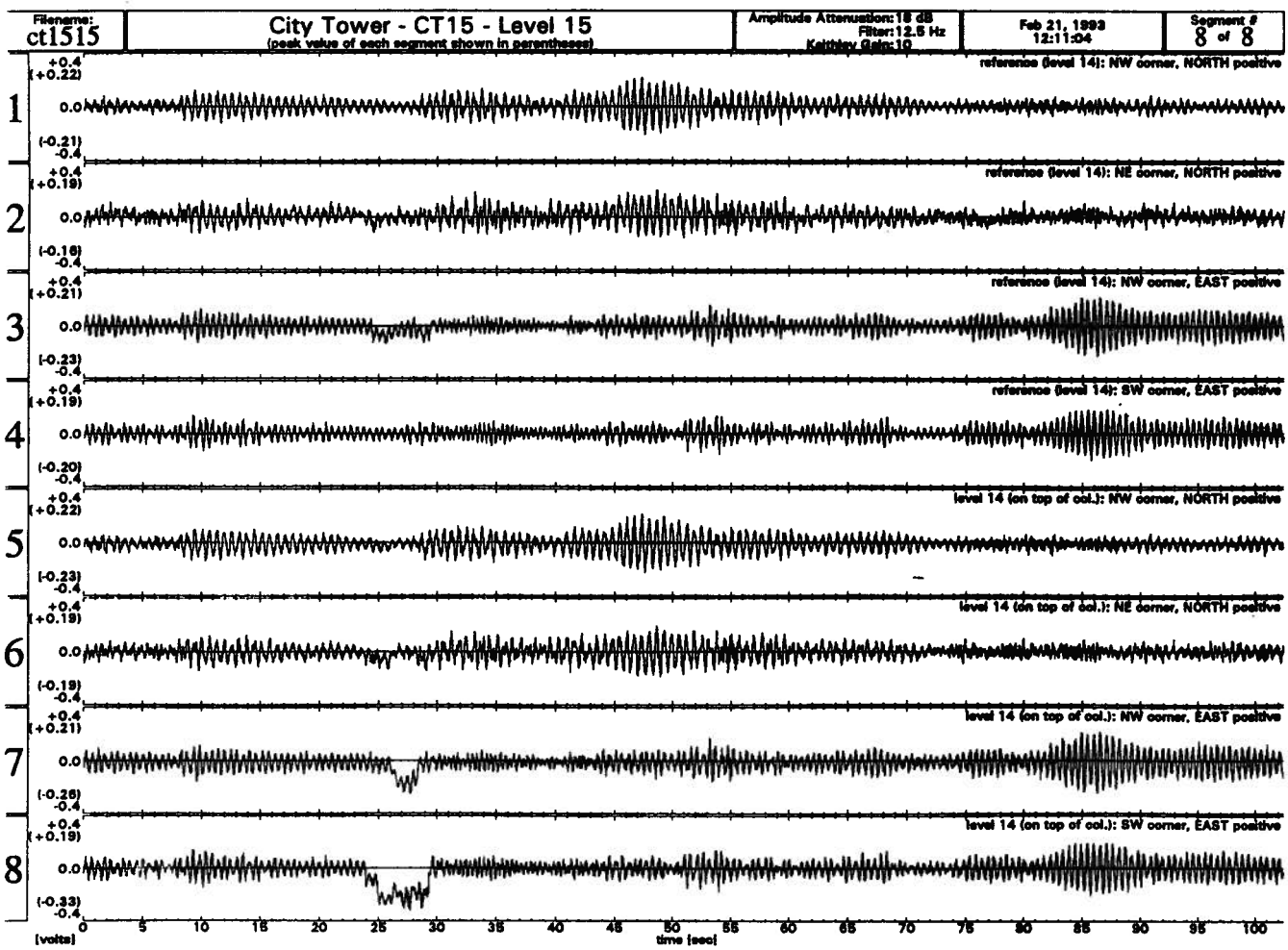

Figure C.1. Typical ambient vibration time history produced by HPPlot.

The header contains several information about the data files. These include the filename prefix, an optional title, conditioning information, the time at which the data was collected, and the segment number. Each plot contains the channel number, peak values for that particular channel (shown in parentheses), an optional label, and finally the time signal itself. All of the plots are scaled according to the peak value of all of the channels shown on that page.

C.2 INSTALLATION AND SYSTEM REQUIREMENTS

This program should run on any PC computer with a 80286 processor or higher. Also, since this program sends printing instructions directly to the printer, it must be used with a printer which supports Hewlett Packard's printer control language PCL5 (Hewlett-Packard Company, 1990) such as a HP LaserJet III.

This program can be copied into any directory and executed from any other directory provided there is a *path* to it.

C.3 PROGRAM EXECUTION

C.3.1 RUNNING THE PROGRAM

To run the program, several parameters must be specified on the command line. A list of these parameters will be displayed by executing the program without any arguments, i.e. by typing

```
HPP <enter>
```

at the DOS prompt. By doing so, the screen shown in Figure C.2 will appear.

The speed of this program depends on the speed of the computer, and more importantly, the speed of the parallel port (which connects the computer to the printer). It takes about 5 minutes to generate the plots for a typical setup, but it takes about one hour[1] for a LaserJet III to print the

[1] This is based on 8 data files containing 32768 data points, 2 sets of calibration files, executed on a PC computer with an 80486DX processor

entire setup. Since this is such a long period of time, and since there are usually several setups, this program is best used *over night* since the printer and the computer must be dedicated to the task. A BATch file can be created to execute the program with all the necessary parameters (see §C.3.3 for an example).

```
HPPlot   BBB Time History File Plotter · 1.0
         (requires HP/PCL5 based laser printer)
         A Program by Norman Schuster

Please specify the following parameters when executing this program:

HPP  dest  datafile  nf  [cal]  [filter]  [att]  [labelfile]  [warnings]

       dest = destination for printer commands (either PRN or a file)
   datafile = first 6 characters of "BBB" files to be plotted
         nf = the number of "BBB" files to be plotted
      [cal] = calibration "flag" -> 0 = print; 1 = don't print; default = 1
   [filter] = filter setting on signal conditioner [Hz]
      [att] = attenuation setting on signal conditioner [dB]; if multiple
                values, use: att_1,seg_1,seg_m;att_2,seg_m+1,seg_n...
[labelfile] = file containing "header" title, and individual plot titles
 [warnings] = warnings "flag" -> 0 = display; 1 = suppress; default = 0

ex.1 (minimum)                HPP prn corona 8
ex.2 (multi att. values)      HPP lpt1 corona 8 0 12.5 12,1,1;18,2,8
ex.3 (file dest.; label file) HPP myFile.ext corona 8 0 12.5 12 corona.hpp
```

Figure C.2. Instructions displayed when HPPlot is executed with no command line parameters.

C.3.2 COMMAND LINE ARGUMENTS

The following is a detailed description of each parameter. Note that only the first four parameters are required and that the rest are optional.

C.3.2.1 Destination (dest)

This is the destination of the printer commands. If "prn" or "lpt1" is specified, the printer commands will be sent directly to the printer. If the name of a file is specified (name and extension arbitrary), the printer commands will be written to that file. However, the user should note that these files take up a lot of disk space (over 5 megabytes[2]). To later print this file, enter

[2]This is based on 8 data files containing 32768 data points and 2 sets of calibration files

the following command at the DOS prompt:

```
copy filename.ext prn
```

where "filename.ext" is the name of the file previously specified. DO NOT print this file using the DOS utility PRINT since it interferes with the PCL instructions.

C.3.2.2 Filename Prefix (datafile)

This is the file prefix of the "BBB" files; i.e. the characters which precede the "labels" which are appended to the file (01, 02, a1, b1, ...) during data acquisition.

eg. to print the files "ct100901.bbb", "ct100902.bbb", etc. use "ct1009"

eg. to print the files "test01.bbb", "test02.bbb", etc. use "test"

C.3.2.3 Number Of Files (nf)

This is the number of files which make up the setup.

C.3.2.4 Calibration Flag (cal)

If the user wishes to print the calibration files, a zero (i.e. "0") should be specified, otherwise unity (i.e. "1") should be specified. This argument is optional and defaults to "1".

C.3.2.5 Filter Setting (filter)

This is the filter setting that was used on the signal conditioner (Hz) during data acquisition. This number appears in the header of each page (except calibration which defaults to "OUT"). If no value is specified, "N/A" (not available) is displayed instead. A negative one (i.e. "-1") can also be specified to indicate that this value is unavailable.

C.3.2.6 Attenuation Setting(s) (att)

This is the attenuation setting on the signal conditioner (dB). This number appears in the header of each page (except calibration which defaults to "66"). If no value is specified, "N/A" (not

available) is displayed instead. A negative one (i.e. "-1") can also be specified to indicate that this value is unavailable.

The program assumes that this setting is the same for all the files. However, if the attenuation was changed in between segments, these different values can be specified using the following format:

att_1, seg_1, seg_m; att2, seg_m+1, seg_n [,att_3,...]

For example, if segments 1 and 2 were attenuated at 12 dB while segments 3 to 8 were attenuated at 18 dB, specify the following:

```
12,1,2;18,3,8
```

DO NOT SEPARATE THE NUMBERS WITH ANY SPACES!

C.3.2.7 Filename With Plot Labels (labelfile)

If the user wishes to add a custom label to the header as well as individual plots, he/she may specify the name of an ASCII file (name and extension arbitrary) which contains the following strings (max. 80 characters):

<title appearing in header>
<label of plot #1>
<label of plot #2>
.
.
.
<label of plot #nf>

The first string appears in the header while the other strings appear in the top right corner of the corresponding plot (right-justified).

C.3.2.8 Warning Flag (warnings)

If the program is unable to locate any of the files specified on the command line, it will prompt

the user as to whether it should continue or stop. If the program is being used in a BATch file, this interruption could be very inconvenient.

To suppress these warnings, specify a "1". By default, these messages are displayed.

C.3.3 EXAMPLE OF GENERATING PLOTS WITH A BATCH FILE

Suppose all eleven data files from the CT15 test are to be plotted. Further, it is desired that all the relevant conditioning information appear in the header, and that each plot is to contain a label describing the location of each sensor. To accomplish this, follow these steps:

1) With the information from Table A.2 (see Appendix A), create a BATch file called "CT15_HPP.BAT" which contains the following lines:

```
hpp prn ct15pv 8 0 12.5  0 ct15pv.hpp 1
hpp prn ct15ph 8 0 12.5  0 ct15ph.hpp 1
hpp prn ct1515 8 0 12.5 6,1,1;18,2,8 ct1515.hpp 1
hpp prn ct1513 8 0 12.5 12 ct1513.hpp 1
hpp prn ct1511 8 0 12.5 18 ct1511.hpp 1
hpp prn ct1509 8 0 12.5 12 ct1509.hpp 1
hpp prn ct1507 8 0 12.5 18 ct1507.hpp 1
hpp prn ct1505 8 0 12.5 12 ct1505.hpp 1
hpp prn ct1503 8 0 12.5 12 ct1503.hpp 1
hpp prn ct1502 8 0 12.5 12 ct1502.hpp 1
hpp prn ct1501 8 0 12.5 12 ct1501.hpp 1
```

Note that this BATch file executes HPPlot along with the required parameters to satisfy the task described above. Also, the label files have the same name as the filename prefix for the corresponding file (for consistency). Finally, all warnings from the program are to be suppressed so that such warnings do not interrupt the BATch job.

2) Create the label files following the format described in §C.2.7. To illustrate, the contents of the label file "CT1511.HPP" is shown below:

```
CT15 - City Tower - Ambient Vibration Measurements
<Reference> Level 14 - column base at NW corner; NORTH Positive
<Reference> Level 14 - column base at NE corner; NORTH Positive
<Reference> Level 14 - column base at NW corner; EAST Positive
<Reference> Level 14 - column base at SW corner; EAST Positive
Level 11 - column base at NW corner; NORTH Positive
Level 11 - column base at NE corner; NORTH Positive
Level 11 - column base at NW corner; EAST Positive
Level 11 - column base at SW corner; EAST Positive
```

The first line will appear in the header; the second line will appear in the top right corner of the plot for channel 1; the third line will appear in the top right corner of the plot for channel 2; and so on.

3) Copy all of the BBB files from the CT15 test to the same directory on the computer's harddrive which contains the BATch file and label files described above.

4) Turn on the printer and ensure that there is sufficient paper and toner. In this case 11*(8+2) or 110 sheets will be required to plot all of the time histories.

5) Finally, execute the BATch file by typing the following at the DOS prompt:

```
ct15_hpp <return>
```

This will execute the instructions in the BATch file, and if all goes well, in approximately 11 hours, all of the data files from the CT15 test will be plotted.

D

APPENDIX D
SLAVE NODE GENERATOR SOFTWARE (SLAVE) - OPERATING INSTRUCTIONS AND DOCUMENTATION

D.1 DESCRIPTION

In some cases, the measured motions of each floor provide an incomplete picture of the building's vibration mode. In order to improve this, motion at other points on the floor is interpolated by treating each floor as a rigid body, and then using the measured components of the mode shapes (*master nodes*) to calculate corresponding motion at these *slave nodes*.

D.2 INSTALLATION AND SYSTEM REQUIREMENTS

This program was written in C++ (Stroustrup, 1993) and compiled with a Borland C++ 3.1 compiler. The program should run on any PC computer with a 80386 processor (with an 80387 FPU) or higher, and at least 1Mb of memory.

The program can be copied into any directory and executed from any other directory provided there is a *path* to it.

D.3 PROGRAM EXECUTION

D.3.1 REQUIREMENTS AND RESTRICTIONS

This program uses the potential modal ratio files (*.mod) created by the program ULTRA as *master* files to interpolate for unmeasured points of motion (POM) which are referred to as *slave* nodes. The output files are created using the *.mod format so that the companion program, VISUAL, can use them. There are several prerequisites:

(1) The coordinates of the master nodes must not have identical x or y coordinates

eg.
x1 = (50, 100); x2 = (60, 80) <---- OK
x1 = (**50**, 100); x2 = (**50**, 80) <---- unacceptable
x1 = (**51**, 100); x2 = (**50**, 80) <---- OK

As shown above, the user can get around this restriction by slightly offsetting the coordinates (since the motion probably doesn't vary that much anyway)

(2) A minimum of 3 master files is required and must be of the following combinations:

XXY	- 2 in the *x* direction, 1 in the *y* direction
XYY	- 1 in the *x* direction, 2 in the *y* direction
XXYY	- 2 in the *x* direction, 2 in the *y* direction
XXYZZZ	- 2 in the *x* direction, 1 in the *y* direction, 3 in the *z* direction

Also, the *.mod files should have the same attributes (same reference sensor, same resolution, same coherence cutoff, etc.). SLAVE will check to see that these requirements are met, but if necessary these *verifications* can be suppressed by entering the appropriate code on the command line.

(3) the underlying assumption of this program is that the inputted motion are those of a rigid body (or at least they can be treated as such).

D.3.2 RUNNING THE PROGRAM

To run the program, several parameters must be specified on the command line. A list of these parameters will be displayed by executing the program without any arguments, i.e. by typing:

```
SLAVE <enter>
```

at the DOS prompt. By doing so, the message shown in Figure D.1 will be displayed on the screen.

D.3.2 COMMAND LINE ARGUMENTS

The following is a detailed description of each parameter. Note that only the first parameter is required while the rest are optional.

```
S L A V E

Slave Node Generator - Object Oriented Version (3D) - 1.0

SLAVE inputFile [flags : acdfnprsx] [thetaCutOff]\n";

  inputFile : input file containing slave node details (extension "slv")
      flags : specify which fields in the "mod" files to ignore:
              [a] - don't compare reference signals
              [c] - don't compare coherence cutoff
              [f] - don't compare frequency resolution
              [n] - don't compare number of points
              [p] - don't compare phase cutoff

              [x] - use XXYY formulation exclusively
              [d] - allow dual entries in formulae
              [s] - allow split entries in formulae

              [r] - create rigid body motion files
thetaCutOff : rigid body rotation cutoff (0-90°)
```

Figure D.1. Message displayed when SLAVE is executed with no arguments.

D.3.2.1 Filename (INPUTFILE)

This is the name of the input filename. It should have the extension "slv" but do not specify this extension on the command line. The format of this file is described in §D.3.3.

D.3.2.2 Options (FLAGS)

There are several program options. First, if the user wishes to use *.mod files which do not have identical parameters in its headers (such as different reference signals), the user can instruct the program to ignore that particular parameter when it compares the files. These options are as follows:

option	description
a	don't compare reference signals
c	don't compare coherence cutoff
f	don't compare frequency resolution
n	don't compare number of points
p	don't compare phase cutoff

The other options have to do with the two-dimensional (2D) formulations. These options are as

follows:

option	description
x	use XXYY formulation exclusively
d	allow dual entries in formulae
s	allow split entries in formulae
r	create rigid body motion file

The *x* option instructs the program to use the XXYY formulation exclusively (see §D.4 for more information). A *dual* entry means that either both *x* motions are non-zero while the *y* motion(s) are zero (at a particular frequency) or vice versa. A *split* entry means that only a single *x* and single *y* measurement are non-zero.

Finally, the user can specify an *r* to instruct the program to output the rigid body motions (RBM) at a specified centre of rotation so that comparative studies can be done with analytical mode shapes generated by a program such as ETABS (see Appendix E for further information). In this case, the RBM files will be created instead of the *.mod files.

D.3.2.3 Rigid Body Rotation Cutoff (THETACUTOFF)

The XXY and XYY formulations check to see if the rotation of the rigid body does not exceed this value (typically 70-80° is specified - default is 90°). See the formulations section for further details.

D.3.3 INPUT FILE

The input file is an ASCII file whose name should have the extension "slv". The format of this file is as follows:

```
n  filename.str filename.mes
slaveFilename_1 xcr ycr zcr mr1 mr2 mr3 [mr4] [mr5] [mr6]
slaveFilename_2 ...
.
.
.
slaveFilename_n ...
```

All of these parameters are described below.

n The number of slave files to be generated.

filename.str SLAVE uses the nodal coordinates specified in a *structure* file[1] when generating the slave nodes. Note that the coordinates of the slave nodes must also be included in this file.

filename.mes SLAVE uses the direction cosines from a *measurement* file[1] to determine the direction of the motion. These direction cosines are cross-referenced with the nodal coordinates in the structure file. Note that the direction cosines and corresponding filename of the slave node files must also be included in this file. Also the direction cosines must be either unity (±1) or zero (0) i.e. the motion must occur along the X or the Y axis.

slaveFilename_# The name of the output slave file (or RBM file)

ccr / ycr / zcr These are the x, y, and z coordinates of the centre of rotation. These must correspond to the coordinate system used in the structure file.

mr# These are the name of the master files (*.mod). A combination of 3, 4, or 6 filenames may be listed, and they need not be in any particular order.

Note that if the next slaveFilename in the list has the same centre of rotation and master files as the preceding slaveFilename, then these parameters do not need to be specified.

D.3.4 EXAMPLE

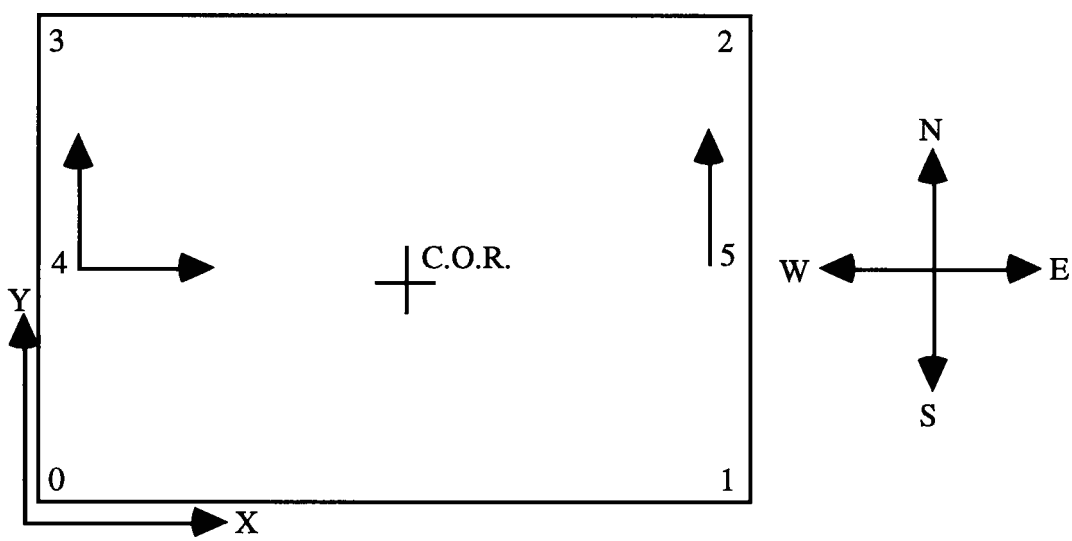

Figure D.2. Floor plan of a rectangular building with three instruments.

[1]See the VISUAL documentation in Felber, 1993.

To illustrate the use of this program, consider a building with rectangular floors as shown above. The corners are located at nodes 0,1,2,3 while sensors are located at nodes 4 and 5. Motion in the X and Y direction were measured at 4 while only Y direction motion is measured at 5. Also, the origin is taken to be at the bottom left corner while the centre of rotation (COR) is located in the centre of the floor. To generate the motion of each corner of the floor, the following files must be prepared:

structure file (sample.str)

```
Structure File Sample
200 -200  200 -200
6
0    0.0   0.0  20.0
1  100.0   0.0  20.0
2  100.0  70.0  20.0
3    0.0  70.0  20.0
4    0.0  35.0  20.0
5  100.0  36.0  20.0
4
0 1
1 2
2 3
3 0
```

Note that the y coordinates of nodes 4 and 5 have been slightly offset in order to satisfy one of the restrictions discussed in §D.3.1

measurement file (sample.mes)

```
Measurement File Sample
11
4eo4e  4  1 0 0
4no4e  4  0 1 0
5eo4e  5  1 0 0
0eo4es 0  1 0 0
0no4es 0  0 1 0
1eo4es 1  1 0 0
1no4es 1  0 1 0
2eo4es 2  1 0 0
2no4es 2  0 1 0
3eo4es 3  1 0 0
3no4es 3  0 1 0
```

slave input file (sample.slv)

```
8 sample sample
0eo4es  50.0 35.0  0.0  4eo4e 4no4e 5eo4e
0no4es
1eo4es
1no4es
2eo4es
2no4es
3eo4es
3no4es
```

The modal files *4eo4e.mod*, *4no4e.mod* and *5eo4e.mod* must already exist (created using ULTRA).

After the program has been executed, the following files will be created:

0eo4es.mod
0no4es.mod
1eo4es.mod
1no4es.mod
2eo4es.mod
2no4es.mod
3eo4es.mod
3no4es.mod

These files can be used like regular *.mod files. Also, when animating the mode shapes, it isn't necessary to use the original (master) mod files unless desired. If, in the above example, the user specified that rigid body motion (RBM) files were to be generated, the following files (with corresponding filenames) will be created instead.

0eo4es.rbm
0no4es.rbm
1eo4es.rbm
1no4es.rbm
2eo4es.rbm
2no4es.rbm
3eo4es.rbm
3no4es.rbm

The RBM files contains formulation information in the header. This is followed by tabulated rigid body motions; along with corresponding frequencies.

D.4 FORMULATION

The objective of this formulation is to develop expressions which can be used to calculate motion at other points of a floor in a building which has been instrumented.

D.4.1 REQUIREMENTS

The following formulation has been adapted from Çelebi, Safak, et al. (1987). The sensor locations should be positioned with the following considerations

(1) sensor locations should not lie on a straight line.

(2) directions of the sensors should not all be parallel

(3) all sensor directions should not intersect at one point.

D.4.2 NOMENCLATURE

The nomenclature is consistent with that of Çelebi, Safak, et al. (1987). The relevant variables are listed here:

x_i, y_i, z_i	Cartesian coordinates of point *i*
u_{xi}, u_{yi}, u_{zi}	displacement of point *i* in the *x*, *y*, and *z* directions, respectively
u_{x0}, u_{y0}, u_{z0},	rigid-body translations in the *x*, *y*, and *z* directions, respectively
$\theta_x, \theta_y, \theta_z$	rotation about the *x*, *y*, and *z* axis, respectively

D.4.3 TWO-DIMENSIONAL FORMULATION

The basis of the following formulae are two equations which describe the displacement of point *i* in the *x* and *y* directions. These equations are:

$$u_{xi} = u_{x0} + x_i(\cos\theta_z - 1) - y_i(\sin\theta_z) \quad \text{(D.1a)}$$

$$u_{yi} = u_{y0} + y_i(\cos\theta_z - 1) + x_i(\sin\theta_z) \quad \text{(D.1b)}$$

In these equations, u_{xi} and u_{yi} represent motion of the master nodes while u_{xo} and u_{yo} represent the motion of the floor at its centre of rotation. It is the latter two variables which must be solved

for. For this exercise, it will be assumed that 4 measurements have been made. Two of these measurements are aligned with the positive x direction while the other two are aligned with the positive y direction. Further, it is also assumed that none of the sensor share the same Cartesian coordinates. With this basis, Equation D.1 can be rewritten for these four measurements:

$$u_{x1} = u_{x0} + x_1(\cos\theta_z - 1) - y_1(\sin\theta_z) \quad \text{(D.2)}$$

$$u_{x2} = u_{x0} + x_2(\cos\theta_z - 1) - y_2(\sin\theta_z) \quad \text{(D.3)}$$

$$u_{y3} = u_{y0} + y_3(\cos\theta_z - 1) + x_3(\sin\theta_z) \quad \text{(D.4)}$$

$$u_{y4} = u_{y0} + y_4(\cos\theta_z - 1) + x4(\sin\theta_z) \quad \text{(D.5)}$$

This can also be written in matrix notation by treating the trigonometric expressions as distinct variables (even though one can be derived from the other):

$$\begin{Bmatrix} u_{x1} \\ u_{x2} \\ u_{y3} \\ u_{y4} \end{Bmatrix} = \begin{bmatrix} 1 & 0 & x_1 & -y_1 \\ 1 & 0 & x_2 & -y_2 \\ 0 & 1 & y_3 & x_3 \\ 0 & 1 & y_4 & x_4 \end{bmatrix} \begin{Bmatrix} u_{x0} \\ u_{y0} \\ (\cos\theta_z - 1) \\ \sin\theta_z \end{Bmatrix} \quad \text{(D.6)}$$

Since there are only three unknowns, only three of Equations D.2 to D.5 are required. However, if the trigonometric expressions are treated as distinct variables (as they were with Equation D.6), then all 4 equations can be used. Both of these treatments are used in the formulations presented below.

D.4.3.1 XXYY Formulation - Utilizing 4 Measurements

Subtracting Equation D.3 from Equation D.2 and subtracting Equation D.5 from Equation D.4 gives:

$$\beta_x = (\cos\theta_z - 1) - \alpha_x \sin\theta_z \quad \text{(D.7)}$$

$$\beta_y = (\cos\theta_z - 1) + \alpha_y \sin\theta_z \quad \text{(D.8)}$$

where

$$\alpha_x = \frac{y_1 - y_2}{x_1 - x_2} \quad \beta_x = \frac{u_{x1} - u_{x2}}{x_1 - x_2}$$
$$\alpha_y = \frac{x_3 - x_4}{y_3 - y_4} \quad \beta_y = \frac{u_{y3} - u_{y4}}{y_3 - y_4}$$

Subtracting Equation D.7 from Equation D.8 gives:

$$\sin\theta_z = \frac{\beta_y - \beta_x}{\alpha_y + \alpha_x} \quad \text{(D.9)}$$

The other trigonometric term can be solved for using the identity

$$(\cos\theta_z - 1) = \sqrt{1 - \sin^2\theta_z} - 1 \quad \text{(D.10)}$$

The rigid body translations can then be solved for by rearranging Equation D.1.

Finally, the displacement of the *slave* POM can be found by using Equation D.1 after substituting the rigid body translation and rotation and the slave node's Cartesian coordinates.

D.4.3.2 XXY Formulation - Utilizing 3 Measurements

Subtracting Equation D.3 from Equation D.2 gives:

$$\beta_x = (\cos\theta_z - 1) - \alpha_x \sin\theta_z \quad \text{(D.7)}$$

where

$$\alpha_x = \frac{y_1 - y_2}{x_1 - x_2} \quad \beta_x = \frac{u_{x1} - u_{x2}}{x_1 - x_2}$$

Two identities need to be introduced at this time; these being:

$$\sin 2\phi = \frac{2\tan\phi}{1 + \tan^2\phi} \quad \text{(D.11a)}$$

$$\cos 2\phi = \frac{1 - \tan^2\phi}{1 + \tan^2\phi} \quad \text{(D.11b)}$$

or

$$(\cos 2\phi - 1) = \frac{-2\tan^2\phi}{1+\tan^2\phi} \quad \text{(D.11c)}$$

By letting $2\phi = \theta_z$ and substituting Equations D.11a and D.11c into Equation D.7, and then rearranging gives:

$$\tan\phi = \frac{-2\alpha_x \pm \sqrt{\alpha^2 - \beta(\beta+2)}}{(\beta+2)} \quad (12)$$

Upon substituting Equations D.11a and D.11c into Equation D.7, a quadratic is created with an extraneous root. The correct root can be determined in a computer algorithm (as will be discussed in §D.5).

The trigonometric terms can now be solved for by substituting Equation D.12 into both Equation D.11a and Equation D.11c. The rigid body translations can then be solved for by rearranging Equation D.1.

Finally, the displacement of the *slave* POM can be found by using Equation D.1 after substituting the rigid body translation and rotation and the slave node's Cartesian coordinates.

D.4.3.3 XYY Formulation - Utilizing 3 Measurements

The following formulation is similar to that of the previous section except now two of the signals are in the y direction as opposed to the x direction.

Subtracting Equation D.5 from Equation D.4 gives:

$$\beta_y = (\cos\theta_z - 1) + \alpha_y \sin\theta_z \quad \text{(D.8)}$$

where

$$\alpha_y = \frac{x_3 - x_4}{y_3 - y_4} \quad \beta_y = \frac{u_{y3} - u_{y4}}{y_3 - y_4}$$

The identities introduced in the previous section are also used here. As before, by letting $2\phi = \theta_z$,

and substituting Equations D.11a and D.11c into Equation D.8, and then rearranging gives:

$$\tan\phi = \frac{+2\alpha_x \pm \sqrt{\alpha^2 - \beta(\beta+2)}}{(\beta+2)} \quad \text{(D.13)}$$

As with the XXY formulation, an extraneous root is created. The correct root can be determined in a computer algorithm (as will be discussed in §B.5).

The trigonometric terms can now be solved for by substituting Equation D.13 into both Equation D.11a and Equation D.11c. The rigid body translations can then be solved for by rearranging Equation D.1.

Finally, the displacement of the *slave* POM can be found by using Equation D.1 after substituting the rigid body translation and rotation and the slave node's Cartesian coordinates.

D.4.4 THREE-DIMENSIONAL FORMULATION

The basis of the following formulae are three equations which describe the displacement of point i in the x, y, and z directions. These equations are:

$$u_{xi} = u_{x0} + x_i(\cos\theta_y + \cos\theta_z - 2) - y_i(\sin\theta_z) + z_i(\sin\theta_y) \quad \text{(D.14a)}$$

$$u_{yi} = u_{y0} + x_i(\sin\theta_z) + y_i(\cos\theta_x + \cos\theta_z - 2) - z_i(\sin\theta_x) \quad \text{(D.14b)}$$

$$u_{zi} = u_{z0} - x_i(\sin\theta_y) + y_i(\sin\theta_x) + z_i(\cos\theta_x + \cos\theta_y - 2) \quad \text{(D.14c)}$$

There are several combinations of these equations but at least 6 are required to solve for the 6 unknowns. In this exercise, it will be assumed that 6 measurements have been made. Two, one, and three of these measurements are aligned with the positive x, y, and z directions, respectively. Further, it is also assumed that none of the sensor share the same Cartesian coordinates. Equation D.14 can be rewritten for the aforementioned measurements. However, the *closed form* solution is very tedious to formulate and very difficult to implement since the equations must be solved simultaneously and since several extraneous roots appear in the solution. Since the

rotations associated with building floors are small, the following approximations can be made:

$$\sin\theta_i \approx \theta_i$$
$$\cos\theta_i \approx 1$$

Using the above approximations in Equation D.14, the following six expressions can be written for the aforementioned displacements:

$$u_{x1} = u_{x0} - y_i\theta_z + z_i\theta_y \quad \text{(D.15)}$$

$$u_{x2} = u_{x0} - y_i\theta_z + z_i\theta_y \quad \text{(D.16)}$$

$$u_{y3} = u_{y0} + x_i\theta_z - z_i\theta_x \quad \text{(D.17)}$$

$$u_{z4} = u_{z0} - x_i\theta_y + y_i\theta_x \quad \text{(D.18)}$$

$$u_{z5} = u_{z0} - x_i\theta_y + y_i\theta_x \quad \text{(D.19)}$$

$$u_{z6} = u_{z0} - x_i\theta_y + y_i\theta_x \quad \text{(D.20)}$$

Equations D.15 through D.20 can be assembled into a matrix and solved simultaneously. The matrix equation is as follows:

$$\begin{bmatrix} 0 & 1 & 0 & -z_1 & 0 & x_1 \\ 1 & 0 & 0 & 0 & z_2 & -y_2 \\ 1 & 0 & 0 & 0 & z_3 & -y_3 \\ 0 & 0 & 1 & y_4 & -x_4 & 0 \\ 0 & 0 & 1 & y_5 & -x_5 & 0 \\ 0 & 0 & 1 & y_6 & -x_6 & 0 \end{bmatrix} \begin{Bmatrix} u_{xo} \\ u_{yo} \\ u_{zo} \\ \theta_x \\ \theta_y \\ \theta_z \end{Bmatrix} = \begin{Bmatrix} u_{y1} \\ u_{x2} \\ u_{x3} \\ \theta_{z4} \\ \theta_{z5} \\ \theta_{z6} \end{Bmatrix} \quad \text{(D.21)}$$

D.5 COMPUTER ALGORITHM CONSIDERATIONS

For the two-dimensional formulation, the objective was to first calculate the rigid body rotation about the center of rotation, and then use this value to calculate the rigid body translations. Because of the numeric problems associated with inverse trigonometric routines (arcsine, arccosine, etc.), the value of θ_i was never calculated directly since it is not actually needed.

In general, the XXYY formulation is stable while the other formulations can become unstable if

the *correct* root is not used in subsequent formulae. It was found that the extraneous root led to excessively high rigid body rotations (somewhere in the range of 80°-180°). Therefore, the correct root can be determined by calculating θ_z and then checking to see if it is excessive (or conversely checking to see if it is a reasonable value).

Another problem arises when the rigid body translations are calculated. Equations D.2 and D.3 will generally give different answers for u_{xo}, and similarly, Equations D.4 and D.5 will generally give different answers for u_{yo}. One way to deal with this is to calculate a known displacement, and then comparing it with the given displacement. The value which is closest can then be used in subsequent calculations. This problem arises for several reasons including: (a) loss of precision, (b) inaccurate Cartesian coordinates of the sensors, and (c) that the structure to which the sensors were mounted is not a rigid diaphragm although its behavior is assumed to be similar.

The three-dimensional formulation is generally stable. In the event that the matrix becomes singular, the formulation reverts to an appropriate two-dimensional formulation.

A

B

C

D

E

F

G

H

APPENDIX E
MODAL ASSURANCE CRITERIUM SOFTWARE (MAC) - OPERATING INSTRUCTIONS

E.1 DESCRIPTION

Comparison of dynamic modal characteristics are made on the basis of both frequencies (periods) and vibration mode shapes. One method of correlating mode shapes is to perform a modal assurance criterium (MAC) analysis. This involves a formulation which has been described in Chapter 2; and is reproduced here for reference (Equation E.1).

$$MAC(a,x) = \frac{\left[\{\phi_a\}^T\{\phi_x\}\right]^2}{\left[\{\phi_a\}^T\{\phi_a\}\right]\left[\{\phi_x\}^T\{\phi_x\}\right]} \quad \text{E.1}$$

This program takes two sets of mode shapes (analytical and/or experimental) and assembles a matrix of MAC values. This permits the user to correlate mode shapes which have been obtained from different sources.

E.2 INSTALLATION AND SYSTEM REQUIREMENTS

This program was written in C++ and compiled with a Borland C++ 3.1 compiler. The program should run on any PC computer with a 80386 processor (with an 80387 FPU) or higher, and at least 1Mb of memory.

The program can be copied into any directory and executed from any other directory provided there is a *path* to it.

E.3 PROGRAM EXECUTION

E.3.1 RUNNING THE PROGRAM

In order to assemble a MAC matrix, the names of the two mode shape files as well as a name for

the output file must be specified on the command line. For assistance, executing the program without any arguments, i.e. by typing:

```
MAC <enter>
```

at the DOS prompt will display the correct sequence of these filenames as well as some additional information (as shown in Figure E.1).

This program supports several different mode shape formats, which are described in more detail in §E.3.2. However, some of these formats (such as the ETABS *.EIG format) are saved in a more efficient format. Therefore, MAC can also be executed with only one or two of the mode shape filenames specified so that they can be translated into a better format. These translated files can be used in subsequent MAC analyses.

```
MAC   Modal Assurance Criterium Analysis · 1.0
      A Program by Norman Schuster

MAC  modeShapeFile1  [modeShapeFile2]  [macFilename]

modeShapeFile#: mode shape file
   macFilename: output file (required for MAC analysis)

DO NOT include the file extension when specifying the files!

supported mode shape file formats (in scanning order):
Analytical    (*.ams)
Experimental  (*.xms)
ETABS         (*.eig) (saves in *.ams format)
SLAVE         (*.sms) (saves in *.xms format)
```

Figure E.1. Message displayed when MAC is executed with no arguments

E.3.2 SUPPORTED MODE SHAPE FORMATS

This program supports several different mode shape formats. However, it will only save mode shape files in either the AMS or XMS format. Further, this program will scan for the following extensions in this order: *.AMS, *.XMS, *.EIG, and *.SMS. For example, if there are two files with identical names but different extensions, such as FILENAME.EIG and FILENAME.AMS, the file with the name FILENAME.AMS will be opened, not the other one.

E.3.2.1 ETABS Mode Shape (EIG)

One application of this program was to compare experimental mode shapes with analytical mode shapes obtained from dynamic analysis using the program ETABS (CSI Ltd., 1992). To facilitate this process, a routine was developed which would read the ETABS *.EIG files. This routine determines the number of periods and storeys in this file, and then extracts the frequencies, storey labels, and corresponding motion of each floor. This information is later saved in the AMS format (see §E.3.2.3 for details).

E.3.2.2 Slave Mode Shape (SMS)

The ETABS mode shapes consist of only 3 degrees-of-freedom per floor (two translation and one rotation) with respect to the centre-of-mass of that floor. Since the experimental mode shapes were not specified in this manner, a file format was developed which would transform the experimental mode shape (of a building) into planar motion relative to the centre-of-rotation. This allowed a proper comparison between the two types of mode shapes. This process was facilitated by the program SLAVE (see Appendix D) which performs this transformation in the process of creating slave nodes.

The format of this file is given below:

```
file_header (max. 80 characters)
number_of_storeys (NS)
label_1  RBM_Filename_1
.
.
.
label_NS  RBM_Filename_NS
number_of_frequencies (NF)
freq_1
.
.
.
freq_NF
```

The `file_header` is for adding a description. This is followed by the number of storeys as well as the storey labels and corresponding modal displacements specified in a RBM file. The

RBM files must already exist from a previous execution of the program SLAVE. Also, the storey labels must be identical to the corresponding storey label in the ETABS model. Finally, the number of frequencies and a list of the frequencies which correspond to the mode shapes to be assembled are specified in the input file. These frequencies MUST correspond exactly (4 decimal precision) to those in the RBM files.

The mode shapes which are assembled in this process are later saved in the XMS format (see §E.3.2.4 for details).

E.3.2.3 Analytical Mode Shape (AMS)

This mode shape file contains all the pertinent information required for the MAC analysis. This consists of the modal frequencies, and the corresponding modal displacements for each storey. The format of this file is given below:

```
file_header (max. 80 characters)
number_of_frequencies (NF)
            <TAB>freq_1  <TAB>freq_2  . . .   <TAB>freq_NF
number_of_storeys (NS)
label_1  Ux  <TAB>Ux_1    <TAB>Ux_2    . . .   <TAB>Ux_NF
label_1  Uy  <TAB>Uy_1    <TAB>Uy_2    . . .   <TAB>Uy_NF
label_1  Qz  <TAB>Qz_1    <TAB>Qz_2    . . .   <TAB>Qz_NF
<BLANK LINE>
label_2  Ux  <TAB>Ux_1    <TAB>Ux_2    . . .   <TAB>Ux_NF
.
.
.
label_NS Qz  <TAB>Qz_1    <TAB>Qz_2    . . .   <TAB>Qz_NF
```

The `file_header` is for adding a description. This is followed by the number of frequencies with the specified frequencies on the following line. Note that each frequency is preceded by a <TAB>, and that they need not be in any particular order. Following the frequencies is the modal displacements for each storey. This consists of 3 lines for each direction (translation in the x and y directions, and rotation about the z axis). Each of these lines begins with the storey label (which must be identical to the corresponding storey label in the other mode shape file), the direction (Ux, Uy, or Qz), followed by the displacement corresponding to each frequency

specified at the top of the column. Each displacement must be preceded by a <TAB>.

This file can be readily imported into a spreadsheet for easy manipulation and exported just as easily. This format is used for saving modal information obtained from an ETABS *.EIG format file. It can also be used to assemble other analytical mode shapes to be used in a MAC analysis.

E.3.2.4 Experimental Mode Shape (XMS)

This file format is identical to the AMS format. A different extension is used so that analytical mode shapes (AMS) can be distinguished from experimental mode shapes (XMS).

E.3.3 EXAMPLE

Suppose a comparison is to be made between analytical mode shapes obtained from using ETABS and experimental mode shapes obtained using ULTRA. The output file from ETABS will be in the EIG format and can be used as is. The mode shape obtained from using ULTRA requires further manipulation.

First, rigid-body-motion (RBM) files must be created using the program SLAVE. The corresponding input file for this purpose is given below.

slave input file (ct32r52n.slv)

```
17 ct32s ct32s52n
3252nP06  0.0  0.0  0.0  04eo52n  06eo52n  04no52n  05no52n
3252nL01  0.0  0.0  0.0  07eo52n  09eo52n  07no52n  08no52n
3252nL02  0.0  0.0  0.0  10eo52n  12eo52n  10no52n  11no52n
3252nL05  0.0  0.0  0.0  16eo52n  18eo52n  16no52n  17no52n
3252nL07  0.0  0.0  0.0  19eo52n  21eo52n  19no52n  20no52n
3252nL09  0.0  0.0  0.0  22eo52n  24eo52n  22no52n  23no52n
3252nL11  0.0  0.0  0.0  25eo52n  27eo52n  25no52n  26no52n
3252nL13  0.0  0.0  0.0  28eo52n  30eo52n  28no52n  29no52n
3252nL15  0.0  0.0  0.0  31eo52n  33eo52n  31no52n  32no52n
3252nL17  0.0  0.0  0.0  34eo52n  36eo52n  34no52n  35no52n
3252nL19  0.0  0.0  0.0  37eo52n  39eo52n  37no52n  38no52n
3252nL21  0.0  0.0  0.0  40eo52n  42eo52n  40no52n  41no52n
3252nL23  0.0  0.0  0.0  43eo52n  45eo52n  43no52n  44no52n
3252nL25  0.0  0.0  0.0  46eo52n  48eo52n  46no52n  47no52n
3252nL27  0.0  0.0  0.0  49eo52n  51eo52n  49no52n  50no52n
3252nL29  0.0  0.0  0.0  52eo52n  54eo52n  52no52n  53no52n
3252nL32  0.0  0.0  0.0  55eo52n  57eo52n  55no52n  56no52n
```

The program SLAVE must then be executed by specifying this filename along with "r" in the list of options (see Appendix D for exact details of running SLAVE). After this, the RBM files listed in Table E.1 will be created.

Now, in order to perform the MAC analysis with the ETABS file, the corresponding storey labels must be specified. A list of the storey labels used in the ETABS file and the corresponding floors which were measured experimentally are shown in the table below.

Table E.1. Corresponding storey labels required for the MAC analysis.

ETABS Storey Labels	Corresponding RBM File
L32	3252nL32
L31	
L30	
L29	3252nL29
L28	
L27	3252nL27
L26	
L25	3252nL25
L24	
L23	3252nL23
L22	
L21	3252nL21
L20	
L19	3252nL19
L18	
L17	3252nL17
L16	
L15	3252nL15
L14	
L13	3252nL13
L12	
L11	3252nL11
L10	
L09	3252nL09
L08	
L07	3252nL07
L06	
L05	3252nL05
L04	
L03	
L02	3252nL02
L01	3252nL01
P02	
P04	
P06	3252nP06

The next step is to create a slave mode shape (SMS) file. The contents of this file are given

below:

slave mode shape (ct32_52n.sms)

```
City Tower - 32 Storeys
17
P06 3252nP06
L01 3252nL01
L02 3252nL02
L05 3252nL05
L07 3252nL07
L09 3252nL09
L11 3252nL11
L13 3252nL13
L15 3252nL15
L17 3252nL17
L19 3252nL19
L21 3252nL21
L23 3252nL23
L25 3252nL25
L27 3252nL27
L29 3252nL29
L32 3252nL32
4
0.5469
2.3047
4.8828
7.5391
```

As can be seen, the storey label and the corresponding RBM file have been specified together near the beginning of this file. The list of storey labels and RBM files is followed by the number of frequencies and the frequencies of the mode shapes to be assembled from the RBM files. These frequencies need not be in any particular order.

Once, this file is created, the MAC analysis can be performed by typing the following at the DOS prompt:

```
MAC  ct32_52n  ct32d  ct32d52n
```

where "ct32d" is the name of the ETABS mode shape file. Following the analysis, the following files will be created:

ct32_52n.xms
ct32d.ams
ct32d52n.mac

The first two files contain the information derived from the original mode shape files, and can be

used again in subsequent analyses. The last file contains the MAC matrix. The contents of this file is shown below. Note that 4 matrices are created - one for each direction and one which contains the sum of all three matrices. Also, the frequencies from the first mode shape file (ct32_52e.xms) appear at the top of each column while the frequencies from the second mode shape file (ct32d.ams) appear at the beginning of each row. Furthermore, the format of this file is such that it can be readily imported into a spreadsheet for formatting and/or further manipulation.

MAC output file (ct32d52n.mac)

```
Modal Assurance Criteria (MAC) Analysis
(1) ct32_52e.xms City Tower - 32 Storeys
(2) ct32d.ams  CITYTOWER, VANCOUVER B.C. - CT32D

ct32_52e.xms runs left to right; ct32d.ams runs top to bottom

All components

             0.5469       2.3047       4.8828       7.5391
0.4729       2.3709       0.1974       0.3675       0.1580
0.6205       2.2581       0.5275       0.1572       0.1031
1.1840       1.7152       0.8798       0.1238       0.2618
2.3815       0.1088       2.0465       0.7719       0.0695
3.2243       0.0122       1.6249       1.1772       0.0389
3.5687       0.0194       1.7435       1.1506       0.0988
4.8618       0.0182       0.5759       2.2417       0.3185
6.2659       0.0060       0.2937       1.7850       0.7622
7.3189       0.1219       0.0406       0.3143       2.3099
7.7835       0.0793       0.1940       0.8762       2.3945

Ux component

             0.5469       2.3047       4.8828       7.5391
0.4729       0.8409       0.0093       0.3538       0.1099
0.6205       0.9765       0.0519       0.1269       0.0796
1.1840       0.9059       0.1688       0.1013       0.1942
2.3815       0.0435       0.1210       0.5316       0.0429
3.2243       0.0053       0.1211       0.6858       0.0122
3.5687       0.0190       0.1278       0.8028       0.0412
4.8618       0.0075       0.1423       0.3440       0.1863
6.2659       0.0001       0.0174       0.0356       0.6634
7.3189       0.0018       0.0116       0.1490       0.7386
7.7835       0.0014       0.0130       0.1162       0.6883

Uy component

             0.5469       2.3047       4.8828       7.5391
0.4729       0.8275       0.0135       0.0044       0.0415
0.6205       0.6399       0.1978       0.0004       0.0092
1.1840       0.1087       0.5215       0.0004       0.0546
2.3815       0.0001       0.9832       0.0004       0.0011
```

3.2243	0.0000	0.6891	0.1963	0.0109
3.5687	0.0000	0.7950	0.2086	0.0454
4.8618	0.0027	0.1189	0.9208	0.0003
6.2659	0.0059	0.1530	0.8573	0.0403
7.3189	0.0556	0.0228	0.1649	0.8469
7.7835	0.0510	0.0130	0.0819	0.9267

Qz component

	0.5469	2.3047	4.8828	7.5391
0.4729	0.7024	0.1745	0.0092	0.0065
0.6205	0.6417	0.2779	0.0299	0.0143
1.1840	0.7006	0.1895	0.0220	0.0131
2.3815	0.0652	0.9423	0.2399	0.0255
3.2243	0.0068	0.8147	0.2950	0.0158
3.5687	0.0004	0.8207	0.1393	0.0123
4.8618	0.0080	0.3148	0.9769	0.1319
6.2659	0.0001	0.1233	0.8922	0.0585
7.3189	0.0646	0.0062	0.0004	0.7245
7.7835	0.0269	0.1679	0.6781	0.7795

F

APPENDIX F
ERROR ANALYSIS

This appendix contains several signal processing plots which were used to assess the accuracy of the instrumentation (FBA sensors) which was used to measure the ambient vibrations of the building.

Figures F.1 to F.8 were used to determine if any aliasing was occurring during measurements of the ambient vibrations. These figures show power spectral densities (PSD) of two measurements using the same sensor arrangement but with different sampling rates; these being 40 Hz and 80 Hz. For the PSD corresponding to the 80 Hz sampling rate, the data in the 20 to 40 Hz range was plotted in reverse order to facilitate locating aliases.

Figures F.9 to Figures F.14 were used to compare the different sensitivities of the FBA sensors. Coherence functions, frequency response functions, and phase functions were generated to determine variances between different sensors.

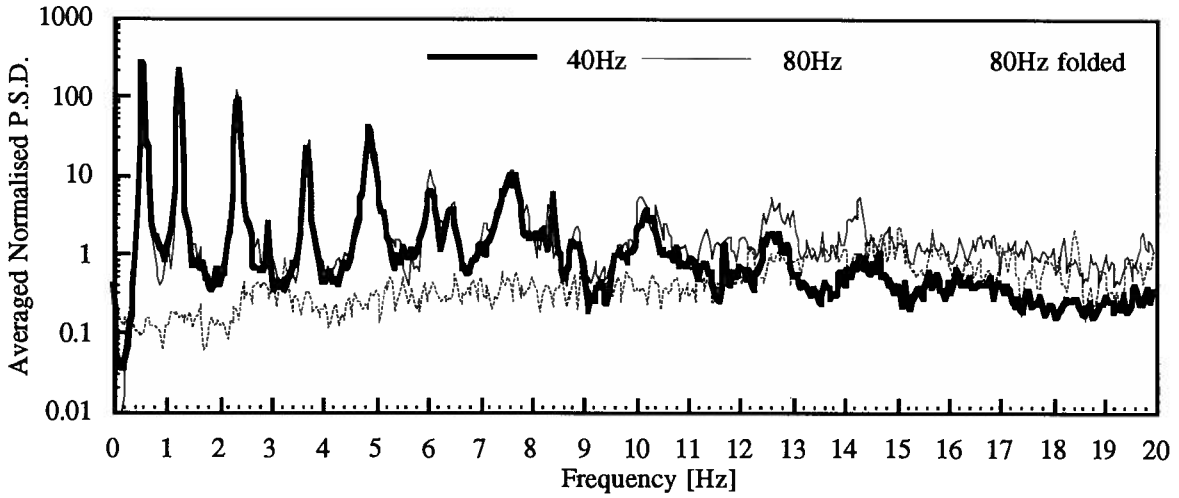

Figure F.1. Comparison of power spectral density functions of signals sampled at different rates (40 Hz and 80 Hz) using FBA #1 oriented in the NS direction.

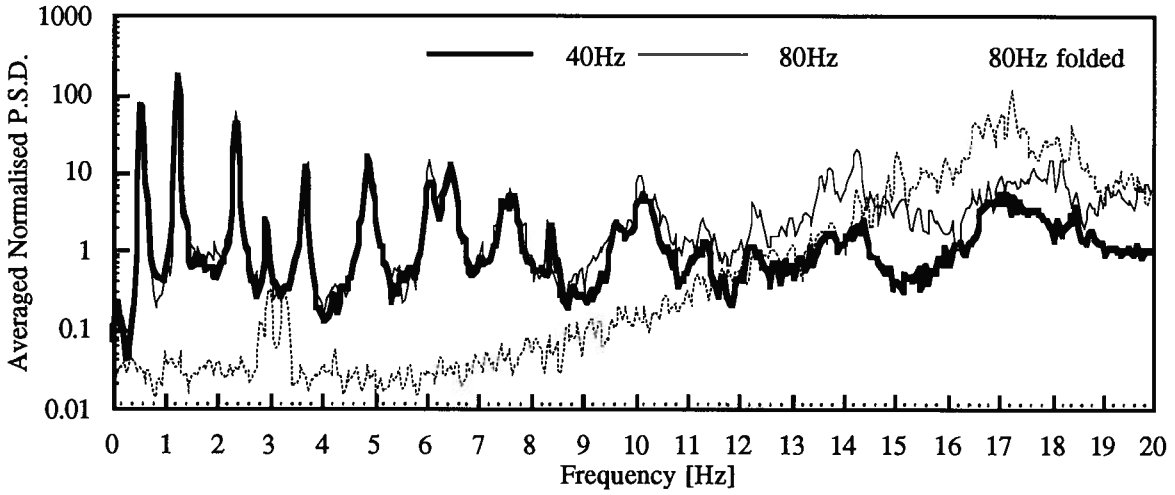

Figure F.2. Comparison of power spectral density functions of signals sampled at different rates (40 Hz and 80 Hz) using FBA #3 oriented in the NS direction.

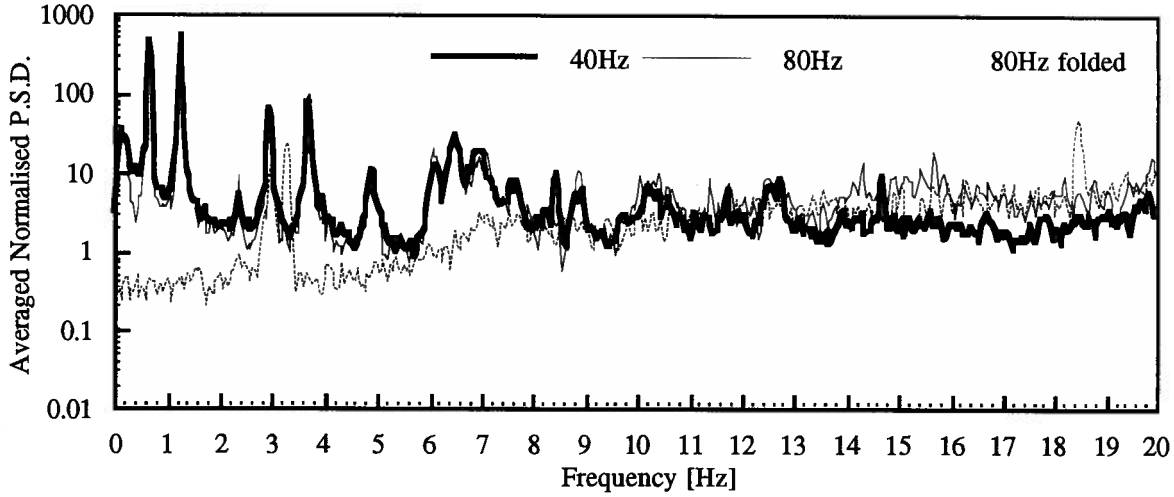

Figure F.3. Comparison of power spectral density functions of signals sampled at different rates (40 Hz and 80 Hz) using FBA #2 oriented in the EW direction.

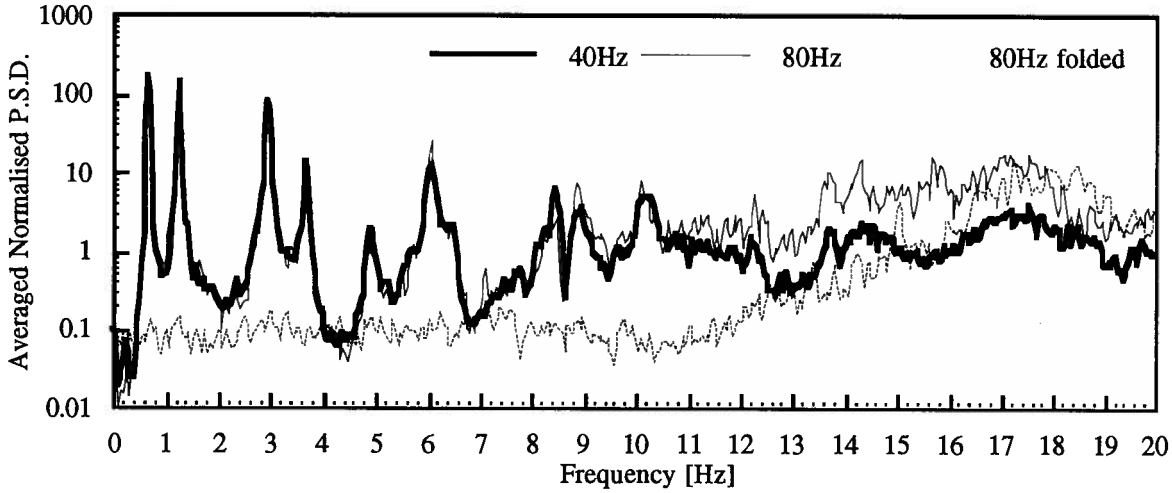

Figure F.4. Comparison of power spectral density functions of signals sampled at different rates (40 Hz and 80 Hz) using FBA #4 oriented in the EW direction.

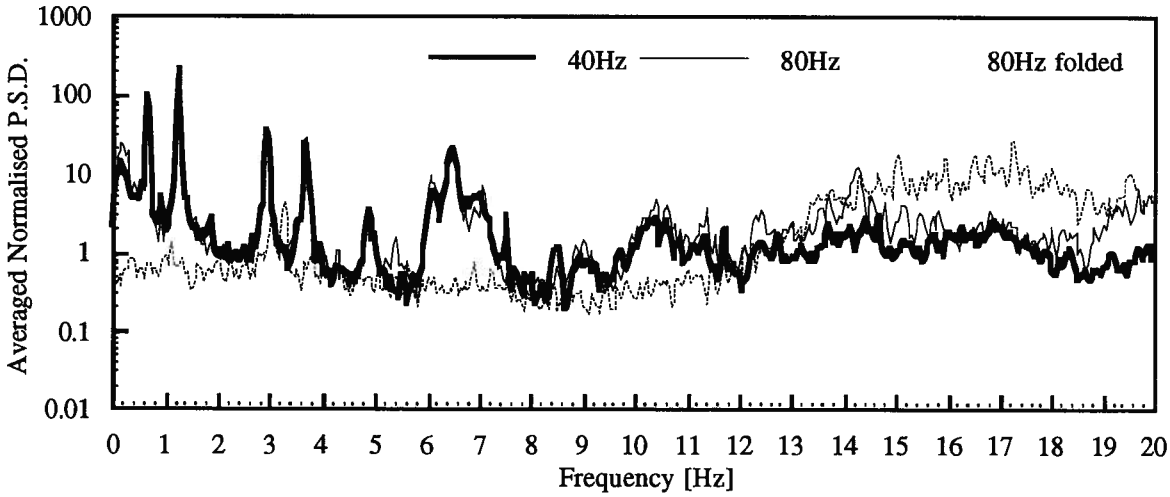

Figure F.5. Comparison of power spectral density functions of signals sampled at different rates (40 Hz and 80 Hz) using FBA #5 oriented in the EW direction.

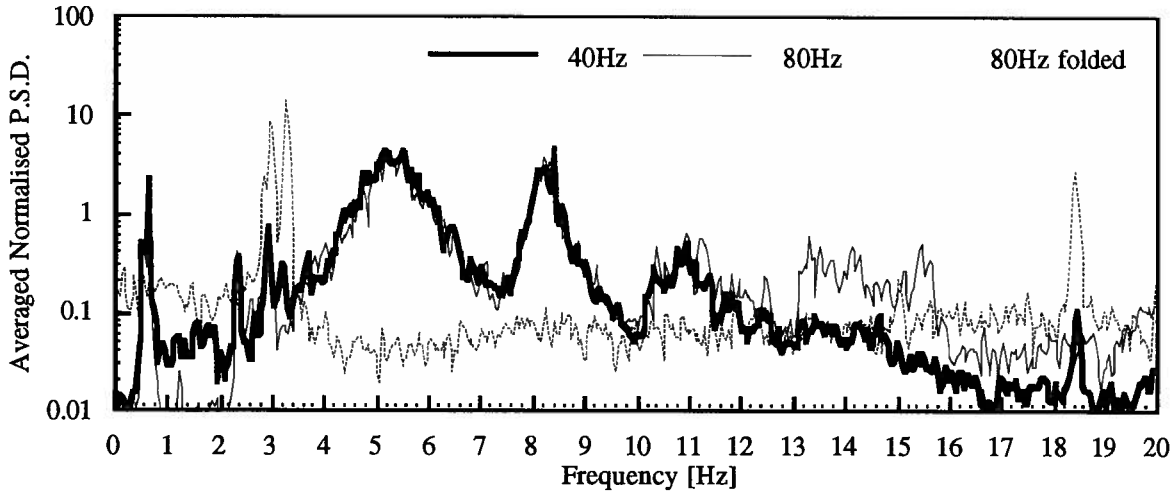

Figure F.6. Comparison of power spectral density functions of signals sampled at different rates (40 Hz and 80 Hz) using FBA #6 oriented in the vertical direction.

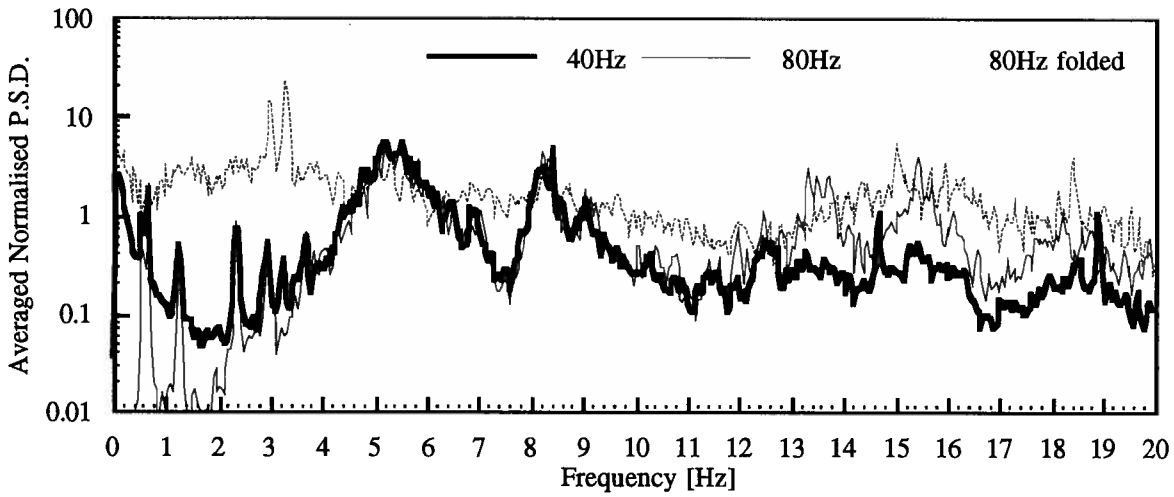

Figure F.7. Comparison of power spectral density functions of signals sampled at different rates (40 Hz and 80 Hz) using FBA #7 oriented in the vertical direction.

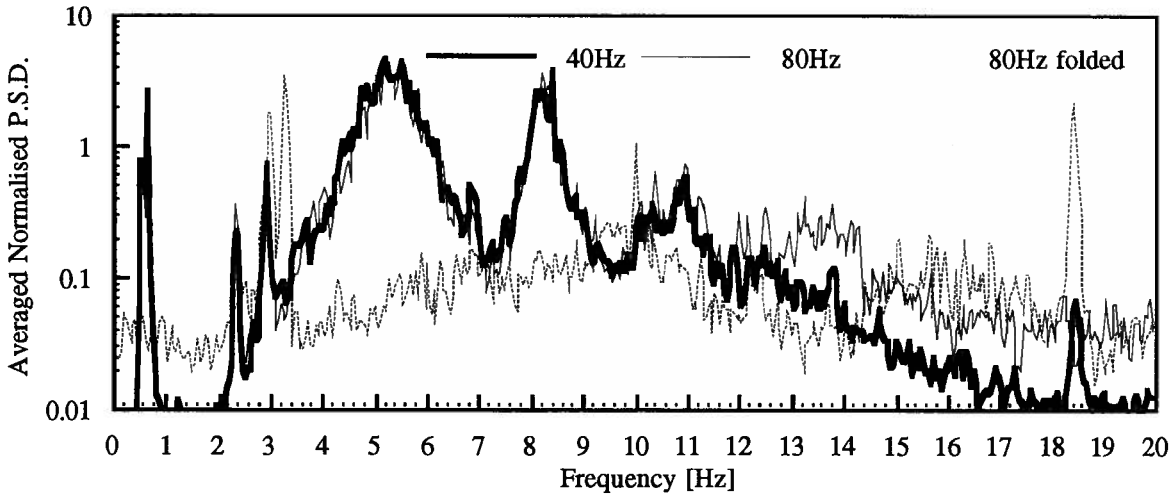

Figure F.8. Comparison of power spectral density functions of signals sampled at different rates (40 Hz and 80 Hz) using FBA #8 oriented in the vertical direction.

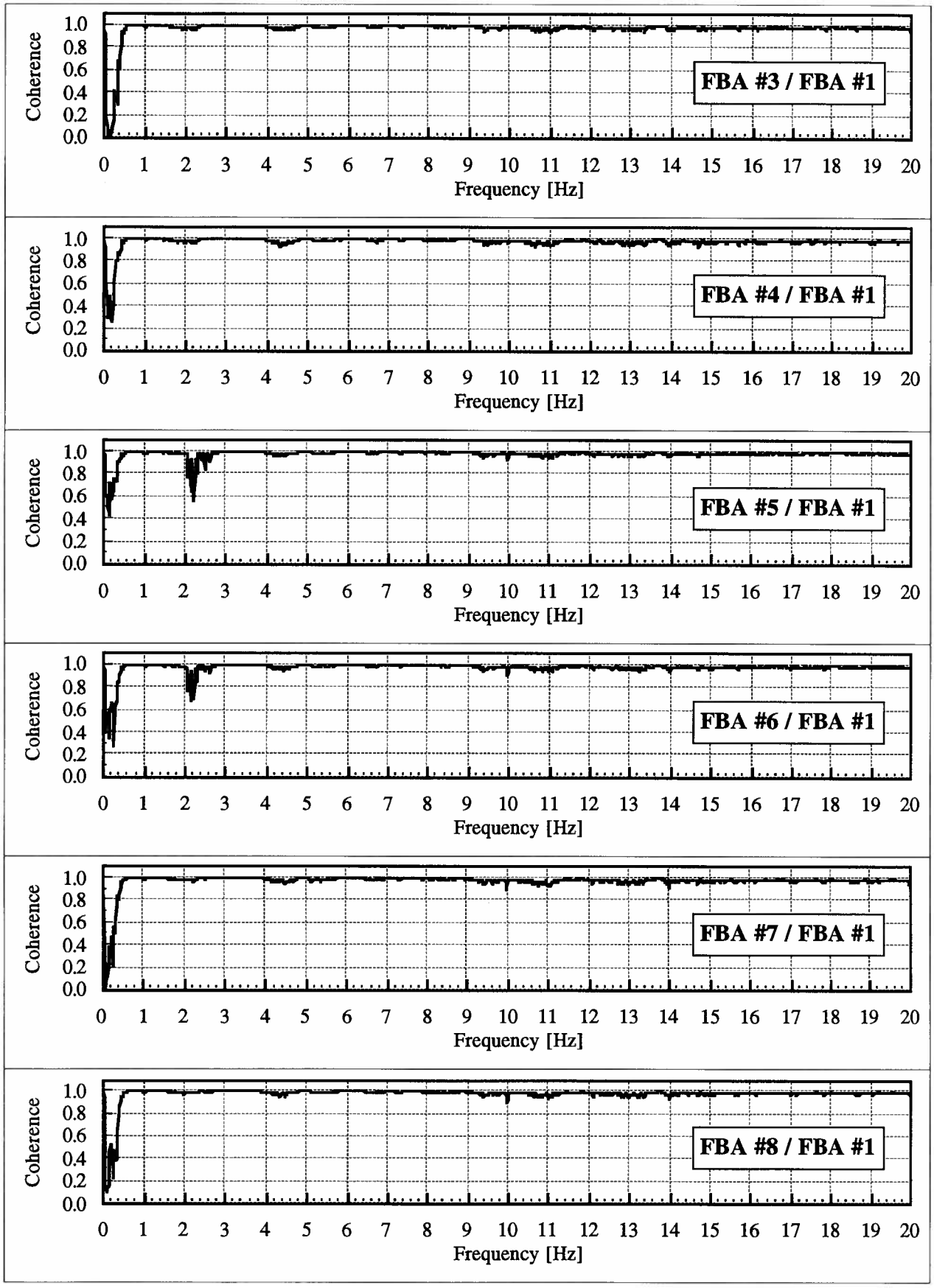

Figure F.9. Coherence functions of FBA #3,4,5,6,7, and 8 w.r.t. FBA #1.

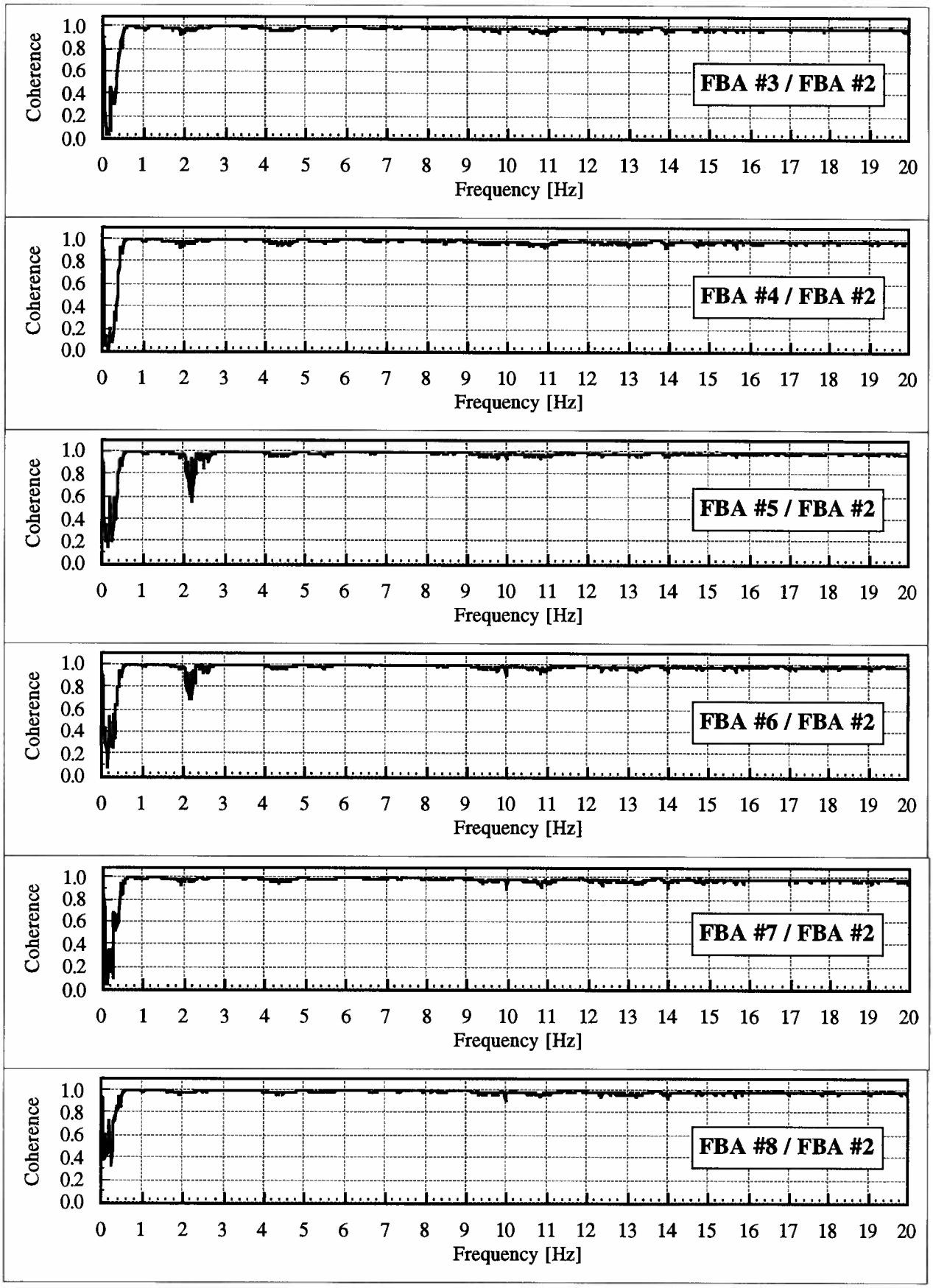

Figure F.10. Coherence functions of FBA #3,4,5,6,7, and 8 w.r.t. FBA #2.

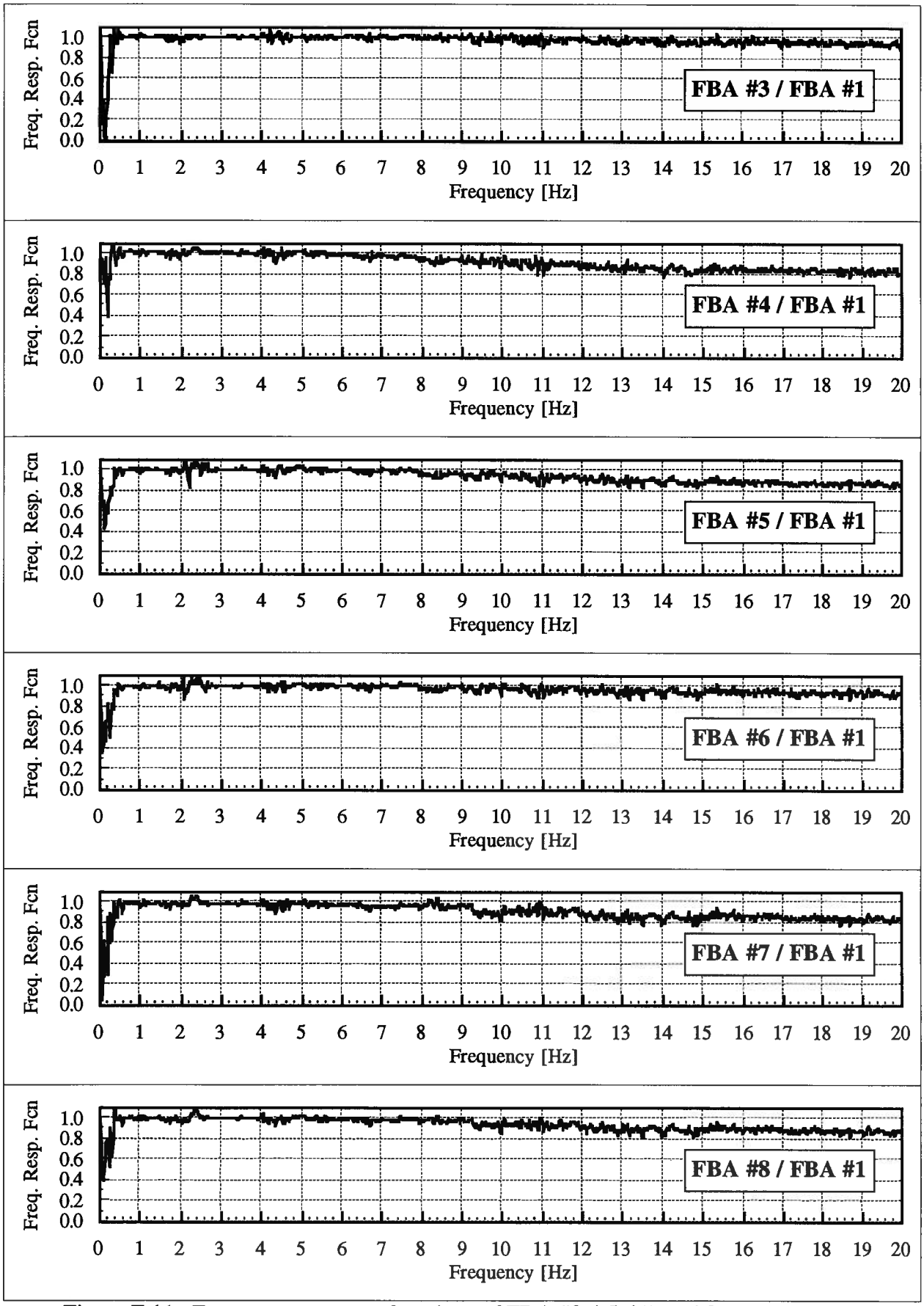

Figure F.11. Frequency response functions of FBA #3,4,5,6,7, and 8 w.r.t. FBA #1.

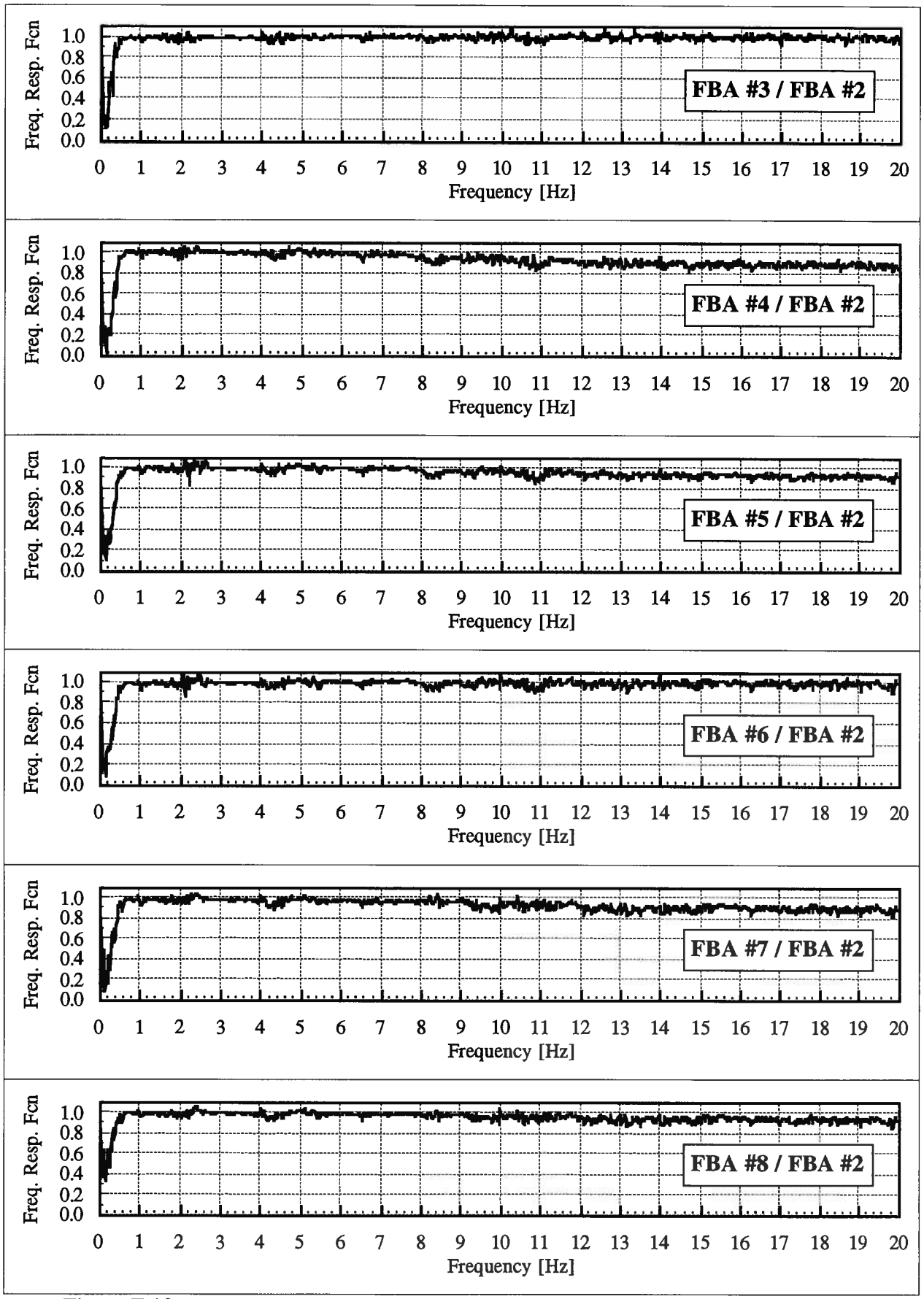

Figure F.12. Frequency response functions of FBA #3,4,5,6,7, and 8 w.r.t. FBA #2.

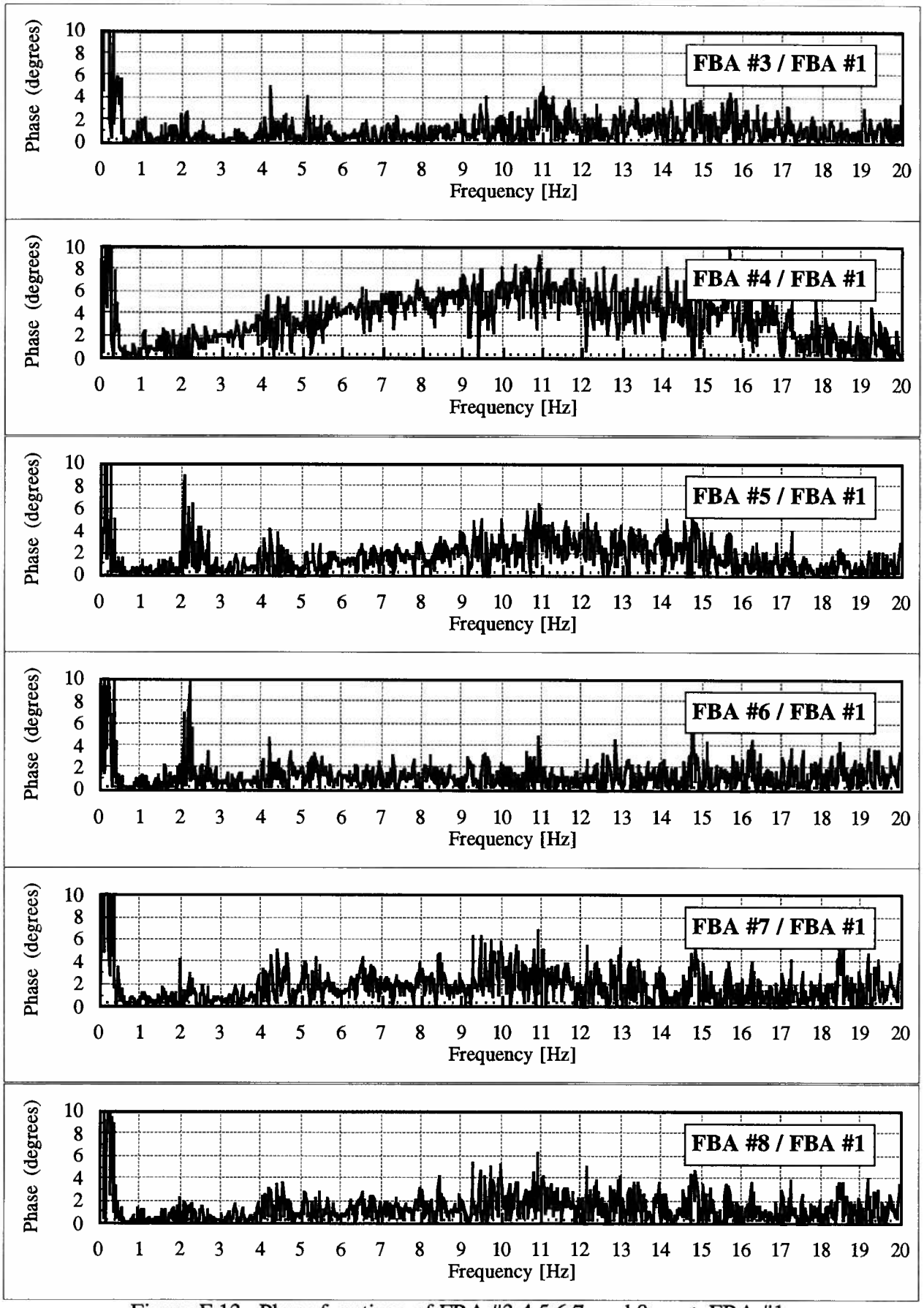

Figure F.13. Phase functions of FBA #3,4,5,6,7, and 8 w.r.t. FBA #1.

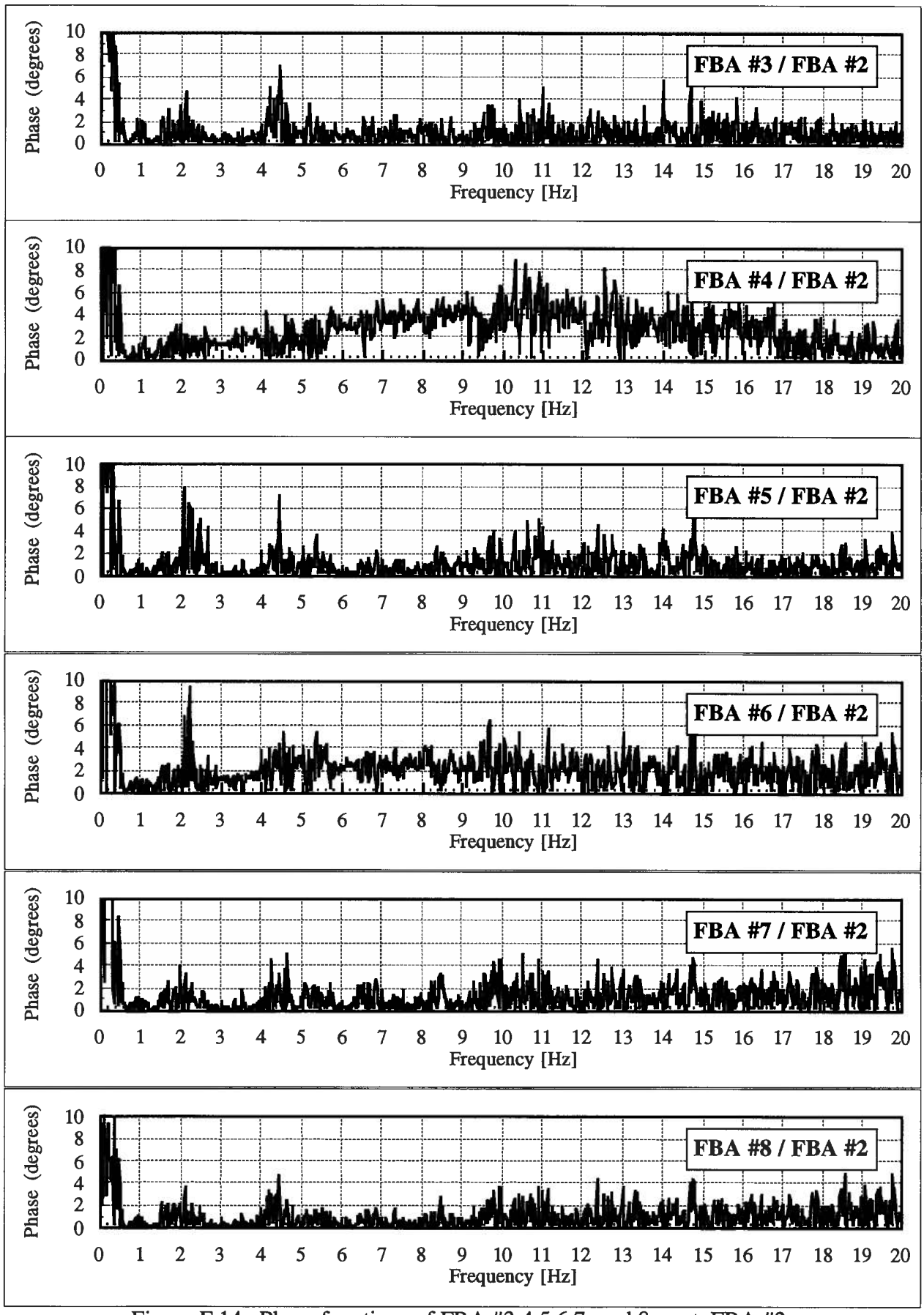

Figure F.14. Phase functions of FBA #3,4,5,6,7, and 8 w.r.t. FBA #2.

G

APPENDIX G
POWER SPECTRAL DENSITY PLOTS

This appendix contains several of the averaged normalized power spectral density (ANPSD) plots which were used to locate natural frequencies of the building. Pairs of signals, in both the North-South and East-West direction of the building, were added and subtracted to produce spectra isolating translational and torsional motion respectively. These spectra are shown in figures G.1 through G.6. In addition, the spikes corresponding to natural frequencies are labeled with the corresponding vibration mode. The naming convention for these modes is explained in Table 5.1.

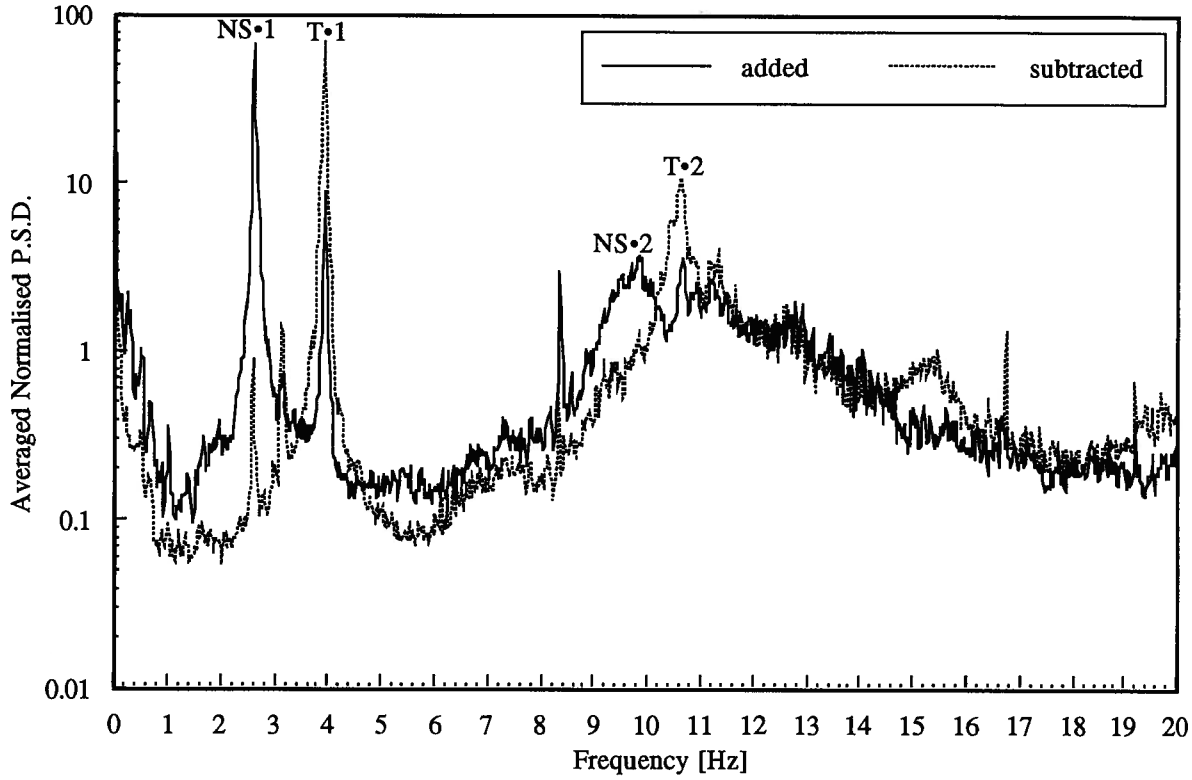

(a) Signals in the North-South direction of the building

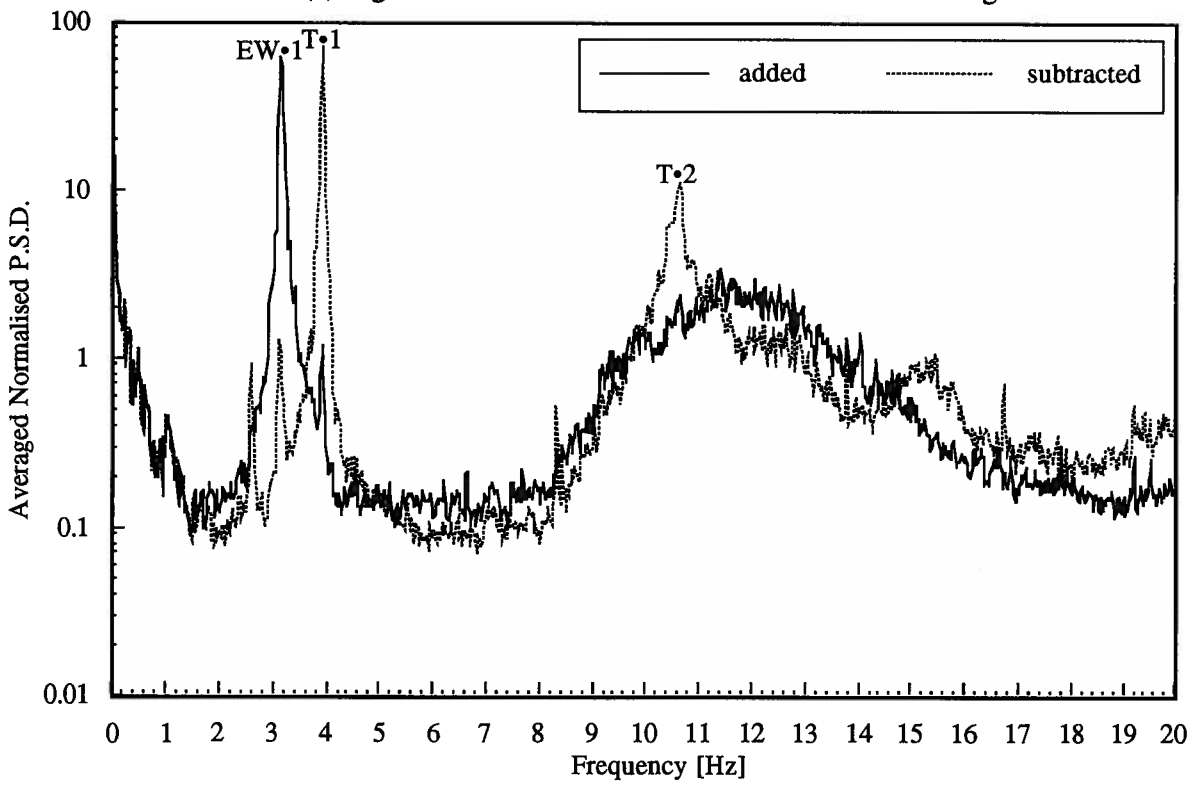

(b) Signals in the East-West direction of the building

Figure G.1. ANPSD plots for all of the lateral signals from the CT10 test. Peaks corresponding to natural frequencies are labeled with the corresponding mode.

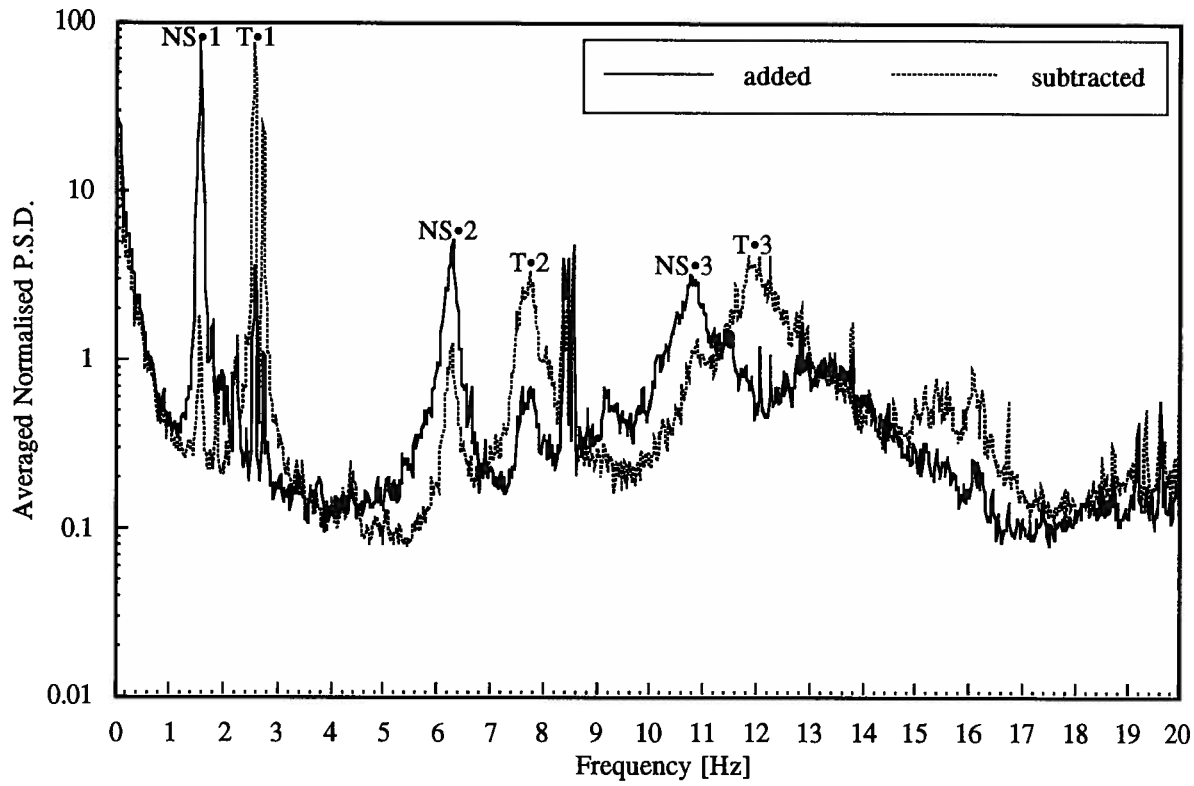

(a) Signals in the North-South direction of the building

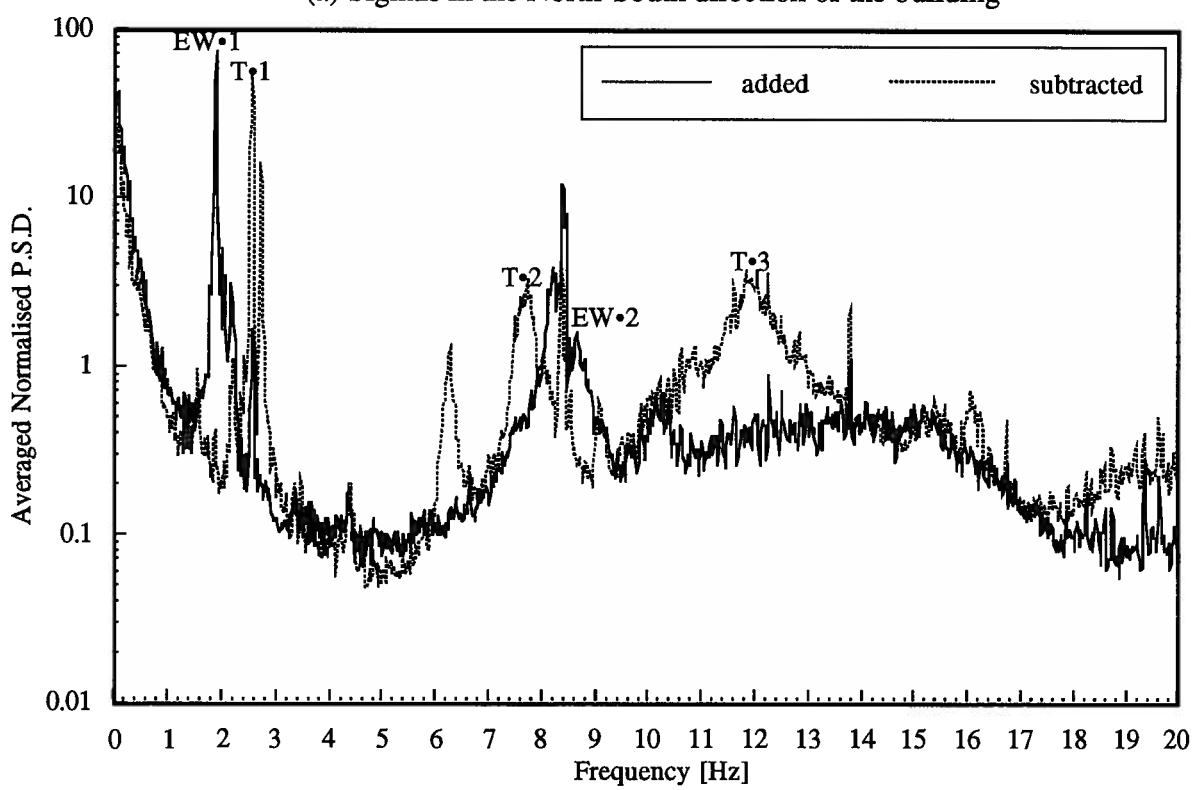

(b) Signals in the East-West direction of the building

Figure G.2. ANPSD plots for all of the lateral signals from the CT15 test. Peaks corresponding to natural frequencies are labeled with the corresponding mode.

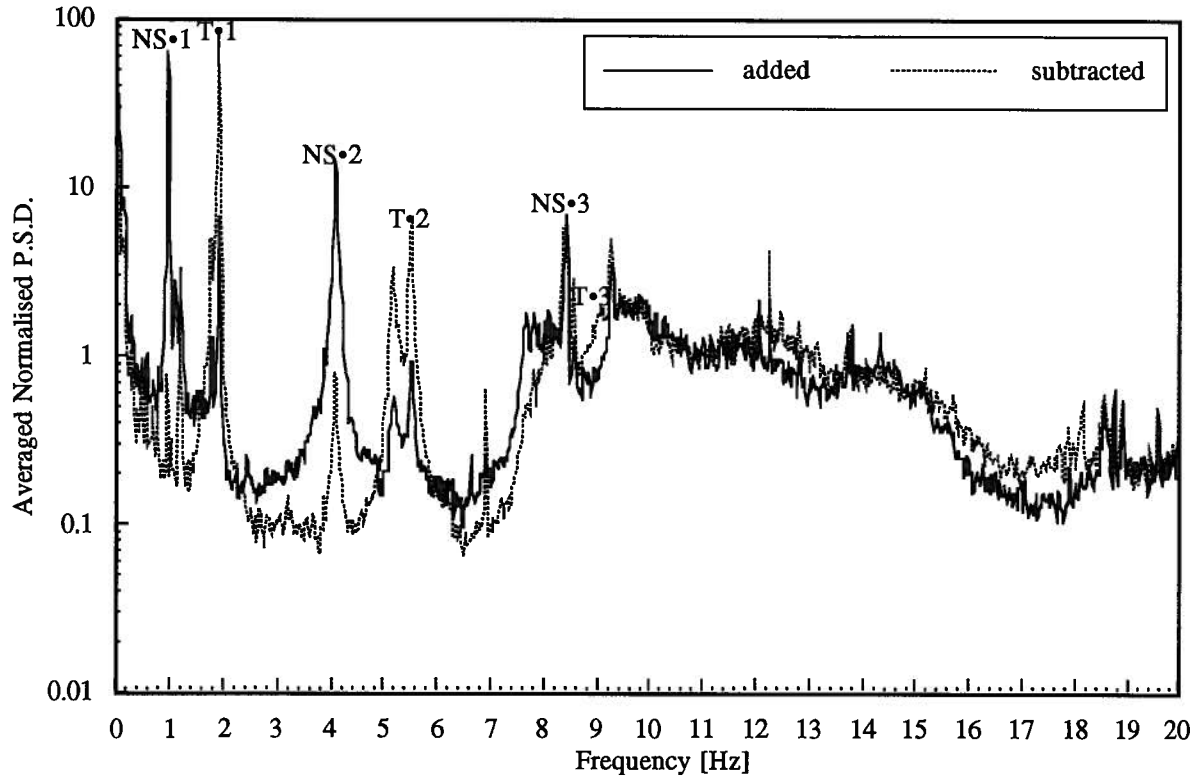

(a) Signals in the North-South direction of the building

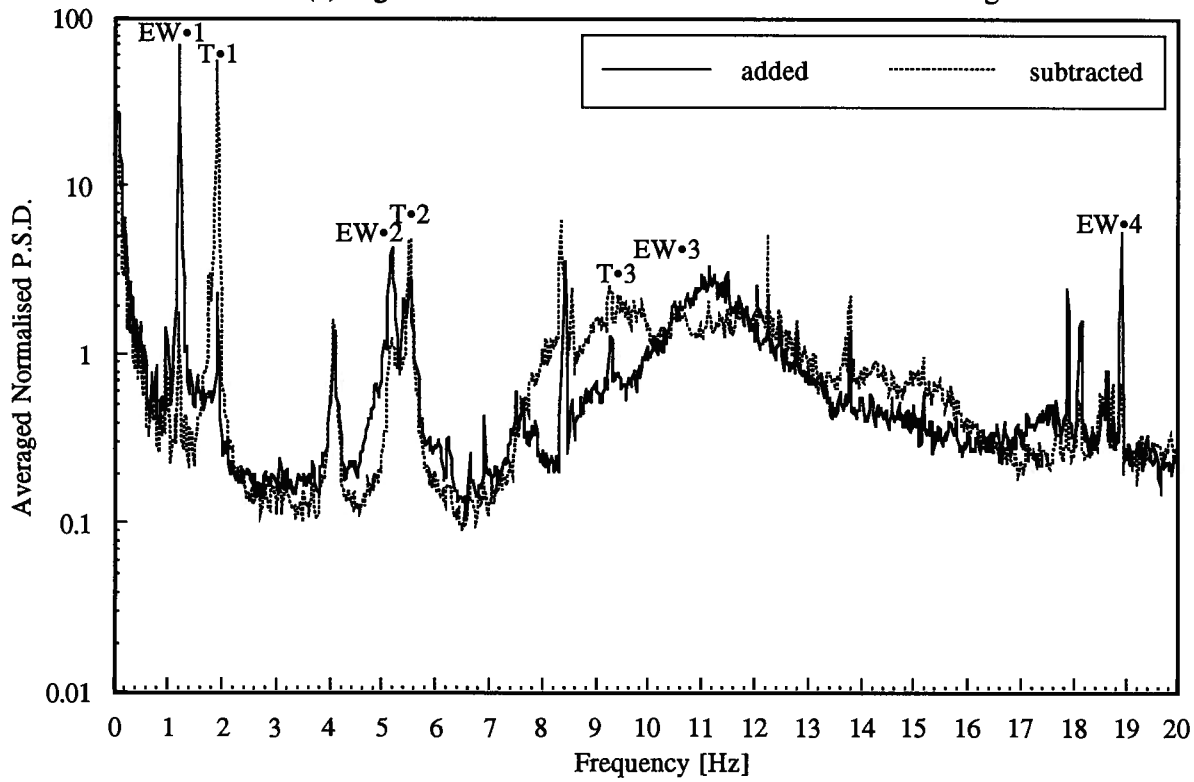

(B) Signals in the East-West direction of the building

Figure G.3. ANPSD plots for all of the lateral signals from the CT20 test. Peaks corresponding to natural frequencies are labeled with the corresponding mode.

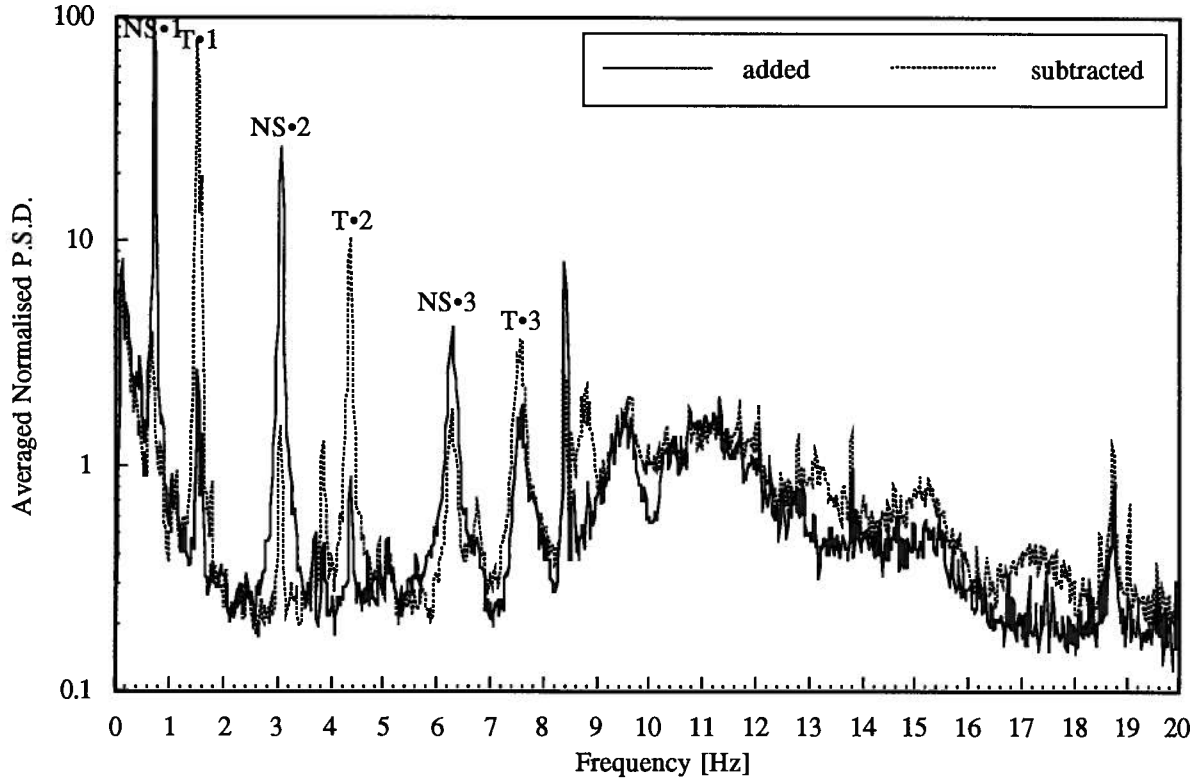

(a) Signals in the North-South direction of the building

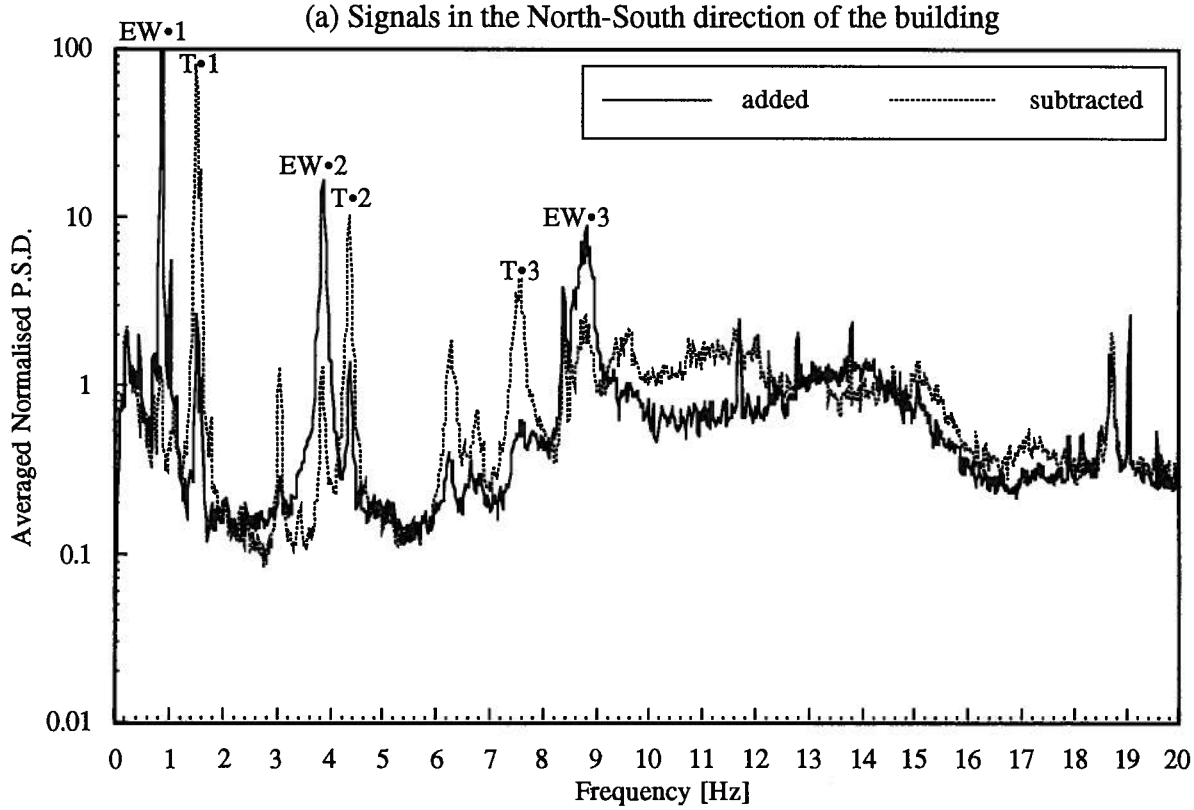

(b) Signals in the East-West direction of the building

Figure G.4. ANPSD plots for all of the lateral signals from the CT25 test. Peaks corresponding to natural frequencies are labeled with the corresponding mode.

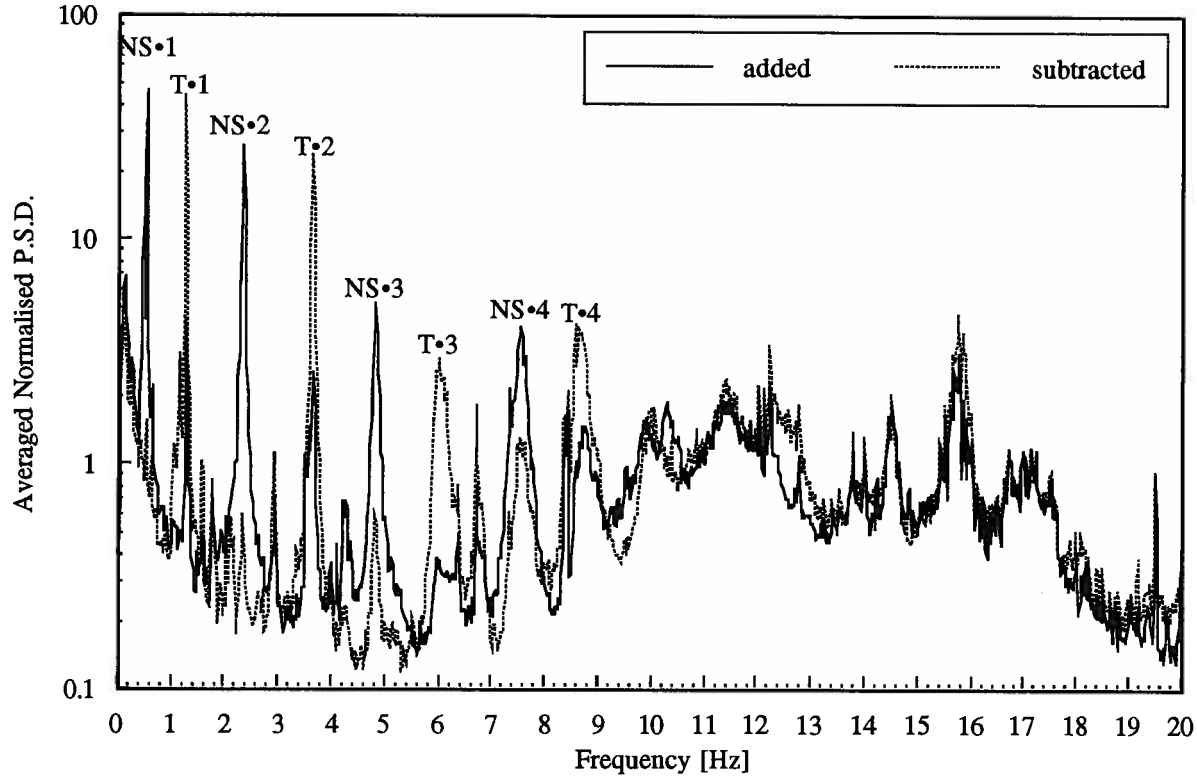

(a) Signals in the North-South direction of the building

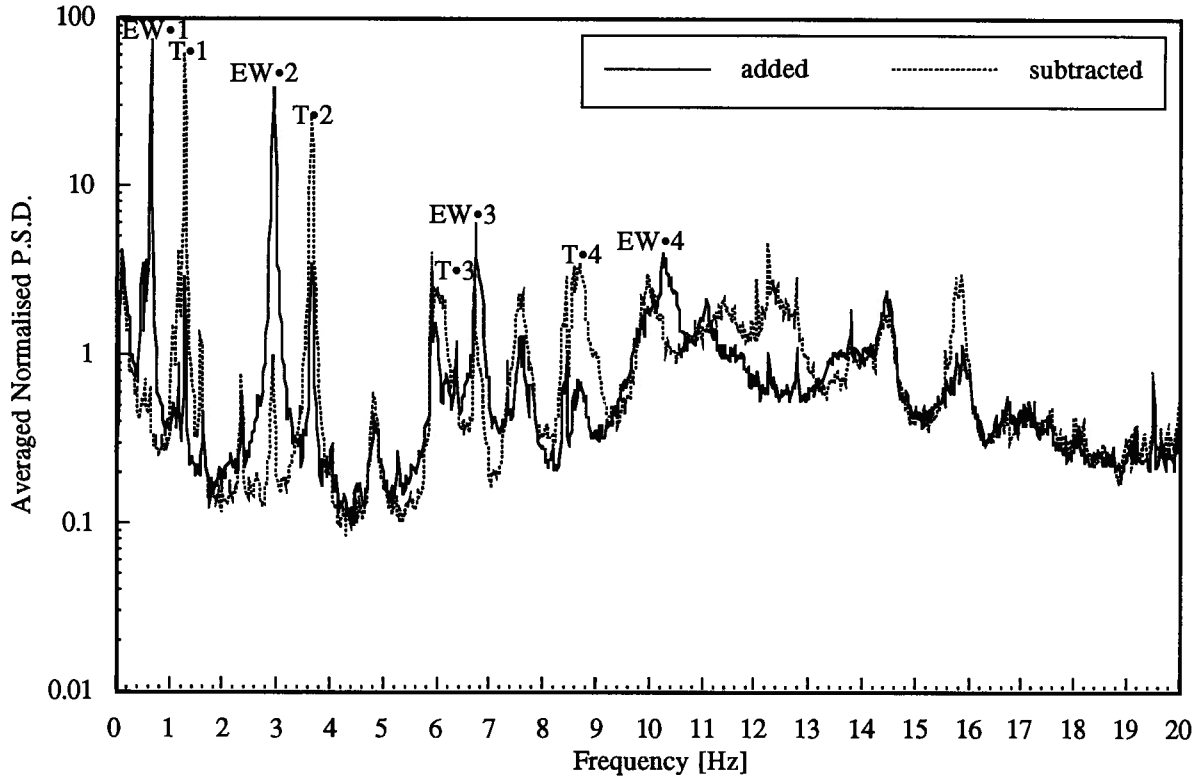

(b) Signals in the East-West direction of the building

Figure G.5. ANPSD plots for all of the lateral signals from the CT32 test. Peaks corresponding to natural frequencies are labeled with the corresponding mode.

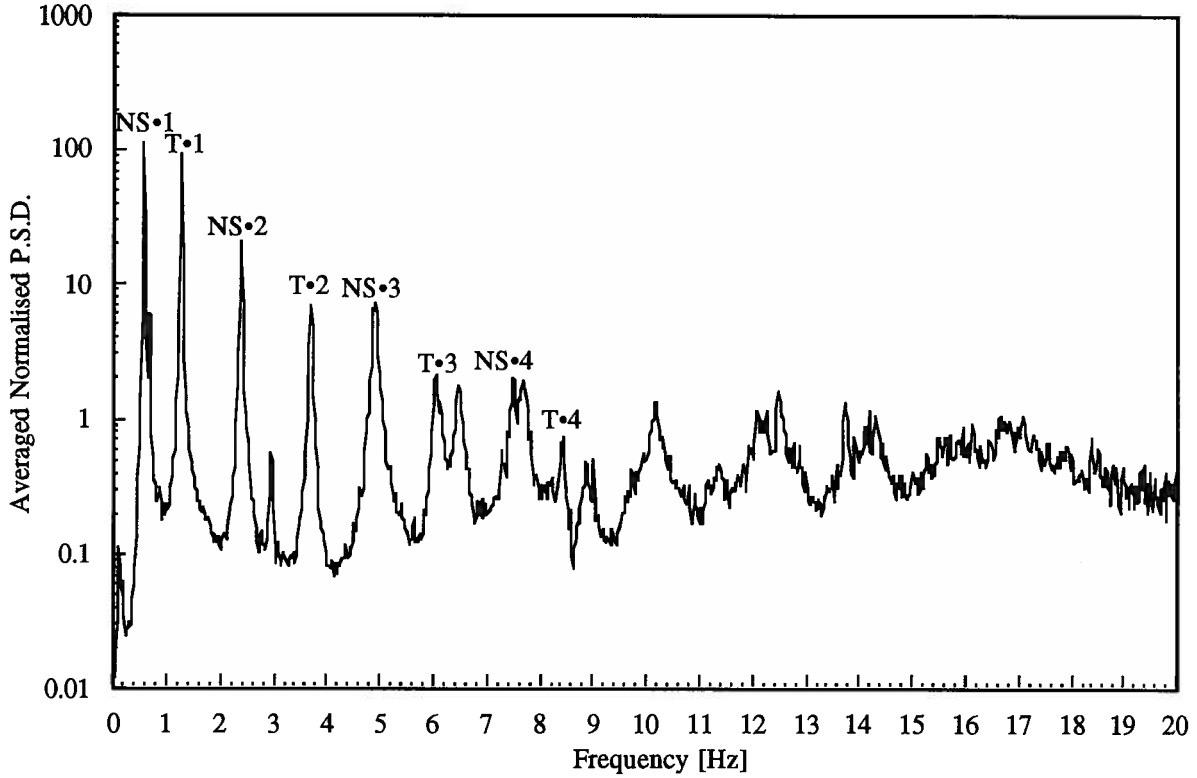

(a) Individual signals in the North-South direction of the building

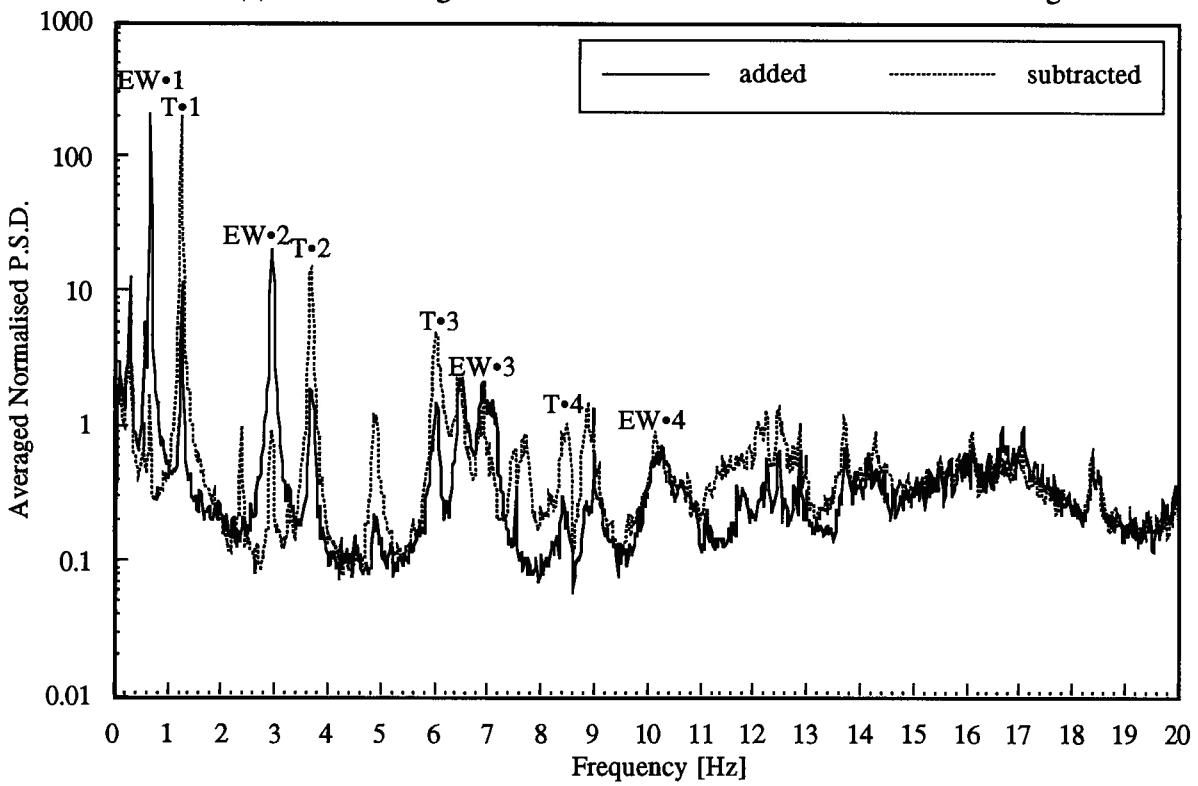

(b) Signals in the East-West direction of the building

Figure G.6. ANPSD plots for all of the lateral signals from the CTTC test. Peaks corresponding to natural frequencies are labeled with the corresponding mode.

H

APPENDIX H
COMPARISON OF ANALYTICAL AND EXPERIMENTAL RESULTS

This appendix presents a comparison between frequencies and mode shapes obtained experimentally (measurements) and analytically (dynamic analysis) using the software program ETABS (CSI Ltd., 1992). Tables H.1 through H.5 compare experimental and analytical frequencies. Also shown in these tables are the percentage difference in these frequencies along with the modal direction factors corresponding to the frequencies obtained using ETABS.

Figures H.1 through H.12 show comparisons between experimental and analytical mode shape components. Each of these figures show the modal displacements for each principal direction of the building; namely translation in both the North-South (NS) and East-West (EW) directions and rotation about the center of mass of each floor. In general, the match was excellent for the dominant component of the mode shape (i.e. the NS component for the NS translational modes showed good correlation; the rotational component of the torsional modes showed good correlation, etc.). In some cases the other components of the modes matched very well while in other cases, the match was poor. Due to space limitations, only the modes from the CT32 model are shown.

Table H.1. Comparison of experimental and analytical frequencies for 10 levels of the building completed (CT10).

	frequencies			modal direction factors (%)		
mode designation	measured (Hz)	ETABS (Hz)	difference (%)	EW direction	NS direction	rotational
NS•1	2.617	2.471	-6	1	97	2
EW•1	3.125	3.233	3	99	1	0
T•1	3.906	3.673	-6	0	2	98
NS•2	9.688	9.800	1	0	92	8
T•2	10.469	10.965	5	1	8	91
EW•2		13.033		99	0	1
NS•3		18.043		2	33	64
T•3		20.692		2	66	32

Table H.2. Comparison of experimental and analytical frequencies for 15 levels of the building completed (CT15).

	frequencies			modal direction factors (%)		
mode designation	measured (Hz)	ETABS (Hz)	difference (%)	EW direction	NS direction	rotational
NS•1	1.563	1.537	-2	0	98	2
EW•1	1.875	2.018	8	99	0	1
T•1	2.578	2.528	-2	1	2	96
NS•2	6.250	5.927	-5	0	86	14
T•2	7.773	7.526	-3	10	13	76
EW•2	8.633	8.546	-1	89	1	9
NS•3	10.703	11.694	9	1	55	45
T•3	11.875	13.107	10	4	44	52

Table H.3. Comparison of experimental and analytical frequencies for 20 levels of the building completed (CT20).

	frequencies			modal direction factors (%)		
mode designation	measured (Hz)	ETABS (Hz)	difference (%)	EW direction	NS direction	rotational
NS•1	0.938	0.997	6	0	99	1
EW•1	1.172	1.310	12	99	0	1
T•1	1.914	1.853	-3	1	1	98
NS•2	4.102	4.046	-1	0	90	10
EW•2	5.156	5.244	2	15	10	75
T•2	5.508	5.787	5	84	1	14
NS•3	8.242	8.449	3	1	54	45
T•3	9.023	10.284	14	4	47	48
EW•3	10.039	12.407	24	33	18	49

Table H.4. Comparison of experimental and analytical frequencies for 25 levels of the building completed (CT25).

	frequencies			modal direction factors (%)		
mode designation	measured (Hz)	ETABS (Hz)	difference (%)	EW direction	NS direction	rotational
NS•1	0.703	0.665	-5	0	99	1
EW•1	0.859	0.874	2	99	0	0
T•1	1.484	1.415	-5	1	1	99
NS•2	3.047	3.003	-1	0	92	8
EW•2	3.945	3.988	1	41	6	53
T•2	4.453	4.269	-4	58	2	39
NS•3	6.250	6.135	-2	2	64	34
T•3	7.578	7.696	2	9	35	56
EW•3	8.828	9.473	7	28	27	45

Table H.5. Comparison of experimental and analytical frequencies for 32 levels of the building completed (CT32).

	frequencies			modal direction factors (%)		
mode designation	measured (Hz)	ETABS (Hz)	difference (%)	EW direction	NS direction	rotational
NS•1	0.547	0.473	-14	0	100	0
EW•1	0.645	0.621	-4	100	0	0
T•1	1.289	1.184	-8	0	1	99
NS•2	2.305	2.382	3	1	95	4
EW•2	2.930	3.224	10	92	2	7
T•2	3.652	3.569	-2	7	4	89
NS•3	4.883	4.862	0	1	85	13
T•3	6.055	6.266	3	11	14	75
EW•3	6.856	7.319	7	55	28	18
NS•4	7.539	7.783	3	34	44	21
T•4	8.652	9.593	11	6	27	67
EW•4	10.488	10.331	-1	4	60	35

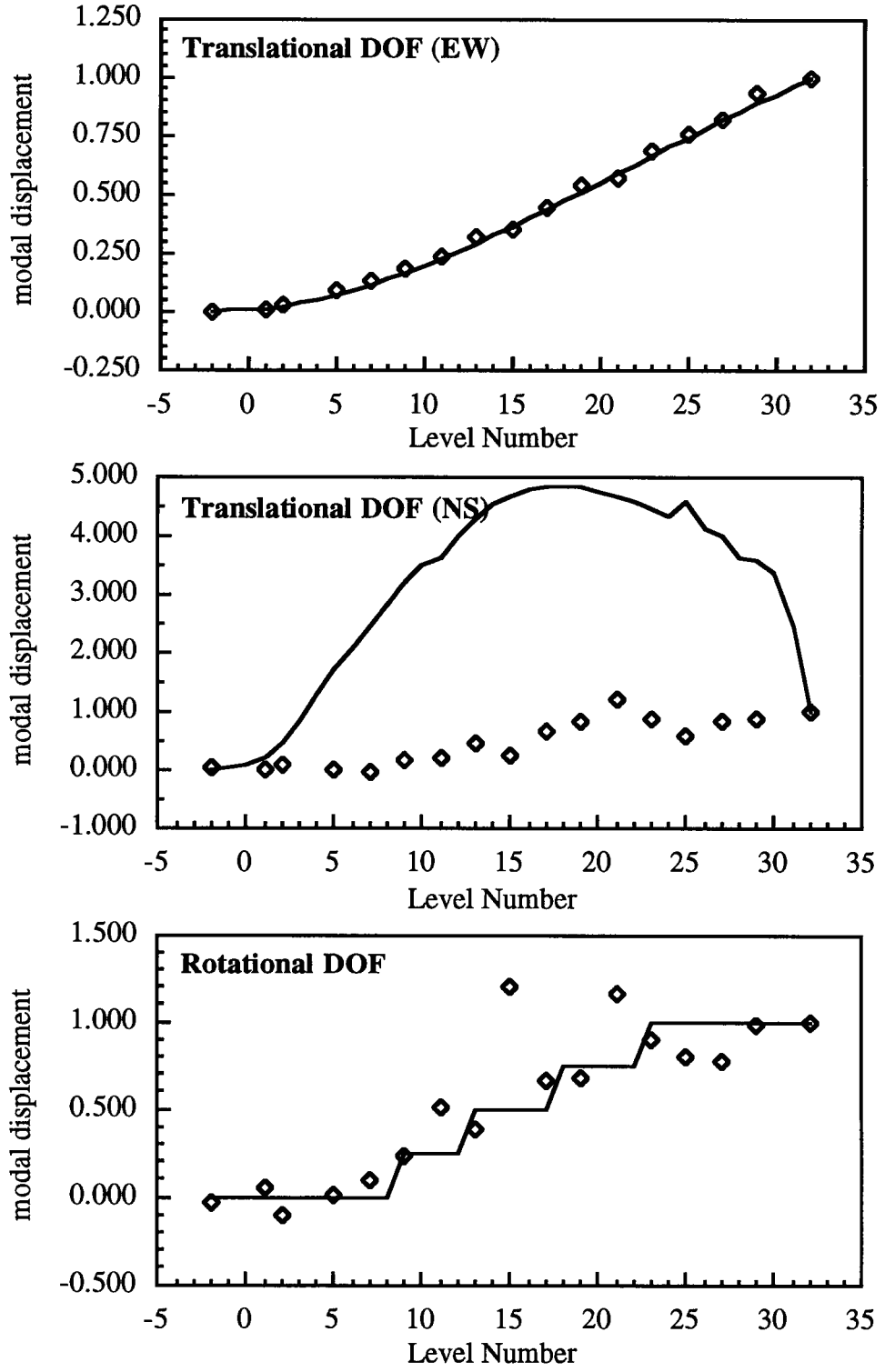

Figure H.1. Comparison of experimental (◊) and analytical (——) mode shapes for fundamental EW translational mode (EW•1)

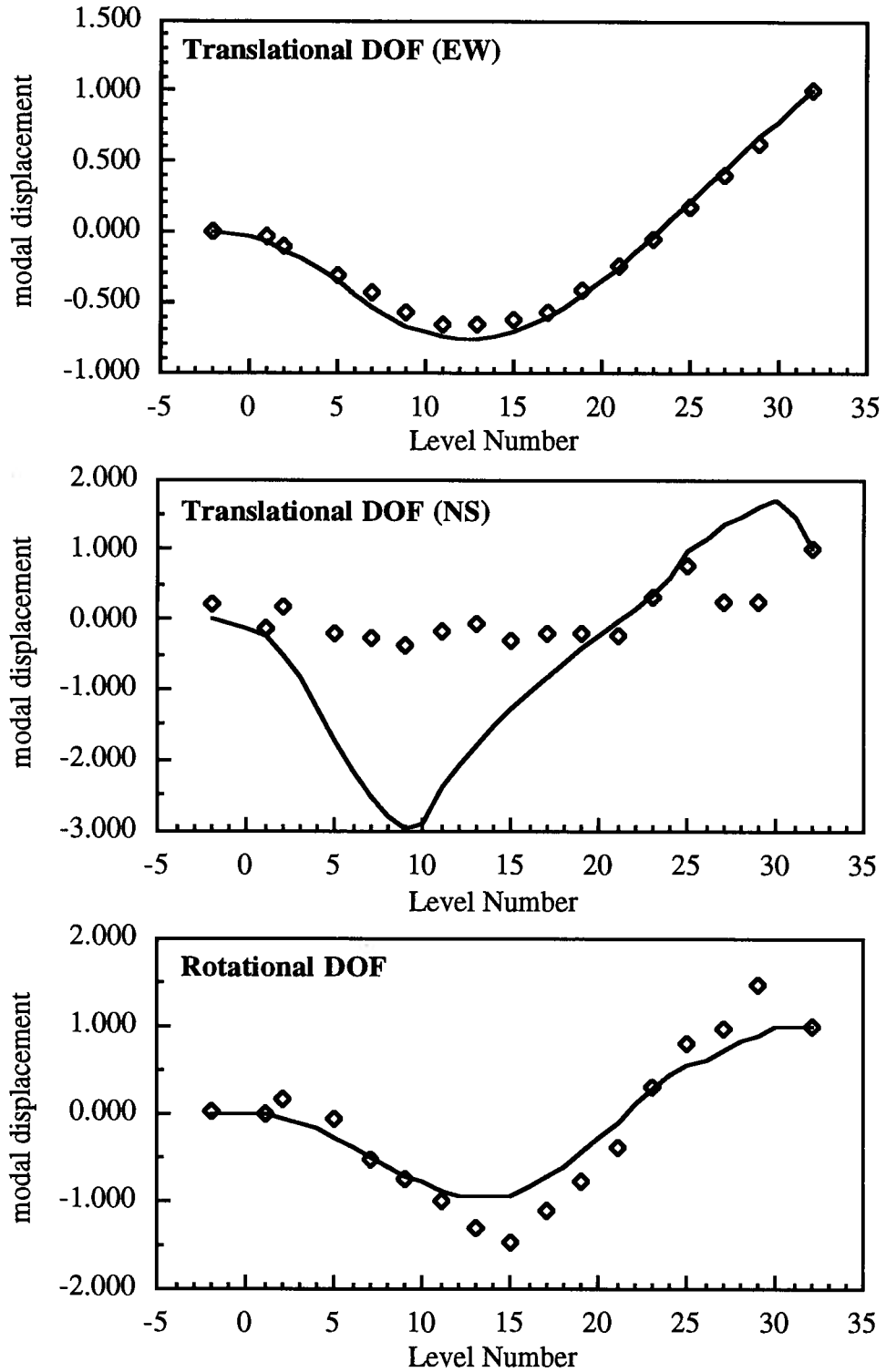

Figure H.2. Comparison of experimental (◊) and analytical (——) mode shapes for second EW translational mode (EW•2)

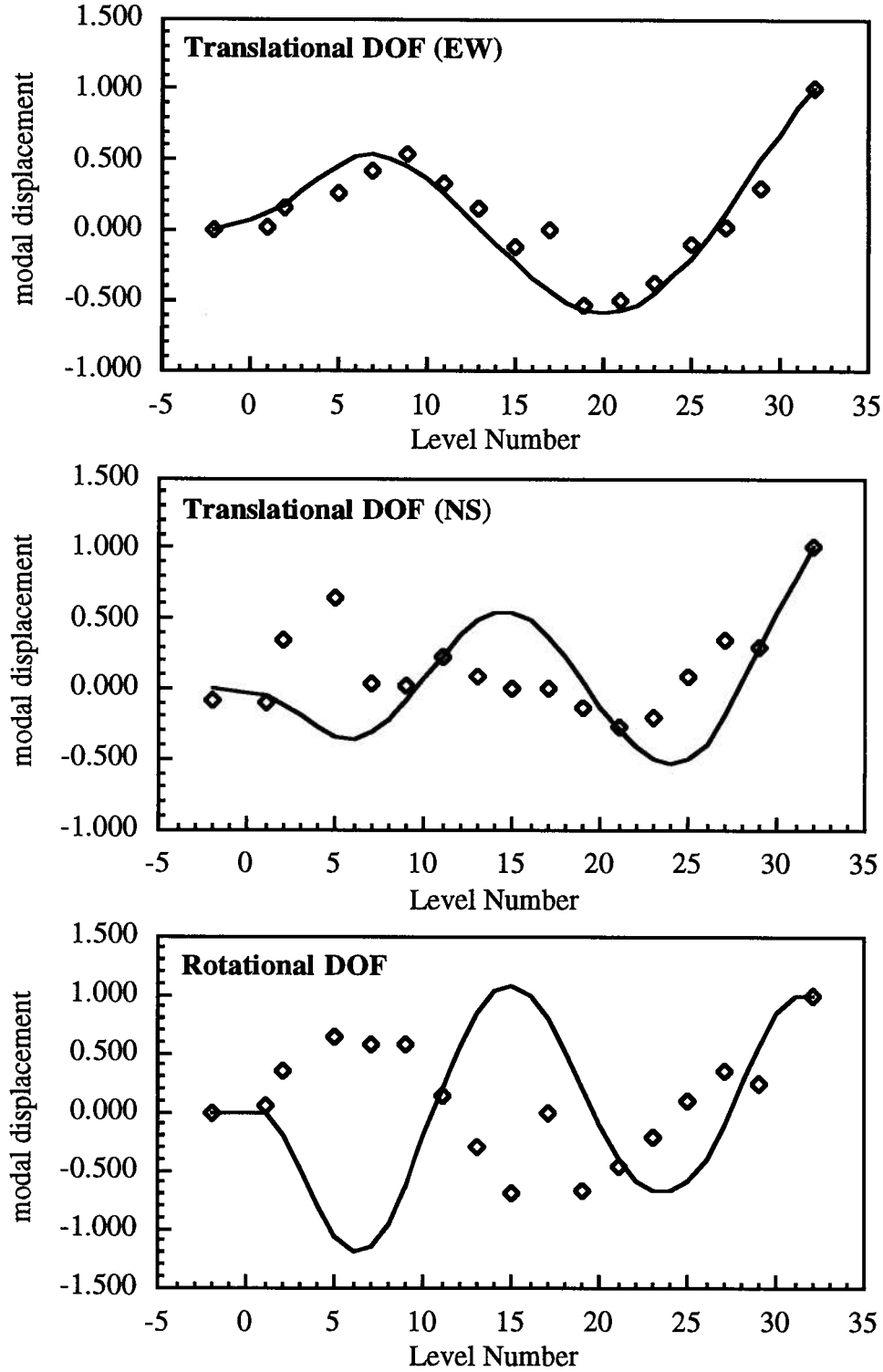

Figure H.3. Comparison of experimental (◊) and analytical (——) mode shapes for third EW translational mode (EW•3)

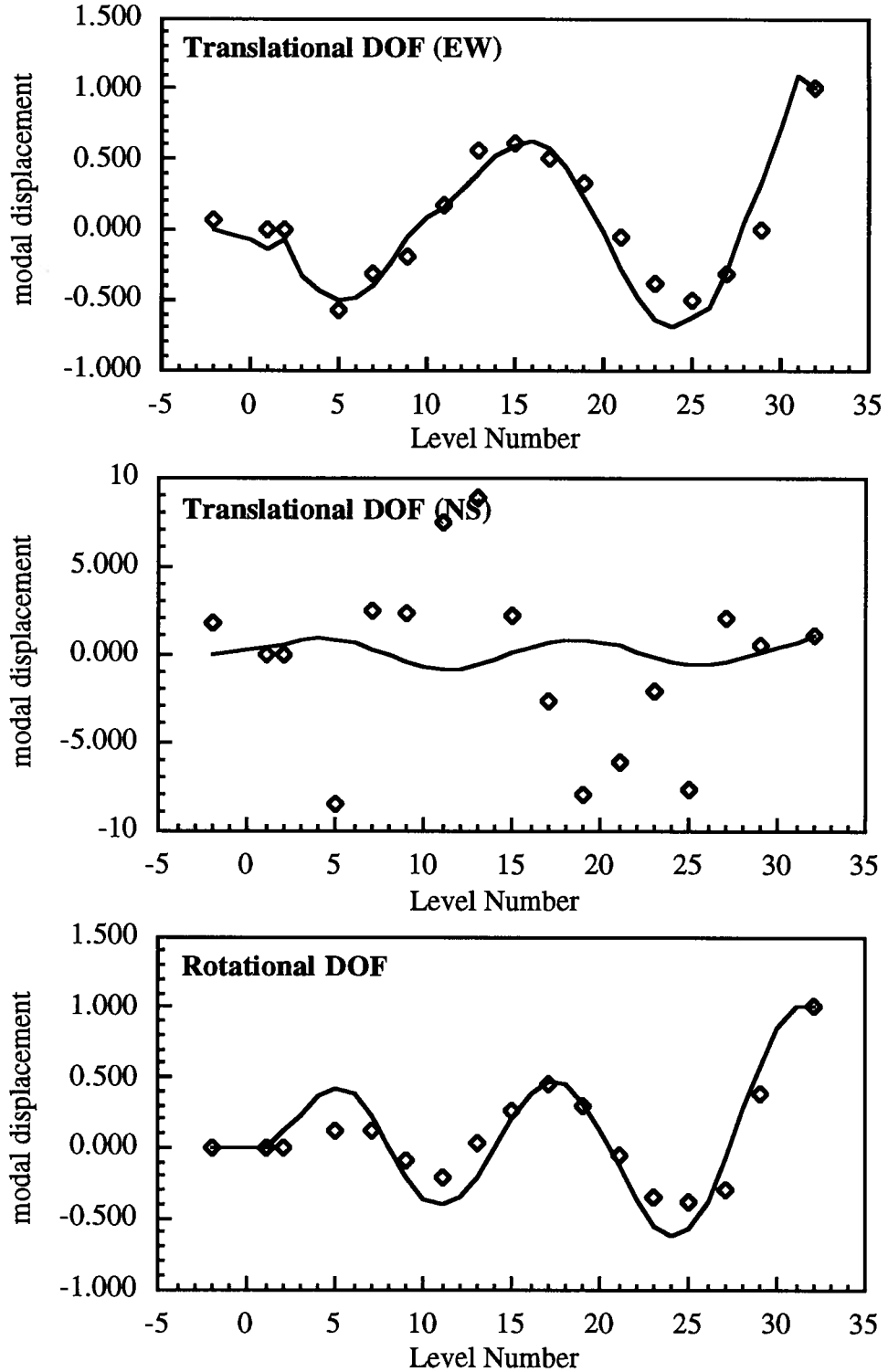

Figure H.4. Comparison of experimental (◊) and analytical (——) mode shapes for fourth EW translational mode (EW•4)

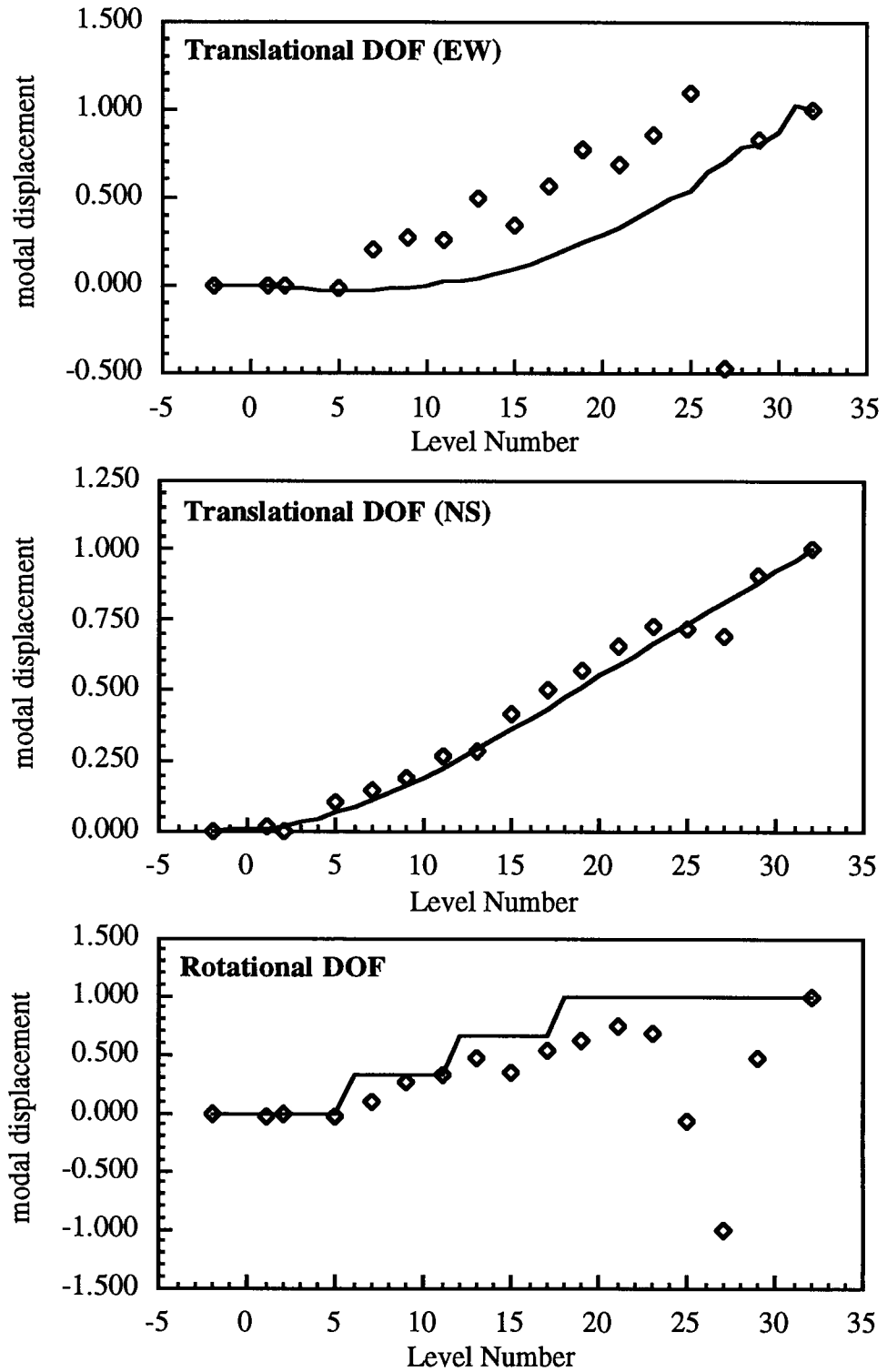

Figure H.5. Comparison of experimental (◊) and analytical (——) mode shapes for fundamental NS translational mode (NS•1)

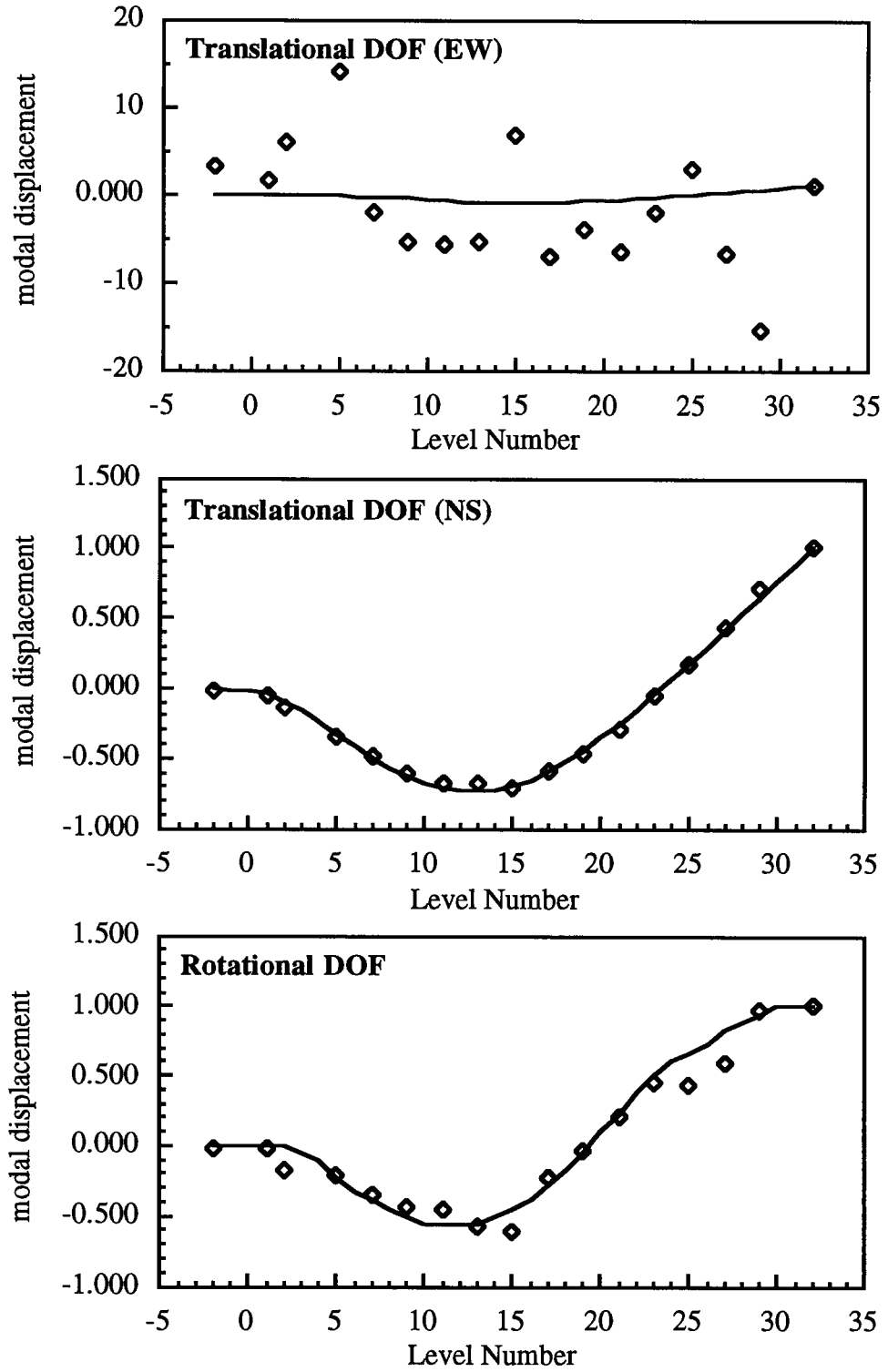

Figure H.6. Comparison of experimental (◊) and analytical (——) mode shapes for second NS translational mode (NS•2)

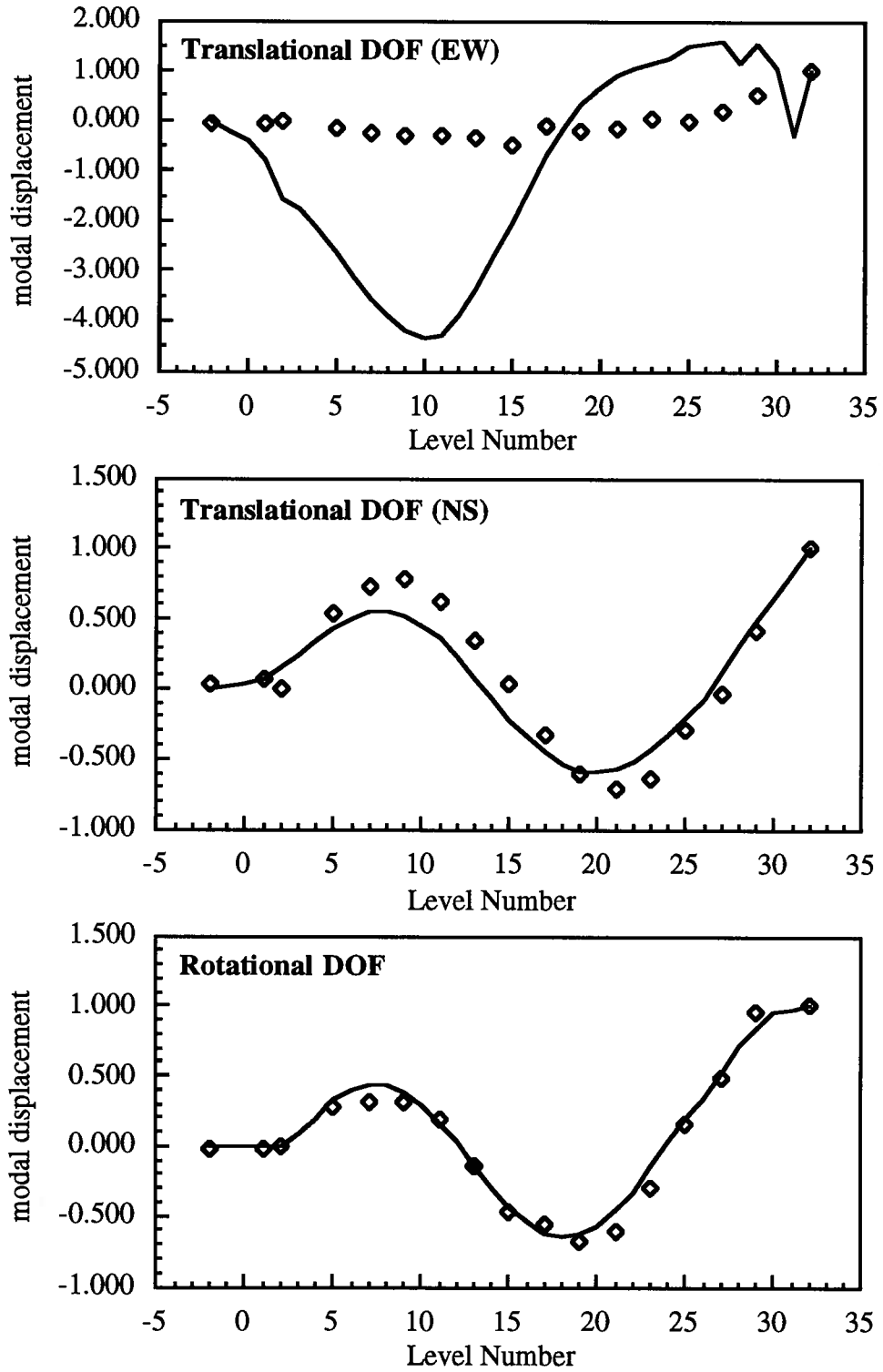

Figure H.7. Comparison of experimental (◊) and analytical (——) mode shapes for third NS translational mode (NS•3)

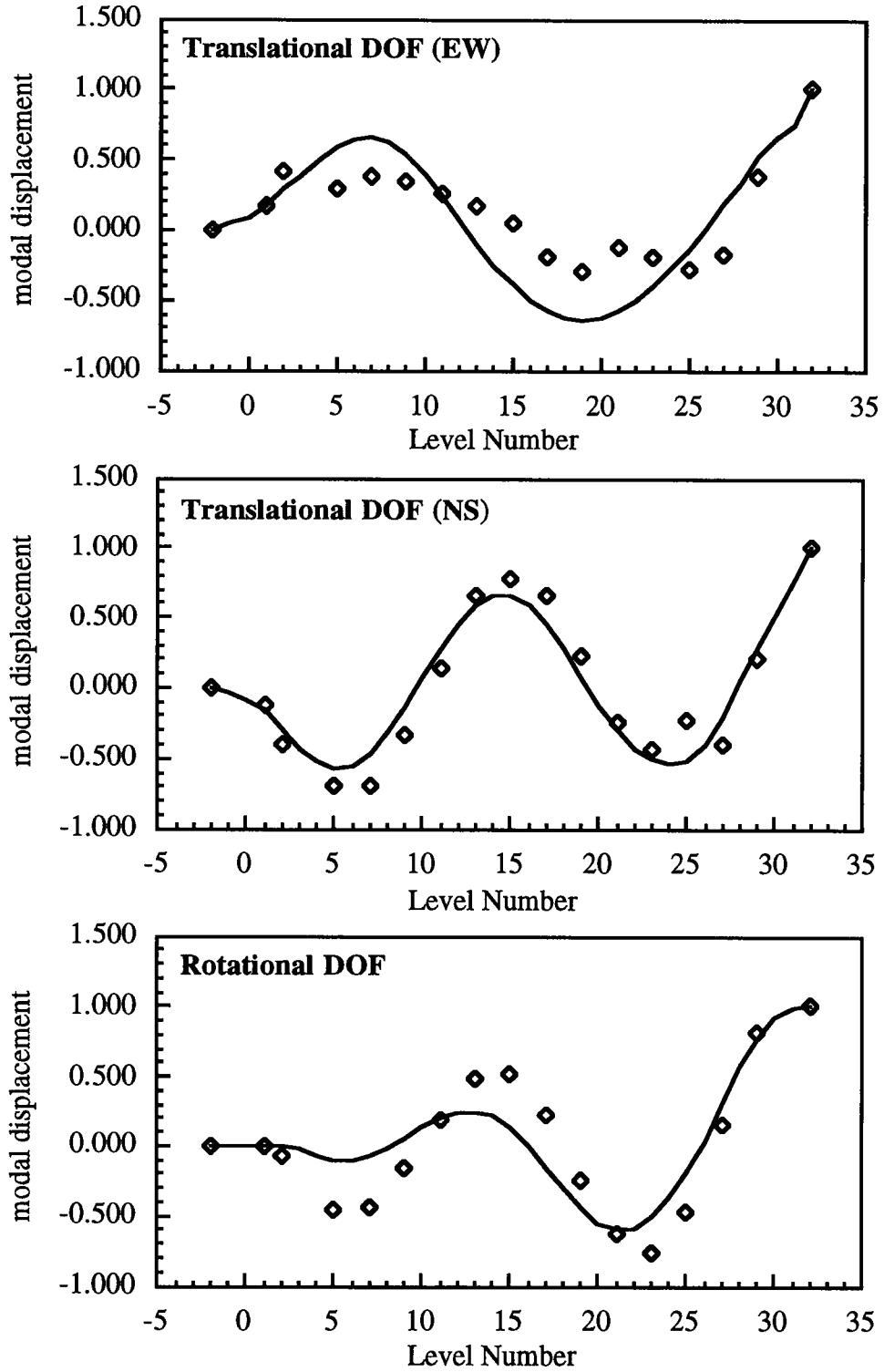

Figure H.8. Comparison of experimental (◊) and analytical (——) mode shapes for fourth NS translational mode (NS•4)

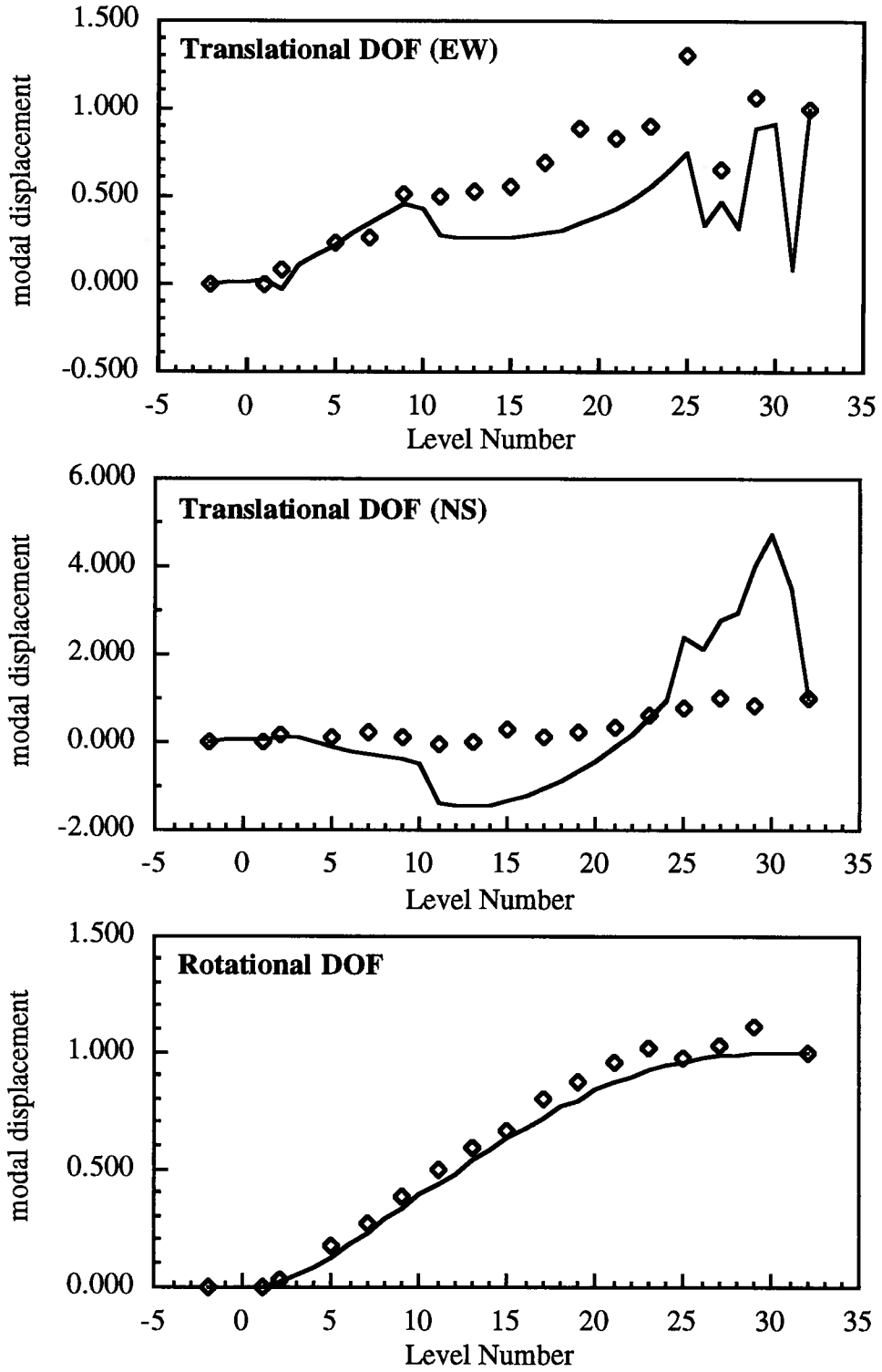

Figure H.9. Comparison of experimental (◊) and analytical (——) mode shapes for fundamental torsional mode (T•1)

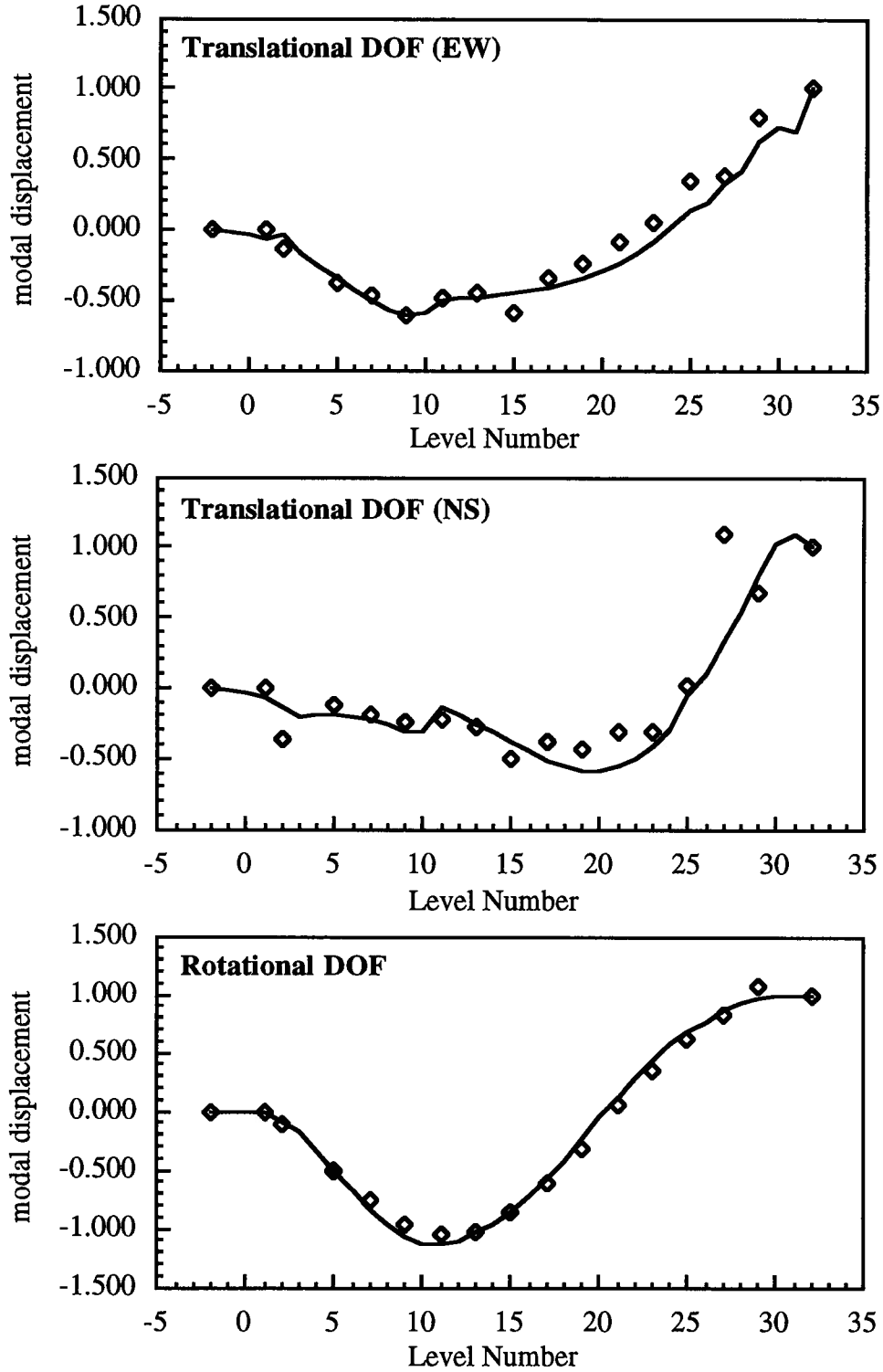

Figure H.10. Comparison of experimental (◊) and analytical (——) mode shapes for second torsional mode (T•2)

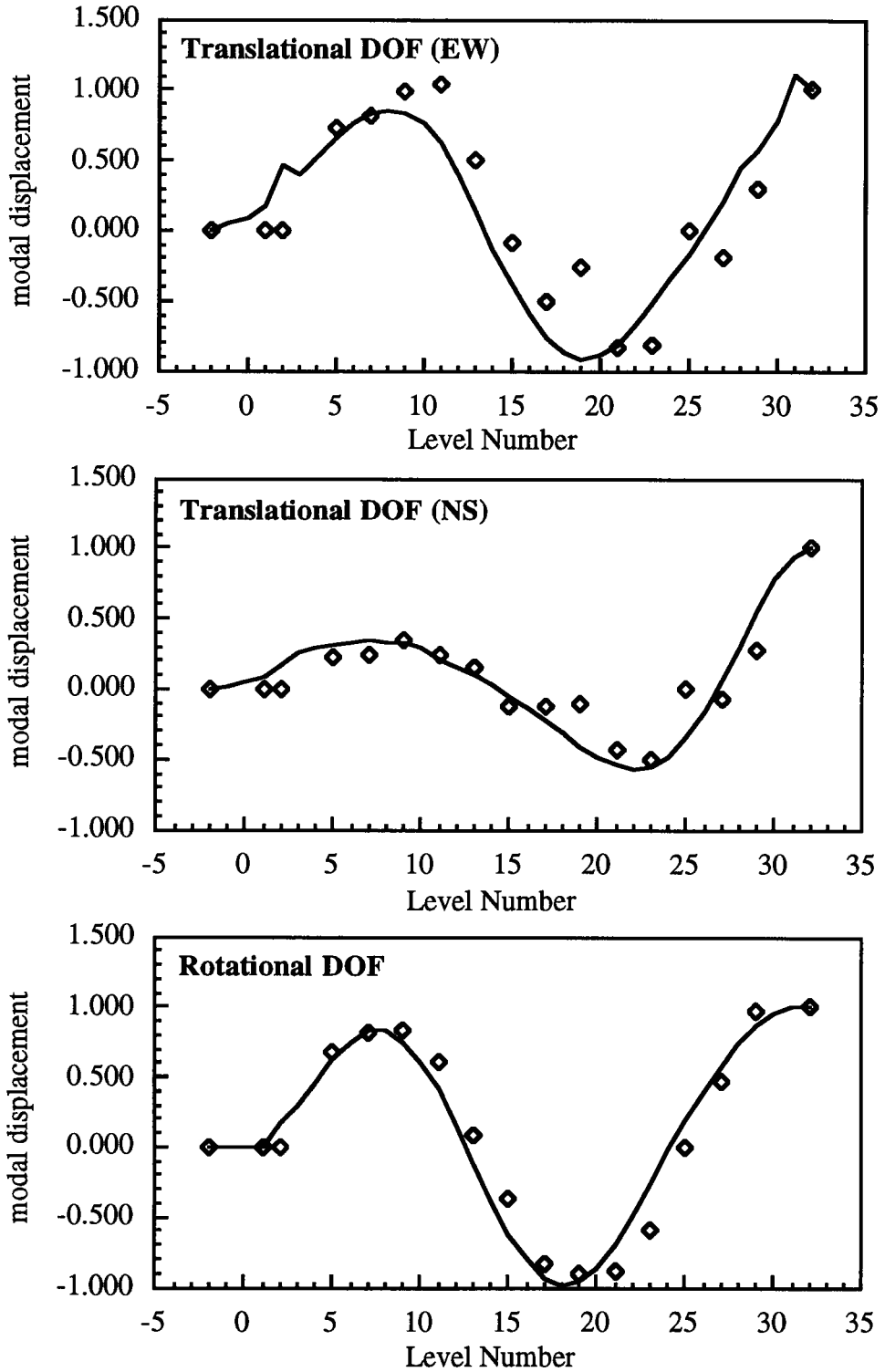

Figure H.11. Comparison of experimental (◊) and analytical (——) mode shapes for third torsional mode (T•3)

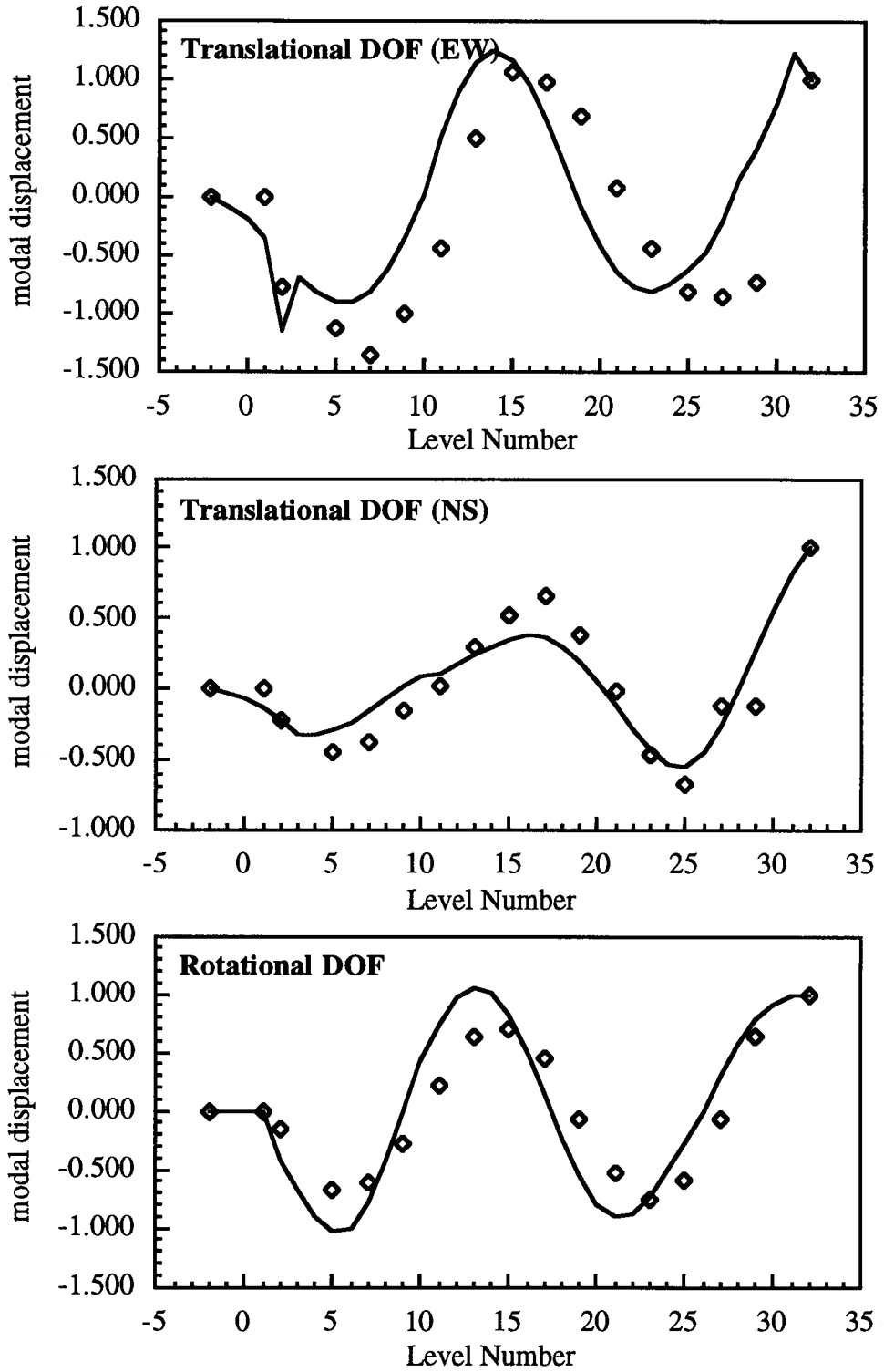

Figure H.12. Comparison of experimental (◊) and analytical (——) mode shapes for fourth torsional mode (T•4)